

**“To investigate the role of nanosecond laser
technology in rejuvenating transport in the aged outer
retina.”**

Dr Ling Zhi Heng

The Department of Genetics

Institute of Ophthalmology

Doctor of Philosophy

In the subject of

Ophthalmology

University College London

London, Great Britain

I, **Ling Zhi Heng**, confirm that the work presented in this thesis is my own. Where information has been derived from other sources, I confirm that this has been indicated in the thesis.'

Dr Ling Zhi Heng
2014

Foreword

This PhD signified a beginning of my life. The experience gained in the pursuit of this course saw me grow from a girl to a young lady. It has been an arduous journey but I am glad I managed to see through it. I am especially grateful to the many individuals who saw me through this period.

In particular, I would like to dedicate this PhD to my beloved father for his 60th birthday and I am glad I made it in time for this! Without my father's financial and constant support, not just for this PhD, for the last 30 years of my life, I would never have come so far. Of course, my mother played the role of my father's ears and without her and her sacrifices she has made for me and my family, nothing today could have ever been achieved.

I am very lucky to have several mentors who have been relentlessly supportive, gracious and always by my side.

I am immensely grateful to Professor Marshall for being my mentor, supervisor and advisor through this PhD and much more. Professor has always provided sound guidance and support, and one that I have and will always look up to as the ultimate role model. Especial thanks also to Judith Marshall and her patience for putting up with my troubles throughout the years and disturbances during the writing period.

I would also like to thank Dr Sobha Sivaprasad, my second supervisor for being a source of constant support and guidance and without her, I won't be where I am today.

Especial appreciation for Mr. Philip Hykin, 'Mr Nice', who has always been there for me, always patient, always kind. One who has taught me so much both in and out of the world of Ophthalmology and medicine.

Last, but certainly very importantly, I was told 'I had better thank this fella', who was there, most times of the days, most times of the year, the one who left me in peace to do my research every weekend in the laboratory and the one who I guess was just 'there'-Michael Chan, A 'mention' perhaps was not enough, but this PhD would celebrate with us the year of our engagement.

This PhD and the sweat, tears and hard work, I dedicate to all of the above.

Acknowledgements

I would like to extend especial appreciation to the following for their help and contribution to the thesis.

Mr Robin Hamilton, PI of RETILASE trial, Moorfields Eye Hospital

Dr Ali Hussain, Institute of Ophthalmology, UCL

Ms Ann Patmore, Institute of Ophthalmology, UCL

Ellex Pty Ltd for providing the 2RT laser for the thesis

Department of Genetics, Institute of Ophthalmology, UCL

Department of Ophthalmology, King's College Hospital

**Research and Treatment Centre, Moorfields Eye Hospital, NIHR
biomedical research unit**

This thesis would not have been possible without the financial support from **JP
Moulton Charitable Trust**

Contents

Abstract	
Abbreviations	
List of Figures	14
List of Tables	18
Chapter 1. Introduction	
1.1 Introduction.....	20
1.2 Lasers for Retinal Therapy.....	26
1.2.1 Mechanism of Retinal Lasers Damage.....	26
1.2.2 Concept of Primary and Secondary Laser Damage.....	33
1.2.3 Underlying Concepts of the 2RT Laser.....	35
1.3 Anatomy of the outer retina	39
1.3.1 Retina	39
1.3.1.1 Neurosensory Retina.....	41
1.3.1.2 The Photoreceptor Layer	42
1.3.1.3 Retinal Pigment Epithelium	44
1.3.1.4 Bruch's Membrane	46
1.3.2 Transport Mechanism of the Outer Retina	47
1.4 Ageing of the outer retina	51
1.4.1 Ageing retina pigment epithelial.....	51
1.4.2 Ageing Bruch's.....	52
1.5 Matrix Metalloproteinase	59
1.5.1 Molecular Biology of Matrix Metalloproteinases.....	59
1.5.2 Systemic Involvement of Matrix Metalloproteinases.....	61
1.5.3 Involvement of Metalloproteinase in Ageing Bruch's Membrane	66
1.6 Treatments of early AMD.....	69
1.7 Problems and Aims at Commencement of this Thesis	77
1.7.1 Problems.....	77
1.7.2 Aims and Objectives.....	81

Part 1

Chapter 2. Assessment of the Discontinuous Beam Energy distribution/ “Speckled Laser Beam” of the 2RT Laser

2.1 Introduction 86

2.2 Methods and materials 87

2.2.1 Physical modelling of beam energy distribution of the 2RT laser 87

2.2.1.1 Assessment of laser beam profile 87

2.2.1.2 Laser application on Neutral Density Filter 88

2.2.1.3 Assessment of laser beam profile through a neutral density filter 88

2.2.2 Assessment of Biological Effects across the Lesions Produced by 2RT laser on Porcine RPE 90

2.2.2.1 Dissection porcine eyes 90

2.2.2.2 Laser application 90

2.2.2.3 Flat mount histology 92

2.2.2.4 Measurement of diameter of laser damage 92

2.2.2.5 RPE viability 92

2.2.2.6 Determination of ED50 of 2RT laser 93

2.3 Results 94

2.3.1 Physical Modelling of Energy Distribution of 2RT Laser 94

2.3.1.1 Assessment of laser beam profile 94

2.3.1.2 Results from Neutral Density Filter analysis of 2RT laser beam 94

2.3.1.3 Laser beam analysis after passing through a NDF 96

2.3.2 Results from Biological Assessment of 2RT Energy Beam Distribution 102

2.3.2.1 Diameter of laser damage with varying energy levels on porcine flat mount histology 102

2.3.2.2 Morphology of RPE Damage from the 2RT laser 104

2.3.2.3 Probit analysis of laser damage 109

2.4 Discussion 110

2.5 Conclusions 113

Chapter 3. The Release of Matrix Metalloproteinases (MMPs) from Porcine and human RPE-BrM explant cultures

3.1.1 Introduction	114
3.1.2 Principles of Gelatin Zymography	115
3.2 Methods and materials	116
3.2.1 Porcine RPE-BrM-Choroid Explant culture	116
3.2.2 Human RPE-BrM-Choroid Explant culture	117
3.2.3 Gelatin Zymography	119
3.3 Results	122
3.3.1 MMP release characteristics of porcine RPE-BrM explant culture as a function of time	122
3.3.2 MMP release characteristics of Human RPE-BrM explant culture as a function of time	126
3.3.3 Histology of Porcine and Human RPE-Bruch's membrane choroid Complex Subsequent to Incubation in Culture Medium	130
3.4 Discussion	132
3.5 Conclusions.....	134

Chapter 4. Effect of Nanosecond Laser on the Release of Metalloproteinases from Porcine RPE-Bruch's choroid Explants

4.1 Introduction	134
4.2 Methods and Materials	136
4.2.1 Set up of explant culture	136
4.2.2 Laser application.....	136
4.2.3 Collection of samples	137
4.2.4 Determination of MMPs (Gelatin zymography)	137
4.2.5 Analysis of gelatin zymography	137
4.2.6 Histology.....	138
4.3 Results	139
4.3.1 Type of MMP release post laser as a Function of Time.....	139
4.3.2 Description of Histology of Laser Lesion at End of Incubation Period	147
4.4 Discussion	149
4.5 Conclusions.....	152

Chapter 5. The effect of exogenously applied MMPs on hydraulic conductivity across the Aged Bruch's membrane

5.1 Introduction.....	153
5.2 Methods and materials	155
5.2.1 Preparation of Human Bruch's-Choroid sample	155
5.2.2 Activation of MMP	156
5.2.3 Measurement of hydraulic conductivity	159
5.3 Results	161
5.3.1 Baseline Hydraulic Conductivity	161
5.3.2 Change in Hydraulic Conductivity.....	162
5.4 Discussion	168
5.5 Chapter conclusion.....	171

Part 2

Chapter 6. Efficacy and safety of retinal rejuvenation using Ellex 2RT laser in age-related maculopathy (RETILASE trial)-background to investigation plan

6.1 Summary of Investigation plan.....	172
6.2 Background to design of RETILASE trial	176
6.2.1 Introduction	177
6.2.2 The International grading of age related maculopathy	178
6.2.3 Summary of Current Clinical Understanding of Pathology of AMD	181
6.2.4 Bruch's Membrane (BrM)	181
6.2.5 Ellex 2RT laser.....	182
6.2.6 Prior research work	183
6.3 Theoretical Concepts for Delaying Ageing in the Outer Retina .	184
6.4 Objectives of RETILASE trial in reference to this thesis.....	185
6.5 Study Design	186
6.5.1 Study Design	186
6.6 Population.....	188
6.6.1 Inclusion Criteria.....	188
6.6.2 Exclusion Criteria.....	188
6.7 Summary of study assessments	190

6.8 Treatment Regime	195
-----------------------------------	------------

Chapter 7

RETILASE results I. Efficacy Evaluation of RETILASE trial

7.1 Introduction	196
7.2 Baseline characteristics of trial participants	197
7.2.1 Data Sets Analysed	197
7.2.2 Baseline Characteristics	197
7.2.3 Morphology of AMD status of patients recruited	199
7.3 Methods of Analysis of efficacy	201
7.3.1 Mean change in VA, Contrast Sensitivity, Microperimetry, Flicker Perimetry	201
7.3.2 Changes in Fundus Morphology	201
7.4 Results	205
7.4.1 Visual acuity outcome	205
7.4.2 Contrast Sensitivity	210
7.4.3 Microperimetry	212
7.4.4 Flicker Perimetry	218
7.4.5 Changes in Fundus Morphology	220
7.5 Statistical/analytical issues	222
7.6 Discussion	223
7.7 Conclusions	227

Chapter 8

RETILASE Results II. Safety of the 2RT laser in patients with early AMD

8.1 Introduction	228
8.2 Methods of Analysis of Safety	229
8.2.1 Fundus Autofluorescence	229
8.2.2 Optical Coherence Tomography	229
8.2.3 Color Fundus Photography	232
8.2.4 Microperimetry	232
8.3 Summary of Results of Safety Analysis	234
8.3.1 Changes on Fundus Autofluorescence	234

8.3.2 Optical Coherence tomography.....	239
8.3.3 Color Fundus Photography.....	240
8.3.4 Microperimetric analysis of laser lesions	241
8.4 Discussion	252
8.5 Conclusions.....	256

Chapter 9. Discussion

9.1 Discussion	257
9.2 The Role of the 2RT Laser in Rejuvenating the Aged Outer Retina	258
9.3 Safety profile of the 2RT laser	262
9.4 Evaluation of tools to monitor early AMD.....	273
9.5 Conclusions and future direction.....	280
References.....	282
Presentations and publications.....	296
Appendix.....	297

Abstract

The transport capacity of the retina plays a major role in maintaining health of the photoreceptors cells. In particular, age-related changes in the Bruch's membrane(BrM) correspond to a decrease in the transport of nutrients and waste products across the Bruch's. Matrix metalloproteinase(MMP), an extracellular matrix regulator was found to be sequestered in aged BrM, with decreased availability for activity. Hence, it was hypothesized that a plausible target to rejuvenate the transportation across BrM and prevent the age-related processes in the macular was to increase the activity of MMP in BrM. Previous studies have shown an increase in MMP release secondary to RPE migration initiated by deliberate injury using lasers. However,conventional lasers causes collateral photoreceptor cell damage via primary thermal denaturation and secondary apoptosis. The nanosecond laser used in the present study with its speckled beam configuration and nanosecond pulse is designed to limit the primary damage profile. The main objectives of this PhD was to determine if this novel laser was a viable option to improve transport across BrM while preserving photoreceptor function, further to ascertain its efficacy and safety for use in human subjects to delay or prevent onset of AMD.

Laboratory results from this thesis confirmed the importance of MMPs but demonstrated the inadequacy of the speckled beam configuration at higher energy levels. Corroborative clinical results also found beam profile inadequacy with the suprathreshold nature of the current energy-dose but desmonstrated minmal collateral damage. Clinical evaluation found a short term improvement of visual function. It may be concluded this novel laser has potential to be used as a therapeutic modality to delay AMD, but further work needs to be done to address the current issues of beam configuration and energy dosing for its optimal use in the future.

Abbreviations

Abbreviations	
2RT	Retinal Rejuvenative Therapy
AMD	Age related macular degeneration
AGE	Advanced Glycation End Product
ALE	Advanced Lipoxidation End Product
AREDS	Age Related Eye Disease study
BJO	British Journal of Ophthalmology
BrM	Bruch's membrane
CAPT	Complications of Age related macular degeneration trial
CC	Choriocapillaries
CFP	Color fundus photograph
CNV	Choroidal neovascularization
CNVPT	Choroidal neovascularization prevention trial
CW	Continuous wave
DLS	Drusen Laser study
DR	Diabetic Retinopathy
ECM	Extracellular matrix
ELM	External limiting membrane
FA	Fatty acids
FAF	Geographic atrophy
GA	Fundus autofluorescence
HMW	High molecular weight
ILM	Inner limiting membrane
IS	Inner Segment
LMMC	Large macromolecular weight complex
MP1	Microperimetry
MMP	Matrix metalloproteinase
OCT	Optical Coherence Tomography
OS	Outer Segment
PRL	Photoreceptor layer
RPE	Retinal pigment epithelium
SRT	Selective Retinal Therapy
TIMP	Tissue Inhibitor of MMP
UK	

WHO	United Kingdom World Health Organisation
-----	---

List of Figures

Chapter 1 Figures

Figure 1.1 Laser energy distribution in spot sizes in millisecond duration	30
Figure 1.2a, 1.2b RPE damage using a non Q switched and Q switched laser	31
Figure 1.3 Pictorial demonstration of mechanism of laser damage in different time domain.....	32
Figure 1.4 Illustration of primary and secondary laser damage in the retina	34
Figure 1.5 Schematic diagrams of the effects on the retina and Bruch's membrane caused by a) a millisecond laser, b) a microsecond laser and c) a nanosecond laser.	36
Figure 1.6 Pictorial diagram of the anatomy of the retina	40
Figure 1.7 Diagram of anatomy of neural retina.....	41
Figure 1.8 Pictorial demonstration of rod outer segment renewal.....	43
Figure 1.9 Transport pathways across the Bruch's membrane.....	49
Figure 1.10 Transport of metabolites in the outer retina	50
Figure 1.11 HC plots across Bruch's membrane at (a) macular and	56
Figure 1.12 Role of MMPs in systemic diseases	65
Figure 1.13 MMP Pathway in elderly Bruch's-choroid.....	68
Figure 1.14 Progression of AMD.....	76
Figure 1.15 Concept of quantitative MMP release	80

Chapter 2 Figures

Figure 2.1 Pictorial demonstration physical modeling of energy beam distribution of the 2RT laser	89
Figure 2.2 Pictorial demonstration of laser application in varying laser energy levels in porcine flat mount.....	89
Figure 2.3 Pictorial demonstration of laser application in varying laser energy levels in porcine flat mount.....	91
Figure 2.4 Analysis of laser beam profile at 0.5mJ	94
Figure 2.5 Impact of varying 2RT laser energy on gelatin Neutral Density Filter	95
Figure 2.6 Enlarged image to demonstrate speckle profile of laser beam on NDF at 0.1mJ.	95
Figure 2.7 Laser beam analysis	97

Figure 2.8 Morphology of RPE damage in terms of energy range	105
Figure 2.9 Probit curve of exvivo porcine energy levels vs ophthalmoscopically visible threshold	109
Figure 2.10 RPE damage from low energy 2RT laser	110

Chapter 3 Figures

Figure 3.1 Modified Ussing chamber	118
Figure 3.2a Dissection of Porcine Eyes Figure 3.2b Ussing chamber	118
Figure 3.3a Example of method to determine gelatinase molecular weight	121
Figure 3.3b Comparison of porcine and human RPE-BrM choroid explant samples with molecular weight standards	121
Figure 3.4 Zymogram of Porcine RPE-BrM choroid explants	123
Figure 3.5 Time course of MMP release in porcine RPE-BrM choroid explant culture	124
Figure 3.6 Zymogram of Human RPE-BrM choroid explant culture	126
Figure 3.7 MMP release profiles of Human RPE-BrM explant culture	127
Figure 3.8a, b Histology of porcine vs human RPE-BrM explants	130

Chapter 4 Figures

Figure 4.1 Pattern of laser spot application in porcine explants.....	137
Figure 4.2 Zymogram of apical release of MMP in porcine explant culture post laser	141
Figure 4.3 Zymography of basal release of MMP in porcine explant culture post laser	141
Figure 4.4 MMP profiles of explant culture post laser	142
Figure 4.5 MMP profiles of porcine explant culture post laser in varying number of laser shots.....	144
Figure 4.6 Levels of active-MMP2 basal release with different number of laser spots.....	146
Figure 4.7 Total quantity of active-MMP2 release at Day 7 of incubation	146
Figure 4.8 Histology of porcine RPE-BrM explant culture day 10 of incubation	147

Chapter 5 Figures

Figure 5.1 Representative zymogram of APMA activated MMP2 in varying concentrations	157
Figure 5.2 Graph comparing MMP densitometric quantity with concentration of active MMP2.	158
Figure 5.3 Schematic diagram of modified Ussing chamber for measurements of HC	160
Figure 5.4 Photographic diagram of Ussing chamber water tank	1600
Figure 5.5 Baseline Hydraulic Conductivity of samples	161
Figure 5.6a Plot of pre and post HC with varying levels of activity of MMP-2 with age	163
Figure 5.6b Change in HC versus concentration of Active-MMP2.....	164
Figure 5.7 Individual Plots of HC pre and post addition of Active-MMP2	167

Chapter 6 Figures

Figure 6.1 Pictorial demonstration of druse size grading, International Classification	177
Figure 6.2 Pictorial demonstration of biochemical impact of nanosecond laser on the RPE.....	184
Figure 6.3 Microperimetry	193
Figure 6.4 Flicker perimetry	194

Chapter 7 Figures

Figure 7.1 Photographic demonstration of measurement of druse size using AREDS maculopathy grading grid	204
Figure 7.2 Mean VA, cases versus controls.....	208
Figure 7.3a Individual plot of change in VA, controls	209
Figure 7.3b Individual plot of change in VA, cases	209
Figure 7.4a Individual plot of change in CS, controls.....	211
Figure 7.4b Individual plot of change in CS, cases	211
Figure 7.5a Individual plot of change in MP1 at 4 degrees, controls	215
Figure 7.5b Individual plot of change in MP1 at 4 degrees, cases.....	215
Figure 7.6a Individual plot of change in MP1 at 12 degrees, controls	217
Figure 7.6b Individual plot of change in MP1 at 12 degrees, cases.....	217
Figure 7.7a Individual plot of change in Flicker perimetry for controls	219

Figure 7.7b Individual plot of change in Flicker perimetry, cases	219
---	-----

Chapter 8 Figures

Figure 8.1 OCT and infra-red image obtained from Spectralis	230
Figure 8.2 FAF and infrared overlay	230
Figure 8.3 Presumed OCT anatomical layers as defined in this thesis...	231
Figure 8.4a,b. Demonstration of MP1 analysis	235
Figure 8.5a Recovery of RPE damage post laser	236
Figure 8.5b Dynamic Process of RPE laser lesion recovery.....	237
Figure 8.6 A-C FAF classification of laser lesions.....	238
Figure 8.7 Full fields FAF image at 15 months post laser.....	238
Figure 8.8 Comparison of laser lesion on CFP and FAF	240
Figure 8.9 Evolution of laser scars on CFP.....	241
Figure 8.10a Example of Hyperflorescent type I laser lesion.....	240
Figure 8.10b Example of hyperflorescent type II laser lesion	244
Figure 8.10c Example of hypoflorescent laser lesion.....	246

Chapter 9 Figures

Figure 9.1 Demonstration of possible effects of rejuvenating the aged outer retina	260
Figure 9.2 Demonstration of speckling of 2RT laser beam	262
Figure 9.3 Pictorial demonstration of impact of energy levels on speckling of 2RT laser beam.....	262
Figure 9.4 Damage profile of lasers in mili to nanosecond time domain on OCT.....	265
Figure 9.5 Pictorial demonstration of imaging resolution as compared to anatomical structure	275

List of Tables

Chapter 1 Tables

Table 1.1 Pulse duration and thermal diffusion distance, by Birngruber, Roeder and team	29
Table 1.2 Hydraulic conductivity in ageing physiology	57
Table 1.3 Changes in the BM secondary to ageing	58
Table 1.4 Types of MMP	62
Table 1.5 Inducers and inhibitors of MMP	62
Table 1.6 Biological activities mediated by MMP cleavage.....	63
Table 1.7 Gelatinase activity age-matched control versus AMD.....	68

Chapter 2 Tables

Table 2.1 Energy levels versus mean diameter of RPE damage	103
Table 2.2 Table describing laser damage morphology on RPE flat mount	108

Chapter 5 Tables

Table 5.1 Dilution and concentration of active-MMP2	156
---	-----

Chapter 6 Tables

Table 6.1 Summary of RETILASE investigation plan	174
Table 6.2 AREDS simplified severity scale grading table	176
Table 6.3 Summary of RETILASE study assessments.....	190

Chapter 7 Tables

Table 7.1a Baseline characteristics of study cohort.....	199
Table 7.2a Morphological profile of study cohort	200
Table 7.2b Morphological profile of cases cohort.....	200
Table 7.2c AMD Morphological profile of control cohort	200
Table 7.3 AREDS classification	202
Table 7.4a RETILASE: MEAN VA baseline, 6 and 12 months	207
Table 7.4b RETILASE: MEAN change of VA 6 and 12 months	207
Table 7.5a RETILASE: Mean Contrast Sensitivity baseline, 6 and 12 months	210
Table 7.5b RETILASE: Change in Contrast Sensitivity 6 and 12 months.....	210

Table 7.6a RETILASE: Microperimetry Analysis at 4 degrees, Baseline,6 and 12 months	214
Table 7.6b RETILASE: Change in microperimetry at 4 degrees at 6 and 12 months	214
Table 7.7a RETILASE: Microperimetry analysis at 12 degrees, baseline, 6 and 12 months	216
Table 7.7b RETILASE: Change in microperimetry at 12 degrees, 6 and 12 months	216
Table 7.8a RETILASE: Flicker perimetry analysis at baseline, 6 and 12 months	218
Table 7.8b RETILASE: change in Flicker perimetry.....	218
Table 7.9a RETILASE : Morphological change in druse at 6 months	220
Table 7.9b RETILASE: Morphological change in druse at 12 months	221

Chapter 8 Tables

Table 8.1 FAF classification of 2RT laser lesions	237
Table 8.2 RETILASE: Mean diameter of laser lesion on CFP	241
Table 8.3a RETILASE: change in MP1 at 4 degrees for laser lesions....	249
Table 8.3b RETILASE: change in MP1 at 12 degrees for laser lesions..	249
Table 8.4 Individual laser lesion MP1 defect.....	250
Table 8.5 Classification of Q switched nanosecond laser changes based on FAF findings	254
Table 8.6 FAF classification and implications	255

Chapter 9 Tables

Table 9.1 Clinical assessment of laser damage in varying laser time domains	266
Table 9.2 Laser protocols used in prior laser-drusen studies	269
Table 9.3 Summary of study design and outcome of laser-drusen studies ..	270

Chapter 1. Introduction

1.1 Introduction

The concept of the effects of radiation on vision has been described since Plato, when Socrates advised against direct gazing at solar eclipses. Later, Theophilus Bonetus described central vision loss from sun gazing in the early 17th century. However, it was Meyer Schwickerath who first published his findings of using natural sunlight to treat melanomas in 1949.(G., 1960) This method was of course limited by constraints of the weather, season and the long exposure time. In the 1950s, he then specified the development of the first xenon arc lamp by Carl Zeiss Laboratories, which produced radiation through passage of high intensity electricity through a xenon gas filled chamber. This method stimulated huge interest amongst ophthalmologists. He achieved effective treatment of melanomas, but also noticed the disappearance of surrounding vessels on the optic disc and other parts of peripheral retina even though the laser treatment site was remote. It was then that he suggested the use of photocoagulation using xenon arc to arrest retinal changes in proliferative diabetic retinopathy. (Meyer-Schwickerath, 1954)

Although effective, the xenon arc treatment was painful, long and caused numerous complications such as scarring, visual field defects (scotomas) and damage to other structures of the eye such as the cornea and lens.(L'Esperance, 1966a, L'Esperance, 1966b)

In the late 1950s, MASER (microwave amplification by stimulated emission of radiation) was developed by Townes at Bell Laboratories and a Russian team with Basov and Prokhorov who received the Nobel Prize in Physics for their work.(Gordon JP, 1954, Basov NG, 1954) Schawlow then proposed a similar effect using visible light, using ruby as laser medium.(AL., 1959) With this, in 1960, the era of lasers began. Theodore Maiman and workers produced the first working laser, a solid state ruby laser which was initially designed for range-finding for military purposes.(TH, 1960)

During the same period, some researchers were engaged in the study of the pathophysiology of diabetic retinopathy, which were consequent to the design of treatment algorithm of laser photocoagulation in this disease. Patz and Ashton were the first to describe the production of a particular 'factor x' that was vasoproliferative in nature and was produced during ischemia of the retina

which resulted in retinal neovascularization.(Ashton et al., 1954, Patz et al., 1953)

As such, early interventions of proliferative diabetic retinopathy consisted of full thickness laser burns which were designed to eliminate involving ischemic retina to prevent release of 'factor x'. Subsequently, it was thought that an ideal laser system would be one that could directly close off the blood vessels and the argon laser met this criteria.

In 1964, Bridges discovered the argon laser with emission in the blue (488nm) and green (514nm) spectrum and found these wavelengths to be strongly absorbed by hemoglobin and melanin with the possible potential of closing off blood vessels and vascular lesions.(L'Esperance, 1969) This was a misconception as some investigators subsequently showed that the main absorption site was the RPE, which was not dependent on the blue-green emission of the argon laser. Furthermore, 70% of emission of the argon laser was at 418nm which was found to be absorbed by macular pigment and caused unwanted side effects. (Marshall et al., 1975)

However, it was since then that lasers became the gold standard for treatment of numerous retinal diseases such as proliferative diabetic retinopathy, diabetic macular oedema, vein occlusions etc.

An advancement that preserved much more retina was conceived by Wolbarsht who postulated a model for the rationale of photocoagulation therapy for proliferative diabetic retinopathy. The model stated that destruction of photoreceptors by photocoagulation would decrease its oxygen demand and constrict retinal vessels, by restricting angiogenic factors.(Wolbarsht and Landers, 1980)

Much later, some investigators have found that laser therapy itself causes release of cytokines and other factors such as MMPs, transforming growth factor- β (TGF- β), pigment epithelial derived factor (PEDF) and angiostatin. These biochemical substances modulated the effects of laser.(Wolbarsht and Landers, 1980, Jennings et al., 1991, Caldwell et al., 2005, Sanchez et al., 2007, Matsumoto et al., 1994) Given that the RPE has the highest temperature rise during laser, it was postulated that a basis of laser therapy could be focal to RPE injury with the secondary release of the various cytokines, anti-angiogenic and growth factors.

Although effective for treatment of proliferative diabetic retinopathy and limiting the growth of peripheral neovascularization, lasers had not met with equal success in the treatment of macular diseases. Results from the ETDRS demonstrated that macular laser was only effective at preventing visual loss at 3 years in diffuse macular oedema, but had limited role in improving vision.(1985) A possible reason could be the limitation of treatment areas close to the fovea and the damage of the very cells (photoreceptors) the treatment was aimed to protect.

Anderson and Parrish coined the term 'selective photothermolysis' defined by the 'confinement of damage by brief laser pulses'.(Anderson and Parrish, 1983) Several investigators such as Birngruber et al in Germany and Marshall et al in London have carried out various experiments to define the optimal laser physical parameters that aimed to target selective RPE cells. Several laser parameters were examined which included wavelengths and time domain. With regards to wavelength of incident radiation of the laser, Mainster found that there was minimal impact of wavelength on RPE selectivity, except that impact of longer wavelengths extended further to into the choroid.(Mainster, 1986) In the 1980s, Sliney and Marshall suggested that pulse trains with high repetition rates could maximize therapeutic effect while minimizing collateral damage.(Sliney, 1992)

Q-switching, a technique first proposed in 1958 by Gordon Gould, and subsequently demonstrated independently in the 1960s by R.W. Hellwarth and F.J. McClung, used electrically switched Kerr cell shutters in a ruby laser to produce laser of light pulses with low pulse repetition rates, higher pulse energies, and longer pulse durations. (Taylor, 2000, McClung, 1962) Marshall investigated the mechanism of action of various Q switched and non Q-switched retinal lasers and evaluated the impact of such modalities on the retina. Publications in the last few decades on various animal models have shown that lasers in the Q-switched domain have limited collateral damage when compared to cw laser using various wavelengths.(Marshall et al., 1975, Marshall and Mellerio, 1968)

Earlier on, it was stated that lasers were a successful treatment modality for numerous retinal vascular diseases. During treatment of diabetic retinopathy, Gass had previously observed the disappearance of drusen post laser photocoagulation. Based on this observation, several investigators carried out clinical investigations on the use of laser prophylaxis in non-exudative or early AMD.(2003, 2006, Frennesson et al., 2009, Friberg et al., 2006) The mechanism of disappearance of drusen observed was unknown. However, although the studies did show significant decrease in drusen, the outcome of the studies did not prove satisfactory because they also showed an increase in rates of neovascularization and no improvements in visual outcomes.(2003, 2006, Frennesson et al., 2009) It was noted that the lasers used in these studies were in the milli to microsecond time domain and were in continuous wave mode. Further analysis found these neovascularization to be associated with higher laser intensity.(Kaiser et al., 2001) These results were not surprising given the knowledge of Stephen Ryan's earlier model of laser induced subretinal neovascularization.(Miller et al., 1990) In this model, it was indicated that the impact of laser on the RPE-BrM-choroid complex and the ability of RPE cells to proliferate to reconstitute its monolayer determined the resultant formation of subretinal neovascularization. Hence, based on these knowledge, it was reasonable to assume that the lasers used in the prior studies was of too high intensity and caused adjacent damage to surrounding structures such as breaks in BrM and subsequent neovascularization.

Age related macular degeneration is the leading cause of blindness amongst those aged 65 and above and causes 5% of total global blindness from data released by WHO in 2010.(Pascolini and Mariotti, 2012). In America, studies found that 3.8% of Americans between ages 50-59 have either intermediate or advanced form of the disease and this number escalates to 14% in the age range of 70-79. In the UK, by 2020, it was estimated that more than 650,000 people will have advanced AMD, which is 150,000 more than the current number. It has been further estimated that 44,000 new cases of wet AMD a year in the UK will require intravitreal anti-angiogenic agent therapy.(Owen et al., 2012) This problem will be even more prevalent as we face a global aging population. The WHO has estimated that the proportion of the world's population over 60 years will double to 22% by 2050, to more than 2 billion in

absolute numbers. (Subramanian, Ness et al 2009.; Global brief for World Health Day 2012 by WHO).

Visual impairment results in both undesirable personal and socioeconomic consequences. The costs of treatment, rehabilitation and hospital labor demands a significant economic contribution from the individual, government and society, both directly and indirectly. The global cost of visual impairment from direct health-care costs such as treatment was estimated to cost US \$255 billion and US \$89 billion indirectly. (Rein et al., 2006, Alliance for Aging Research, 2011) In the UK, the cost of AMD already accounts for 1% of the annual NHS budget (which was 96 billion pounds in 2013/14)

Clinically, AMD can be classified into early, intermediate or advanced (neovascular or geographic atrophy) under the International Classification. (Ferris et al., 2013) In this classification, the five year risk of progression to advanced AMD ranges from 0.5% in the ageing retina (early AMD) to 50% amongst the intermediate group. (Ferris et al., 2013) Currently, there are available treatment for neovascular stage of the disease in the form of anti-angiogenic agents, such as Bevacizumab (Avastin), Ranibizumab (Lucentis), aflibercept (Eylea). The therapeutic regime for wet AMD (using Ranibizumab) starts with 3 mandatory injections, and retreatment is dependent on evaluation of fluid resolution. (Brown et al., 2009, Brown et al., 2006, Subramanian et al., 2009, Regillo et al., 2008, Ophthalmologists., 2012) Studies have shown that the average number of Ranibizumab injections at 12 months was 5.6. In the UK, the NICE approved AMD treatment (Lucentis) costs 700 pounds per injection and this accounts for the exorbitant direct cost AMD therapy.

Currently, there is no treatment for dry or atrophic types of AMD and a paucity of prophylactic therapy for the ageing retina. Prevention is always better than cure. Understanding the etiologies of the ageing retina and its ageing transport systems would be key to developing a prophylactic therapy to delay or prevent AMD.

The metabolic oxidative requirements of the neural retina are one of the highest of all tissues in the body (Cohen and Noell, 1960, Ahmed et al., 1993, Winkler et al., 1983) The choroid contains numerous blood vessels with a high potential supply of oxygen and nutrients. Thus, there is a constant chain of supply of nutrients and substrates to the photoreceptor cells which have the highest concentration of mitochondria of any cells in the inner segment layer. This high

metabolic oxidative requirement increases the level of free radical releases from the electron transport chain in the cellular mitochondrial. (Skulachev, 1996, Korshunov et al., 1997) Studies previously demonstrated the daily shedding of lipid rich membranous disc from the distal end of the outer segments of photoreceptor cells, consisting of free radical damage. This allows the removal of damaged membranous waste products to the RPE cells, for final removal through the choroidal blood stream. At the proximal end, new discs are synthesized(Bok, 1985, Young, 1976). Henceforth, an intact transport system is crucial to maintain the nutritional status and waste removal for maintenance of the RPE. Over the last two decades, experiments conducted by Marshall and Hussain have demonstrated BrM as the rate limiting location of decline in the transport system and shown the age-related decrease in transport functions.(Hillenkamp et al., 2004, Hussain et al., 2002, Hussain et al., 2010c, Moore et al., 1995a) In addition, the same team had demonstrated the involvement of the metalloproteinase pathway in the maintenance of transport across the BrM.(Kumar et al., 2010, Ahir et al., 2002, Hussain et al., 2011) Hence, clinical observations by Gass with regards to laser and decreased drusen load become more intriguing. One possible postulation could be the effect of laser on causing RPE injury with subsequent RPE proliferation which causes release of MMPs that cleans the BrM.

In the following, these background knowledge on the development of retinal lasers in recent years as well as the transport mechanism of the outer retina and the physiological changes in ageing in the outer retina would be discussed. The background to the nanosecond laser, termed 2RT laser, would be elaborated.

1.2 Lasers for Retinal Therapy

The early history and development of retinal lasers have been discussed. The following details the literature on the mechanism of laser damage and the profile of laser damage on the retina from lasers in different time domain.

1.2.1 Mechanism of Retinal Lasers Damage

Retinal photocoagulation was and is still the widely accepted clinical therapy for numerous ocular conditions such as proliferative diabetic retinopathy, diabetic macular oedema (DMO), central serous retinopathy (CSR).

The mechanism of retinal lasers damage involves tissue destruction from forces generated by thermal degradation of incident energy absorbed by the target tissue. (Marshall, 1970) The amount of energy absorbed by the target tissue was thought to be dependent on the wavelength of incident radiation and absorption characteristics of irradiated tissue. The extent of tissue destruction is related to 1. degree of exposure energy; 2. area of irradiation (laser spot size); and 3. duration of exposure.

The fundamental changes in the laser mechanism of action are in accordance with the laser time domain. The biological effects of laser are the result of one or a combination of several mechanisms such as photochemical, thermal, thermo-mechanical, which with the exception of photochemical effects are virtually independent of wavelength. In the millisecond domain, thermal damage is the predominating mechanism. Depending on spot size, energy and pulse duration, damage initiated in the RPE may be conducted to adjacent tissue. By contrast, several authors have shown that pulse in the nano to microsecond domain resulted in heat absorption by melanosomes, causing microcavitation and mechanical disruption of the RPE. (Kelly and Lin 1997; Lin et al.

1999;Brinkmann et al. 2000;Roegener et al. 2004; Schuele et al. 2005; Lee et al. 2007). Subnanoseconds and picoseconds exposures may result in optical breakdown and plasma formation or ionization (Cain et al. 2005; Roach et al. 2004;(Edsall, 1997)

Current lasers are continuous wave with pulse domains in millisecond to 0.1 second regime. They result in thermal denaturation of adjacent retinal layers and distance of its internal spread is time-dependent.(Table 1.1) The neuroretinal impacts of conventional and current lasers in millisecond time domain have been widely investigated.(Bowbyes et al., 1973, Marshall et al.,

1975, Wolbarsht et al., 1965, Zweng et al., 1967, Muqit et al., 2010a, Borland et al., 1978) Numerous researchers concur with the theory that RPE is the primary layer responsible for absorption in laser light. RPE contain melanosomes which absorbs up to 50% of the incident laser energy. This results in RPE cell death and subsequent migration and cell division with consequent release of cytokines, anti-angiogenic factors and matrix metalloproteinase (MMPs).(Ahir et al., 2002, Chidlow et al., 2013)

In the 1980s, Birnruiger studied the effects of various wavelengths and found that there were minimal differential effects caused by different wavelengths, except that longer wavelengths was penetrated deeper. In the same study, he found an inverse relationship between length of damage and laser pulse duration.(Table 1.1) Improvements in laser technology from long to shorter time domains saw significant benefits in reducing the length of damage through the inner retina.

With regards to area of irradiation, image spot size was found to be interdependent on pulse duration and functions differently at milliseconds and nanoseconds time domain. For example, in the millisecond time domain, thermal damage was found to be highly dependent on retinal image size. (Lund et al. 2007; Schulmeister et al. 2008a) (Figure 1.1) In the millisecond domain, the smaller image size would result in greater radial cooling effects and a smaller increase in peak energy. In contrast, pulses in the sub nanoseconds domain was found to have limited therapeutic index due to the very high peak energy from these exposures which must be overcome by large spot sizes to maximize heat flow and prevent outer retinal hemorrhages.(DH., 1988)

Multiple pulsing can reduce the overall temperature increases in the RPE and limit the extent of damage from thermal diffusion. For example, single pulses of millisecond duration will lead to high temperature increase which will cause neuroretinal effects and disruptive effects such as choroidal bleeding whilst multiple pulses which reduces peak temperatures through the theory of additive effects of thermal energy will therefore cause a reduction in peak temperatures and greater selectivity of organelles and/or anatomical layer as target.(Sloney, 1999) The Arrhenius equation can be used to predict additivity for pulses in the thermal damage mechanism pulse duration. (Lukashev et al. 1996; Schulmeister 2007). In accordance to Arrhenius model, there is a proportional rate of increase in thermal damage to tissue with increasing temperature. Based on

extensive retinal injury studies conducted to derive safe exposure limits, the limited additivity of thermal coagulation from pulse and inter-pulse rest periods allows accumulation of thermal energy without subsequent effects of thermal mechanical disruption of adjacent tissues such as the inner retina. This thermally additive exposure had been described mathematically as number of pulses N raised to $-1/4$ power ($N^{-1/4}$). This empirical formulation means that the threshold energy per pulse will only be 10% of single pulsed threshold when $N=10,000$ pulses. This additivity is dependent on thermal confinement and thermal relaxation time, which is in turn dependent on the absorption molecule and tissue (melanin and RPE). Brinkmann et al have determined the thermal confinement period of melanin and RPE to be 0.5 to 1.0 μ s and 20 to 25 μ s respectively.(Brinkmann, 2005) (Neumann and Brinkmann 2005)

Another form of pulsed mode systems is the Q switched technology. Q switched systems are used in ophthalmology for its high peak energy to cause photo-disruptive effects. Examples of its use include Yag capsulotomy where there is no biological heat absorber and the capsular damage is a function of the transmitting laser parameters only. At the level of the retina, the resultant damage is dependent upon the laser transmission and the biological absorption, which in this case, is mainly the melanin in the RPE. Marshall first described the differences in various plausible mechanisms of laser photocoagulation in 1970 by comparing Q-switched and non Q-switched lasers in various short pulsed domains in Dutch rabbits. In Q switched lasers, the mean output power is much higher than a cw laser such that RPE cells undergo complete degeneration in the center of the laser lesion, whilst at RPE cells at the periphery undergo 'blast' forces from the micro-explosions generated in the center. This resulted in the pigment granules and cytoplasm disintegrating and breaking away from the cellular boundaries. The explosive nature of the center of laser lesion resulted in subretinal hemorrhage. (Marshall 1968 experimental eye research)(Figure 1.2)

This effect can be reduced with increasing the diameter of the laser beam, by diffusing the laser energy.(Marshall, 1970)

Hence, it can be concluded that conventional and current laser in the millisecond time domain results in a degree of neuroretinal damage. The shorter time duration in micro-nanoseconds transits from thermal to mainly mechanical mechanism of action with improved selective damage of the RPE layer. Flat mount histology compared the limited impact on RPE cells using Q switched

lasers as compared to non Qswitched lasers in single and multipulsed modes. (Marshall, 1970) Roider and group have also demonstrated with invitro experiments the limitation of damage using ultrashort pulses.(Roider et al. 1993; Brinkmann et al. 2000; Roegener et al. 2004).

Even until now, the lasers used in clinical scenarios are in the cw mode and in the millisecond or microsecond time domain. Although effective in treatment vascular disease, it causes thermal diffusion damage to the surrounding layer. 2RT laser is the first doubled-frequency Nd:YAG laser in the nanosecond time domain using a Q switched system, with a large spot size which is postulated to have limited effects to within the RPE.

Table 1.1 Pulse duration and thermal diffusion distance, by Birngruber, Roider and team

Pulse Duration	Thermal Diffusion Distance / μm
1 second	1000
0.5 seconds	707
100msec	320
50msec	225
10msec	100
1msec	32
100 μsec	10
10 μsec	3.2
1 μsec	1
1nanosec	0.5

Figure 1.1 Laser energy distribution in spot sizes in millisecond duration

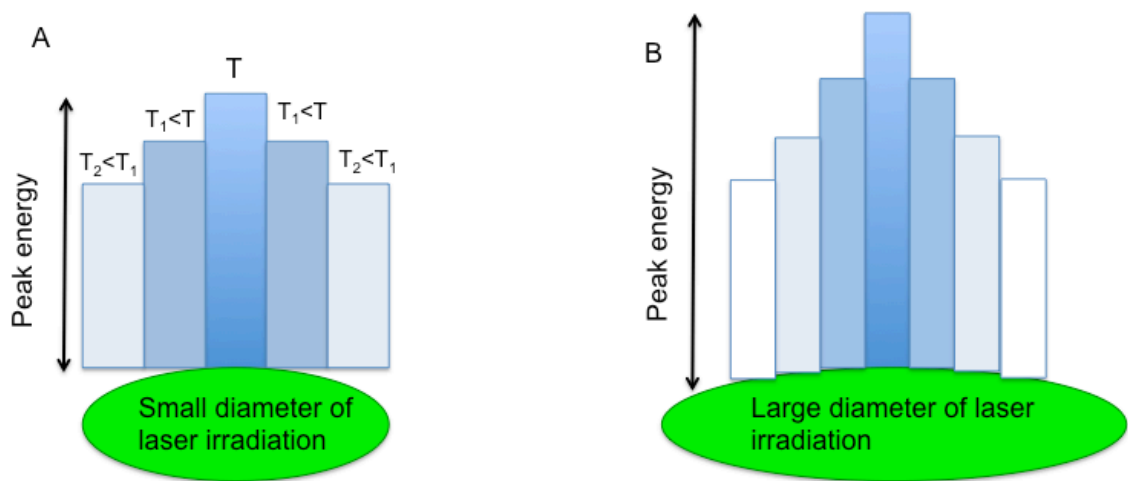


Figure 1.1 is a pictorial representation explaining the effect of laser irradiation size (retinal laser spot) on peak energy. A, represents the peak energy effect of small laser spot size whilst B represents effect from large laser spot size. In A, the smaller spot size allows cooling effect to reach the center of laser spot quickly and hence, a lower peak energy. In B, retinal irradiance profile is too large for any consequential cooling effect to effectively reach the center of the irradiated spot during pulse exposure. This results in a high effective peak energy. Hence, the smaller the spot, the shorter the time to reach its center and faster cooling effect and lower peak energy or exposure limit.

Adapted from Schulmeister, Theory of the basis of radial cooling

Figure 1.2a, 1.2b RPE damage using a non Q switched and Q switched laser

Figure 1.1a

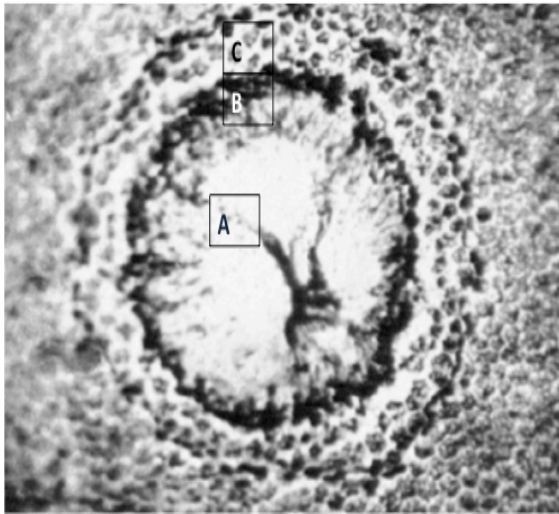


Figure 1.1b

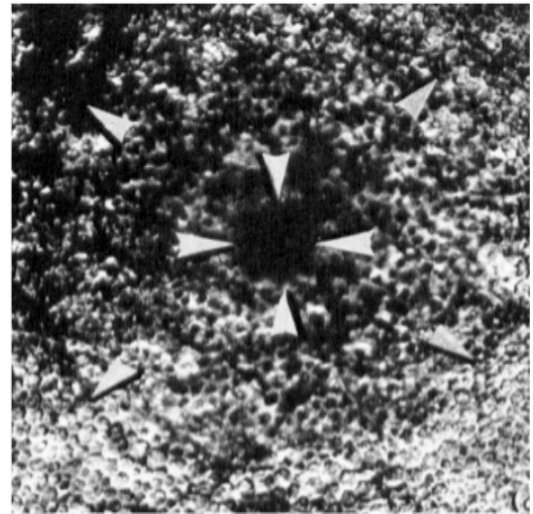


Figure 1.2a shows the zones of laser damage on the RPE using a non Q switched laser. Note the 3 zones of laser damage; Central zone (A) with destroyed pigment epithelial cells the size of incident beam; Peripheral zone B with a ring of pigments, from the radial streaming of pigmentation from the central zone and zone (C) demonstrates an area of reduced pigmentation from further outward displacement of pigment granules.

Figure 1.2b shows zones of RPE damage from Q switched laser. The inner arrows show complete void of RPE cells from microexplosions of individual RPE cells from the high energy and a peripheral zone of 'blast' effects from the center of the lesion.

Pictures are taken from Marshall. 1970.

Figure 1.3 Pictorial demonstration of mechanism of laser damage in different time domain

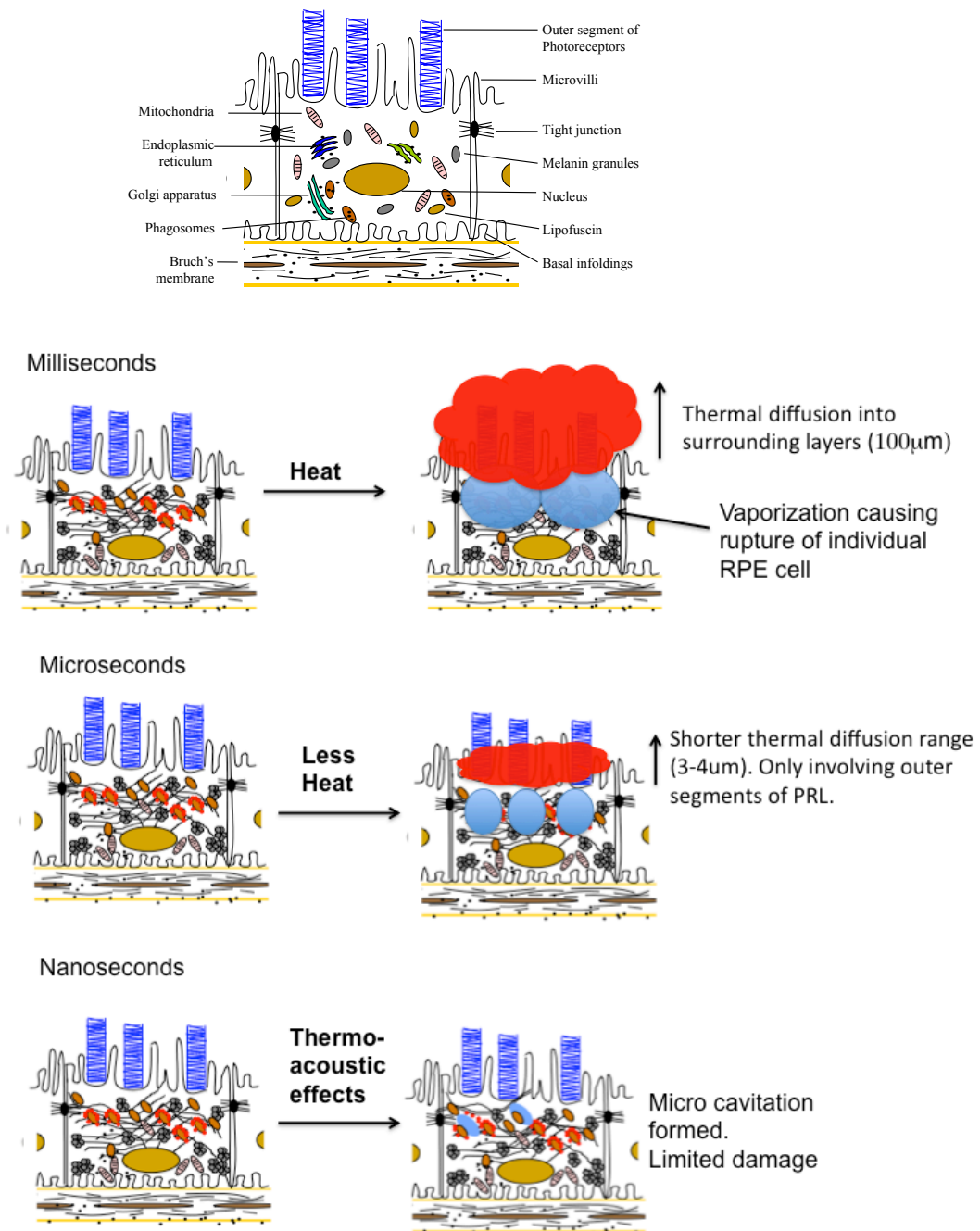


Figure 1.3 is a pictorial demonstration of mechanism and length of damage in varying time domains. The millisecond time domain shows heat absorption in thermal mechanism of action, with resulting vaporization and 'micro explosion' of individual RPE cells. This results in thermal diffusion distance in the range of 100 μ m. In the microsecond time domain, there is less heat energy absorption with a shorter thermal diffusion distance of 3-4 μ m. Still, the tips of outer segment of PRL are affected. In the nanosecond time domain, energy absorption results in microbubble formation and damage to surrounding organelles, with micro cavitation and death of discrete RPE cell. This results in limitation of damage to RPE layer.

1.2.2 Concept of Primary and Secondary Laser Damage

It was established earlier that the ideal retinal laser would be one that is between 400 to 600 μm wavelength, with a short time domain, sufficiently low energy, multipulsed and with an adequately large spot size. The reason for this is to prevent primary damage which is defined by the laser-tissue interaction at the level of the RPE, photoreceptor cells and beyond. This happens acutely to within 48 hours post laser.

Less is known of the secondary induced damage by laser. This is a much-neglected concept, which holds importance for long term prognosis for visual function. Secondary laser damage is defined by the apoptosis of photoreceptor outer segments from the lack of support mechanism resulting in a dysfunctional transport to and from the photoreceptor cells. The reason for this is because the time period for a physiological disc renewal and shedding is 48 hours, however, with the current size of laser beam used clinically (ie, 100 to 200 μm), the time period for RPE wound healing takes approximately 7 days. Hence, the imbalance resulting from time taken to re-establish RPE layer and facilitating the metabolic needs for photoreceptor cells, in theory, will cause secondary damage to photoreceptor cells. In contrast to primary damage, this secondary effect takes days to occur. (Figure 1.4)

Figure 1.4 Illustration of primary and secondary laser damage in the retina

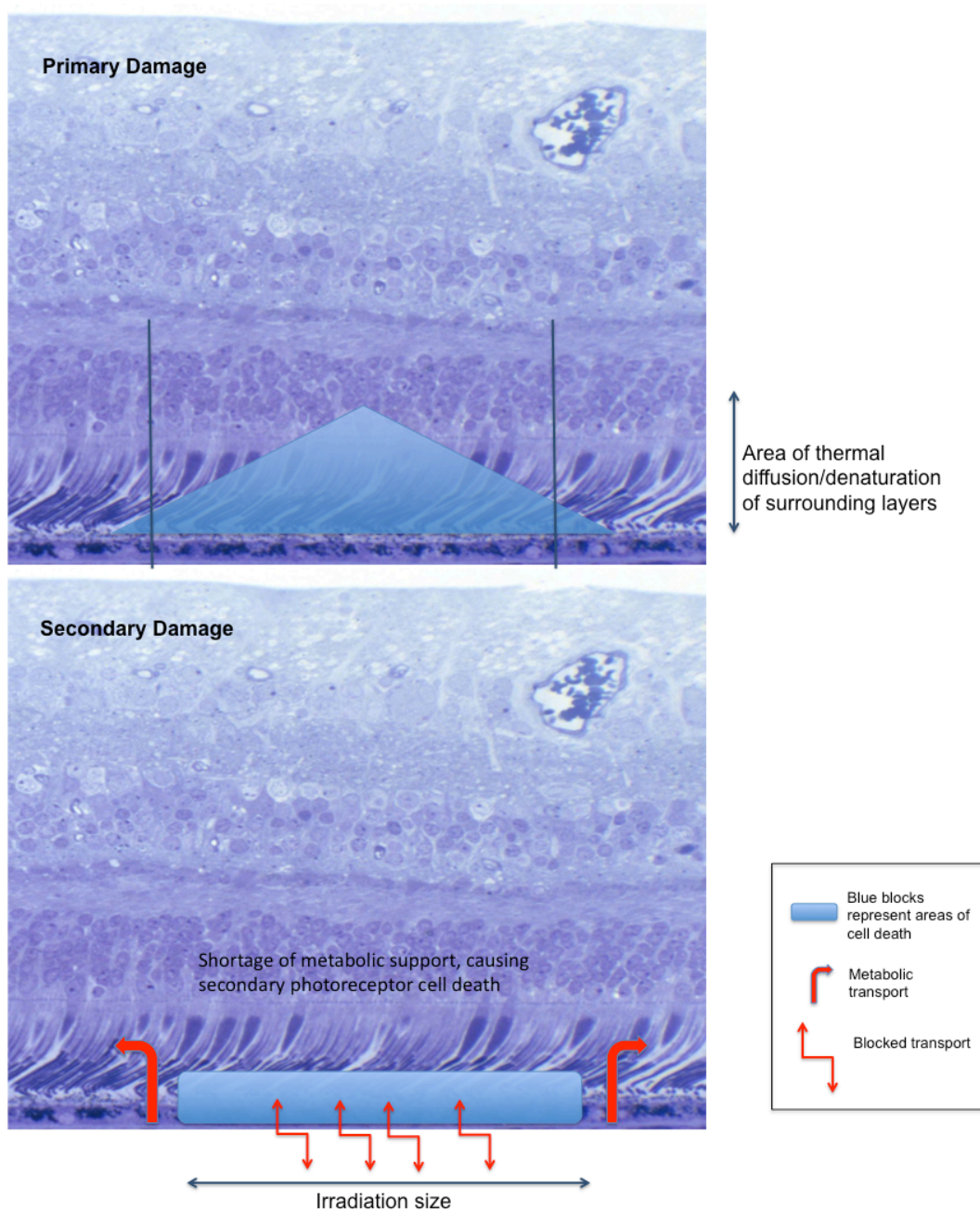


Figure 1.4 illustrates the concept of primary and secondary laser damage in the retina. Primary damage is defined by the acute phase of laser-tissue interaction, with consequential damage to the surrounding layers. Secondary damage is defined by death of photoreceptor cells from the lack of support mechanism such as the RPE and hence, dysfunctional transport mechanism.

1.2.3 Underlying Concepts of the 2RT Laser

Fundamentally, one of the aims of modern lasers would be to allow the use of laser in the fovea avascular zone, without harmful effects to the neural layer. The edge of the fovea avascular zone was defined as a limit to current and conventional lasers due to the extensive laser damage described earlier. (Muqit et al., 2010a, Bowbyes et al., 1973, Marshall et al., 1975) This limited the use of laser in the treatment of macular diseases. The concepts of primary and secondary damage has been described. The following describes the underlying concepts in the design of a nanosecond, speckled beam laser, which was aimed at circumventing primary and secondary damage of retinal lasers. With the speckled beam configuration, this laser was hypothesized to cause disparate groups of RPE cell death in a 400 μ m spot size. With this, there would be islands of preservation of RPE cells and timely reconstitution of the single RPE layer. This would hence prevent secondary apoptosis of photoreceptor cells. In addition, with the larger areas available for RPE migration, there should be in effect a higher release of cytokines and immune-modulatory factors released from RPE migration.

The 2RT laser functions in a single 3 nanosecond pulse laser. The ultrashort pulse duration in the nanosecond time domain would in theory limit the length of damage. Nanosecond lasers was shown in animal models to have a smaller therapeutic range than the longer time domains.(Framme et al., 2002) This decrease in therapeutic range have a risk of causing secondary subretinal bleeds. This therapeutic range may be increased by first, repetitive pulsing and second, increasing the laser spot size (as in the 2RT laser). Fully knowing that an enlarged spot size will be subject to secondary damage as mentioned above, the indication of the current laser design was meant to address this problem.

Figure 1.5 shows the mechanism of laser damage in the different time domain as compared to the 2RT laser.

Preliminarily, this laser was used by Pelusconi et al in treatment of diffuse diabetic macular oedema and found to have less functional defects on the retina as compared to conventional laser. Guymer and team in Australia performed a small pilot study with the use of the 2RT to treat early AMD. Unfortunately, the team have mis-concocted a treatment algorithm with 12 laser lesions and

average laser energy of 0.3mJ, which resulted in minimal improvements using flicker perimetry but otherwise no visual acuity changes. (ARVO abstract 2012) Thus far, there is no proper assessment of this unique laser as a modality to prevent AMD.

Figure 1.5 Schematic diagrams of the effects on the retina and Bruch's membrane caused by a) a millisecond laser, b) a microsecond laser and c) a nanosecond laser.

Figure 1.5a. 10msec laser

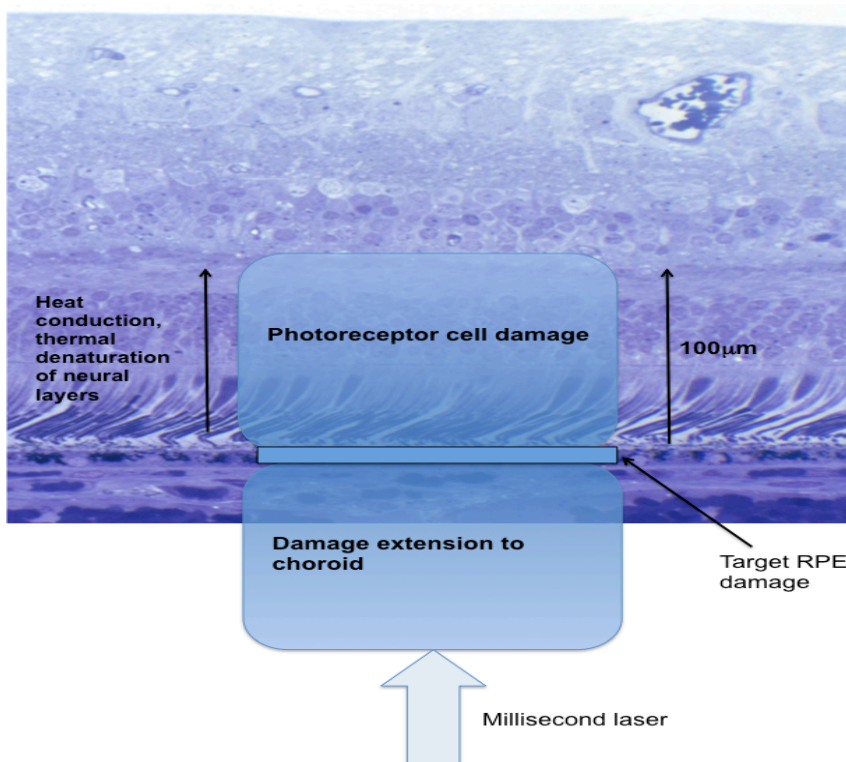


Figure 1.5a The 10msec laser.
Mechanism of Action: Diffusion of thermal denaturation to the photoreceptor cells and inner retina. Secondary damage results from the impeded transport system across the RPE cell layer resulting in apoptosis of the photoreceptor cells.

Figure 1.5b Microsecond laser

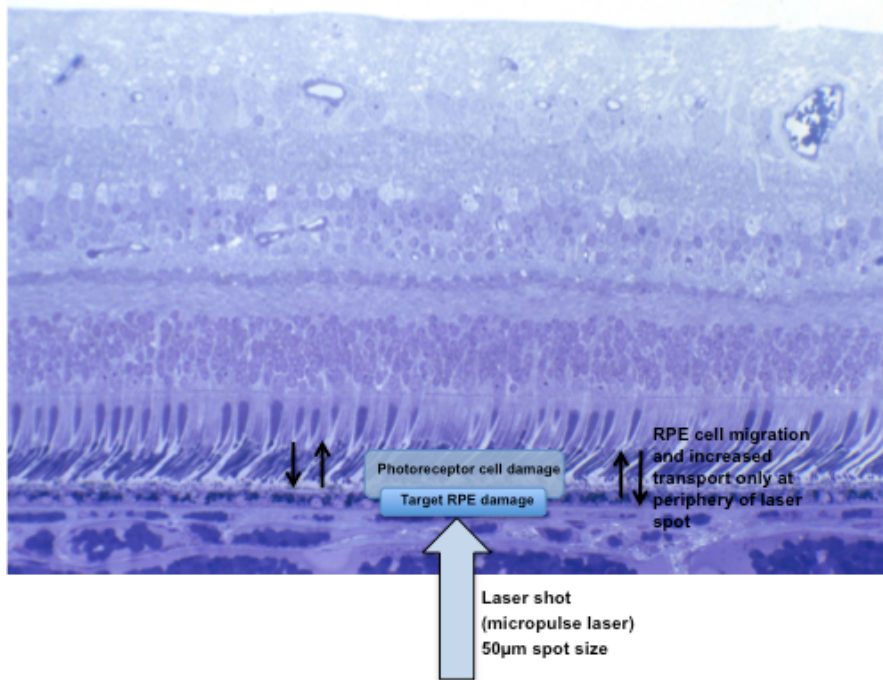


Figure 1.5b: The microsecond laser.

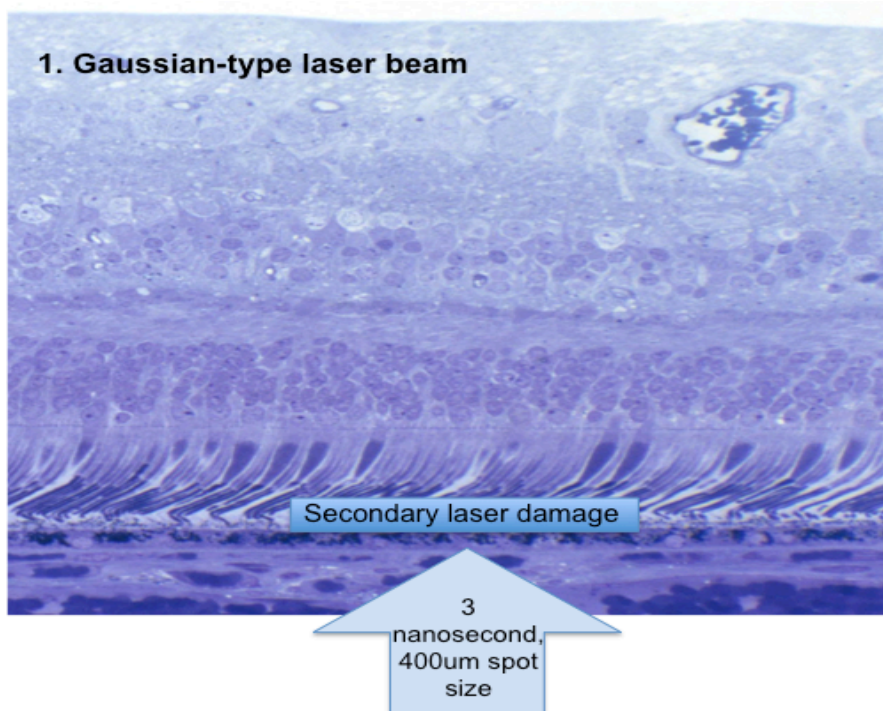
Mechanism of action:

Primary damage: photoreceptor cell damage reduced, however, the tips of the outer segments are still prone to secondary damage.

Secondary damage: Impedes transport mechanism across RPE-Bruch's membrane complex, resulting in less nutrient availability for photoreceptor cells.

Thermal diffusion distance of approximately 10µm.

Figure 1.5c. Nano-second laser



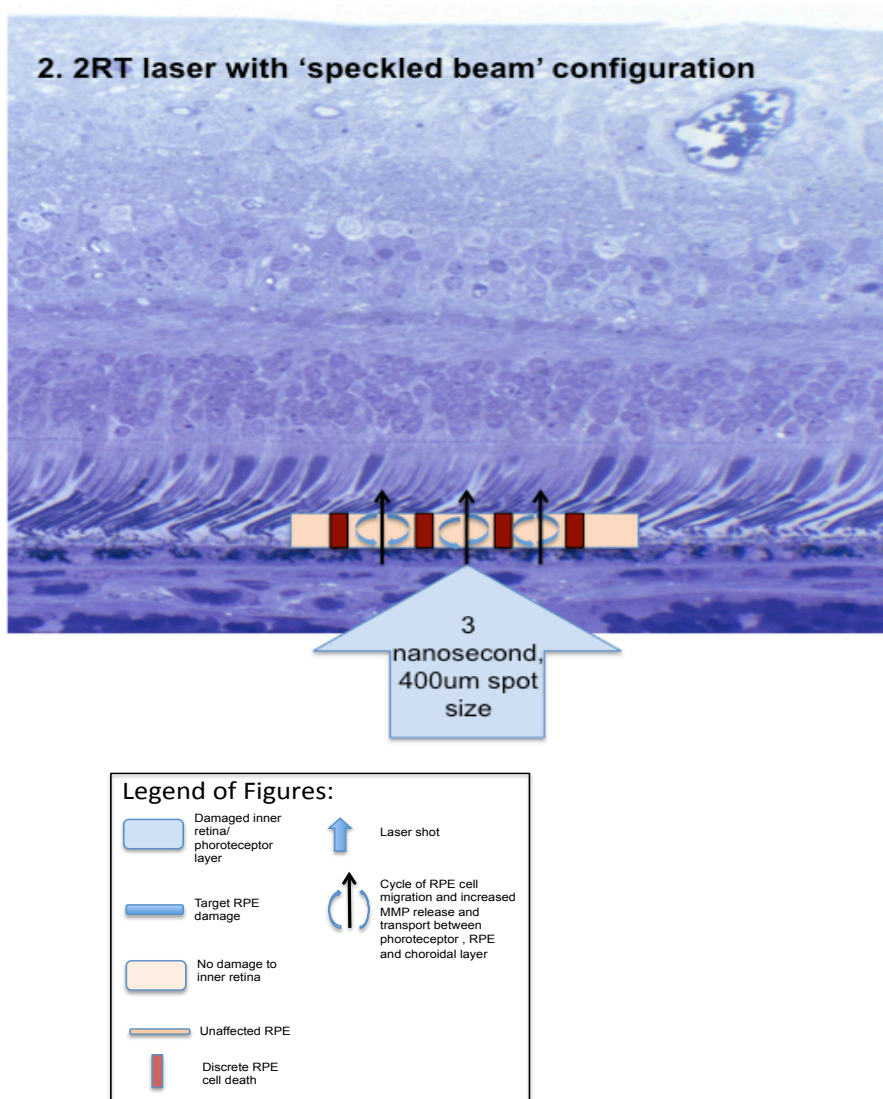


Figure 1.5c: The nanosecond laser

In the pictorial diagram of the nanosecond laser (1), the Gaussian beam type nanosecond laser shows secondary damage from a large area of irradiation. In (2), the 2RT laser has a 'speckled beam configuration' of which there are discontinuous areas of RPE cell death and migration that occur in each 400µm spot size, ensuring continuous and maximal improvement of transport mechanism across the retina.

Mechanism of action: 2RT is a nanosecond pulsed laser, which uses very low energy levels to produce a limited effect that selectively targets melanosomes within the retinal pigment epithelium cells. It is the first laser that employs the technology of diffusion of the laser beam. This novel therapy means that only 25% of the laser energy reaches the RPE in a grid pattern within the 400µm beam. This laser energy absorption by melanosomes within RPE cells causes microbubbles and cavitations to form, damaging a percentage of RPE cells within the laser spots without rupture of the cell membranes.

1.3 Anatomy of the outer retina

1.3.1 Retina

As mentioned above, the balance between nutrient transport and waste removal is of utmost importance in maintaining the health of the photoreceptor cells. In the following, basic background knowledge of the transport system across the inner and outer retina would be reviewed. The following is a brief description of the anatomy of the retina, with particular focus to the outer retina.

The retina is the innermost layer of the eye and is important for the conversion of information from the external environment as neural impulses to the brain for intricate analysis. There are two layers of the retina, the inner neurosensory layer and the outer retina, consisting of the RPE which is bound on its posterior surface by the BrM and choroid.

The following gives a brief description of the important topographical regions of the anatomy of the retina (Figure 1.6)

The posterior pole: A 5 to 6mm diameter circular zone of retina between the arcades of the temporal retinal arteries which is shown in histology to have highest concentrations of cones and has more than single layer of ganglion cell bodies.

The macula lutea: known in latin as the 'yellow spot'. 1.5mm diameter area in the posterior pole, approximately 1.5 disc diameter lateral to the optic disc. Consists of high concentration of xanthophyll carotenoid pigments (zeaxanthin and lutein) which acts as a filter for protection against ultra-violet irradiation.

The fovea: 0.35mm diameter area of depression in the macular consisting only of cones where the cones are concentrated at maximum density.

The peripheral retina: remaining of the retina outside posterior pole to the ora serrate. Rich in rods and has only one layer of ganglion cell bodies.

Ora serrate: Transitional zone where the neuroretina is continuous with nonpigmented epithelial cells of pars plana.

Figure 1.6 Pictorial diagram of the anatomy of the retina

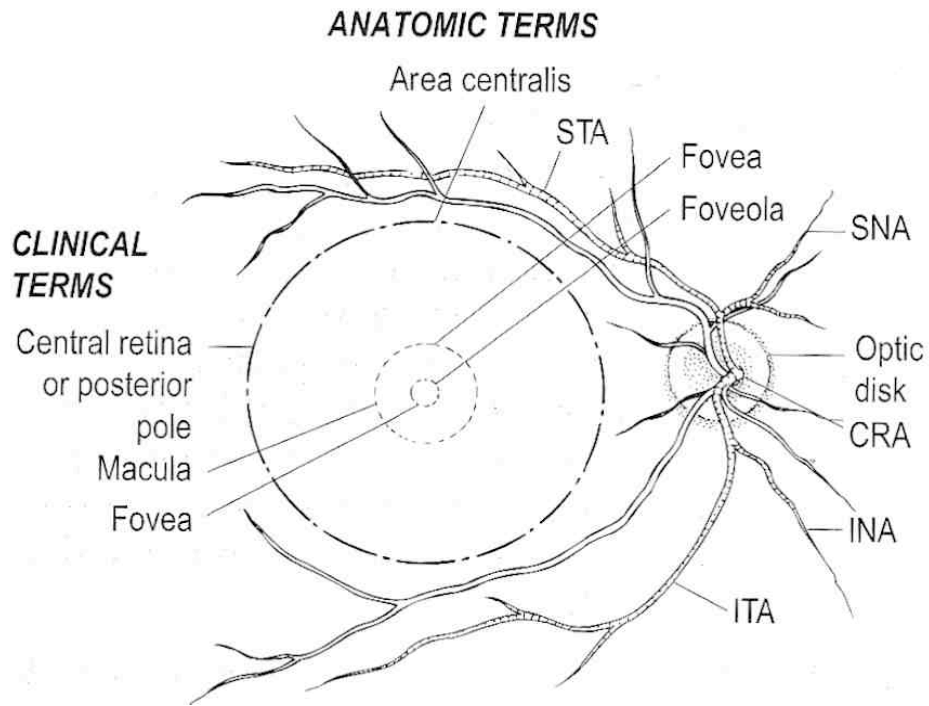


Figure 1.6 is a pictorial representation of the anatomy of the retina, adapted from Forrester's, *The Eye, Basic science in practice*, Third edition

1.3.1.1 Neurosensory Retina

The neurosensory retina is a 300µm thick matrix of neural tissue. Very importantly, the three main layers that are involved in the transduction, transmission and conduction of impulses from light are the photoreceptor cells, bipolar cells and ganglion cells whose activity are modulated by the horizontal cells and amacrine cells respectively. (Figure 1.7)

Figure 1.7 Diagram of anatomy of neural retina

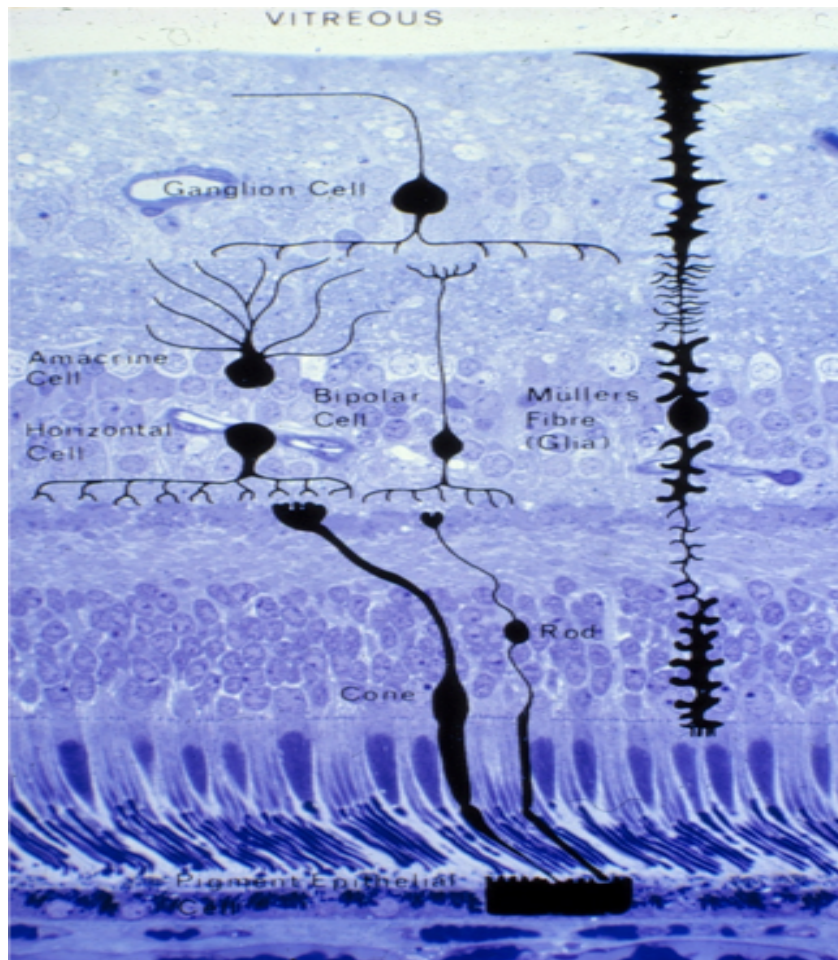


Figure 1.7 is a diagrammatic representation of the anatomy involved in the neurosensory retina in terms of transduction, transmission and conduction pathways of light impulses to electrical signals to the brain.

1.3.1.2 The Photoreceptor Layer

There are 2 types of cells in the photoreceptor layer (rods and cones). There are approximately 115million rods and 6.5 million cones in the human eye. Rods are responsible for contrast, bright and motion whilst cones co-ordinate color vision, spatial resolution and fine visual resolution. Rods dominate the peripheral retina, whilst cones are mostly concentrated in the macular, and the fovea is exclusively cones.

Each rod and cone is a long and narrow cell with an inner and outer segment joined by a modified cilium. These inner and outer segments are connected to the cell body by the outer limiting membrane which then passes into the outer nuclear layer of the retina and axons pass into the outer plexiform layer to form synapses with bipolar and horizontal cells. The inner and outer segments contain visual pigments which aid in the photochemical transduction of light into neuronal impulses.

As mentioned, photoreceptor cells (rods and cones) of the vertebrate retina are highly specialized cells which responds to the stimulus of light, and relays this response to surrounding neurons as optical input to the brain. To facilitate its function, photoreceptor cells undergoes series of metabolic activities to maintain necessary visual components, regeneration and waste removal.

Early autoradiographic studies demonstrated similar pathways of photoreceptor metabolism in rats, frogs, rhesus monkey. Light-sensitive outer segment of the retinal rods consists of a stack of a thousand densely packed discs, each with a double layer of infolded plasma membrane . Bok and Young have traced the pathways from protein synthesis, which includes the visual pigment rhodopsin, in inner segment of cell through transfer through the cilium to base of the outer segment where the protein are then incorporated into newly formed membranous disc. This addition of new membranous discs at the base of a photoreceptor cell outer segment requires the synchronized removal of old disc through phagocytosis of RPE cells.(Young and Bok, 1969) The rate of rod renewal varies between species and location within the retina; with rats having a range of 8 to 14 days for complete turnover and rhesus monkey with a range of 9 to 13 days.(Bok, 1970) (Figure 1.8)

Figure 1.8 Pictorial demonstration of rod outer segment renewal

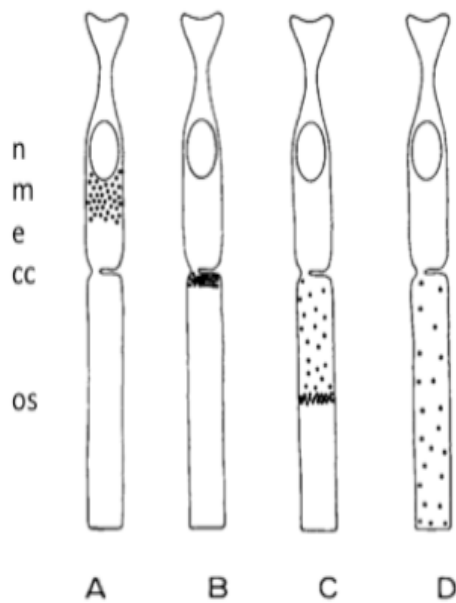


Diagram from Young and Bok 1969.

Renewal of rod outer segments as revealed by radioautography after injection of radioactive amino acids. The location of radioactive protein is indicated by black dots. OS: outer segment; cc: connecting cilium; e: ellipsoid; m: myoid; n: nucleus.

A- Minutes after injection, radioactive protein is concentrated in the myoid portion of the inner segment, the major site of protein synthesis.

B- Hours later, newly formed protein aggregates at the base of the outer segment, the site of membrane assembly.

C- The heavily labeled membranous discs are gradually displaced by the repeated formation of newer discs at the base of the outer segment. These new discs are weakly labeled, due to the continued presence of low levels of labeled precursor in the tissue fluids.

D- The moving band of intense radioactivity disappears when it reaches the apex of the cell.

Ambient temperature and light variation in the microenvironment of photoreceptor cells also increases rate of renewal and formation of outer segment disc. (Bok 1967 J of sci biology)

Dysfunctional RPE has been hypothesized to be the cause of some retinal dystrophic diseases. Experiments on RCS rats have demonstrated the involvement of poor phagocytosis of outer segments by RPE to be causative factor for eventual photoreceptor demise (Herron et al., 1969). Kroll and Machemer first demonstrated that photoreceptor metabolic functions decline very rapidly from retinal detachment. (Kroll and Machemer, 1969) In vitro amphibian culture also showed that rod renewal becomes dysfunctional within 2 days of retinal detachment. (Hale et al., 1991) Hence, from the knowledge obtained from early experiments, it may indirectly be concluded that the area of RPE death induced by laser may induce a 'dystrophic-like' microenvironment where photoreceptor renewal rate is stagnated from the lack of nutrition from regenerated visual pigments and the buildup of old disc, which inhibits the metabolic removal of waste from the choriocapillaries.

The work done previously provided an understanding to the impact of laser on secondary damage as defined earlier. In simple terms, the larger the laser spot size, the larger the area denuded of RPE and the longer it would take to re-

establish complete RPE cell layer, which may hinder the reparative period for photoreceptors and result in secondary apoptosis and long term damage.

1.3.1.3 Retinal Pigment Epithelium

The RPE is a single cuboidal layer of epithelial cells lining the BrM with its apical microvilli interdigitating with the outer segments of the photoreceptor cells. RPE vary in size and shape and is dependent on age and location. By and large, RPE cells closer to the center of the retina or the macular are 14 μ m in height and 10 μ m in lateral dimension, whilst in the periphery, the cells are 14 μ m in height and up to 60 μ m laterally. The total number of RPE cells per human eye ranges from 4.2 to 6.1 million with more cell loss in older eyes. The RPE has low regenerative potential and in the event of injury, reacts by hyperplasia of adjacent cells.

The main functions of the RPE are as per follow:

1. to assist in directional nutritional and waste transport between the choroidal and neuronal layer;
2. to facilitate visual pigment through cis-trans formation of retinoid and to act as a reservoir to store retinoids.
3. eliminating fluid from subretinal space.

It is crucial to understand the repair mechanism of the RPE and photoreceptors, especially post injury or induced injury from laser. RPE plays a crucial role in the exchange of materials from the photoreceptors to choroidal capillaries. This one cell layer structure is strategically located between the photoreceptors and choroidal layers and forms one of the blood-retina barriers with its tight junction between cells. Autoradiography studies from Bok and Young in the 1960s have demonstrated the direct participation of the RPE in outer segment disc removal processes in frogs. RPE was found to be involved in the metabolic process of vitamin A, which is an important light-detecting pigment located in the outer segments of photoreceptor cells. Vitamin A from old outer segment disc entering the RPE was released through isomerization into its useful form back to photoreceptor cells. The RPE also synthesizes and secretes components of the mucopolysaccharide materials lying between spaces of outer segments. (Young, 1976, Bok, 1970, Young and Bok, 1970) Hence, the RPE plays a crucial role in

maintaining the health of photoreceptor cells.

It is an established fact that RPE do have limited regenerative and repair capabilities.(Al-Hussaini et al., 2008, Wallow and Tso, 1973b) Histological studies have demonstrated initial necrosis of RPE, budding of individual RPE cells and multilayered RPE formation in laser lesion within 7 days after conventional continuous wave argon laser application.(Smiddy et al., 1986, Wallow, 1984) In vitro experiments demonstrated the capacity of RPE to migrate following laser therapy. Local RPE lesions were also found to induce a global RPE cell division, with repaired tissue having pronounced reduced pigmentation.(Al-Hussaini et al., 2008) Time course of repair for ARPE 19 cell culture with applied laser of 300mW power 200 μ m spot size, 0.1s duration was found to complete in 7 days. In the same study, the authors attributed repair of laser lesion to involve both cell migration and proliferation, with changes not limited to the lesions. Changes were found in expression of genes involved in regulation of cell proliferation, migration and tissue repair and induction of alarmin IL33 and heat shock protein HSPA6.(Tababat-Khani et al., 2013)

1.3.1.4 Bruch's Membrane

The BrM is an acellular connective tissue layer whose thickness is 2-4 μ m, but this increases with age and pathology. The BrM is a pentalamina layer which consists of 5 layers: the RPE basal lamina; the inner collagenous zone; a middle elastic layer with perforations; an outer collagenous zone and the basement membrane of the endothelial cells in the choriocapillaries.

Given an understanding of the anatomy of the retina and in particular the outer retina, the following will focus on the integration of these anatomical structures in relation to the transport functions of the outer retina.

1.3.2 Transport Mechanism of the Outer Retina

Nutrient transport across Bruch's membrane and RPE

Branches of the central retinal artery supply the inner human retina whilst the capillaries of the choroidal circulation supply the outer retina. It was shown that the latter accounts for most of the metabolic needs of photoreceptor cells. (A, 1970, Wilson et al., 1973, Alm and Bill, 1973)

The ease of transport across the BrM and RPE is dependent upon a particular molecule's size, charge, hydrophobic/hydrophilic nature. (Figure 1.9, 1.10) . The BrM is the first barrier down the transport system. By default, the BrM is an acellular pentalaminated extracellular matrix (ECM) and can only allow passive transport as per Fick's law of diffusion. However, its collagenous and fibrillar layout renders it a 'sieve-like' configuration, giving it apparent 'pore' size distributions in discrete layers of the membrane. (Marshall J, 1988) The 'pore' theory of fluid transport and diffusion was further supported by ultra structural studies and transport studies using various sized fluorescein isothiocyanate (FITC) labeled dextrans, which demonstrated the presence of different 'pore sizes', with the inner collagenous layer containing the smaller pores and hence, the rate limiting structure. A size exclusion limit was obtained from experimental studies by Starita et al (Starita et al., 1997), which explained the effect of size of molecules traversing the BrM to the neural retina.

Having passed through the BrM, the molecule would traverse the monolayer RPE. The convoluted basolateral aspect of the RPE is in direct contact with BrM, minimizing diffusional distance for rapid transport of released metabolites and increasing the surface area for metabolic exchange. The RPE cells are joined by tight junctions known as 'zonulae occludentes' which were known to constitute the outer blood retinal barrier. (Shakib et al., 1972) To gain access through the RPE, metabolites either diffuse down their concentration gradients, or are carried via membrane carriers. (Heller and Bok, 1976, Miyamoto and Del Monte, 1994, Kundaiker et al., 1996)

Having been transported through the BrM and RPE, metabolites would be released to the photoreceptor cells via 2 plausible pathways. First, released metabolites diffuse freely or carried by carrier proteins for uptake by inner segments, or second, by direct transport through the microvilli extensions from the RPE cytoplasm to the interdigitating distal part of outer segment. (A.A Hussain, 2004)

Transport of Waste across RPE and Bruch's membrane

The transport pathway for waste products traverse in the opposite direction to nutritional transport described above. In general, waste products are small soluble substances that can easily diffuse down their concentration gradients into the choroidal capillaries for final removal. After being released from the outer segment, the RPE phagocytose an approximate level of 6000-8000 discs daily (Feeney-Burns et al., 1980, D, 1994) which then undergo biochemical breakdown with lysozymes within the cytoplasm of the RPE. Some basic amino acids, fatty acids and retinoid from the break down would be recycled to the photoreceptors for use. Other waste products such as urea would then diffuse down their concentration gradients into the vascular network. However, with a large amount of free radical damage, some waste material degradation by RPE would still be incomplete and this would result in production of residual bodies such as lipofuscin (Feeney-Burns et al., 1980, Dorey et al., 1989). Some of these smaller fragments may escape the RPE but ultimately get trapped within the inner layer of Bruch's, other larger fragments will become deposited on surface of BrM, forming lipo-proteinases products known as drusen.

Hydraulic conductivity is an important part of the system transport. In normal eyes, fluid flow had been observed to have a posterior direction, from retina to choroid. In a study by Marmor et al, most of the outward fluid flow across the RPE were found to be conducted via active transport, from apical to basal compartments whilst a smaller percentage was driven by passive osmotic gradients between the subretinal space and choroid. (Negi and Marmor, 1986), The inner collagenous layer of the BrM had been demonstrated to contribute significantly to the resistance between the RPE and BrM.(Starita et al., 1997, Moore et al., 1995a). Hence, the small pore radii in this region make it the rate limiting structure for hydraulic conductivity. An equation based on geometric analysis across this resistance barrier shows that a slight change in the radii of the pores would cause huge changes to hydraulic conductivity across the BrM.(Equation 1)(Renkin, 1954, Wyler et al., 1979, Lebrun and Junter, 1993)From this equation, the radii (r) was raised to a power of 4, thus, any age related changes to it's the structure of the BrM would result in deleterious effects.

Equation 1:

$$L_p = \sum_i \frac{\pi r_i^4}{8\eta l} \times \sigma_i$$

L_p : HC
 r : radius
 l : path length of conducting pore
 η : viscosity of fluid in pore
 σ_i : density of pore of various radii

Figure 1.9 Transport pathways across the Bruch's membrane

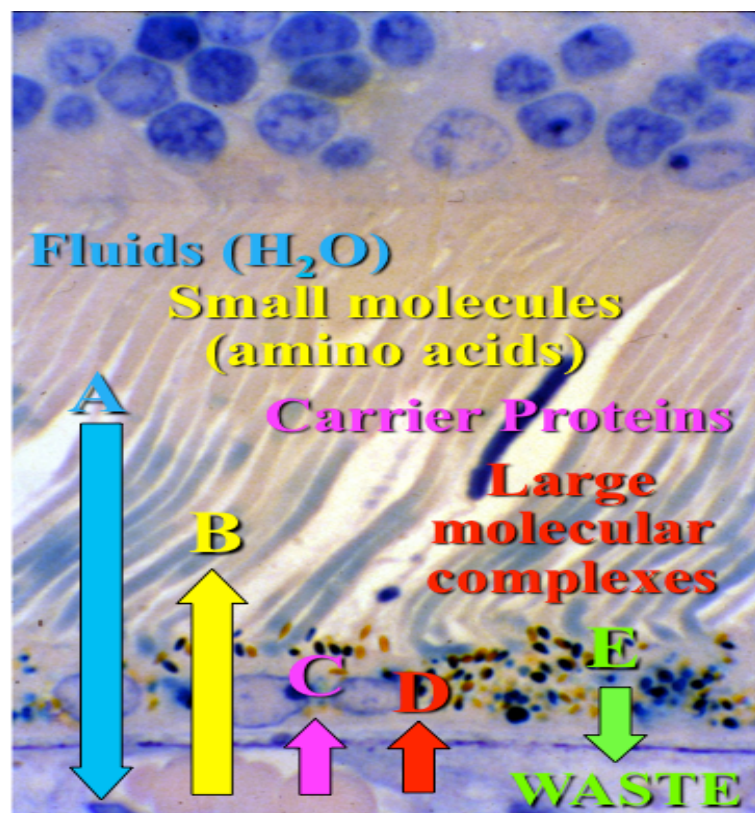


Figure 1.9 is a simplified diagram of the fluid and molecular transport in and out of the retina across the BrM.

Figure 1.10 Transport of metabolites in the outer retina

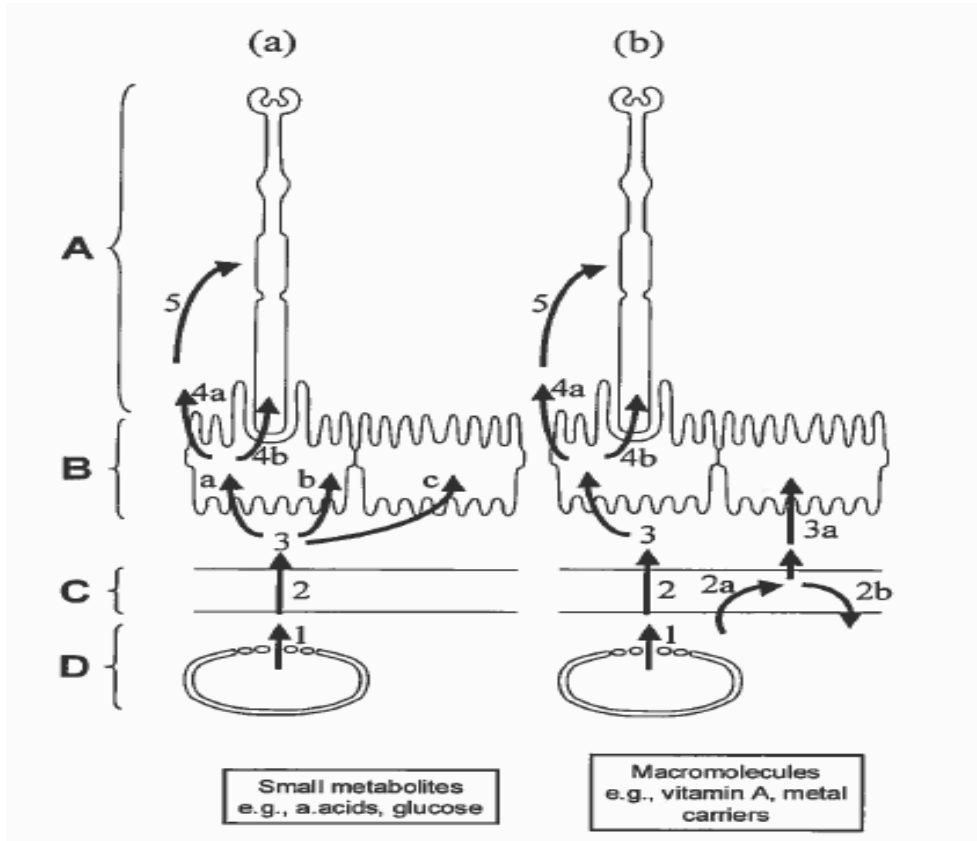


Figure 1.10 Transport pathway for metabolites between choroid to photoreceptor cells. (a) represent small solutes, (b) represent macromolecules.

- (1) After release from choriocapillaries,
- (2) Metabolites passively diffuse across Bruch's membrane
- (3) Taken up at the basal convoluted surface of RPE either by free diffusion or carrier mediated active or passive transport.
- (4) (a,b) Metabolites are then released into the interphotoreceptor matrix(IPM)
- (5) Diffuses down a concentration gradient across the IPM to be taken up by inner segment layer.

Figure from Hussain et al (A.A Hussain, 2004)

1.4 Ageing of the outer retina

Ageing changes are seen in neural retina, RPE, BrM and choriocapillaries. Of these, the most important cause of changes was in the RPE and BrM. As such, these structures are dealt with in further details.

1.4.1 Ageing retina pigment epithelial

Ageing causes a spectrum of degenerative structural and biochemical changes in the RPE. With age, there is a loss of effective cellular volume from retention of phagocytic material in the form of residual body and lipofuscin. Changes with consequences to the transport element can be seen in the loss of the complexity of basal convolution and microvilli. Despite this, experiments have shown that RPE cells can be loaded with lipofuscin and yet still function. Hence, it is not the rate limiting factor in terms of ageing transport and metabolic dysfunction.

Further downstream, in pathology such as age related macular degeneration (AMD), investigators have found degenerative RPE, which included changes ranging from hyperplasia, hypertrophy, atrophy with associated thinning of choriocapillaries, thickening of BrM and photoreceptor cell death. (Sarks et al., 1988)

The term 'senescent' RPE refers to a stage whereby normally mitosing RPE cells no longer divide. This happens when the cycle of telomere-telomerase becomes deregulated beyond a certain point when cells no longer divide. In fact, this concept had been proven both in vivo in primate eyes and in in-vitro experiments. (Mishima et al., 1999) Despite this, the senescent RPE cells were still found to be still metabolically active and release secretory enzymes and proteins. (Cao et al., 2013) This created a pro-inflammatory environment, which some authors hypothesize to be a causative factor in AMD.(Bandyopadhyay and Rohrer, 2012)

1.4.2 Ageing Bruch's

Structural

Structurally, the BrM increases from 2µm in thickness in the first decade of age to 7µm by the 10th decade.(Ramrattan et al., 1994b) Furthermore, Pauleikhoff et al have previously found an increase in lipid content in the BrM, hence introducing a hydrophobic barrier amongst aged eyes.(Pauleikhoff et al., 1990) Furthermore, these changes were found to be more pronounced in the macula as compared to the periphery.(Holz et al., 1994)

GE Marshall et al also found increased collagen type IV in choroidal endothelial cell basement membrane.(Marshall et al., 1992) They have attributed the increase in type IV collagen to be associated with the focal thickening between choriocapillaries and BrM due to ageing.(Marshall et al., 1992) Starita et al have also demonstrated that the highest resistance in aged BrM was between the inner collagenous layer and layer of elastin.(Starita et al., 1997) Hence, it may be assumed from various experimental data that the increase in type IV collagen and formation of dysfunctional collagen from AGEs play a significant role in causing resistance and decrease in transportation function across the BrM with age.

Physiological

There are dynamic changes in terms of molecular and physiological aspects of BrM throughout life. With age, investigators have found notable molecular modification and reconfiguration in the BrM, resulting in increase in thickness and its reduced filtration capacity. (van der Schaft et al., 1992, Ramrattan et al., 1994b, Moore and Clover, 2001a) The following summarizes the constellation of molecular changes in the BrM:

1. Increased cross linkage of collagen, which resulted in the increase of strength, and density of the collagen network but decreased in elasticity, flexibility and filtration capabilities. (Ugarte et al., 2006)
2. Higher turnover rate of BrM proteoglycans; proteoglycans are glue of extracellular matrices in BrM. As proteoglycan size increases, heparin sulphate fraction increases. Heparin sulphate is known to have anti-inflammatory properties either by interacting with complement factor H, an important regulator of the complement cascade and the local immune

response or by modulating complement activity via inhibition of the cleavage of complement factors B and C3, to respectively Bn and C3b.(Meri and Pangburn, 1994) Given the association between the complement system and development of AMD, the interaction between heparin sulphate and PGs may be one of the key molecular switches that turn normal RPE/BrM ageing into AMD pathology.(Scholl et al., 2008, Charbel Issa et al., 2011)

3. Increased mineralisation of BrM:

Some authors claim to have demonstrated a link between BrM calcification and AMD. It was postulated that extensive calcification of the BrM renders it brittle resulting in breaks, forming neovascularisation. (Spraul et al., 1999a) However, in empirical studies, the elasticity of membrane cannot be broken even when subject to pressures way outside its physiological limits. (Ugarte et al., 2006)

4. Increased content of advanced AGEs in BrM were noted; AGEs are glycosylated or oxidised fat or proteins. AGEs accumulate on structural protein, like collagen in BrM where they inhibit protein function and cause AMD.(Glenn et al., 2009, Baynes, 2001)

5. Accumulation of lipids in BrM. The increase of age found progressive accumulation of lipids such as phospholipids, triglycerides, FA and free cholesterol in BrM. This was noted especially in the macular.(Baynes, 2001, Sheraidah et al., 1993, Holz et al., 1994, Pauleikhoff et al., 1990) Some authors have found a 7x-increased concentration of cholesterol esters in the macular amongst the elderly as compared to its periphery. The accumulation of lipids with increasing age, reduces the capacity of BrM to facilitate fluid and macromolecular exchange between the choroid and the RPE or vice versa which is essential for retina function.(Marshall J, 1988)

6. Abnormalities in the MMP system were found with increased levels of TIMP 3 inhibitor and AGEs and reduced active MMP2 and 9 from AMD donors compared to age-matched controls(Kamei and Hollyfield, 1999b, Hussain et al., 2011)

7. Additional high molecular weight MMP species (HMW 1 and 2) consisting of polymers of MMP 2 and 9 and much larger macromolecular weight complex (LMMC) with HMW1, HMW2, Pro MMP 9, Pro MMP 2 identified in BrM. (Kumar et al., 2010)

Functional changes of Ageing Bruch's membrane

Hydraulic conductivity defined as a measure of water transport through a system, which in this case is across the BrM. With age, this basic transport need was found to be compromised. (Starita et al., 1996a) Foulds et al performed early experiments to determine the direction and rate of flow of water across the retina. (Moseley and Foulds, 1982) However, limited studies were done to specifically determine rate of fluid output by RPE in a normal eye. One clinical study using B scan ultrasonography to determine rate of regression of retinal bleb in a non-rheumatogenous retinal detachment had found the rate of RPE transport to be approximately $0.11 \mu\text{l}/\text{hour}/\text{mm}^2$. (Chihara and Nao-i, 1985) A presumed pressure on the RPE-Bruch's membrane complex is 4mmHg as found in experiments using monkey eyes. (Emi et al., 1989) (Maurice et al., 1971) Based on the information above, a well accepted equation for hydraulic conductivity calculation is $\text{HC} = \text{flow}/\text{pressure}$, and the calculated minimal HC for baseline requirements would be $0.65 \times 10^{-10} \text{m/s}/\text{Pa}$. (A.A Hussain, 2004) This calculated value was noted to be low because the calculation did not consider the drop in pressure across the BrM and had not considered the age related decrease in transport across the BrM. Experiments by Moore et al (1995a) had shown that an approximately 11% of human Bruch's sample taken from a set of donors aged 50 and above did not meet this calculated basic requirement. (Moore et al., 1995a)

Invitro studies by Moore et al (1995) and Starita et al (1996) previously demonstrated the compromise of hydraulic conductivity across the BrM with ageing and have found these changes to be exaggerated in the macular region. (Moore et al., 1995a, Starita et al., 1996a) (Figure 1.11) From the previous experiments, it was demonstrated that ageing causes exponential decrease in hydraulic conductivity across the BrM in both macular and peripheral region and the calculated half-life for this decrease was 16 and 23 years respectively. With these results of exponential decay, Moore et al

hypothesized that the mechanisms of decrease in fluid transport had been 'programmed' from birth and calculated the 'finite period of viable function' to be 101 and 131 years respectively.(Figure 1.11) (Moore et al., 1995a) However, in reality, individual ageing rates will also be dependent upon environmental and behavioral issues such as diet, light exposure, smoking etc.

Amino acids are required for regeneration of outer segment disc and to replace neurotransmitter stores. Eight amino acids of varying sizes have been used to investigate the diffusional transport across the human Bruch's and shown a linear decrease with age.(Hussain et al., 2002) Further studies with large molecules (Macromolecules), Hussain et al previously calculated using FITC dextrans as quasispherical probes that the exclusion radii for the inner collagenous resistance layer was 5.88nm, in the amino acid studies, the solute flux rates were reduced to 60% when solute radius was 10% of pore radius. Hence, in theory, large proteins such as albumin, transferrin and ceruloplasmin with radii of 3.58nm, 4.3nm and 4.68nm (61, 73, 79% pore radius) would not be able to pass through the conducting pore, restricting their transport. (Hussain, 1999)

Thus, with age, fluid and nutritional transport are certainly compromised.

Figure 1.11 HC plots across Bruch's membrane at (a) macular and (b) periphery

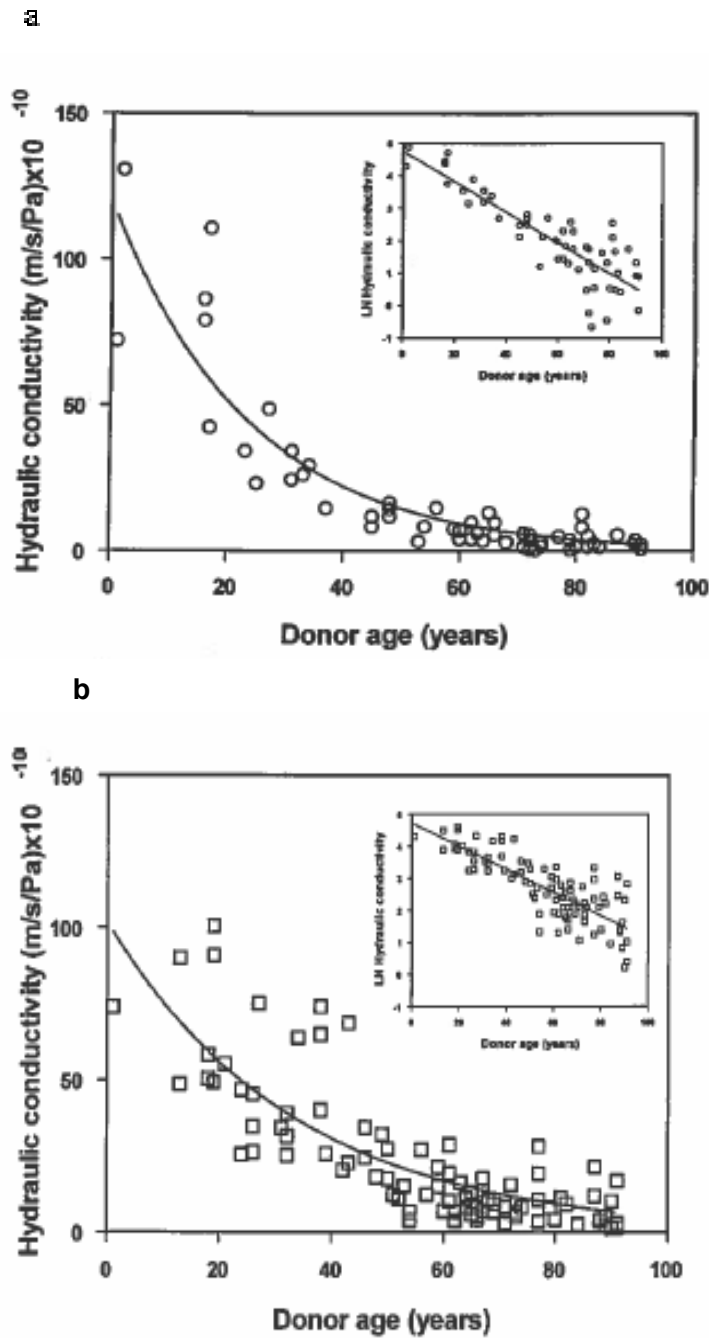


Figure 1.11 a and b shows age dependent variation of HC of human BrM. In this experiment by Hussain et al, HC of BrM was determined in 58 donors (1-81 years of age). Half life of macular region was calculated to be 16 years (a), whilst that of the periphery was 25 years (b). Graphs adapted from Moore et al, 1995 and Starita et al 1996.

Table 1.2 Hydraulic conductivity in ageing physiology

REFERENCE	INVITRO MODEL	RESULTS	CONCLUSION
Fisher RF Eye 1987(Fisher, 1987b)	Human eyes	HC decrease across BrM with age and Young's modulus increase. Opposite results to lens capsule. Static measurement of HC.	Implications on ageing macula and cataract.
Moore et al 1995(Moore et al., 1995a)	Human BrM-Choroid complex	Age related exponential decrease in HC. 1. HC decrease is greater in first 4 decades of life; 2. HC decrease more centrally then peripherally. Dynamic measurement of HC.	The findings could be attributed to changes in BrM and CC with age. Other studies have found increased lipid deposits more centrally than peripherally.
Starita et al(Starita et al., 1997)	Human BrM-choroid (old and young donors)	Using excimer laser in series of 3 pulses(0.75um) to ablate Bruch's membrane, it was found that the greatest resistance of HC was in the inner collagenous layer. Dynamic measurement of HC.	No corresponding morphological or histological data to correlate with this finding.
Ahir et al(Ahir et al., 2002)	Cultured RPE medium, HC across BrM using various methodologies with a latent and activated MMPs (MMP 2 and 9)	Both activated MMP 9 and 2 were released during cell proliferation. Activated MMP 9 and 2 both causes increases of HC across BrM complex up to 3 folds. MMP9 effect was found to be more pronounced in older eyes.	Activation of MMP coincides with cell cycle and is a promising pathway to regulate the ECM of the BrM.
Hillenkamp et al(Hillenkamp et al., 2004)	Bovine eyes(<2years), human eyes(13 to 81 years). Excimer laser to ablate BM and investigate the effect of path length in the macromolecular transport mechanism across BM.	Path length and matrix component influenced the macromolecular transport mechanism across BrM with age. Choroidal thinning was not associated with restriction of transport.	

Table 1.3 Changes in the BrM secondary to ageing

Structural	Physiological	Functional
Increase in vesicles and membranous materials first in the inner collagenous layer with age.(Feeney-Burns and Ellersieck, 1985)	Increase in TIMP3 in Bruch's membrane.(Kamei and Hollyfield, 1999b, Fariss et al., 1997a)	Hydraulic conductivity across BrM decreases exponentially with age.(Starita et al., 1997, Moore et al., 1995a)
Progressive increase in membranous lipids with age in BrM.(Newsome et al., 1987b, Bird and Marshall, 1986, Bird, 1992, Sarks et al., 1999)	Active-MMP 2 and 9 more prominent in peripheral than macular region in Bruch's membrane.(Guo et al., 1999b)	Macromolecular permeability across BrM decreases linearly with age.(Hussain, 2002;Moore, 2001)
Increased crosslinking from AGEs and advanced lipoxidation products in BrM with age.(Karwatowski et al., 1995b, Handa et al., 1999)	Presence of MMP 1, 3 , 2 and 9 in Bruch's membrane with increased inactivation with age.(Guo et al., 1999b)	Macromolecular permeability decreases comparatively further in macular area in aged BrM.(Hussain et al., 2010c, Starita et al., 1996a, Moore et al., 1995a)
Type IV collagen increases in BrM with age along RPE basement membrane and choroidal endothelium. Laminin increased in inner collagenous layer and basal linear deposits.(Marshall et al., 1992, Marshall et al., 1994)	Increased bound MMP 2 and 9 in ageing Bruch's membrane, decreasing free pool for activation.(Kumar et al., 2010)	
Increase in thickness of BrM from 2 to 5um from 1 st to 10 th decade of life. (Ramrattan et al., 1994b)		
Increased deposition of material between RPE and BrM (drusen).(Sarks, 1976b, Green and Key, 1977)		

1.5 Matrix Metalloproteinase

Matrix Metalloproteinase(MMP) is an extracellular matrix regulator which was shown to be involved in the pathophysiological pathways leading to ageing in the retina. The following will review the molecular biology of MMPs, the involvement of MMPs in other parts of the body, and in particular reference to the outer retina and AMD.

For the purpose of this thesis, pro or latent MMPs refer to the inactive or bound state of MMPs and active-MMPs refer to MMPs in the active or free form.

1.5.1 Molecular Biology of Matrix Metalloproteinase

Gross and Lapiere first discovered Metalloproteinases 50 years ago during tadpole tail metamorphosis.(Gross and Lapiere, 1962) Since then, it was found that the complex turnover process of the extracellular matrix(ECM) is regulated by a family of 20 zinc-binding, calcium dependent enzymes, the matrix metalloproteinases (MMP). MMPs are classified to the type of ECM regulated, namely collagenases, gelatinases, stromelysins etc(Table 1.3). MMP activity are regulated by its inducers such as inflammatory marks (TNF-beta, ILF) and its inhibitors (TIMPs) (Table 1.4). In addition to its role to cleave proteins of the extracellular matrix, it also acts as a feedback to activate or inactivate other signaling pathways, including receptors, adhesion molecules and growth factors. (Table 1.5)

MMPs have a common structure which includes a pro-peptide consisting of 80 amino acids, a catalytic domain of 170 amino acids, a 'hinge region' which connects to the hemopexin C-terminal domain of 200 amino acids. Exceptions to this include MMP-7, -23 and -26. All MMPs are released as inactive zymogens which consists of a 'cysteine switch' in the pro-peptide domain that binds to the zinc ion in the catalytic domain. This prevents MMP activation by preventing a water molecule to bind to zinc, preventing catalysis to its active form. The hemopexin C-terminal domain has a large surface for protein-protein interaction and serves as substrate recognition and for interaction for specific tissue inhibitor of matrix metalloproteinase (TIMPs).

Proenzymes of MMPs (or ProMMPs) are activated in a step-wise fashion. First, other tissue or plasma proteinase bind to a 'bait' region in the pro-peptide domain which then undergoes cleavage to remove part of the pro-peptide. The

second step involves complete removal of the pro-peptide by action of either MMP intermediates or other active MMPs. (Nagase et al., 1990, Peppin and Weiss, 1986)

MMPs can also be activated artificially by treatment using mercurial compounds, or chaotropic agents. This technique is used in the laboratory to activate inactive MMPs.

For the purpose of this thesis, only MMP 9 and 2 would be further elaborated.

Human Matrix Metalloproteinase 9:

Human matrix metalloproteinases are released as pro-forms, requiring activation for its activity. Both MMP 2 & 9 are thought to have collagenolytic activities, playing particularly important roles in final pathway of fibrillar collagens degradation, particularly collagen type I. Hence, both play a vital role in ECM remodeling.

Human MMP 9 is a type IV collagenase and participates in degradation of a wide range of substrates, which includes gelatin; type IV, V, XIV collagens; X2-macroglobulin; elastin; vitronectin and proteoglycan. Activation of Pro MMP 9 is currently still poorly understood but some data has suggested the influence of MMP 2 in cleaving pro-domain of MMP 9.(Toth et al., 2003)

Human MMP 2

Activation of MMP 2 is complex and mediated by MMP 14 and TIMP 2. First, the proMMP 2 forms a complex with TIMP 2 through its hemopexin C terminal domain with the non-inhibitory C terminal domain of TIMP 2. This complex then binds to an active MMP 14 via the free N-terminal MMP inhibitory domain of TIMP 2. The propeptide of the proMMP 2 then links to another molecular of active MMP14. The two adjacent MMP14 molecules interact through their hemopexin C terminal domains. A tetrameric quaternary compound of proMMP2 is formed, whereby one molecular of MMP14 acts as a proMMP2-TIMP2 receptor and the other activates the proMMP2 by cleaving the pro-peptide. (Alcazar et al., 2007, Smine and Plantner, 1997, Butler et al., 1998)

1.5.2 Systemic Involvement of Matrix Metalloproteinases

MMP activation has widespread important biological physiological functions such as embryonic development wound healing and angiogenesis, but could overtly cause injuries and disorders involving cancer, inflammation and several auto-immune diseases.(Li et al., 2012, Said et al., 2014, Schveigert et al., 2013) The balance between the latent and stimulated forms of MMP is required under physiological conditions, but deregulated MMP profiles have been reported in several diseases such as coronary artery disease, myocardial infarction, coronary aneurysm and stroke. (Nagase et al., 2006, Longo et al., 2002, Wang et al., 2002) (Figure 1.10)

More recently, several protective functions of MMP have been found. These include the role of MMP 9 in chronic renal failure, stroke recovery by remodeling of neuronal extracellular matrix and Alzheimer's disease by the regulation of the β -amyloid deposits by MMP9.(Aston-Mourney et al., 2013, Okada et al., 2012)

Table 1.4 Types of MMP

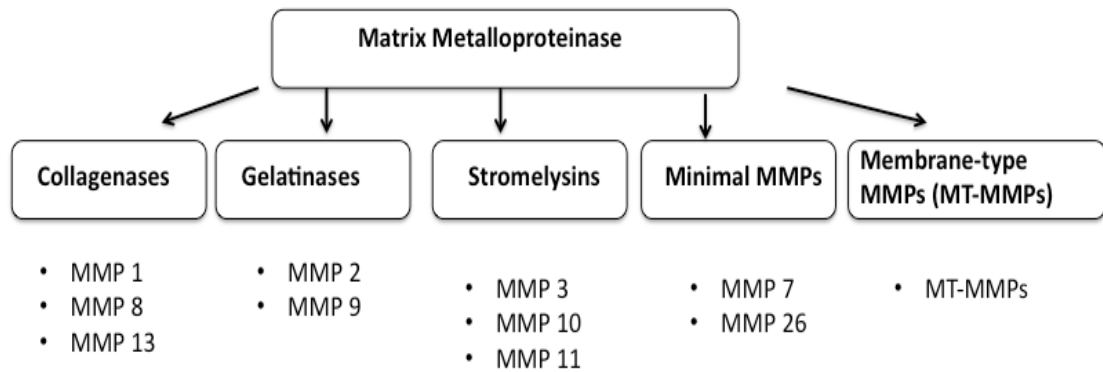


Table 1.5 Inducers and inhibitors of MMP

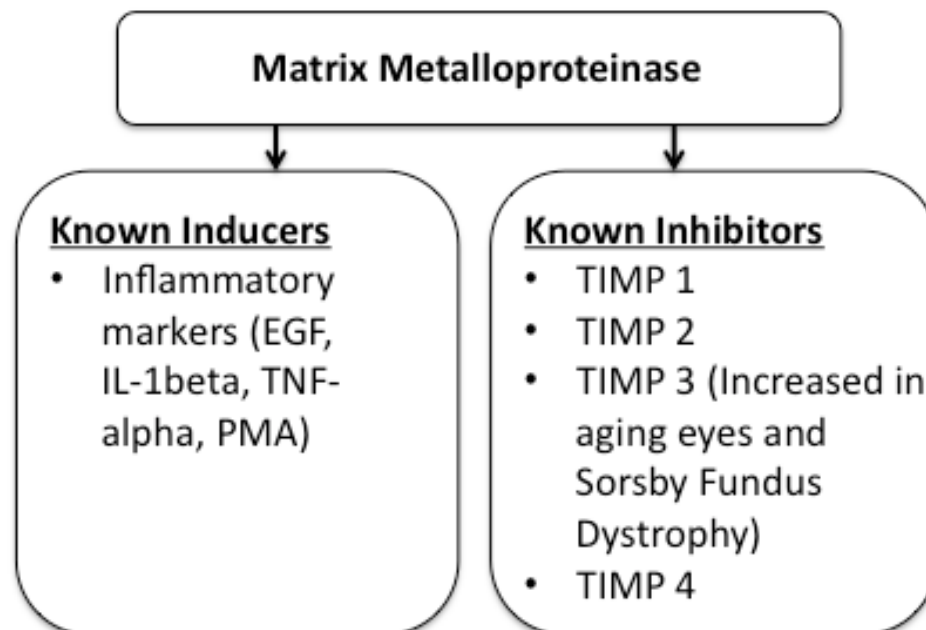


Table 1.6 Biological activities mediated by MMP cleavage

Biological effect	Responsible MMPs	Substrate cleaved
Keratinocyte migration and reepithelialization	MMP-1	Type I collagen
Osteoclast activation	MMP-13	Type I collagen
Neurite outgrowth	MMP-2	Chondroitinsulphate proteoglycan
Adipocyte differentiation,	MMP-7,	Fibronectin
cell migration	MMP-1,-2, and -3	Fibronectin
cell migration	MT1-MMP	CD44
Mammary epithelial cell apoptosis	MMP-3	Basement membrane
Mammary epithelial alveolar formation	MMP-3	Basement membrane
Epithelial-mesenchymal conversion (mammary epithelial cells)	MMP-3	E-cadherin
Mesenchymal cell differentiation with inflammatory phenotype	MMP-2	Not identified
Platelet aggregation	MMP-1	Not identified
Generation of angiostatin-like fragment	MMP-3	Plasminogen
MMP-7	Plasminogen	
MMP-9	Plasminogen	
MMP-12	Plasminogen	
Generation of endostatin-like fragment	MMPs	Type XVIII collagen
Enhanced collagen affinity	MMP-2, -3, -7, -9, and -13 (but not MMP-1)	BM-40 (SPARC/Osteonectin)
Kidney tubulogenesis	MT1-MMP	Type I collagen
Release of bFGF	MMP-3, and -13	Perlecan
Increased bioavailability of IGF1 and cell proliferation	MMP-1, -2, -3, -7, and -19	IGFBP-3
MMPs	IGFBP-5	
MMP-11	IGFBP-1	
Activation of VEGF	MMPs	CTGF
Epithelial cell migration	MMP-2, MT1-MMP, MMP-19	Laminin 5 γ 2 chain
MT1-MMP [108]	Lamin 5 β 3	
Apoptosis (amion epithelial cells)	Collagenase	Type I collagen
Pro-inflammatory	MMP-1, -3, and -9	Processing IL-1 β from the precursor
Tumor cell resistance	MMP-9	ICAM-1
Anti-inflammatory	MMP-1, -2, and -9	IL-1 β degradation
Anti-inflammatory	MMP-1, -2, -3, -13, -14	Monocyte chemoattractant protein-3
Increased bioavailability of TGF- β	MMP-2,-3,-7	Decorin
Disrupted cell aggregation and increased cell invasion	MMP-3, MMP-7	E-cadherin

Reduced cell adhesion and spreading	MT1-MMP, MT2-MMP, MT3-MMP	Cell surface tissue transglutaminase
Fas-receptor mediated apoptosis	MMP-7	Fas ligand
Pro-inflammatory	MMP-7	Pro-TNF α
Osteoclast activation	MMP-7	RANK ligand
Reduced IL-2 response	MMP-9	IL-2R α
PAR1 activation	MMP-1	Protease activated receptor 1
Generation of vasoconstrictor	MMP-2	Big endothelin
Conversion of vasodilator to vasoconstrictor	MMP-2	Adrenomedullin
Vasoconstriction and cell growth	MMP-7	Heparin-binding EGF
Neuronal apoptosis leading to neurodegeneration	MMP-2	Stromal cell-derived factor 1 α (SDF-1)
Bioavailability of TGF β	MMP-9	precursor of TGF β
Thymic neovascularization	MMP-9	Collagen IV
Hypertrophic chondrocytes apoptosis and recruitment of osteoclast	MMP-9	Galactin-3
Embryo attachment to uterine epithelia	MT1-MMP	MUC1, a transmembrane mucin

Table by Visse and Nagase et al(Nagase et al., 2006)

Figure 1.12 Role of MMPs in systemic diseases

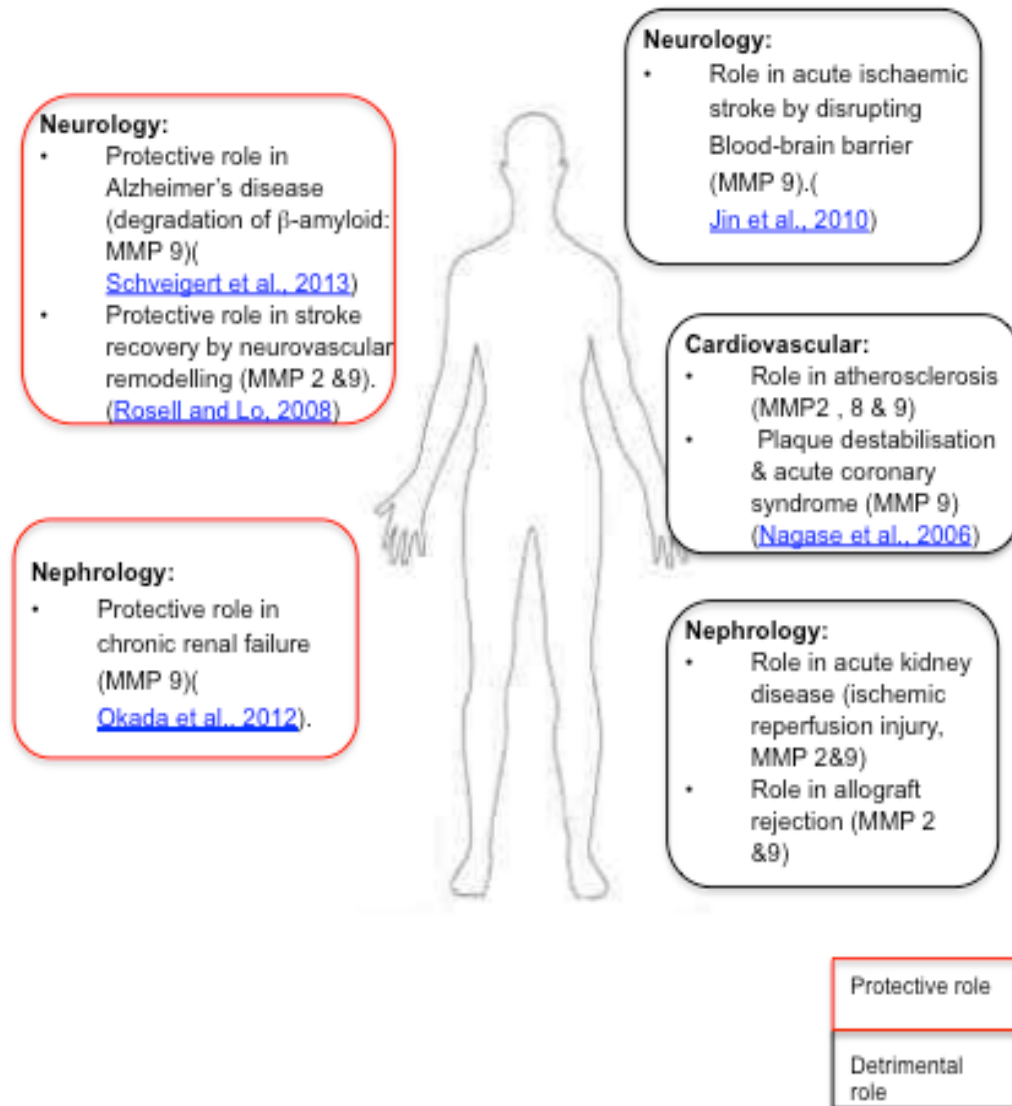


Figure 1.12 Pictorial diagram of detrimental and protective role of MMP in the human body. Because of their effect on various extracellular matrix, MMP serves a multiphasic role in numerous diseases. It has long been thought that MMP causes disease progression (atherosclerosis, cancer, angiogenesis). However, it is now known that MMP (particularly MMP 2 and 9) has a critical role in acute diseases, but serves as a protective protease in chronic conditions, due to its ability to remodel extracellular matrix during recovery periods.

1.5.3 Involvement of Metalloproteinase in Ageing Bruch's Membrane

MMP profile of ageing Bruch's membrane

The extracellular matrix of the BrM is tightly regulated by matrix metalloproteinases. These enzymes are released as pro-enzymes and activated by cleavage of a peptide. The activation pathways of these enzymes are regulated by other MMPs and tissue inhibitors of matrix metalloproteinase (TIMP). Previous investigations have demonstrated the release of MMPs by both RPE and the choroid. (Ahir et al., 2002, Guo et al., 1999b) To date, there are 4 known TIMPs (TIMP 1, 2, 3, 4). (Murphy, 2011) Abnormalities of the degradation and synthesis regulatory coupling can cause structural and functional changes to the BrM. An example is Sorsby Fundus Dystrophy, an inherited disorder consisting of a mutational change in TIMP 3 gene. This results in deregulation of ECM turnover. Histological studies have found an exaggeratedly thickened Bruch's membrane (30µm) amongst patients whose clinical pattern resembles that of early onset of AMD. (Weber et al., 1994) RPE and choroidal endothelial cells secrete MMPs 1, 2, 3 and 9 and TIMPs 1, 2, 3 which were also found in BrM. (Alexander et al., 1990, Della et al., 1996, Vranka et al., 1997, Fariss et al., 1997a, Hunt et al., 1993) Increased inactive MMP 2 and 9 have been found in aged and AMD donors. Similarly, an increase in TIMP 3 had been noted in the BrM of aged donors. (Vranka et al., 1997, Fariss et al., 1997a) This could be a cause of the structural thickening of Bruch's membrane in normal aging. Thus, these evidences suggest a role of MMP/TIMP ratio in regulating the structural integrity of the BrM. In a cross-feedback fashion, it was also suggested that the integrity of the BrM is crucial in the RPE regulation of MMP and TIMP secretion. (Padgett et al., 1997) Work from our group in the past decade had demonstrated the structural and biological effects of MMP-2 and 9 in relation to the ageing retina. Kumar et al have also found an increased proportion of bound MMP in the form of monomeric and heteropolymeric sequestration in ageing BrM, decreasing the free pool available for activation. The heteropolymeric sequestration had been found by chromatography to consist of sequestered Pro MMP 2 and Pro MMP 9. (Kumar et al., 2010, Hussain et al., 2011) It was hypothesized that this depletes the level of MMP available for activation required for the turnover metabolism of the outer retina. This decrease in active MMP levels was

correlated to the decreased hydraulic conductivity and decreased macromolecular transport across the BrM.(Ahir et al., 2002)

In essence, previous studies have shown the following with regards to MMP in the ageing BrM:

- Sequestration of MMP in ageing BrM
- Age related decreased hydraulic conductivity across BrM
- RPE cell proliferation releases activated MMP
- Activated MMP increases hydraulic conductivity across aged Bruch's,

It may be hypothesized that manipulation of the matrix metalloproteinase pathway, ie by increasing the quantity of activated MMP, might enhance regulation of the extracellular matrix of the aged Bruch's, thus improving the transport system and delaying onset of AMD.

Matrix Metalloproteinase in AMD

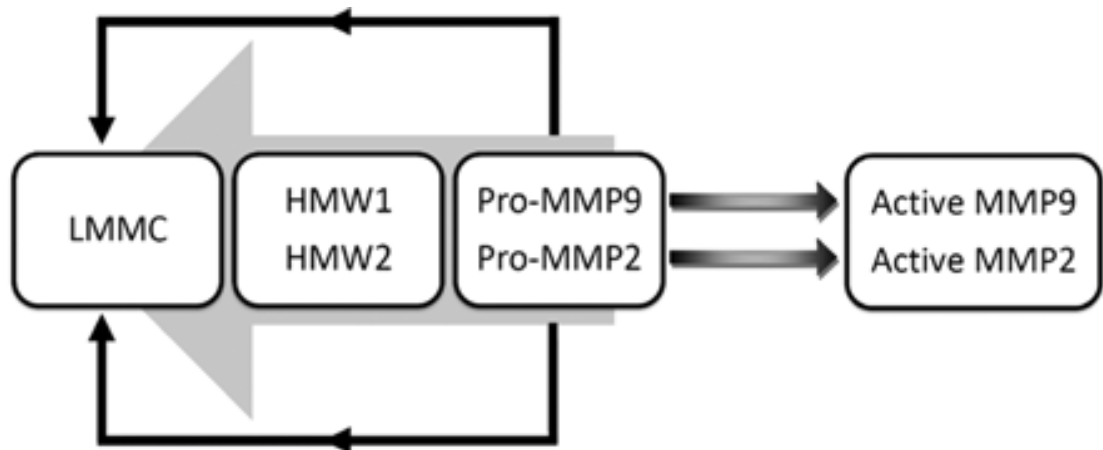
Prior studies implied the contribution of MMP pathway in AMD. Chau et al has found an increase in the plasma levels of pro MMP 9 in patients with early age related maculopathy and neovascularization in comparison to controls.(Chau et al., 2007) Fiotti et al also found longer microsatellite in the region of MMP 9 to be associated with exudative AMD.(Fiotti et al., 2005)

Previous in vitro studies by our team demonstrated the increased sequestration of MMP 2 and 9 into high molecular weight species (HMW 1 and 2) in AMD donors. This would deprive the levels of free pool of pro MMP for activation under normal regulatory circumstances.(Hussain et al., 2011) The following figure demonstrates the pathway for MMP sequestration in AMD.

Table 1.7 Gelatinase activity age-matched control versus AMD

Gelatinase activity Age matched Control & AMD					
MMP species	Donor group	Free	Bound	Total	
HMW2	Control	1435 ± 1520	12702 ± 3940	14137 ± 4725	High Bad Low Good
	AMD	6685 ± 5444*	15195 ± 3018	21880 ± 8182*	
HMW1	Control	1335 ± 2470	5996 ± 2911	7331 ± 4040	
	AMD	6327 ± 7064**	10480 ± 5616	16807 ± 11950*	
Pro-MMP-9	Control	9354 ± 11895	16068 ± 7692	25422 ± 16553	
Pro-MMP-2	AMD	33375 ± 25579***	22572 ± 7274	55947 ± 30662*	
	Control	1567 ± 1753	1393 ± 964	2960 ± 2071	
AMD	379 ± 374*	674 ± 700	1053 ± 854*		
Active MMP-9	Control	NDet	517 ± 376	517 ± 376	High Good Low Bad
AMD	NDet	195 ± 80*	195 ± 80*		
Active MMP-2	Control	357 ± 428	1978 ± 1140	2336 ± 1257	
	AMD	335 ± 519	614 ± 534***	949 ± 885*	

Figure 1.13 MMP Pathway in elderly Bruch's-choroid



Pathway constructed by Hussain et al., 2011

1.6 Treatments of early AMD

AMD extends from the early stages of drusen (Figure 1.14) and /or pigmentary changes with normal visual acuity to either exudative, wet AMD characterized by subfoveal choroidal neovascularisation or dry, geographic atrophy, that results in severe sight impairment (blindness).(Abdelsalam et al., 1999) There are various classifications of AMD. In the early stage of the disease, these classifications are based on the size of the drusen and presence of pigmentation.(Davis et al., 2005, Bird et al., 1995) According to the Age Related Eye Disease Study (AREDS) group, the rate of progression of early AMD defined as AREDS 3 (drusen>250µm, presence of central hyper or hypopigmentation) stands at 10% per annum. (Davis, Gangnon et al. 2005) Prior experimental model for prophylactic therapy for AMD were largely based on nutritional studies, on the basis of antioxidant to counteract the effects of inflammation. Studies have shown the link between complement factors H and complement pathways, classical, alternative and lectin, in particular alternative pathways to play a role in AMD. Epidemiological studies have also found association between groups with consumption of antioxidants in terms of vitamins and vegetables to have a lower prevalence of AMD. In detail, some of the nutrients that was previously investigated or currently undergoing investigation are highlighted below.

(i) Fats

The data from several large nutritional studies have been analyzed in an attempt to correlate the various types of fats with AMD. These studies observed the quantity and quality of each type of dietary fat, including omega 3 and 6, mono and polyunsaturated fats, saturated fats, total fats, trans fats, and cholesterol in relation to the risk of developing AMD.(Weikel et al., 2012). In general, only polyunsaturated fat and omega 3 (EPA and DHA) have been shown to have a beneficial effect in reducing the risk of both early AMD and conversion to neovascularisation.

Studies demonstrated the positive link between long chain omega 3 fatty acids (such as docosahexaenoic acid, DHA and eicosapentaenoic acid, EPA) and decreased rates of chronic diseases, including AMD.(Pilkington et al., 2011, Bacova et al., 2010) The Eye Disease Case Control study (EDCC) group have found higher intake of omega 3 fatty acids to confer retinal protection against neovascular AMD (Seddon et al., 2001) Similar results were found by the US

Twin Study of Age Related Macular Degeneration group and the Age Related Eye Disease Study (AREDS) group, although the results were not statistically significant after adjustment for linoleic acid and arachidonic acid respectively. (Seddon et al., 2001, Sangiovanni et al., 2009) In particular, a prospective study of over 72,000 participants from the Nurses Health Study (NHS) and Health Professionals' Follow up study (HPFUS) demonstrated that the highest intakes of DHA were associated with a reduced risk for AMD (Relative Risk (RR)=0.7, $p < 0.05$ CI 0.52, 0.93). (Cho et al., 2001) The Melbourne Collaborative Cohort group demonstrated that although the group consuming the highest amounts of omega 3 fatty acids had a slightly reduced risk for early AMD (Odds Ratio (OR)=0.85, 95% CI: 0.71, 1.02, $p = 0.03$) there was, however, no association between the type of fatty acid and the disease. (Chong et al., 2009)

There have been several studies that have produced contradictory results, finding deleterious effects of omega-3 fatty acid intake on AMD risk. In the Carotenoids in Age Related Eye Disease Study (CAREDS) (Robman et al., 2007), the investigators have reported an increased risk for intermediate AMD amongst women consuming the highest amounts of omega-3 fatty acids compared to women consuming the least amount of omega 3 fatty acids (OR 2.60, CI 1.60, 4.40, $p < 0.01$). Also, in the NHS and HPFUS study, the group with the highest intake of linoleic acid had an increased risk for any stage of AMD (RR=1.49, 95% CI: 1.15, 1.94, $p = 0.0009$). (Augood et al., 2008)

Fish as a dietary source of omega-3 has also been shown to be associated with a decreased risk for neovascular AMD. The AREDS group found that consumption of at least two servings of fish per week reduced the risk of neovascular AMD (OR =0.61; 95% CI:0.37, 1.00, $p = 0.01$). (SanGiovanni, Chew et al 2007) The NHS and HPFUS group also found that individuals who consumed more than four servings of fish per week had a reduced risk of any stage of AMD compared to those having less than 4 servings per week (RR=0.65; 95% CI: 0.46, 0.91). (Cho et al., 2001)

In contrast, many studies, including the Beaver Dam Eye Study, CAREDS, and the Melbourne Collaborative Cohort did not find any association between consumption of mono unsaturated fatty acids such as oleic acid and any stage of AMD risk. (Cho et al., 2001, Delcourt et al., 2007, Robman et al., 2007) There were, however, reports of increasing risk of early AMD with consumption of

monosaturated fatty acids amongst subjects from the Blue Mountains Eye Study.(Smith et al., 2000)

Increased saturated fats and cholesterol intake are associated with adverse health outcomes. Similar to monosaturated fatty acids, a link was also noted between cholesterol and risk of early AMD in the Beaver Dam Eye Study and the Blue Mountains Eye Study. (Smith et al., 2000)

In summary, other than for long chain polyunsaturated fatty acids, the evidence for all other fats remains relatively ambiguous. However, strong evidential data currently suggests that increased consumption of long chain omega 3 fatty acids such as EPA and DHA reduces the risk for neovascular and early AMD. (Roorda et al.)

(Roorda et al.) Carbohydrates

Carbohydrates have been postulated to contribute to oxidative stress and result in cell and tissue dysfunction Research that investigated carbohydrates intake and AMD utilized the glycemic index as an indicator. The glycemic index is the measure of the ability of 50g of a certain glucose-rich food to raise blood glucose level as compared to the ability of 50g of standard food. A high glycaemic index food would result in higher levels of blood glucose after two hours of food consumption.(Weikel et al., 2012) Almost all epidemiologic data have demonstrated that higher glycemic index foods were associated with higher risk for AMD or AMD progression.(Chiu and Taylor, 2011)

For example, in the cross sectional analyses of the baseline data from AREDS, patients with higher dietary glycemic indices were at increased risk for the manifestation of large drusen and neovascularization.(Chiu et al., 2006) It was calculated that compared with those in the lowest 20% of dietary glycaemic index, those in the highest 20% had a 39% higher risk of advancement of disease.(Chiu et al., 2007). These findings corroborated results from another cross sectional analysis of 526 women in the NHS study. This study found that women who had dietary glycemic indices in the highest one third compared to the lowest one third had an increased risk for AMD (OR=2.71; 95% CI: 1.24, 5.93, p=0.01). From these data, some authors concluded that by changing the dietary glycemic index by 1.0 unit (equivalent to replacing 3 pieces of white bread with 3 pieces of wholegrain bread as a daily consumption), approximately 100,000 cases would be avoided in 5 years.(Chiu et al., 2007)

The Blue Mountains Eye Study also noted a significant trend of decreasing risk for early AMD with increased intake of food with lower glycemic index, which included cereal fiber, breads and grains.(Kaushik et al., 2008)
Hence, the evidence for a positive link between a high glycemic index and early AMD is substantial.(Roorda et al.)

(Roorda et al.) Carotenoids

Carotenoids constitute part of the macular pigments found in the retina. Lutein and zeaxanthin are some of the carotenoids found in the macular region.(Granado et al., 2003)

Several case control and cross sectional studies have reported high intakes of carotenoids such as lutein/zeaxanthin to be protective against neovascular AMD. (1993, Seddon et al., 1994) In the AREDS study, cross sectional analysis have shown that longer-term consumption of lutein/zeaxanthin provided a 20% reduced risk for drusen and late AMD(Chiu et al., 2009) The Carotenoids in Age Related Maculopathy in Italians Study (CARMIS), a randomised clinical trial in which patients received either a combination of 10mg lutein, 1mg zeaxanthin, 4mg astraxanthin and an antioxidant versus no supplements, found that the subjects who received the combination treatment had improved and stabilised visual acuity.(Piermarocchi et al., 2011) The conclusions from this study were reinforced by the Lutein antioxidant Supplement trial (LAST) which showed improvements in visual acuity and contrast sensitivity in subjects who received the supplementation.(Trieschmann et al., 2007)

Despite these encouraging results, there have been several cross sectional studies which did not demonstrate an association between serum levels of carotenoids and risk of any stage of AMD. Several prospective studies, such as the Rotterdam prospective cohort, which has over 10,000 subjects of both genders living in Rotterdam, in the Netherlands, did not find an association between lutein/zeaxanthin intake and AMD.(van Leeuwen et al., 2005) The NHS and HPFUS study, and the Beaver Dam eye study had similar outcomes. (VandenLangenberg et al., 1998, Cho et al., 2004, Cho et al., 2008) On the other hand, few studies have suggested increased risk of early AMD with consumption of high amounts of lutein/zeaxanthin. (Robman et al., 2007, Mares-Perlman et al., 2001)

Beta-carotene, another carotenoid which was investigated in many studies, in general did not have a positive effect on risk reduction in AMD.(Smith et al., 1997, Cardinault et al., 2005)

Studies that evaluated other carotenoids found commonly in food-based products, such as lycopene, in tomato-based products, and cryptoxanthin, in avocados, basil and mangos, did not find a significant correlation with decreased AMD.(Cardinault et al., 2005, Michikawa et al., 2009)

As carotenoids are by-products of vitamin A, which takes the form of retinol in the body, several analyses of vitamin A/retinol intake and plasma levels have been carried out to examine the role of vitamin A in promoting retinal health.

The NHANES I study has found that increased consumption of fruits and vegetables rich in vitamin A results in a decreased risk for any stage of AMD (OR=0.59, 95%CI: 0.37, 0.99, p<0.01), whilst the Beaver Dam Eye study found that past or current intake of beta carotene reduced the risk for the manifestation of large drusen.(VandenLangenberg et al., 1998, Goldberg et al., 1988) All other investigations of vitamin A and the risk of AMD, however, did not find encouraging associations.(Simonelli et al., 2002, Seddon et al., 1994)

In summary, of all the carotenoids studied, lutein and zeaxanthin were found to confer most benefit to the retina and the greatest benefits lie in the most advanced stages of AMD. A large scale clinical trial, the AREDS 2 study is currently recruiting to evaluate the benefits of lutein/zeaxanthin.

(iv) Vitamins

Vitamin C is a strong antioxidant (ascorbic acid) and its effects on AMD have been investigated on the basis of its antioxidant properties. However, results from several clinical studies concluded that there was no correlation between vitamin C status and retinal health.(Blumenkranz et al., 1986, 1993) This can be postulated to be a secondary consequence of the hydrophilic properties of ascorbic acid in an environment where the retina is largely lipophilic, hence limiting its role at this site.

Vitamin D

The general health benefits of vitamin D on chronic disease are well known. However, there had only been one study which investigated the role of vitamin D in AMD. In the NHANES III study, non Hispanic whites with the highest

serum levels of vitamin D had a reduced risk of early AMD compared to those with low serum levels. This effect was however not noted in non-Hispanic blacks or Mexican Americans. (Parekh et al., 2007) Further studies are required to further explore this correlation.

Vitamin E

Vitamin E is a lipophilic antioxidant (alpha-tocopherol) and was a focus of retina research in efforts to diminish the risk for AMD. An earlier case control study of 48 patients demonstrated that plasma vitamin E was significantly lower in patients with late AMD as compared to early AMD, or healthy age matched controls.(Simonelli et al., 2002) Several other analyses from the POLA study involving 2584 participants also found that those with high levels of plasma vitamin E had a reduced risk of early and late AMD, whilst the AREDS study which evaluated vitamin E consumption found that those consuming highest amounts of vitamin E had a slightly reduced risk for late AMD, compared to those consuming the least amounts.(Chiu et al., 2009, Delcourt et al., 1999) Despite these initial encouraging results, research from the Beaver Dam eye study, the NHS and HPFUS study, and the women's health study (WHS) group, which involved a total of approximately 50,000 participants did not find any relationship between vitamin E levels and AMD risk. (VandenLangenberg et al., 1998, Cho et al., 2004, Christen et al., 2010)

Hence, taken in totality, current data from clinical trials does not support a significant effect of vitamin E alone on AMD.

(v) Multivitamins (AREDS preparation):

It was hypothesized that the consumption of several groups of different vitamins would be more effective in their mode of action compared to a single vitamin.(Weikel et al., 2012) Several studies have demonstrated consistently high levels of carotenoids, vitamin C, and vitamin E contributed to reduced risk of neovascular AMD when used in combination.(1993) The AREDS study tabulated a compound score to compare overall diet to the risk for AMD and the compound score included intake of vitamin E, C, zinc, lutein/zeaxanthin, DHA, and EPA.(Chiu et al., 2009) The subjects with the highest score had a reduced risk for drusen (OR=0.75; 95% CI:0.60, 0.93, p=0.048) and late AMD (OR=0.58, 95% CI:0.40, 0.82; p=0.002). Results from the AREDS study also

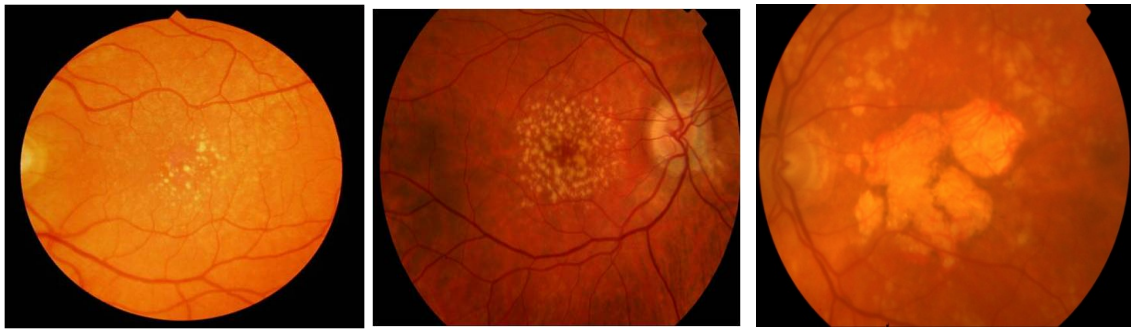
demonstrated that supplementation with a cocktail of beta-carotene, vitamin E, vitamin C, zinc and copper reduced progression from intermediate to advanced AMD (exudative form) by 34% over 6 years of follow up. (Chiu et al., 2009) That said, several authors have disputed the role of zinc in relation to its purpose to delay the onset of AMD. Results from AREDS 2, with the addition of lutein and zeaxanthin were largely equivocal.

Despite the hint that multivitamins may delay onset of exudative AMD, there was no substantial evidence to conclude that multivitamins play a role in dry AMD.

(vi) Statins

Several epidemiologic and genetic studies have found similar risk factors for both AMD and atherosclerosis. This led to the speculation that statins, long known for their beneficial effects on patients with atherosclerosis and hyperlipidemia, may have a protective role in AMD. This hypothesis on the pharmacological mechanism of action of statins in preventing AMD was based on their serum lipid lowering effects, hence altering the structure of BrM and preservation of the choroidal vasculature by protection against atherosclerosis and the anti-inflammatory properties of statins.(Penfold et al., 2001, Friedman, 2004) Prior work demonstrated that statins reduce plasma levels of VEGF by altering the transcription factors involved in VEGF production.(Dichtl et al., 2003) VEGF is an important mediator in the development of choroidal neovascularisation. There were only two other trials which have evaluated the effect of statins on stages of AMD, and they did not demonstrate that statins have a beneficial role.(Guymer et al., 2005)

Figure 1.14 Progression of AMD



Dry/Early AMD →
(multiple small or
intermediate drusen)

Intermediate AMD →
(extensive drusen)

Advanced AMD
(Geographic Atrophy involving the
fovea or Sub-fovea Choroidal
Neovascularisation)

1.7 Problems and Aims at Commencement of this Thesis

1.7.1 Problems

AMD is and will become increasingly prevalent with increasing life span of the population, especially in developed nations. This effect of this will be the surmounting indirect and direct costs both because of treatment (antiVEGF in exudative AMD) and the social costs attributed to blindness. As mentioned earlier, there is no proven prophylactic therapy to delay the onset of AMD. The AREDS1 study have shown minimal advantage of multivitamins (vitamin C, E, Zinc) to delay onset of wet AMD, although several investigators have disputed the role of Zinc. Studies targeting carotenoids with zeaxanthin, lutein etc have equivocal results.

The biggest risk factor in AMD is ageing, therefore, theoretically if the ageing processes in the outer retina were delayed or reversed, the onset of AMD would be significantly delayed. Ageing in the outer retina results in debris in the retinal pigment epithelium and the BrM. It appears that this deposition of debris affects transport of metabolites into and water and waste out of the retina respectively. There is limited evidence that migration of the RPE cells induces release of enzymes which allow the cells to release their hemidesmosomal complexes with BrM and such enzymes also initiate removal of debris. MMPs have been identified as the major class of agent responsible for maintaining healthy acellular membrane systems throughout the body. The cell death associated with laser irradiation of the RPE is known to initiate cell migration within 4 to 7 days of irradiation and in turn this is associated with enzymatic release. Currently, laser parameters used clinically result in collateral damage to photoreceptor cells. To minimize such damage, the pulse duration of lasers have been reduced to microseconds. Whilst this minimizes primary damage, secondary damage may occur as a result of contiguous areas of RPE cells being damaged, thereby resulting in overlying areas where the photoreceptor cells is deprived of nutrients.

The unique configuration of this laser aims to first limit the secondary damage and second, to increase the efficiency of MMP release by increasing the effective circumference available for RPE migration. Although in reality the RPE migration really may involve 4 to 5 layers of RPE cells, for simplicity purposes, the following effective circumference calculations will be based on a single layer

of the peripheral circumference of RPE cells. For example with a Gaussian beam of 400 μ m spot size laser beam, a calculated estimate of effective circumference for RPE migration from laser injury would be 1200 μ m. This would be equivalent to 30 RPE cells (using a lateral dimension of approximately 40 μ m). With an estimated 10 to 15% discrete RPE injury in a discontinuous laser beam, it was expected that there would be a discontinuous areas of RPE injury within the 400 μ m spot size, hence increasing the effective circumference available for RPE migration and biochemical releases of enzymes.(Figure 1.15) This effective circumference of RPE cell migration is a crucial factor in determining the level of MMP release for clearing up of the debris and improving transportation across the BrM. There is minimal evidence that first, laser injury to the RPE results in MMP release, and second the effect of MMP on transport across the BrM. It is postulated that the number of laser spots and laser energy play a role in defining the volume of RPE injury. It is proposed that the number of laser spots have greater effect than laser energy given that a higher energy will result in a higher zone area of RPE damage and less circumferential region for RPE migration and release of enzymes, in addition to the secondary laser damage.(figure 1.15)

Guymer and team in Australia, at the time of commencement of this thesis, was in the initial stages of a pilot study whereby 12 clock hour laser lesions were proposed as the treatment algorithm and flicker perimetry was used as the primary treatment outcome. It is in question whether this minimal number of lesions would have any effect on the macular and the sensitivity of the flicker perimetry to monitor response given the paucity of published data.

When the design of this PhD was initiated, there were no other published clinical assessments of the 2RT laser used in human subjects. With the 12 clock hour lesions, the initial pilot study in Australia had been deemed inappropriate due to the misconception of the treatment algorithm and the use of changes in flicker perimetry to define their outcome. In reality, in early AMD, there are few clinical tests that are sensitive enough to determine subtle changes expected in this select group of patients. This becomes a problem in the design of clinical trials to monitor treatment response. Most clinical trials is almost exclusively dependent on VA changes, however, the problem arises when subjects enter the trial with 6/6 vision and otherwise asymptomatic.

In essence, there are several problems concerning the laser configuration of the 2RT laser and its use in early AMD that have been identified in this thesis. The following lists the problems at time of commencement of this thesis:

Problem 1: Laser is an ideal modality to cause RPE injury and initiate the migratory processes with secondary release of factors such as MMPs and cytokines etc. However, as mentioned, laser in the current form (milliseconds) was found to result in collateral primary damage to the adjacent layers. It was discussed that the nanosecond time domain would be effective in causing limited damage, however, with the large area of irradiation, it would be subject to secondary damage. The 2RT laser with its speckled beam configuration was designed to allow discontinuous injury to the RPE cells in a 400 μ m spot size, with the aim to circumvent this problem. No previous studies have been attempted to qualify this laser beam profile and its effect on the RPE.

Problem 2: Although it was known that that RPE migration results in MMP release which in turn clears up the debris, there is still uncertainty about the minimum volume of RPE migration required for MMP release for BrM 'clean up'. Limited in vitro experiments have shown that MMP is released from RPE migration post laser, but this needs to be ascertained.

Problem 3: Although preliminary studies of measurements have been made on MMP release, the directionality (ie, apical or basal) and time sequence has not been fully studied.

Problem 4: From the experiment by Ahir et al, it was shown that exogenously applied MMP result in increased hydraulic conductivity across the BrM. However, the effect of varying levels of MMP on the BrM with age has not been studied. It is critical to understand the therapeutic impact of MMP especially in the elderly, which will have implications on defining possible treatment algorithm for using the 2RT laser in delaying onset of AMD.

Problem 5: There had been minimal data on the use of this novel laser in human subjects with AMD and the only pilot study by Guymer et al was inappropriate in terms of the their treatment algorithm with 12 laser lesions.

Hence, there is a lack of information with regards to the use of this laser in human subject and its effect in AMD patients to prevent or retard onset of AMD. Also, the treatment algorithm for this laser as a treatment modality is poorly defined.

Problem 6: In terms of clinical assessment, there is currently no easily available tool to evaluate the functional deficit in very early AMD patients, which will make interpretation of structural or functional evaluation of pre and post treatment difficult.

Given these problems, several aims of the thesis were set out in the chapter following.

Figure 1.15 Concept of quantitative MMP release

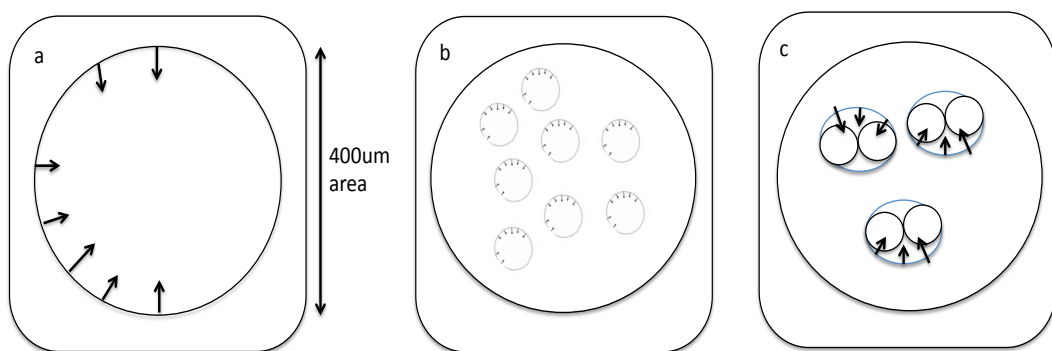


Figure 1.15 is a pictorial representation of the concept of increased efficiency of MMP release per unit circumference of RPE injury. In figure a., a 400µm spot size has a limited available circumference of MMP release from RPE cell migration. In figure b, the discrete RPE damage allows multiple simultaneous areas of RPE migration for MMP release. Figure 1.15c represents a theoretical model of increasing laser energy. With higher, the zone of RPE damage will cause coalescence of laser lesions, thereby forming a larger area of laser damage, again, with the compromise of available circumference for RPE migration, with the added risk of secondary laser damage.

1.7.2 Aims and Objectives

In addressing the above problems, this thesis has been structured into 2 main parts; Part 1 involves laboratory investigations, which aimed to determine the following:

- a. the laser beam configuration of the 2RT laser;
- b. the impact of the nanosecond laser on release of MMPs;
- c. the type, direction and time sequence of release of MMPs;
- d. the effect of varying levels of MMPs on hydraulic conductivity across the ageing BrM
- e. defining a treatment algorithm for clinical use

Part 2 of the thesis would be the clinical evaluation of the use of this laser in delaying the progression of AMD. Ideally, this should have been done in patients without the signs of early AMD, ie druse, hence, targeting to delay the ageing physiology. However, due to constraints of ethics, the clinical evaluation was done in early AMD patients. The clinical assessment of the use of the novel laser in early AMD undertaken was involved in determining the following:

- a. the efficacy of this laser to delay progression of AMD; and
- b. the damage and/or limitation of damage of this nanosecond laser in AMD patients, ie, 'safety'.

During the conceptual stage of design of individual experiments to determine the above objectives, the following detailed main, secondary, tertiary and quaternary aims were defined in accordance to the problems identified.

The first main aim concerning Part 1 of this thesis involved assessing the laser beam design and its impact on RPE.

Main aim: To evaluate the viability of the design of the discontinuous nanosecond to prevent secondary laser damage.

Secondary aims:

1. To assess the beam energy distribution of the 2RT laser on homogenous targets.

2. To evaluate the morphology of laser damage on heterogenous targets such as biological tissues and/or the RPE.

Tertiary aims:

1. To determine the diameter of laser damage as a function of laser energy.
2. To evaluate the effect on energy levels on the effective circumference for RPE migration.
3. To determine the ED50 plot of this laser on damage thresholds.

Quaternary aim:

1. To assess the effectiveness of various methodologies to determine visual damage of the RPE cell.

Before problem 2 may be addressed, it would be important to understand the baseline characteristics of the release profiles of MMP. Hence, an experiment was designed with the following aims:

Main aim: To determine the baseline characteristics of MMP release

Secondary aims:

1. to determine the baseline profile of MMP in an in vitro model using RPE-BrM choroid explant culture

Tertiary aims:

1. To determine the types of MMP release;
2. To determine the time course of MMP release;
3. To determine the direction of MMP release;

Quaternary aim:

1. To assess if there may be differences in MMP release characteristics profile between different species.

After the determination of a baseline MMP profile, problem 2 and 3 may be addressed.

Main aim: To assess the impact of the nanosecond laser on MMP release

Secondary aims:

1. To determine if MMPs are released post laser application in an in vitro model of a RPE-BrM choroid explant culture model;

Tertiary aims:

1. To determine the type of MMP release;
2. To determine the temporal sequence of MMP release;
3. To determine the direction of MMP release;

Quaternary aims:

1. To determine the effect of varying laser parameters on MMP release in the in vitro model

To address problem 4;

Main aim: To evaluate the effect of varying levels of MMP on transport across the BrM

Secondary aim:

1. To evaluate the effect of activated MMP on transport across BrM.

Tertiary aims:

1. To assess the impact of varying quantity of MMP on transport across the BrM.
2. To determine the impact of activated MMP on transport across the BrM as a function of age.

Quaternary aims:

1. To correlate the minimal level of activated MMP required for increasing transport across the BrM in the elderly age group; if any.
2. To correlate the minimum RPE injury required for increase in transport across the BrM in the elderly age group; if any.
3. To determine the laser parameters for clinical use.

The second part of this thesis clinically evaluates the use of this laser in early AMD patients. The main objectives were to evaluate the efficacy and safety (ie, limitation of damage as compared to conventional lasers) of the 2RT laser for clinical use, in patients with early AMD. To address the identified problems, a clinical trial (RETILASE) was designed. However, for the purposes of this thesis, the data obtained was analyzed differently from as set out in the trial protocol, to allow more in depth and scientific evaluation of the information gathered.

The following aims were intended to evaluate the effect of the 2RT laser on human subjects with AMD

Main aim: To clinically evaluate the use of the current laser system to delay progression of AMD.

Secondary aims:

1. To determine changes in visual function tests (visual acuity, contrast sensitivity, microperimetry, flicker perimetry) at 6 and 12 months
2. To determine the proportion of cases treated which converted to advanced AMD.

Tertiary aims:

1. To evaluate the changes in druse morphology post laser at 6 and 12 months.

As mentioned earlier, there is minimal information with regards impact of the 2RT (and/or limitation of damage) on human subjects. The word 'safety' may be used synonymously for the purpose of this thesis.

Qualitative and quantitative analysis of data obtained from clinical imaging in the trial were performed with the following aims.

Main aim: To evaluate the impact of the 2RT laser on human subjects.

Secondary aims:

1. To investigate the limitation of collateral damage (axial damage) of this laser system in human subjects;

2. To investigate the 2RT laser damage on RPE layer in human subjects.
(in view of a possible speckled laser beam configuration)

Tertiary aim:

1. To investigate the functional changes over laser lesions in the macular of human subjects.

Part 1

Chapter 2. Assessment of the Discontinuous Beam Energy distribution/ “Speckled Laser Beam” of the 2RT Laser

2.1 Introduction

The 2RT laser was theoretically designed to limit the primary and secondary laser damage by using a nanosecond time domain and a speckled profile across the laser beam.

The fact that axial laser damage decreases with decreasing time domain is well accepted.

As mentioned earlier in the Introduction chapter (chapter 1), the laser design with its discontinuous beam configuration would minimize the risk of having secondary damage by preserving some cells throughout the irradiated area. This beam energy distribution profile of the 2RT laser has not been evaluated. In this chapter, the main aim would be to assess the viability of the 2RT laser beam to prevent secondary laser damage. It is known that retina laser therapy is a linear process that is dependent on the transmission properties of the laser and the absorption by the biological tissue. To facilitate the evaluation of the laser beam at transmission and absorption, experiments will be performed to analyze the laser beam profile on homogenous and heterogenous targets. This will be further discussed under methods and materials sub-chapter.

Lasers with ultrashort pulse time domain (ie, nanosecond) were found to have high peak energy which can cause secondary break in BrM and subretinal bleed. This may be avoided by increasing the area of laser irradiation to allow a spread of laser energy. The 2RT laser has a large spot size of 400 μ m. The effect of laser damage as a function of laser energy has never been determined. A secondary intention of this chapter would be to evaluate the diameter of laser damage with different laser energies and to determine the ED50 for this laser.

2.2 Methods and materials

2.2.1 Physical modelling of beam energy distribution of the 2RT laser

Physical modeling of the beam energy distribution of the 2RT laser was performed in 3 ways (Figure 2.1):

1. By directly assessing the laser beam,
2. By applying the laser on a homogenous target. The homogenous target used in these experiments was neutral density filter (NDF).
3. By assessing the laser beam after it has passed through a NDF.

2.2.1.1 Assessment of laser beam profile

To preliminarily assess the laser beam profile, laser shots were recorded using a video recording system (HD(720p) up to 30 frames per second and 5 mega pixel camera, Iphone 4). The laser shots were aimed at the camera pinhole in a dark room. The 2RT laser prototype, which has a larger range of energies in the range of 0.3mJ to 1.2mJ, was used. Only few laser shots were taken at 0.5mJ to protect the camera (for subsequent use) from over-exposure to laser beam which would damage the camera.

Post recording, video editing on imovie (MacIntosh system) was done to obtain photograph of individual laser shots of varying energy levels. The images were saved as TIFF files. Individual images of laser shots were imported into the National Institute of Health (NIH) Image J(vers 1.44o) program. After importing the image, the black and white colors were inverted to allow a greater contrast of the images. The edge of the laser lesion was identified and a line was drawn across the middle of the laser beam from end to end using a 'straight line' option in the tool box. This program measures distance in terms of pixels. As such, the unit length was set to 400 μ m, under 'scale', given this was the presumed laser spot size. A plot profile could be obtained using the 'plot profile' sub-category under 'Analyze' on the Image J software. The plot profile obtained would have a 'relative transmission value' in the y-axis.

2.2.1.2 Laser application on Neutral Density Filter

Neutral density filter (Kodak) was used as a homogenous target to determine the transmission of the laser beam. In this experiment, a ND 0.6 was used. The filter was mounted on the headrest of the 2RT system and attached with a cellophane tape. Laser application of varying energy levels 0.6mJ to 0.1mJ, were applied vertically in a row, in ascending-descending order. (Figure 2.2) Each laser lesion was applied 1 spot size apart. Images were taken on Leica microscope (DMC2900) camera at 40x magnification.

2.2.1.3 Assessment of laser beam profile through a neutral density filter

To obtain a full range of energy profile of the laser beam, video recording described in 2.2.1.1 was repeated after the laser beam has been attenuated by NDF. NDF 0.3 was used. The reason why a different NDF stop was used was simply because of its availability during time of experiment. Laser was applied in the range of 0.3mJ to 2.0mJ.

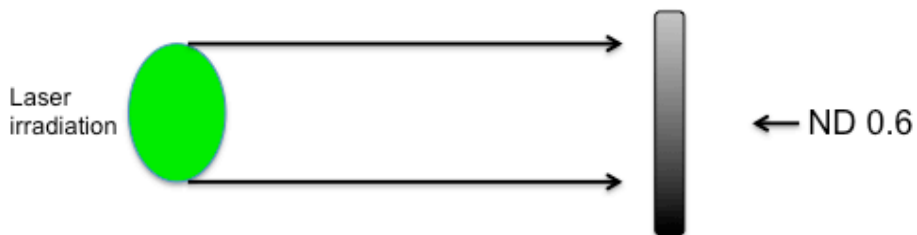
Individual images of laser in varying energy levels were extracted from imovie (as per 2.2.1.1) and imported into image J. In this series, both the images on corresponding NDF and from laser beam were analyzed. Further analysis was undertaken for the laser beam. After obtaining the plot profile for both NDF and laser beam, in image J, under 'image', choose 'color' and click on 'RGB'. This will change the image to red, green and blue colors in accordance to pixel intensity of the image. This was initially done as a 'trial and error' to determine if there might be a difference in intensity of the laser beam with different energies. However, after analyzing multiple images of increasing range of energies (approximately 2-3 images per energy, from 0.3mJ to 2.0mJ), it was noted that the color differentiation may correspond to a presumed differential laser energy intensity, ie, with higher laser energies, there is larger area of red, followed by green and blue depicts least intense areas of laser energy.

Figure 2.1 Pictorial demonstration of physical modeling of energy beam distribution of the 2RT laser

1. Assessment of laser beam profile



2. Assessment of laser beam profile on a homogenous target



3. Assessment of laser beam profile after passing through a NDF.

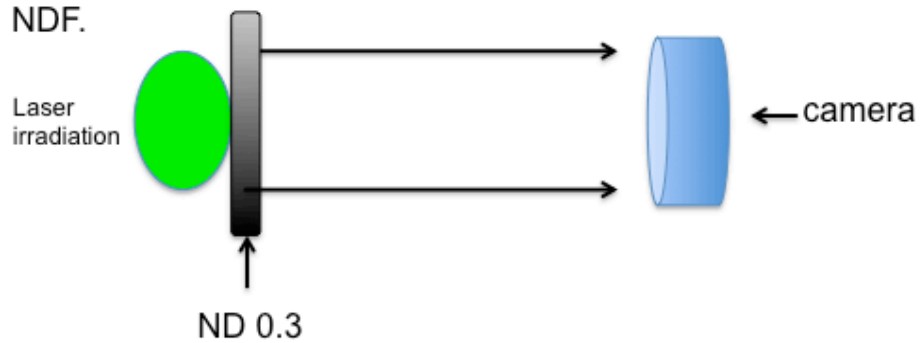
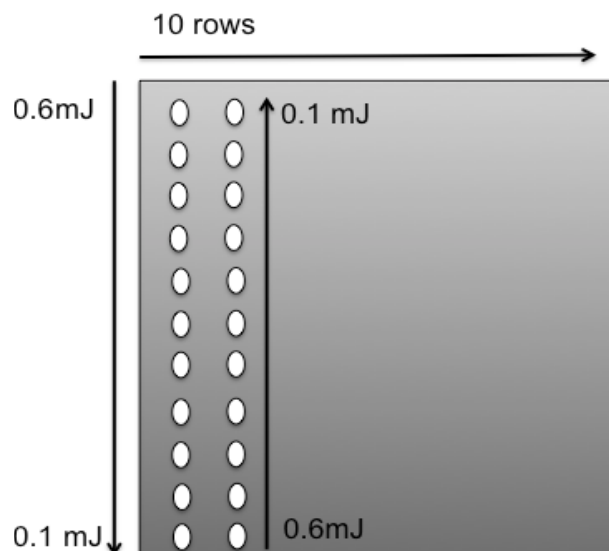


Figure 2.2 Pictorial demonstration of laser application in varying laser energy levels in porcine flat mount



2.2.2 Assessment of Biological Effects across the Lesions Produced by 2RT laser on Porcine RPE

2.2.2.1 Dissection porcine eyes

Fresh porcine eyes were obtained from a local abattoir before steaming and experiments were initiated within 12 hours of death. Whole globes were first briefly rinsed in antiseptic solution before dissection. A circumferential incision at the pars plana was made to remove the anterior segment, lens and vitreous. The retina was gently peeled away thereafter. The leaves the remaining posterior pole with an intact RPE-BM-choroid-sclera which was held in an 'eye' cup (quail egg cup) and affixed using pins to a hard cardboard which was attached to the head rest of laser machine by multiple cellophane tapes. The height of the explant to the laser beam exposure was adjusted by moving the cardboard. The surface exposing the RPE surface was facing the direction of laser beam

2.2.2.2 Laser application

The laser treatment was performed using the clinical slit-lamp delivery system of the 2RT system (Ellex Medical, Australia).

In the samples, laser energy was delivered in a vertical manner towards the optic disc from high energy (0.45mJ per exposure) and reduced sequentially by 0.05mJ per exposure. This was repeated in the opposite direction, forming 2 rows of 8 laser spots each. (Please refer figure 2.3) Spot size of the laser was 400µm in diameter. Each application of the laser was 2 spot size apart. Based on the investigator's brochure for the 2RT laser from Ellex Medical, the visual threshold for the 2RT laser was above 0.30mJ. As such, visibility of the sub-threshold lesions at lower energy levels can be identified as lesion between adjacent 'markers' of higher energy. (Please refer to figure 2.3)

A separate application of millisecond laser, 100µm, 5.57J/cm² (Valon) was applied on a separate flat mount.

Post laser, the tissue samples were immediately fixed in 2.5% glutaraldehyde solution.

Figure 2.3 Pictorial demonstration of laser application in varying laser energy levels in porcine flat mount

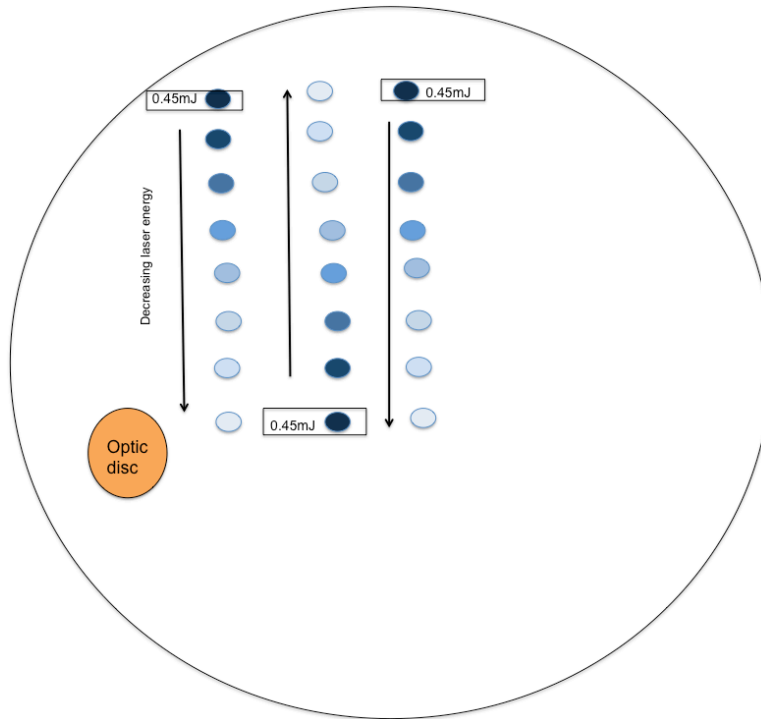


Figure 2.3 demonstrates the method of laser application for the flat mount histology. Laser is applied from high (0.45mJ) to low (0.10mJ) and in the opposite direction in the adjacent row. This allows easy identification of the subthreshold low energy lesions between 2 higher energy lesions which can be taken as 'marker lesions'.

2.2.2.3 Flat mount histology

Post laser, the tissue was fixed in 2.5% Gluteraldehyde buffered in 0.1M Sodium Cacodylate Hcl buffer pH 7.4 with Calcium Chloride 1mg/ml for one hour. It was then rinsed in 0.25M Cacodylate-sucrose buffer with Caclium Chloride 1mg/ml before further dissection of the tissue under dissecting microscopy. The RPE layer was peeled off and dehydrated through ascending series of ethanol concentrations in water - 20%, 50%, 70%, 90% and 100%. The tissue was then cleared in xylene and mounted with XAM on a microscope slide.

Images were then taken using an upright Leica microscope with camera (DMC 2900) at 20x magnification.

2.2.2.4 Measurement of diameter of laser damage

The largest diameter of laser damage was measured the built-in scale (reticule) within an eye piece of the microscope. The measurements were made with direct observation of the scale under the microscope at magnification of 20x. Size of sample is calculated by size noted on reticule, divided by 'Magnification of Microscope'. For example, if the measurement of diameter of laser damage on the reticule measures 4mm, using a microscope magnification of 20x, the 'real size' of sample will be calculated to be 200 μ m.

2.2.2.5 RPE viability

Calcein AM is a cell-permeant dye that can be used to determine cell viability in most eukaryotic cells. In live cells the nonfluorescent calcein AM is converted to a green-fluorescent calcein after acetoxymethyl ester hydrolysis by intracellular esterases. Calcein AM dye test was performed on 0.1mJ and 0.30mJ laser lesions on porcine eyes to determine if there was a discrete pattern of RPE cell death as hypothesized with this laser design. The areas that appeared black signified RPE cell death.

2.2.2.6 Determination of ED50 of 2RT laser

To determine ED 50 of 2RT laser on porcine RPE invitro, laser shots were applied as per figure 2.3 from 0.6mJ to 0.1mJ in a vertical direction. 10 rows of laser were applied, adjacent rows in ascending and descending order of laser energies. Clinically visible laser spots were observed under the slit lamp system of the 2RT laser.

A dose response curve is frequently used in studies determining laser impact on biological tissue. Examination of the slope of the dose response curve may be expressed in terms of a probit plot of a collation of experimental data. By definition, a probit analysis is a type of regression used to analyze binomial response and is used to analyze dose-response experiments.(Finney, 1952)

The ED 50 is a value referred to as the “threshold” which is a reference point on the probit plot, representing a 50% probability of biological injury.

To determine the ED50 of the 2RT laser, the percentage of clinically visible laser spots were tabulated and a probit curve was plotted to determine in vitro ED 50 of the 2RT laser in terms of visibility threshold.

2.3 Results

2.3.1 Physical Modelling of Energy Distribution of 2RT Laser

2.3.1.1 Assessment of laser beam profile

The laser beam profile was assessed at 0.5mJ. The center of the laser beam was noticeably homogenous with increasing scatter towards the periphery. The plotted profile of the laser beam shows a Gaussian-type laser beam with noise.

Figure 2.4 Analysis of laser beam profile at 0.5mJ

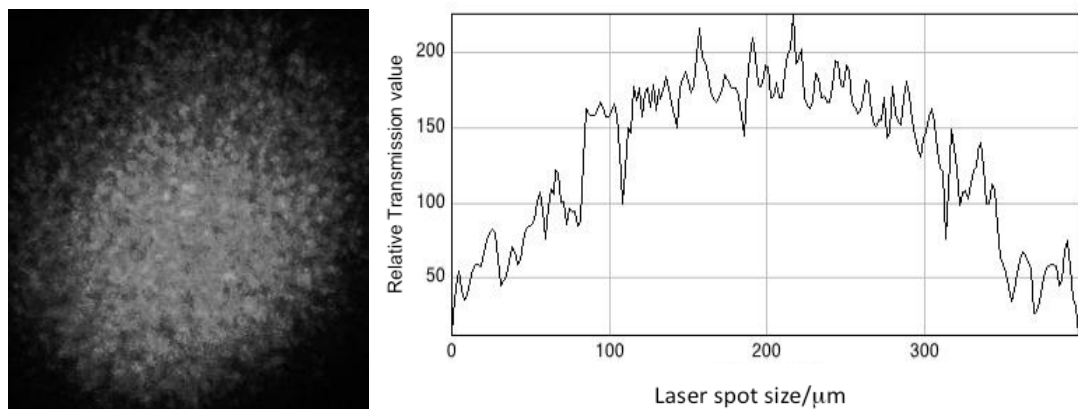


Figure 2.4 shows the imaged laser beam and the beam profile at 0.5mJ. Note that the center of laser beam appears homogenous and the beam profile analyzed appears Gaussian-type with noise.

2.3.1.2 Results from Neutral Density Filter analysis of 2RT laser beam

The images below show the laser uptake on ND 0.6 gelatin filter. NDF microscopic images (figure 2.5) allowed the visualization of damage and showed correlation with beam energy distribution.

It was noted that the size of laser lesion was approximately the same through the differential energy levels.

At high energy levels, from 0.35 to 0.60mJ, the laser beam appeared to have a homogenous center. From 0.35mJ to 0.10mJ, there seemed to be an increasingly 'speckled' appearance. (Figure 2.5) However, the spatial distance between each speckle, even at the lowest energy (0.1mJ) was insufficient for differential damage to the RPE cells. (Figure 2.6)

Figure 2.5 Impact of varying 2RT laser energy on gelatin Neutral Density Filter

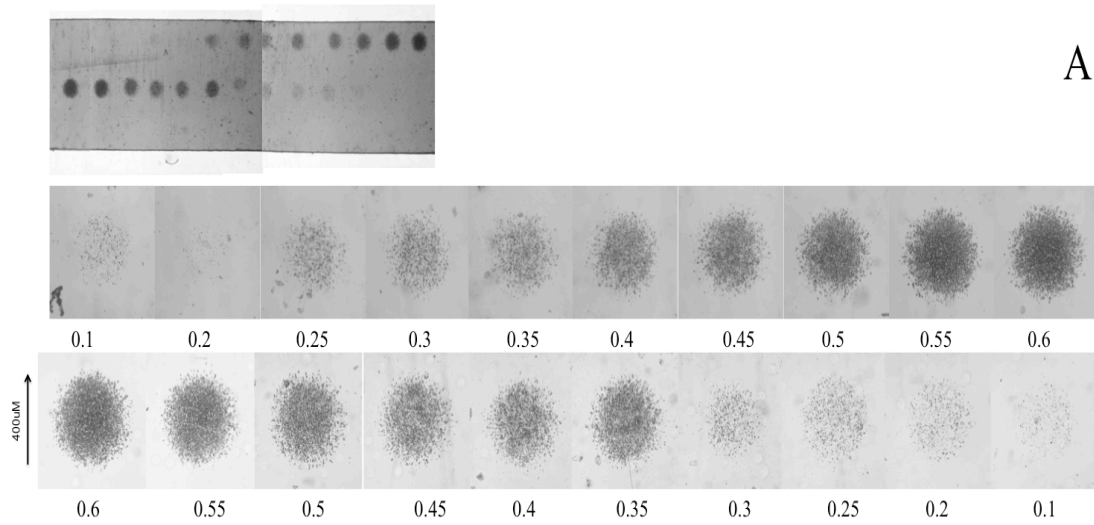


Figure 2.6 Enlarged image to demonstrate speckle profile of laser beam on NDF at 0.1mJ.

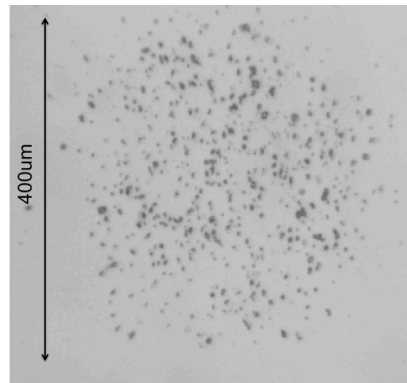


Figure 2.5 shows the NDF microscopy of laser beam in differential energy levels. At lower energies, there appeared to be increasing 'speckle' on NDF uptake.

Figure 2.6 is an enlarged image of laser uptake on NDF at 0.1mJ. Note that although there was 'speckle', the difference in distance between individual 'speckle' was insufficient for differential damage on RPE.

2.3.1.3 Laser beam analysis after passing through a NDF

Laser beam profile was analyzed after passing through a homogenous absorber (NDF 0.3). A range of laser beam energies between 0.3mJ to 2.0mJ was analyzed. Image obtained from NDF was compared with image obtained from laser beam profile. Plot profiles for different energies were plotted using image J(NIH). Plots have been done for every 0.1mJ unit of energy, but only several of the samples analyzed are illustrated below.

3 main zones of laser lesion, shown by the colours red, green, blue were distinctly noted. This could respond to highest area of damage, followed by less lethal damage and sub-lethal damage. Shades of yellow and light blue, may represent 'transition zones.' Red is seen increasingly on the high energy, starting from 0.6mJ (ND 0.3, equivalent to 0.3mJ) in increasing size with smaller areas of green and blue.

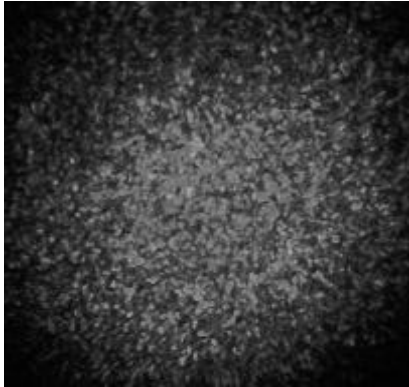
At lower energies, between 0.3mJ to 0.6mJ (after correction for ND 0.3, is equivalent to 0.1mJ and 0.3mJ), corresponding plot profiles of the laser beam show an almost 'top-hat' curve with multiple peaks or 'noise'. This simulates a 'speckled' beam profile, but the inter-peak distance in the plots were too close (<40 μ m). This finding concurred with the previous NDF findings that the spatial differentiation of the current laser beam was insufficient for differential damage on RPE cells.

At higher energies, 0.7mJ to 2.0mJ (after correction for ND 0.3 is equivalent to 0.35mJ to 1.0mJ), curves simulating Gaussian-type distribution were noted.

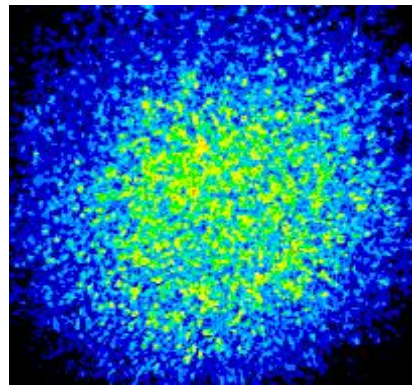
Figure 2.7 Laser beam analysis

0.30mJ

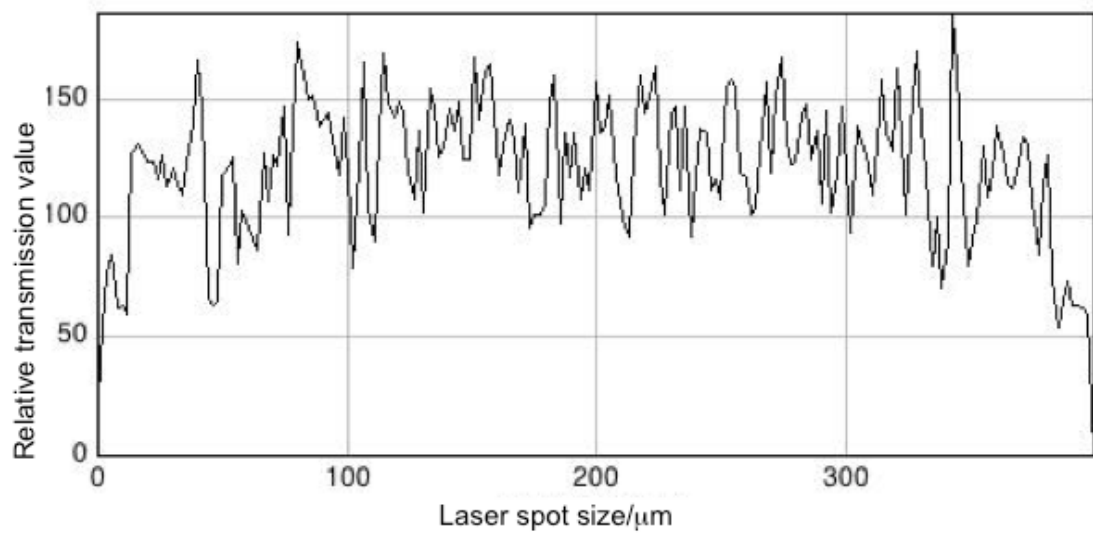
NDF



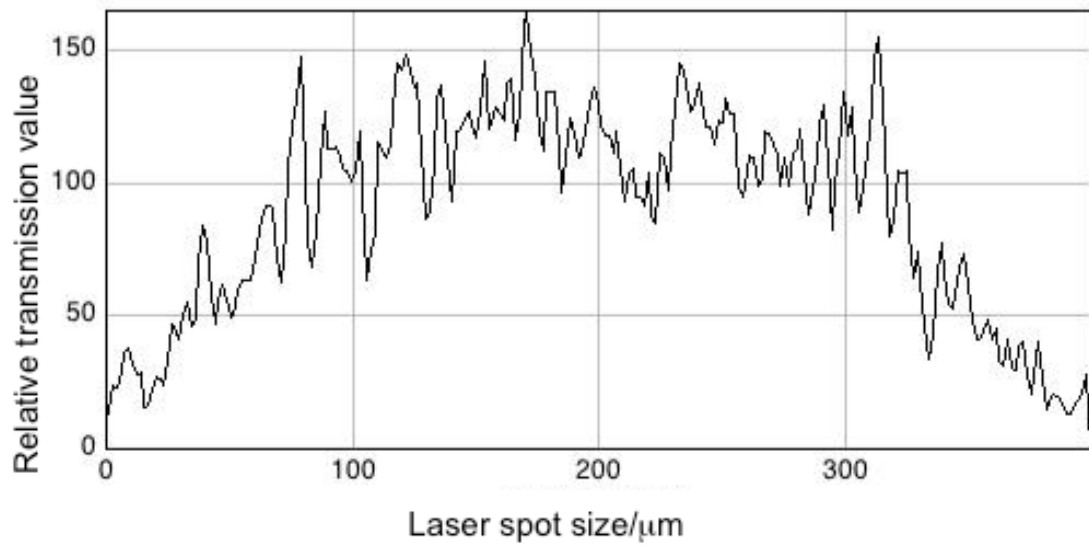
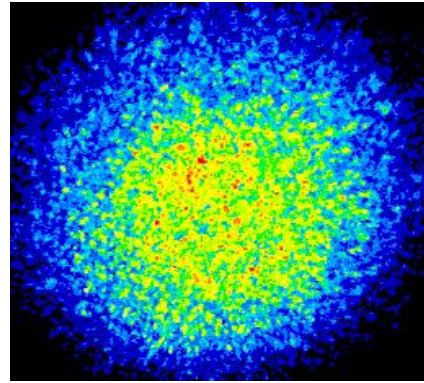
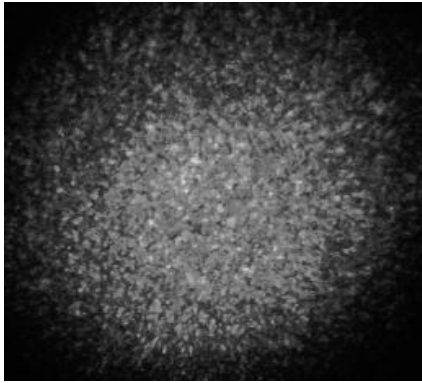
Laser beam analysis



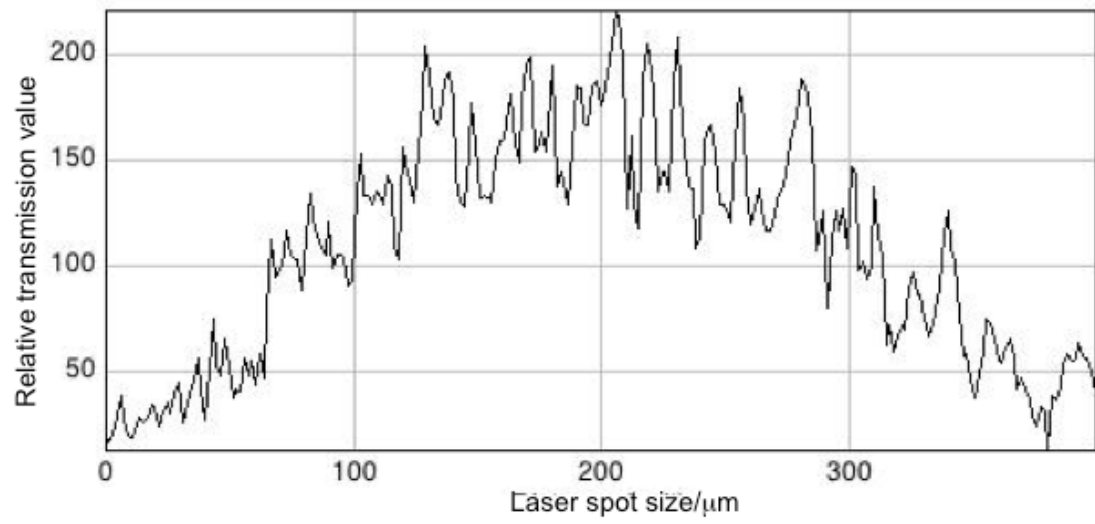
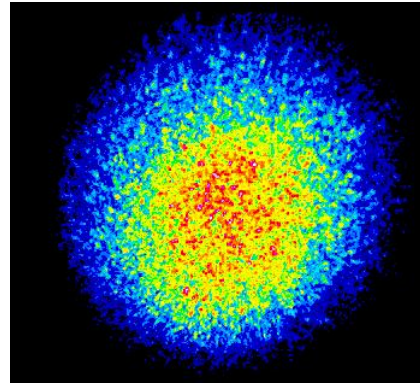
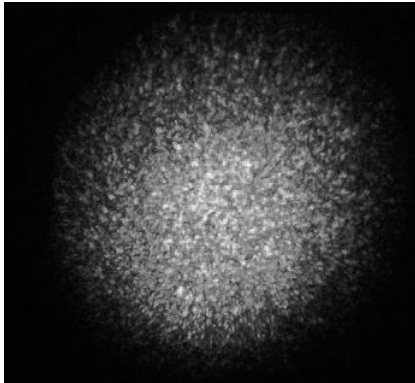
Plot profile of laser beam



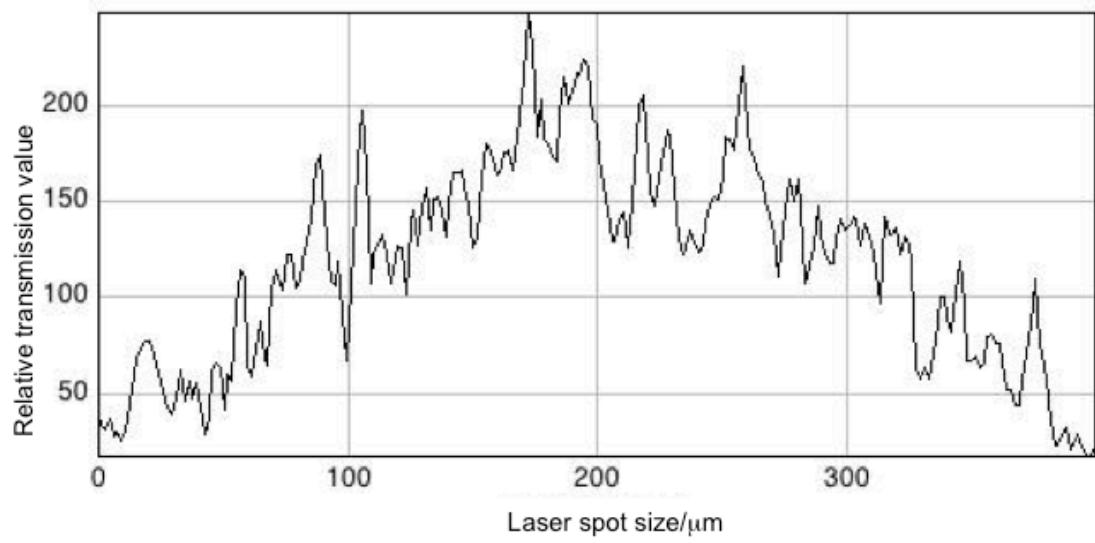
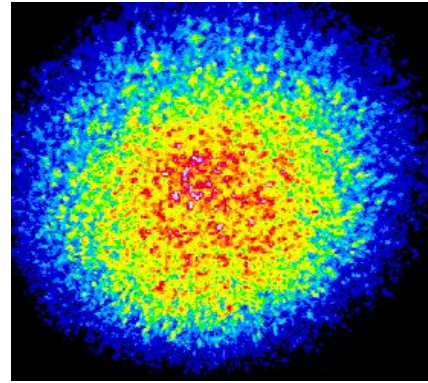
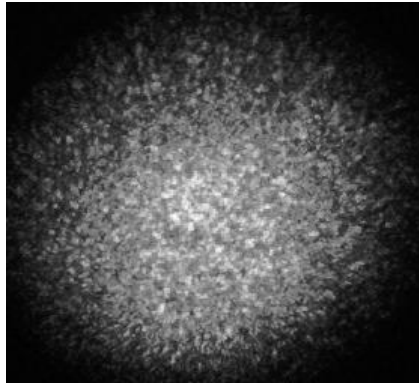
0.70mJ



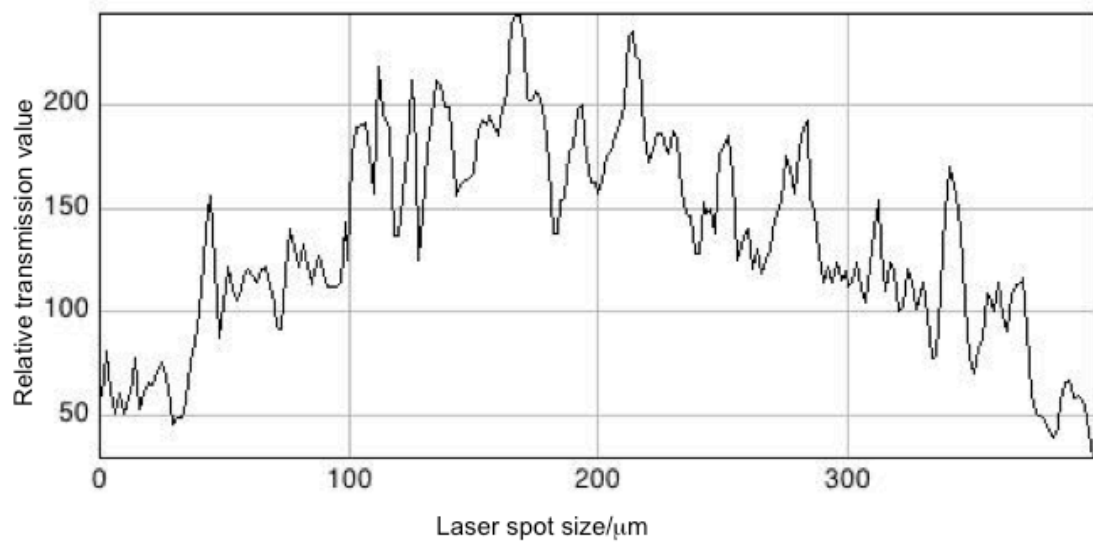
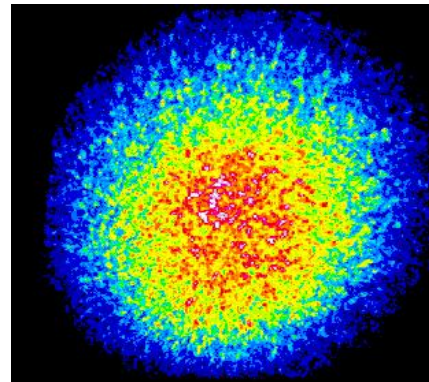
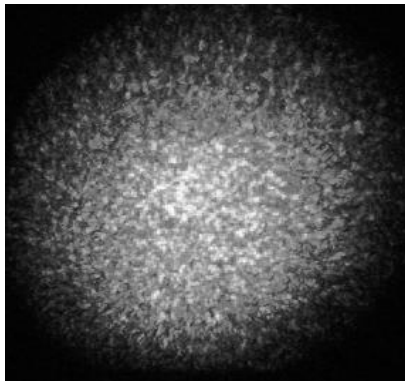
1.2mJ



1.70mJ



2.0mJ



2.3.2 Results from Biological Assessment of 2RT Energy Beam Distribution

2.3.2.1 Diameter of laser damage with varying energy levels on porcine flat mount histology

In this flat mount histology, mean diameter of laser damage across varying energy levels of the 2RT laser were determined. Laser damage was noted to be smaller than the incident laser beam dimension of 400 μm across the range of energy levels studied (0.10 to 0.40mJ). At 0.40mJ, the mean diameter of laser damage is 269.78 (+/-7.59) μm .

The mean of diameter of 2RT laser damage increases with increasing energy, with a range of applied laser energy between 0.10mJ to 0.40mJ. The change in diameter becomes narrower with the lower energy levels. Between 0.1 to 0.2mJ, the change in diameter of laser damage was found to be < 25 μm , which is less than the lateral dimension of a single RPE cell.

In this analysis, it was noted that the diameter of damage could not be accurately measured for laser damage < 0.15mJ as the edge of laser damage is poorly demarcated due to the sub-threshold nature of the laser lesion.

Valon laser applied at 5.57mJ/cm² and 100 μm spot size had a mean diameter approximately equal to size of laser beam (99.70 μm).

Table 2.1 Energy levels versus mean diameter of RPE damage

Energy level	N	Mean Largest diameter/ μm
0.40mJ	4	269.78 (+/-7.59)
0.35mJ	4	243.18 (+/-19.31)
0.3mJ	4	215.4 (+/-3.30)
0.25mJ	3	220.33 (+/-5.51)
0.2mJ	3	197.33 (+/-5.03)
0.15mJ	4	181.25 (+/-11.09)
0.1mJ	6	173.30 (+/-7.76)
Valon (100 μm)	3	99.70 (+/-1.13)

2.3.2.2 Morphology of RPE Damage from the 2RT laser

The morphology of acute RPE damage on flat mount histology corresponded to images obtained from NDF microscopy with the respective energy levels. At 0.4mJ, NDF shows a laser beam with a relatively homogenous center. Histology on porcine flat mount shows a discrete laser burn with loss of individual RPE cell structure. This was surrounded by a ring of highly pigmented RPE cells separated by a ring of empty space between adjacent cells. The morphology of the laser burn is similar to that seen in Gaussian-type lasers. (Marshall, 1970)

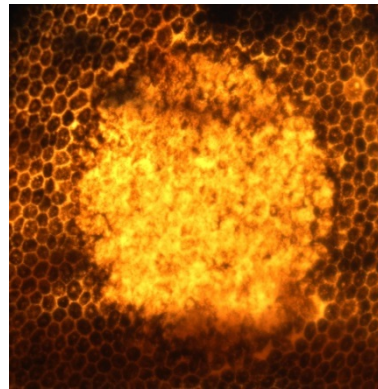
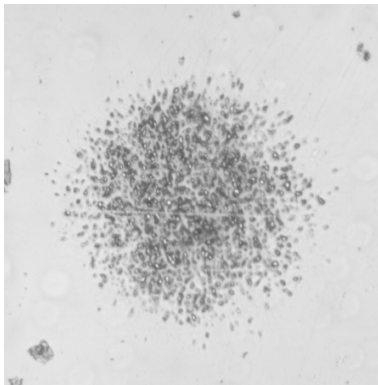
With decrease in laser energy, several changes were noted. First, there was obvious decrease in laser burn size. Also, there was increase in pigmented cells in the laser burn and a smaller proportion of completely damaged RPE cells, with loss of cell structure and pigmentation. At the lowest energies (0.15mJ and 0.1mJ), the edge of laser damage could not be definitely demarcated. There seems to be clusters of sublethal cell death amidst completely destroyed RPE cells on flat mounts without staining.

On calcein AM staining, there seemed to be complete cell death at 0.3mJ. It was noted that there were bright green areas in the lasered areas (Figure 2.8), however, these were likely artefacts as these discrete areas were smaller than an individual RPE cell. At 0.1mJ, there were small clusters of surviving cells, although the small clusters on calcein AM did not match completely with the flat mount. This suggests that most of the cells, although retaining pigmentation and cell structure perhaps have sublethal damage, which was not visible under light microscopy.

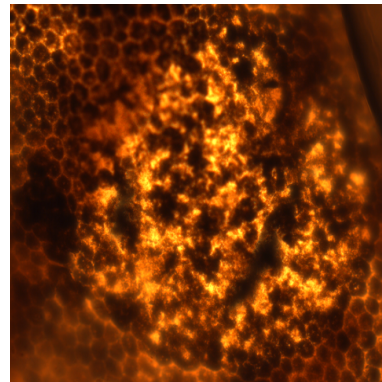
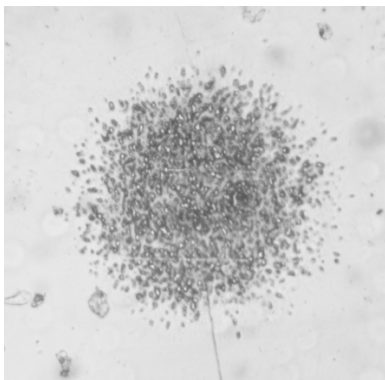
Comparatively, the millisecond laser showed an almost completely blown out laser damage, leaving a ring of pigmentation. This indicated complete cell death. Size of laser damage was found to be approximately the same as laser spot size.

Figure 2.8 Morphology of RPE damage in terms of energy range

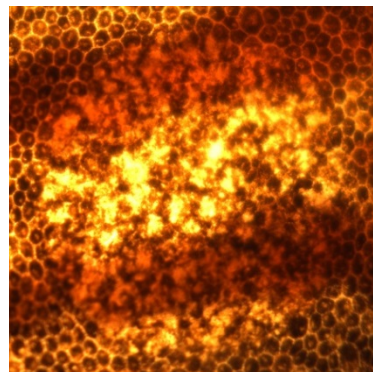
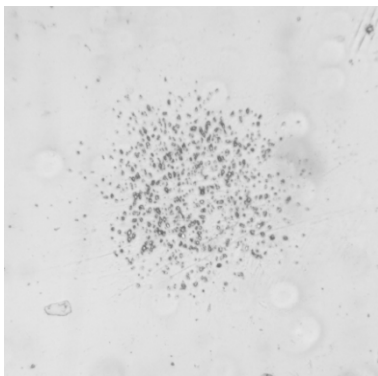
0.40mJ



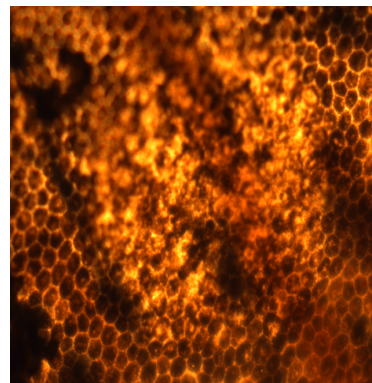
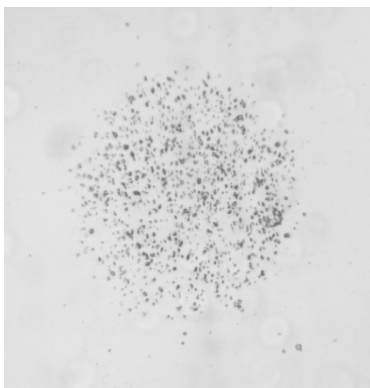
0.35mJ



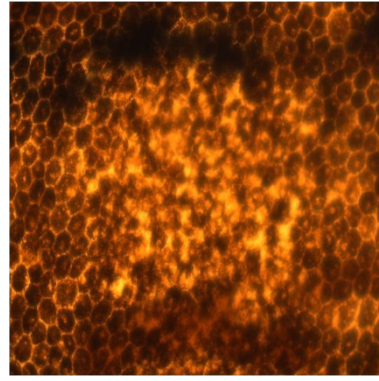
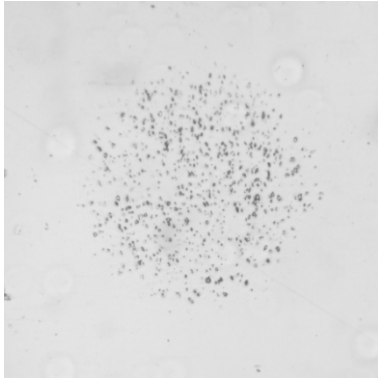
0.30mJ



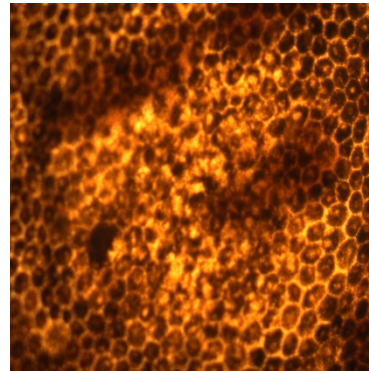
0.25mJ



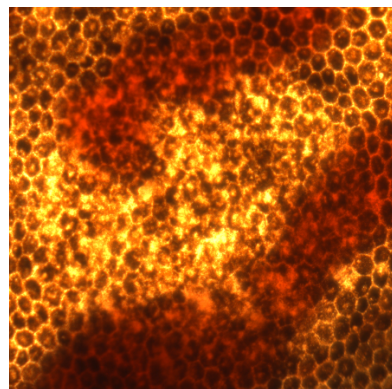
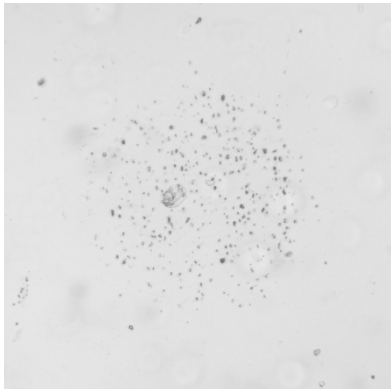
0.20mJ



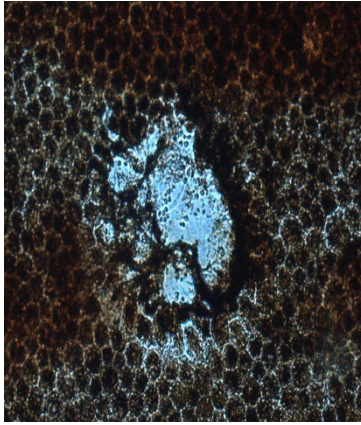
0.15mJ



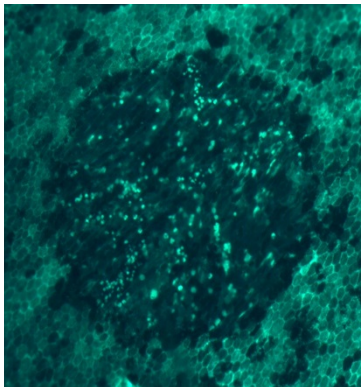
0.10mJ



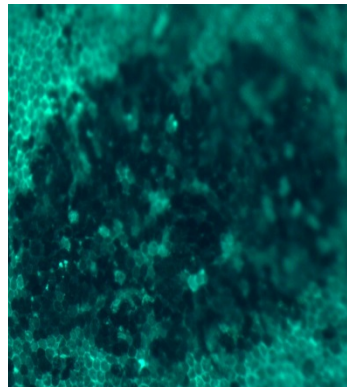
Valon laser



Calcein AM stain



0.3mJ



0.1mJ

Pictures in Figure 2.8 above illustrate laser impact on both neutral density filter and porcine RPE in varying energy levels. All except 0.15mJ has accompanying neutral density filter image. Note the increase in intensity of laser damage with increasing laser energy and the increase in diameter of laser damage. In the calcein-am (live-dead cell assay) pictures, note that in 0.3mJ, there was complete cell death (bright green areas were likely artefacts); and in 0.1mJ, there appeared to be nonconfluent areas of laser RPE cell damage.

Table 2.2 Table describing laser damage morphology on RPE flat mount

Energy	Description
0.4mJ	Discrete laser burn with loss of individual RPE cell structure. This was surrounded by a ring of highly pigmented RPE cells separated by a ring of empty space between adjacent cells.
0.3mJ	A smaller laser burn was noted. There were few pigmented RPE cells in the laser burn which may signify surviving cells. A similar ring of highly pigmented RPE cells noted along edge of laser burn.
0.25mJ	Morphology of laser damage similar to 0.3mJ, but with more pigmented RPE cell in the laser burn.
0.2mJ	Smaller laser burn. Damaged RPE cells with possible sublethally damaged cells seen as pigmented RPE, with intact hexagonal shape. There was a ring of laser damage, but not surrounded by empty cell space between adjacent cells at edge.
0.15mJ	Demarcation of laser damage less obvious. Majority of cells retain hexagonal shape and pigmentation with clusters of RPE cell death. Could signify a mixture of sublethal cell death admist complete cell death.
0.1mJ	Similar change to 0.15mJ

2.3.2.3 Probit analysis of laser damage

Probit analysis was undertaken to determine the ophthalmoscopically visible laser lesion in varying energy levels in porcine ex vivo RPE-BrM explant culture. The 50% cell death based on threshold visibility probit curve was 0.22mJ in this experimental subset for the 2RT laser.

Figure 2.9 Probit curve of exvivo porcine energy levels vs ophthalmoscopically visible threshold

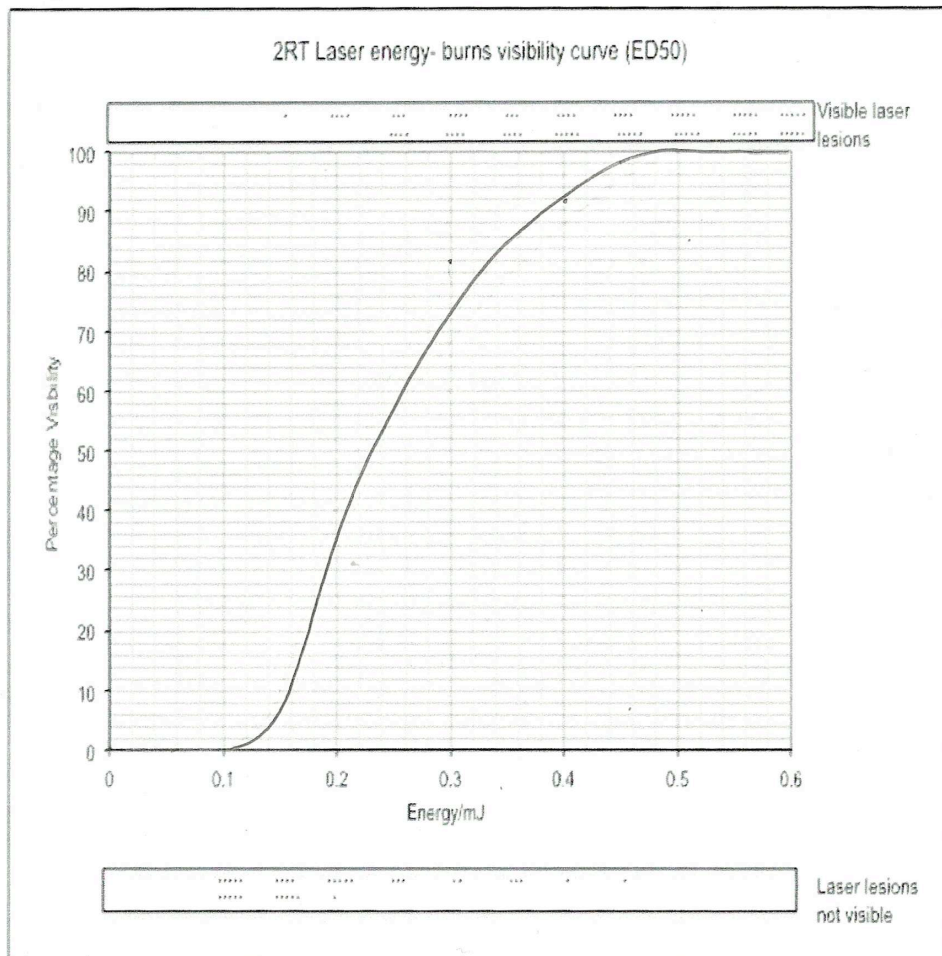


Figure 2.9 shows a probit plot of laser visibility versus laser energy. ED 50 for this set of in vitro experiment on porcine eyes was 0.22mJ for ophthalmoscopically visible lesions.

2.4 Discussion

In this chapter, the profile of the laser beam of the 2RT laser was analyzed using both physical and biological models. The unique design of the 2RT laser aimed to prevent both primary and secondary damage by using a nanosecond laser time domain and a discontinuous laser beam that was designed to preserve RPE cells within an area of laser irradiation.

Results from physical modeling of the laser beam demonstrated increasing Gaussian-like beam profile with higher energy ranges. At energies less than 0.35mJ, there appears to be 'speckling' of the laser beam profile which appeared 'Top Hat' in nature, although the degree of 'speckling' was considered to be inadequate in terms of differential RPE damage. (Figure 2.10)

Figure 2.10 RPE damage from low energy 2RT laser

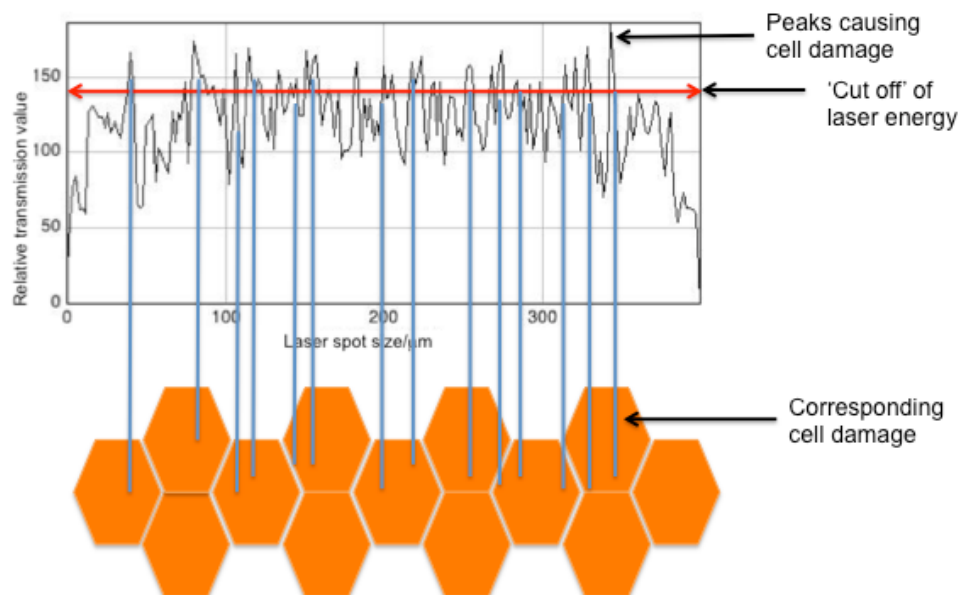


Figure 2.10 demonstrates the possible morphology of RPE damage post 2RT laser at 0.15mJ. The laser energy 'cut off' was set at an insufficiently low level, hence, causing multiple peaks, which were insufficiently separated to cause differential RPE injury.

The current analysis from the porcine RPE flat mount demonstrated acute impact of the 2RT laser, which concurred with findings from the physical modeling. At high laser energies (eg, 0.4mJ), morphology of laser damage showed an almost complete center area of cell death with a periphery row of pigmentation. This was similar to laser burns induced by Gaussian-type beam lasers. With decreasing laser energies, the acute impact of the laser

demonstrated increasing proportion of RPE cell preservation. However, it must be noted that this damage was analyzed at an acute stage and cannot be used to define subsequent changes with time. Hence, it is unknown if these cells were subject to sublethal damage even though they have maintained their cell structure.

Results from the live/dead cell assay (calcein AM) further supported the above results, which show incomplete cell death at low energy levels within irradiated area. Although cell death was incomplete, there appears to be larger proportions of RPE cell death than preservation within the irradiated area which will almost definitely result in secondary laser damage. There is a need to investigate the 24 and 48 hours damage profile of the laser both invitro and in vivo. This is especially so in view of the current findings. It is crucial to determine if the structurally intact cells at low energy on flat mount histology will undergo full death in 24 hours.

Although Wood et al have found similar results in their physical experimental model, they have mistakenly assumed this to be appearance of speckled distribution of the 2RT laser beam when in fact, their own illustrations demonstrate clumping in the center, akin to a gaussian-like laser damage.(Wood et al., 2011) Hence, although similar, the current findings were attributed to a different conclusion

It was noteworthy that in contrast to the millisecond Valon laser (Valon), the laser damage of the 2RT was smaller than the laser beam diameter of 400 μ m, even at threshold and suprathreshold laser energies. There was decrease in size of laser damage with decreasing energy down from 0.40mJ to 0.15mJ. Between 0.10 to 0.20mJ, the difference in diameter of laser damage was found to be smaller than the lateral dimension of a single RPE cell. Hence, it can be argued that within this energy, the effective circumference available for RPE migration for a single laser lesion will be approximately the same.

In this experimental subset, it was found that the ED50 for the 2RT laser on porcine RPE was 0.22mJ. The porcine RPE is a highly pigmented pigmented as compared to human subjects. Furthermore, the experiment was performed after the removal of other energy absorbing structures such as lens, vitreous etc. It is a well-accepted theory that the extent of retinal laser damage is proportionate to degree of retinal pigmentation. (Marshall, Doctor of philosophy thesis) In human, especially in the Caucasian population, the clinical visible

laser lesion could be higher than 0.22mJ. At this level, the approximate diameter of laser damage was 200 μ m. Given that the current results show that the 'speckling' of the laser beam is inadequate, the large diameter of laser damage would imply that secondary laser damage would be unlikely prevented. The question then would be the appropriate level of energy for use. Professor Guymer and the team in Australia, Melbourne had taken an arbitrary value of 70% of the threshold energy level. Threshold in this case would refer to barely visible lesions in human subjects. Calculations based on the ED50 plot obtained in the current in vitro study would obtain a laser energy value of 0.15mJ. There have been suggestions on the use of visible effect threshold(VET) , the setting at which the laser operator first observe an actual effect. This is based on the fact that bubbles were observed at laser treated sites in micro and nanosecond laser energies and produced when intracellular microbubbles coalesce with production of shockwaves. At levels above VET, bubbles often disappeared immediately, while at higher fluence levels, bubbles only disappeared when next laser pulse was applied. VET allows useful titration of laser energy in the clinical setting for individual patients.(Framme et al., 2002, Framme et al., 2004)

Hence, results from different modalities to investigate the topography of the 2RT laser beam did not find an adequately discontinuous or 'speckled' beam profile. An element of Gaussian-type beam with noise was found with increasing laser energy. This suggests that the laser in the current prototype may induce secondary laser damage.

2.5 Conclusions

Combing the analysis of the physical modeling of the laser beam and the biological impact on RPE damage morphology, it may be concluded that the 'speckled' theory in the 2RT laser is held at low energy levels, however, the distance between the speckle is too close for differential RPE injury as intended. Also, increasing laser energy will deviate from 'Top Hat' to Guassian like beams, which will increase noise and become incoherent because of the far greater gradient from center to periphery in the beam.

Although the laser beam configuration did not behave as expected, there is still a need to establish if this current laser in the nanosecond time domain cause any release of MMP by RPE cells and if so, the impact of RPE injury volume on MMP release.

Chapter 3. The Release of Matrix Metalloproteinases (MMPs) from Porcine and human RPE-BrM explant cultures.

3.1.1 Introduction

Even though there were inadequacies to the laser beam, it is still important to evaluate the short pulse (nanosecond) impact on MMP release. Previous work has demonstrated the presence of MMPs in BrM and the expression of ProMMP2 and 9 in RPE cell culture (Guo et al., 1999b, Alexander et al., 1991). Furthermore, experiments have demonstrated the sequestration of latent forms of MMPs 2 and 9 into high molecular weight species in the aged human BrM (Hussain et al., 2011).

Guo et al previously noted the age and topographical differences in the level of latent gelatinases in BrM-choroid explants and the scarcity of active forms in the macular as compared to the periphery. The group have suggested a possible correlation between the reduced level of active MMPs and the age-related thickening, increased presence of denatured collagen, and deposition of debris within BrM, changes that may contribute to the pathophysiology of AMD (Guo et al., 1999b). The recent finding of decreased levels of active MMPs 2&9 in Bruch's from donors supports this hypothesis with AMD compared to age-matched controls (Hussain et al., 2011). More recently, the same group demonstrated that percentage of bound elements increase such an extent that the MMPs are not cleaning the BrM.

Preliminary data from porcine and human studies have demonstrated the release of MMPs post laser. Ahir et al have also shown that RPE cell migration alters the quantity and ratio of pro/active MMPs released (Ahir et al., 2002). In this thesis, it is essential to predetermine the baseline characteristics of the types of MMP release in time and direction (apical vs. basal) in both porcine and human RPE-Bruch's membrane explant culture so as to allow accurate interpretation of data (following experimental laser manipulation) in subsequent chapters. The main objective of this chapter was to quantify the changes in MMP release and/or activation with time with both porcine and human species and to determine if there might be species related differences.

3.1.2 Principles of Gelatin Zymography

Zymography is an electrophoretic technique adapted from sodium dodecyl sulfate (SDS) polyacrylamide gel electrophoresis (SDS-PAGE) containing a substrate, in this case, gelatin, copolymerized in the polyacrylamide, for the detection of gelatinolytic activity in samples. This is a sensitive method to detect gelatinases (MMP2 and 9) and both the pro and active forms.

After electrophoresis, SDS is soaked out from the zymography gel by incubation in a nonbuffered detergent such as Triton X-100 and renatured in an calcium containing activation buffer for a specific length of time and temperature which is dependent upon the enzyme assayed. The partially renatured enzyme then digest the gelatin, leaving a distinguishable zone of digestion that is noted after staining the gel with commassie blue.

The presence of SDS causes denaturation of the enzymes, exposing their active domain which allows both pro and active forms of the enzyme to exhibit activity after partial renaturation. Since the enzyme migrate according to their molecular weight, with the pro form migrating less than active form, both pro and active forms of the enzyme can be detected at the zymogram. (Murphy and Crabbe, 1995, Toth et al., 2012)

3.2 Methods and materials

3.2.1 Porcine RPE-BrM-Choroid Explant culture

Fresh porcine eyes were obtained from a local abattoir and experiments were started within 12 hours of death. Whole globes were first briefly rinsed in antiseptic solution before dissection. An incision was made circumferentially at the pars plana to remove the anterior segment and vitreous. The retina was gently peeled away thereafter. The remaining posterior pole was cut into quadrants and following transfer to phosphate buffered saline, the RPE-BM-choroid layer was gently separated from the sclera using gentle manipulation with forceps and a cutting blade. A suitably intact RPE-choroid preparation was then mounted between the 2 halves of the modified ussing chamber, with exposed tissue diameter of 6mm. The ussing chamber was clamped with screws and both chambers were filled with tissue culture medium. (Figure 3.1) The culture medium used consisted of a mixture of Dulbecco's modified Eagle's medium (with glucose 4.5g/l) (DMEM; sigma) and supplemented with penicillin/streptomycin(1%), L-glutamine, sodium pyruvate(110mg/ml), taurine (100uM), calcium (2mM), and fetal calf serum (FCS 10%). Culture medium was replaced every day and medium that was removed was stored at -40 degrees Celsius until analysis for zymography. A total of 4 explants were examined.

3.2.2 Human RPE-BrM-Choroid Explant culture

Human donor eyes age range, 56–89 years, and postmortem time of 24–48 hours were obtained from the Moorfields Lion Eye Bank. The corneas had been removed at the Eye Bank for use in transplantation surgery, and the remaining globes were transported to the laboratory on saline moistened pads in an icebox. The donor eyes were managed according to the guidelines in the Declaration of Helsinki for research involving human tissue. After a preliminary fundus examination with a dissecting microscope to ensure that the eyes were free of disease and gross handling artifacts, a circumferential incision was made 5 mm posterior to the scleral sulcus, and the remaining anterior segment, lens, and vitreous were discarded. The macular region was located and an 8-mm full thickness trephined section was removed and transferred to PBS. The neural retina was easily detached and discarded, exposing the monolayer of RPE cells. The tissue was examined under high power microscope to ensure coverage of the RPE layer. Tissue without intact RPE layer was discarded. Finally, under low-power magnification, the RPE Bruch's– choroid complex was carefully removed from the underlying sclera by blunt dissection. This technique has been shown to preserve the structural integrity of the explant (Moore et al., 1995a). The explant tissue was then clamped in the modified using chamber as described above.

The culture medium used a mixture of Dulbecco's modified Eagle's medium (with glucose 4.5g/l) and F12-Ham (DMEM-F12; sigma) and supplemented with penicillin/streptomycin(1%), L-glutamine, calcium (2mM), and fetal calf serum (FCS 10%).

A total of 5 explants were examined.

Figure 3.1 Modified Ussing chamber

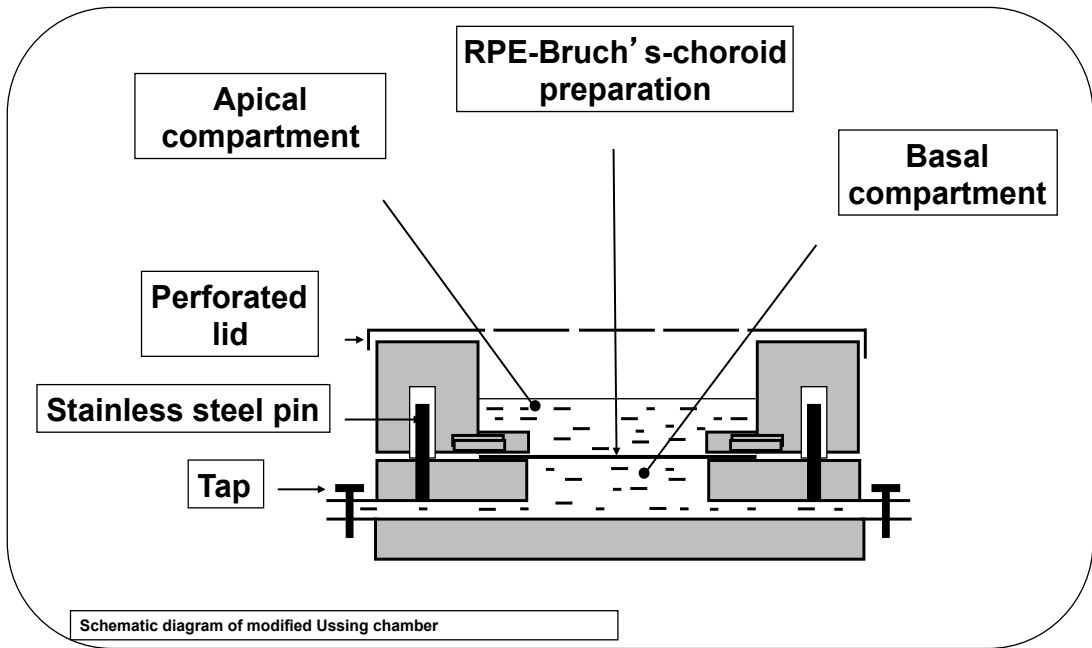
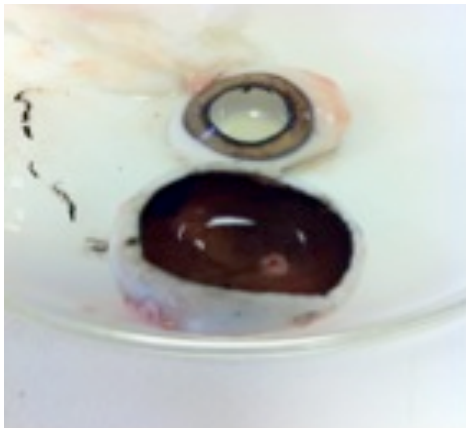
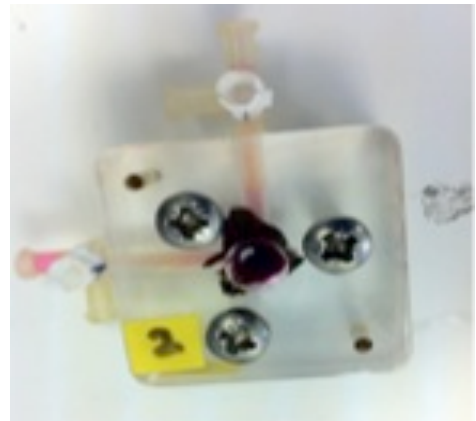


Figure 3.2a Dissection of Porcine Eyes



Porcine eye dissected

Figure 3.2b Ussing chamber with explant



Ussing chamber with explant

3.2.3 Gelatin Zymography

Sodium dodecyl sulfate (SDS) gel electrophoresis was performed (X Cell SureLock Mini-Cell System; Invitrogen, Paisley, UK). The 10% zymogram gels (1-mm thick) contained a 4% stacking layer and 0.1% gelatin in the separating layer (Novex Gels; Invitrogen).

Aliquots of the eluant were diluted (1:2 vol/vol) in Laemmli nonreducing sample buffer (2.5% SDS, 4% sucrose, 0.25 M Tris-HCl, and 0.1% bromophenol blue). Tissue samples were placed in 20 μ L PBS and 40 μ L nonreducing buffer and vortexed for 5 minutes. Twenty microliters of the mixture was loaded onto the gel. Prestained protein molecular weight standards of pro MMP2 and 9 (Invitrogen) and 10% fetal calf serum (FCS; Sigma-Aldrich) were also run on each zymogram. After electrophoresis (150 V, 1 hour), the gels were removed, rinsed in distilled water, and incubated for two half-hour periods in 2.5% Triton X-100, to remove SDS and renature the proteins. They were then transferred to reaction buffer (50 mM Tris-HCl, 10 mM CaCl₂, 75 mM NaCl, and 0.02% NaN₃ [pH 7.4]) and incubated at 37°C for 20 hours to allow proteolytic digestion of gelatin. The gels were rinsed again in distilled water and stained (SimplyBlue SafeStain; Invitrogen) containing Coomassie G-250 blue for a period of 3 hours. Destaining was performed with distilled water for 1.5 hours. MMP activity was observed as clear bands on a blue background. These gels were scanned at a resolution of 2400 dpi (3490 scanner; Epson, Nagano, Japan) and stored in JPEG format. The color images were uploaded into the software (Quantiscan, ver. 3.0; Biosoft, Cambridge, UK) in grayscale format, the colors were inverted so that the MMPs were visualized as dark bands against a whitish background, and the area under individual gelatinase bands was quantified.

The band intensity values for each protein were corrected for background staining for each gel. Pixel analysis determined a graph of intensity and allowed the area under the curve to be calculated. By incorporating the standard in the gel together with the FCS sample and by normalizing staining intensity, MMP bands obtained from different experiments and different gels could be compared.

To determine the accuracy of the bands identified, an initial investigation was performed using porcine and human RPE-BrM choroid explant samples at day 3 of incubation. Ratio of each of the clear bands against the length of the

zymogram were determined and compared against the known molecular weight samples from previous publications by Hussain et al. An example is shown in figure 3.3a. The ratio for pro MMP2 in this case is determined as A / B and compared with samples with known molecular weight standards (as provided by Hussain et al). This method was employed because of the large number of zymography performed in this series of experiments and whilst the using of molecular weight standards was ideal, it was not economically viable.

Figure 3.3a Example of method to determine gelatinase molecular weight

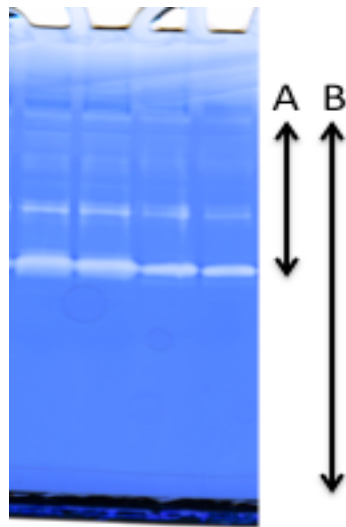


Figure 3.3b Comparison of porcine and human RPE-BrM choroid samples with molecular weight standards.

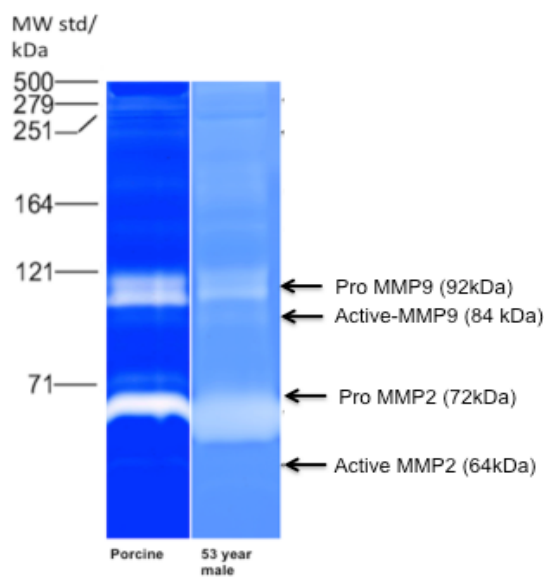


Figure 3.3a. Example of method to determine molecular weight of individual gelatinase. Figure shows a gelatinase zymography. To determine the exact gelatinase species, a ratio was obtained by dividing the length of the clear bands against the length of zymogram. This is then compared against samples with known molecular weight standards.

Figure 3.3b. Molecular weight standards and MMP profile of porcine and 53 year old male in RPE-BrM choroid samples. Hussain et al provided molecular weight and sample of 53 year male.

3.3 Results

3.3.1 MMP release characteristics of porcine RPE-BrM explant culture as a function of time

A zymogram to show the release of MMPs from the RPE-BrM explant into the apical compartment is shown in Fig 3.4. Both Pro-MMPs 2&9 were present as double bands representing isomers of the enzymes and for quantitative analyses, the areas under the doublet was combined. Both active-MMP9 and active-MMP2 were not present in the four explants examined (shown in Fig 3.4). A quantitative analysis of the time-dependent variation in the levels of the various MMP species in both the apical and basal compartments are shown in figure 3.5 The secretion of Pro-MMP9 was high at the start of explant incubation but declined rapidly to reach a steady low baseline in both apical and basal compartments. This decline was rapid in the basal compartment reaching a plateau by day 4 compared to day 6 in the apical compartment. ProMMP2 levels showed a stable level throughout the days of incubation in both apical and basal ends. The levels of MMPs depicted in the graphs of figure 3.5 represent the amount per unit volume of medium retrieved from each compartment and show that these levels in the apical compartment were roughly equal in both compartments.

Figure 3.4 Zymogram of Porcine RPE-BrM choroid explants

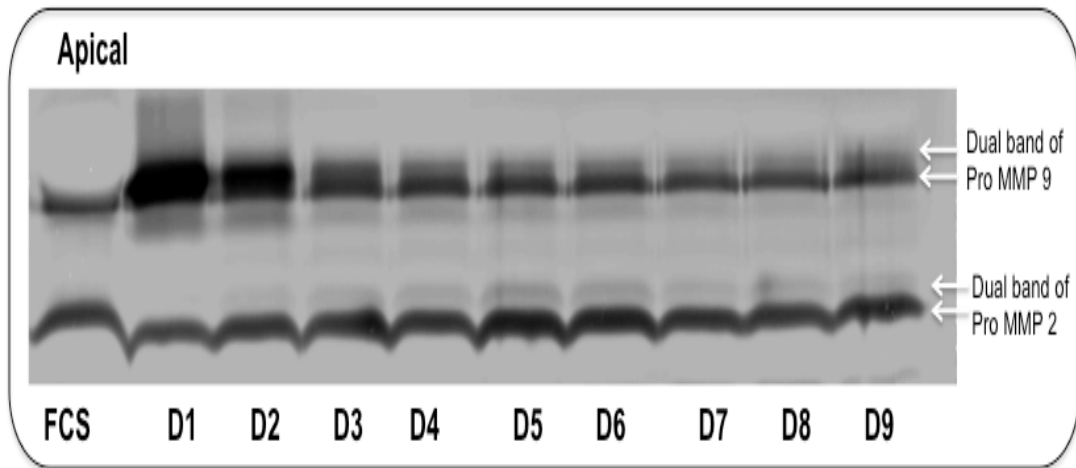
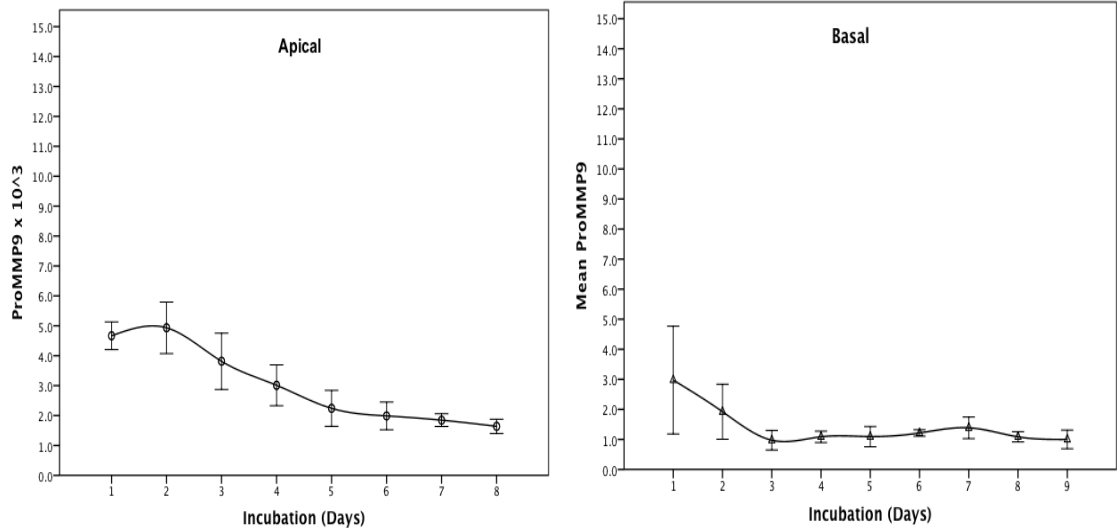


Figure 3.4 shows a zymogram of baseline characteristics of apical MMP release by RPE-BrM explant culture over 9 days. This graph was converted to black and white to highlight the contrast between different bands. Note the presence of dual bands of Pro MMP9 and 2 which represent different isoforms of the MMP species. Note the decrease in intensity of ProMMP9 secretion over time.

Figure 3.5 Time course of MMP release in porcine RPE-BrM choroid explant culture

ProMMP9



Pro MMP2

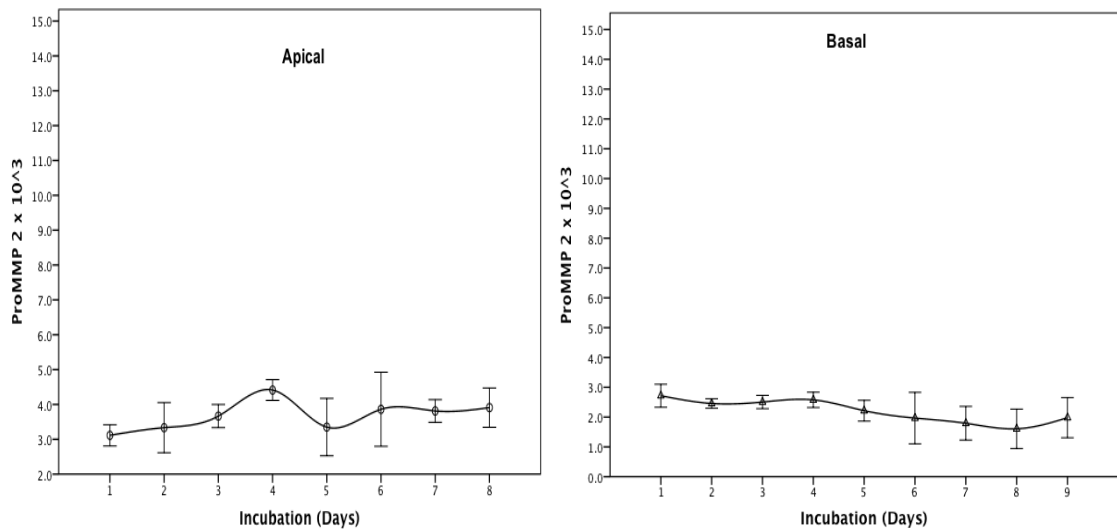


Figure 3.5 Time-course of release of MMPs from porcine RPE-BrM explants in culture. Only profiles for ProMMPs 2&9 are shown since there was no release of activated MMPs 2 & 9 in this experimental series. Level of Pro-MMP9 in both apical and basal compartments showed a decrease over time whilst Pro-MMP2 showed a constant trend. Data is presented as Mean \pm SEM with n=4.

3.3.2 MMP release characteristics of Human RPE-BrM explant culture as a function of time

In the human RPE-BrM choroid explant culture, the explants were maintained for 7 days. Release of Pro-MMPs 2 & 9 and Active-MMP2 were noted in both apical and basal compartments in this experimental series. There was no active-MMP9 secreted (Figure 3.7).

Similar to porcine samples, there was a dual band representing pro MMP9, which suggests the presence of isoforms or different levels of glycosylation of the protein. The level of the higher molecular weight pro-MMP9 isoform was observed to decrease rapidly during the course of the explant culture (Figure 3.6).

A quantitative assessment of the time-dependent release of various MMP species obtained from five human explant cultures is depicted in Figure 3.7. Unlike the situation in porcine samples, the secretory levels of Pro-MMP9 remained fairly stable up to about 4 days in culture followed by a slight decrease. Levels of Pro MMP 2 remained constant throughout the incubation period in both apical and basal compartments.

In the human RPE-BrM-choroid explant cultures, active-MMP2 was always present and remained relatively constant throughout the culture period.

Figure 3.6 Zymogram of Human RPE-BrM choroid explant culture

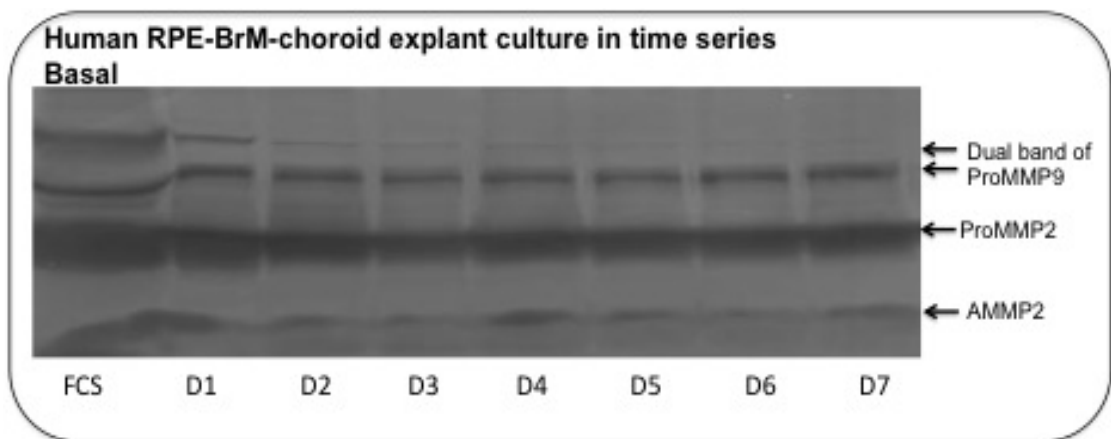
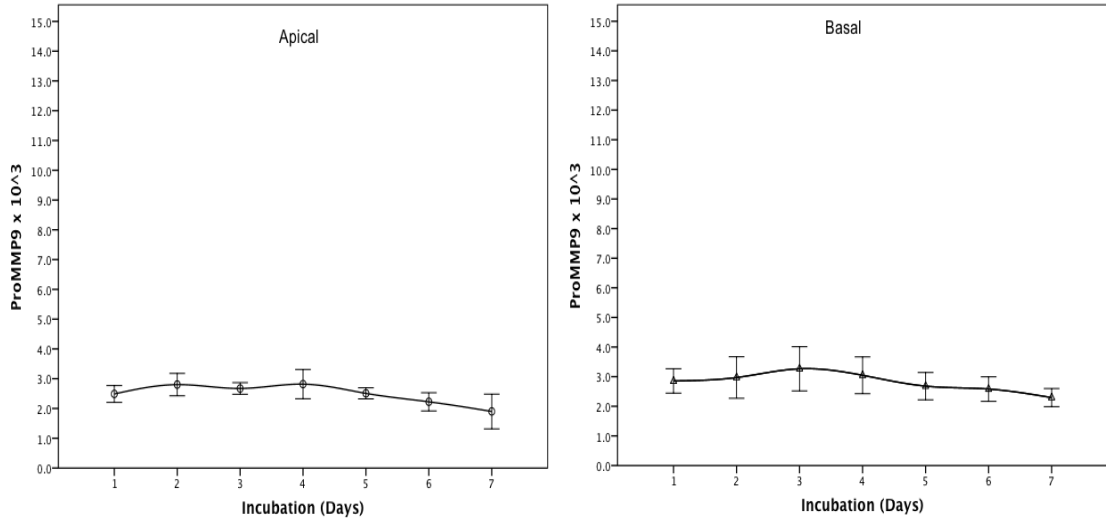


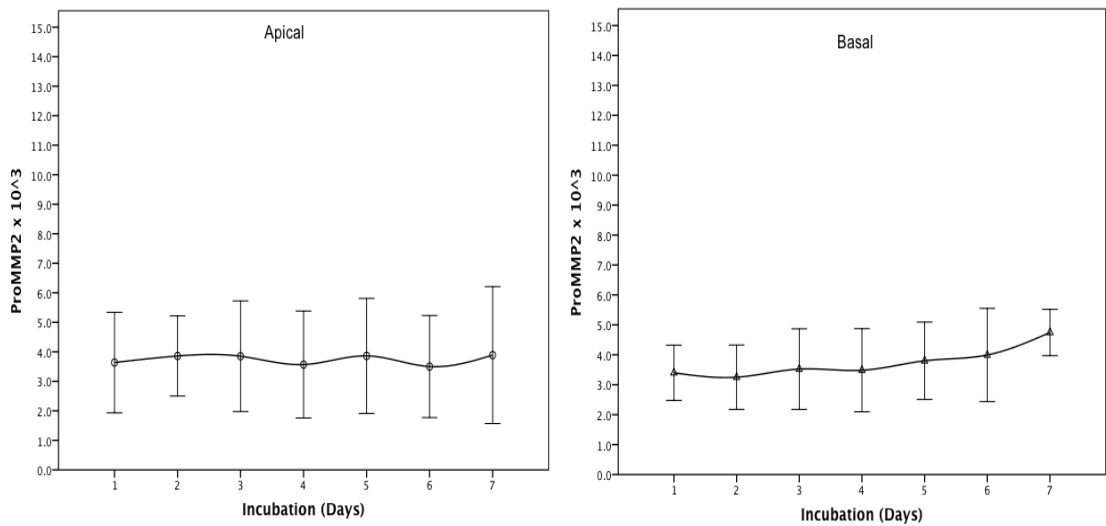
Figure 3.6 shows a zymogram of Human RPE-BrM choroid explant culture with an incubation period of 7 days. There is a noticeable dual band of Pro MMP9 representing different isoforms and a single band of ProMMP2. Active MMP2 was secreted in both apical and basal compartments.

Figure 3.7 MMP release profiles of Human RPE-BrM explant culture culture

ProMMP9



ProMMP2



Active-MMP2

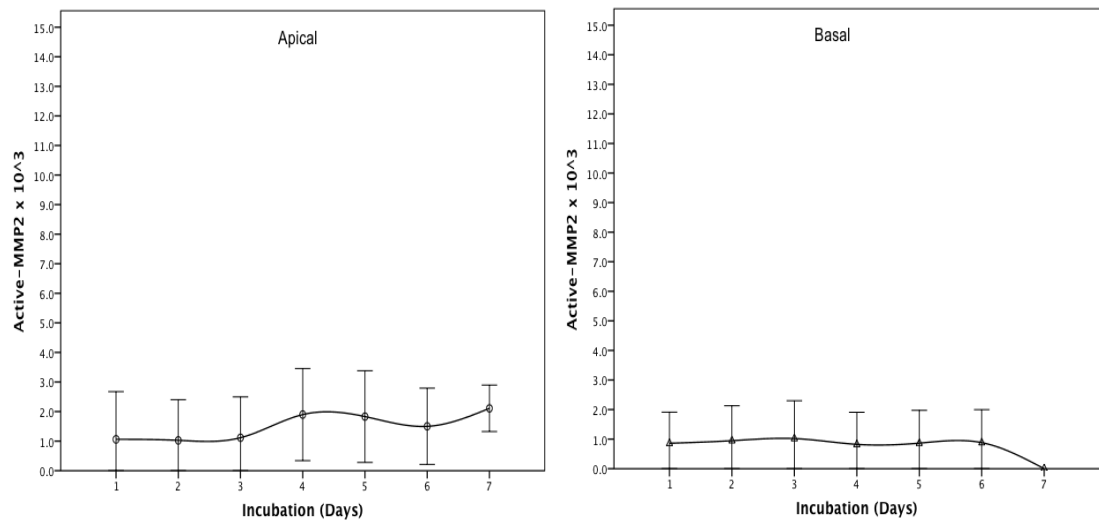


Figure 3.7 MMP release profiles from Human RPE explants over a culture period of 7 days. Levels of pro-MMP9 remained stable over the first four days of culture followed by a slow decline. Pro MMP 2 secretion was constant throughout the incubation period in both compartments. The release of active-MMP2 remained stable throughout the culture period. Data is shown as mean \pm SEM with n=5.

3.3.3 Histology of Porcine and Human RPE-Bruch's membrane choroid Complex Subsequent to Incubation in Culture Medium

Histological assessment was undertaken to determine the integrity of the RPE monolayer following the incubation periods for human (7 days) and porcine (10 days) samples. Although much care was taken in dissecting out an intact RPE preparation, the subsequent mounting of the specimen into the Ussing chamber, edge damage during the clamping process, and the daily replacement of culture medium all pose increasing risk of RPE cell detachment and loss. The post-mortem delays with human tissue also increase the risk of RPE loss. The rapid loss of Pro-MMP9 during the early incubation phase in porcine tissue and the slower loss in human RPE cultures could theoretically reflect loss of RPE cells from the explant. However, the stability of pro-MMP2 levels argues against such a loss in the experimental set-up. The histology of the preparations (Figure 3.8) shows the clear presence and integrity of the RPE monolayer following the long incubation periods such that the time-courses obtained for the various MMPs must reflect secretory changes by the RPE rather than loss of cells into the medium.

Figure 3.8 Histology of porcine vs human RPE-BrM explants

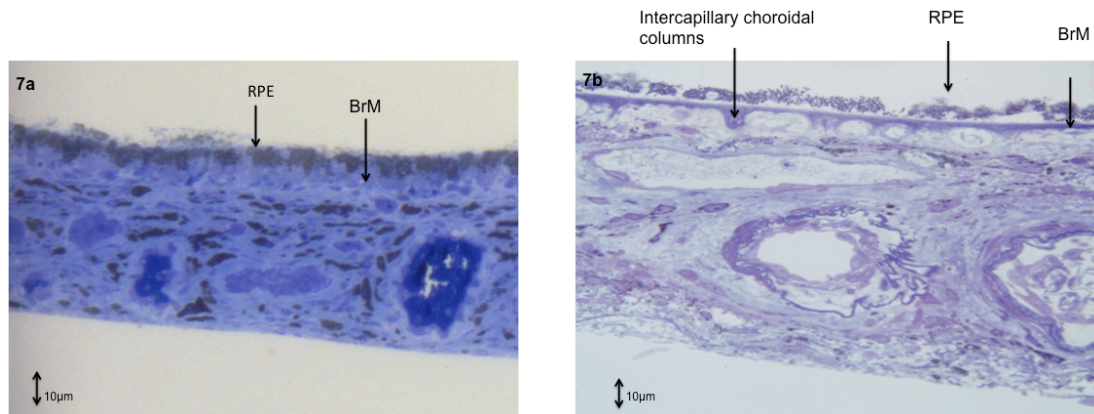


Figure 3.8a shows the histology of a porcine RPE-BrM-choroid explant at day 10 post incubation. There is a continuous layer of RPE.

Figure 3.8b shows the human RPE-BrM-choroid explant at day 7 of incubation, donor aged 72. Note that the RPE layer is beginning to lift away from the BrM. Thickened BrM was noted in this sample.

3.4 Discussion

Previous work has demonstrated the release of latent MMP species in human RPE culture and the presence of equilibrium between bound and free forms of MMPs in BrM.(Hussain et al., 2011, Ahir et al., 2002, Kumar et al., 2010) However, little is known about the time, species-dependency, and vectorial release of MMPs under conditions of explant culture. The understanding of baseline characteristics in the release of MMPs in a given species is essential to help interpret and understand the results of subsequent experimental manipulation. Another reason for undertaking baseline studies is to determine the period of stabilization. In the case of porcine tissue for example, levels of Pro-MMP9 secretion fell rapidly after initiation of the culture stabilizing within 3-4 days. Human explants on the other hand showed stable Pro-MMP9 levels from day 1. These differences may be intrinsic to the species or may be a result of age and post-mortem deterioration of the sample.

In general, porcine eyes were removed from young pigs with minimal post-mortem times and this may have resulted in a more robust response in the stabilization of Pro-MMP9 levels. Porcine samples may also serve as 'young' RPE against the aged human controls utilized in the present study (age 53 to 89 years). As mentioned earlier, with age, RPE undergoes a host of changes ranging from a decrease in melanin content, increase in residual bodies and/or increase in lipofuscin and melanolipofuscin to atrophy/hypertrophy in varying stages of AMD. Morphologically, the crucial alteration that affects transport processes directly is the age-dependent decrease in RPE number and size, hence decreasing available surface area for fluid, nutrient and waste exchange(Mishima et al., 1999, Hjelmeland et al., 1999, Hageman et al., 2001, Kinnunen et al., 2012, MJ, 1971, Feeney-Burns et al., 1980, Feeney-Burns et al., 1984). Furthermore, some investigators have found a decrease in migratory or growth rate with older RPE passage in cell culture, a concept of senescent RPE. Hence, this might in theory result in either qualitative or functional differences in MMP release between porcine and human samples.

Apart from the rapid and early decrease in Pro-MMP9 in porcine samples, there was little difference in the time-related changes in Pro-MMPs in comparison to human samples. The most important difference was the secretion of active-MMP2 in human samples compared to porcine. From this experimental series, there were minimal differences in characteristics of Pro MMP 2 and 9 release

between porcine and human. However, there was secretion of active-MMP 2 which was absent in porcine eyes. Our results agree with Treumer et al, where porcine cultures were noted to secrete isoforms of both Pro MMP9 and 2.(Treumer et al., 2012) However, human RPE-BrM explant culture only secreted isoforms of pro MMP9. It was noted that the isoforms did not appear in BrM-choroid culture. It is possible that since the high MW Pro-MMP9 isoform was in low concentration, it might have been lost in the BrM preparation or it may have been below the detection limit. Whereas in the RPE-BrM preparation, it would have been continuously synthesized.

The current results show the bi-directional release of ProMMPs 2&9 for both species and active-MMP2 for human explant culture. It is essential to determine secretion on the basal end as the BrM is the ultimate target for MMP release to facilitate regulation of the extracellular matrix.

In this sample, only macular RPE-BrM explant samples were used in both porcine and human samples. This is because prior studies have shown differences in RPE characteristics as well as MMP profile in macular and peripheral regions. Hence, using only macular samples allowed comparison between the 2 species.

Guo et al has shown from immunochemistry the presence of MMP 1, 3, 2 and 9 in BrM and a higher level of active-MMP 2 and 9 in periphery but not macular region of BrM.(Kumar et al., 2010, Guo et al., 1999b) In this study, active-MMP2 was found to be secreted by RPE in the macular region in the human species.

3.5 Conclusions

In conclusion, from the current control dataset, porcine and human RPE-Bruch's-choroid MMP profile has been compared over a time period of minimum 7 days. In essence, this current dataset shows that there is an equal bidirectional secretion of MMPs over a time series for both porcine and human species. Secretion profiles of pro MMP 2 and 9 were found to be similar for both porcine and human species, but human species have a low level of active-MMP 2 release in both directions. No active-MMP9 was noted in either species. Hence, the results of this chapter would form the basis of which further laser intervention to RPE/retina in subsequent chapters may be accurately interpreted.

Chapter 4. Effect of Nanosecond Laser on the Release of Metalloproteinases from Porcine RPE-Bruch's choroid Explants

4.1 Introduction

Having established the boundary conditions of release of MMPs as a function of time in the organ culture conditions, it was then possible to evaluate the release of MMPs induced by laser in different exposures (ie, difference in laser number spots).

It is widely accepted that structural and molecular changes of BrM contribute to the ageing of the human eye. (Kumar et al., 2010, Hillenkamp et al., 2004, Moore et al., 1995a, Ramrattan et al., 1994b) This structural modulation compromises the transportation pathway for nutrient supply and metabolic waste removal between the photoreceptors and choroidal blood supply and may over time result in degeneration of the RPE layer as mentioned in the earlier chapter. The tightly regulated remodelling pathway for continuous turnover of the extracellular matrix (ECM) of Bruch's is controlled by a family of extracellular enzymes, known as the matrix metalloproteinase (MMPs) coupled with their tissue inhibitors (TIMPs). In particular, MMPs 1, 2, 3 and 9 and TIMPs 1, 2 and 3 were shown to be secreted by the RPE and were found in BrM (Alexander et al., 1991). Ageing of Bruch's was associated with increased polymerisation and sequestration of Pro MMPs 2 and 9 into high molecular weight species and this was suggested to decrease the availability of free Pro-MMPs the activation process.(Hussain et al., 2011, Kumar et al., 2010)

Active MMPs are potent proteases and have been shown to increase the hydraulic conductivity of BrM, with active-MMP9 being more effective than active-MMP2.(Ahir et al., 2002) Thus, lowered activity of the MMP system (due to MMP polymerisation, inhibition by advanced glycation end-products (AGEs) and by other oxidised and cross-linked collagen species was thought to underlie the ageing process within BrM and therefore in theory, improving MMP activity was expected to lead to reversal.

Previous studies demonstrated that laser irradiation of RPE explants in culture resulted in MMP release.(Zhang et al., 2012, Treumer et al., 2012) However, the results of the experiments have been contradictory regarding the release of activated MMP species. Treumer et al only found active-MMP 2 release from the basal side of porcine RPE-BM and a complete absence of active-MMP9

using a 1.7 μ s Nd: YLF laser (SRT) with a 200 μ m spot size and at threshold laser energies (Treumer et al., 2012). On the other hand, Zhang et al., 2012 found both active-MMPs 2&9 released from both apical and basal sides of aged human explant cultures using the prototype retinal rejuvenation therapy (2RT) system, with 3ns pulse width, 400 μ m spot size and at laser energy of 0.3mJ/lesion.

In the previous chapter, the baseline release profiles for MMPs in both young porcine and aged human RPE-Bruch's choroid explant cultures over time have been determined. In porcine samples, there was no release of active MMPs. Human samples consistently showed the time dependent release of active-MMP2 but absence of activated-MMP9. The volume of RPE damage is important for the levels of MMP release for clearing up debris. In chapter 2, it was shown that at lower energy levels (ie, between 0.1 to 0.2mJ), there was minimal change in diameter of laser damage. Hence, it may be assumed that the available circumference for RPE migration would be minimal in this energy range, and the only way to have a resultant increase in MMP release would be to increase the number of laser spots. Although this novel laser with an ultra short pulse was found to have a disappointingly regular beam distribution, it was still appropriate to evaluate the following:

1. The effect of laser on the RPE with regards to active MMP release;
2. The impact of RPE volume injury on MMP release, ie, would the number of laser spots have an impact on MMP release?
3. The direction of release of MMP from the RPE post laser;
4. The time course of MMP activity post laser

The experiment set up in this chapter was performed using in vitro porcine RPE-BrM-choroid explant culture because of the constraints of getting human tissue.

4.2 Methods and Materials

4.2.1 Set up of explant culture

The set up procedure for explant culture had been described in the Methods section of Chapter 3.

A total of 4 control and 8 lasered samples were set up.

4.2.2 Laser application

Explant cultures were kept in an incubator at 37° C with 5% CO₂ and medium changed every 24 hours. Laser procedure was performed at 48 hours post initiation of culture. This was to allow stabilisation and regrowth of any possible RPE injury in the periphery of the chamber from the clamping process. Prior to laser procedure, the medium was removed from the apical and basal side of the chamber and replaced with PBS solution to prevent laser absorption by the medium and the aperture was covered with a clear film to prevent spillage. For the laser procedure, the chamber was positioned vertically in a holding apparatus on the chin rest of the laser assembly. Probit data from an experiment noting visible lesion from varying laser energy, the ED₅₀ visibility threshold of the laser was determined to be 0.22mJ for porcine eyes and the diameter of laser damage between 0.1 to 0.2mJ had shown minimal change (Chapter 2 of thesis). Thus in this study energy levels between 0.1 to 0.15mJ was used. The laser lesions were delivered 1 spot size apart in a circumferential pattern. Number of laser spots applied ranged was 25 or 50 shots. To prevent lasering the same area twice, the following laser pattern was applied (Figure 4.1). The entire procedure took approximately 3 minutes. Post laser, the PBS was replaced with culture medium and the Ussing chamber assembly returned to the incubator.

In total, 8 explants were lasered. There were 4 explants with 25 laser shots, and 4 explants with 50 laser shots.

Figure 4.1 Pattern of laser spot application in porcine explants

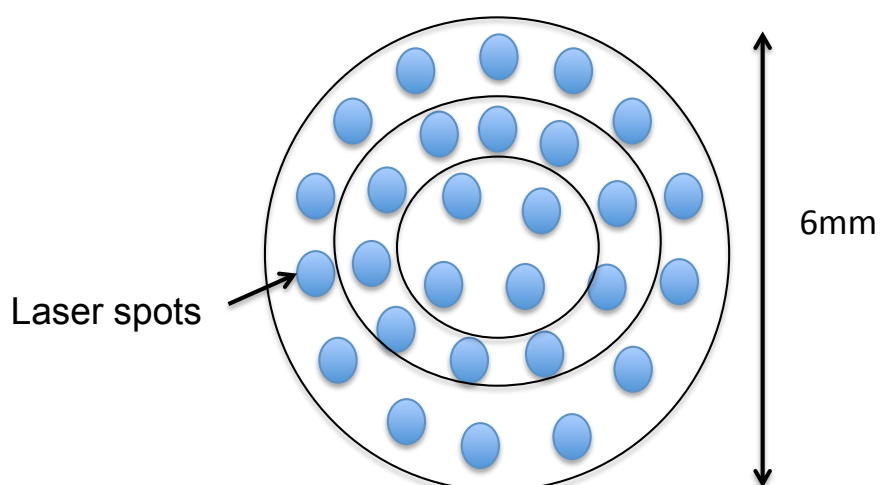


Figure 4.1 is a diagrammatic representation of approximate pattern of laser spot pattern application in this experiment.

4.2.3 Collection of samples

Medium samples were collected from both apical and basal half-compartments every 24 hours and stored at -20°C until analysis of MMPs by zymography.

4.2.4 Determination of MMPs (Gelatin zymography)

The analytical procedure for gelatin zymography has been described in the methods and materials section of Chapter 3.

4.2.5 Analysis of gelatin zymography

Please refer to chapter 3.

Statistics

Statistical analysis was undertaken using SPSS version 19.0. The Mann Whitney U test was used to compare densitometric levels (y-axis) of Pro MMP2 and 9, Active-MMP 2 and 9 from days 3 to 9 (x-axis), at each day of incubation, between 25 versus 50 laser spots. The reasoning for choosing this statistical methodology was because of these were independent random samples and the Mann Whitney U test is a nonparametric test which can also be used as a chi-

square test in determining trends. Apical and Basal samples were analyzed separately. $P < 0.05$ was considered statistically significant.

4.2.6 Histology

For light microscopy, the RPE-choroid preparations were fixed in 4% Gutaraldehyde, dehydrated in a graded series of ethanol and embedded in paraffin. Three μm sections were stained with haematoxylin-eosin and examined under light microscopy.

4.3 Results

4.3.1 Type of MMP release post laser as a Function of Time

In this experimental series, the release and the time-course of release of the various MMP species from control explants was very similar to that obtained for baseline levels in the study of Chapter 3. Levels of Pro-MMP9 released were high at the start of the culture and then showed a steady decline. Released levels of Pro-MMP2 remained fairly steady throughout the culture period. There was no active MMP 2 or 9 released.

Irradiation of RPE-BrM explants with the 2RT laser showed marked differences even on zymographic qualitative analysis as compared to controls (Figure 4.2). In the apical compartment of the Ussing chamber, the emerging presence of active-MMP2 was obvious at D4 (day 2 post laser, D2PL) with much increased levels being maintained over the next four days. The presence of active-MMP2 in the basal compartment was obvious at D6 (D4PL) with increased levels being maintained over the next four days examined. The delay in the appearance of active-MMP2 in the basal compartment may be due to the presence of the large choroidal mass in such tissue preparations. However, active-MMP9 was not observed in any of the lasered explants.

A quantitative assessment of the release of MMP species following laser irradiation is depicted in Fig 4.4. In both control and lasered samples, levels of Pro-MMP9 were relatively high at the start of the culture period followed by a decline to reach a lower plateau. However, in the lasered samples, Pro-MMP9 levels were much higher for most of the culture period.

Unlike control explants where Pro-MMP2 levels remained steady throughout the culture period, lasered explants showed a progressive increase peaking around D5 (D3PL) in the apical compartment and D6 (D4PL) in the basal compartment ($p < 0.05$). A subsequent decline in the apical compartment allowed baseline levels to be reached by D9 (D7PL) but despite the declining phase, levels in the basal compartment remained elevated even at D9 (D7PL).

Lasered samples had release of active-MMP2. Lasered samples have release of active-MMP2 in both apical and basal compartments with levels peaking around days 7 (D5PL) and 6.5 (D4.5PL) for apical and basal compartments respectively. A declining phase was then observed with active-MMP2 reaching

baseline by D9 (D7PL) in the apical compartment. Baseline levels were not reached in the basal compartment by the end of the experimental period. A subanalysis comparing 25 and 50 laser shots and controls is shown in Figure 4.5. The difference between levels of ProMMP9 release is equivocal in both apical and basal ends. There is higher levels of release of ProMMP 2 in samples with 50 laser shots both apically and basally, although it was noted that the MMP release prior to laser (ie, at days 1 and 2) were noted to be of a lower baseline in samples with 25 laser shots. For active-MMP2, there was no difference between number of laser shots in the apical end, although there was twice the levels of active-MMP2 release noted in the group with 50 laser shots on the basal end. Figure 4.6 shows the enlarged figure with a smaller scale to demonstrate the changes. Figure 4.7 shows the total quantity of active-MMP2 released in the basal end in 4 samples of 25 spots and 50 spots (ie, 100 and 200 laser lesions in total respectively) at day 7 of incubation. There were approximately twice the levels of total active-MMP2 release for 200 laser lesions as compared to 100 laser lesions.

Figure 4.2 Zymogram of apical release of MMP in porcine explant culture post laser

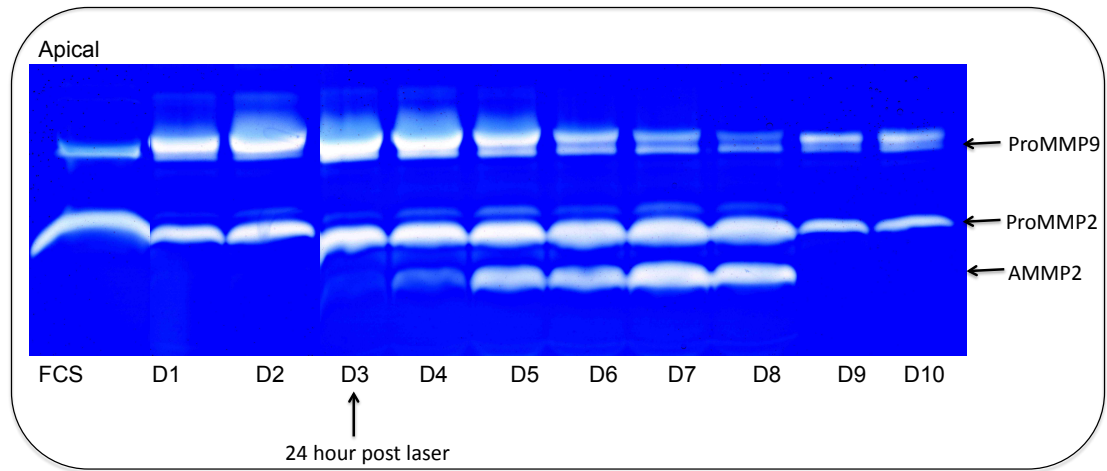


Figure 4.3 Zymography of basal release of MMP in porcine explant culture post laser

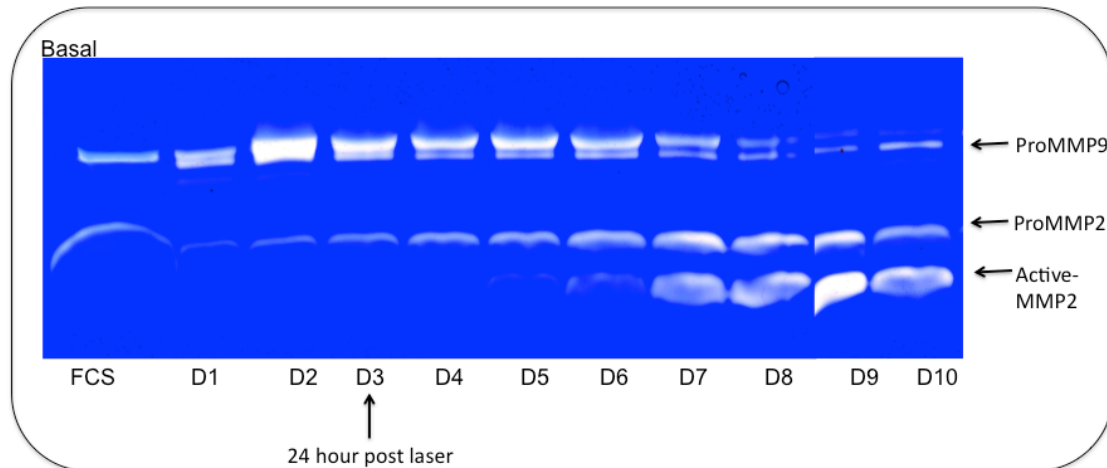
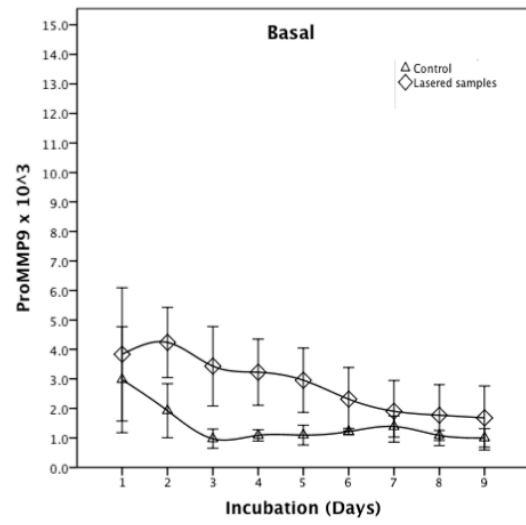
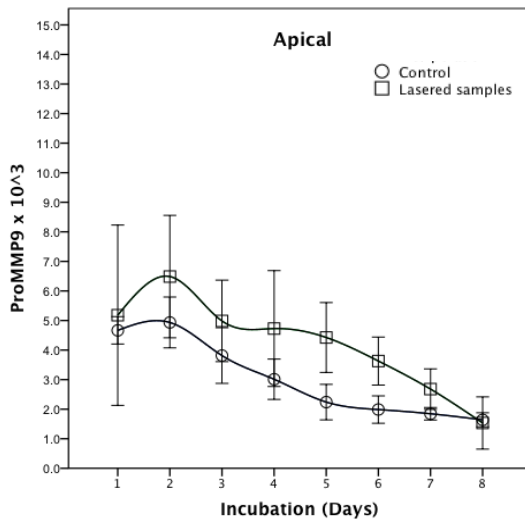


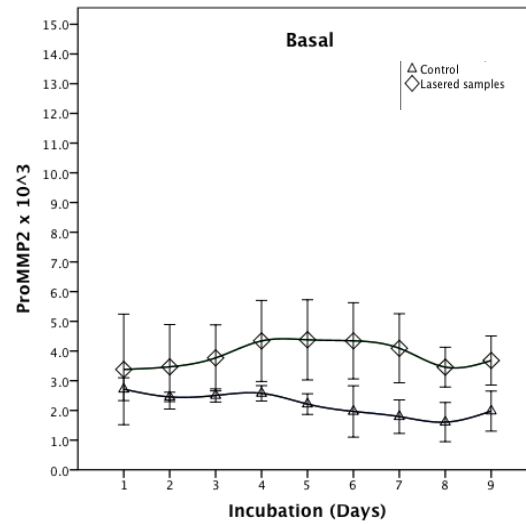
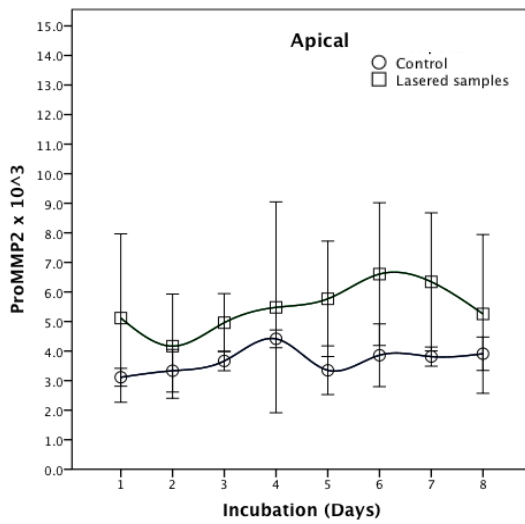
Figure 4.2 and 4.3 shows the zymogram of apical and basal release of MMPs post laser respectively. Note the release of active-MMP2 in both apical and basal compartments.

Figure 4.4 MMP profiles of explant culture post laser

Pro MMP 9



ProMMP2



Active MMP2

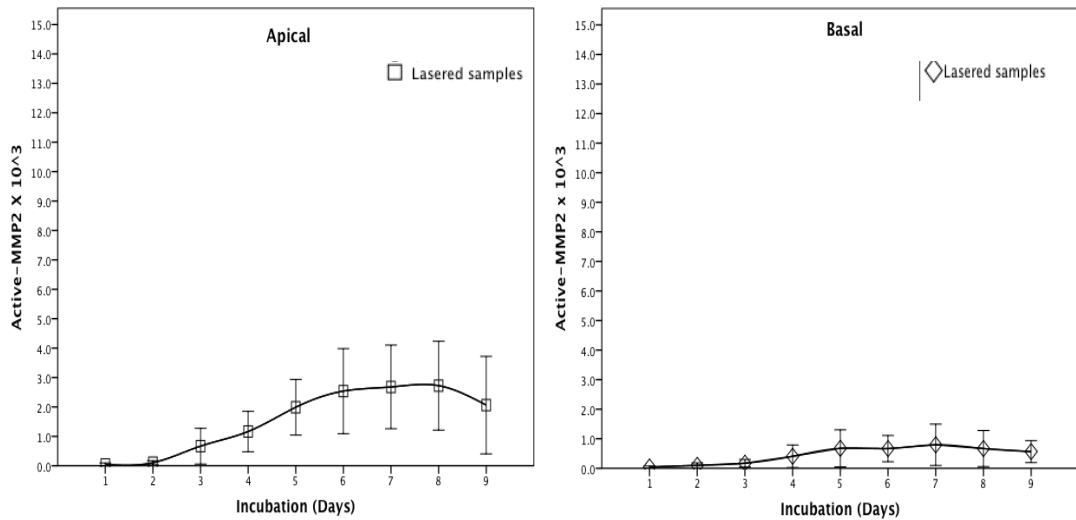


Figure 4.4 shows the release profile of ProMMP 9 and 2, Active-MMP2 both apically and basally of lasered samples(N=8) as compared to controls.(N=4) Laser was performed at Day 2.

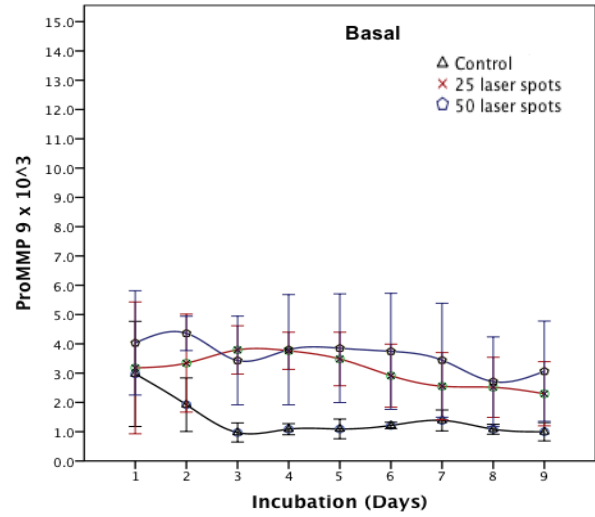
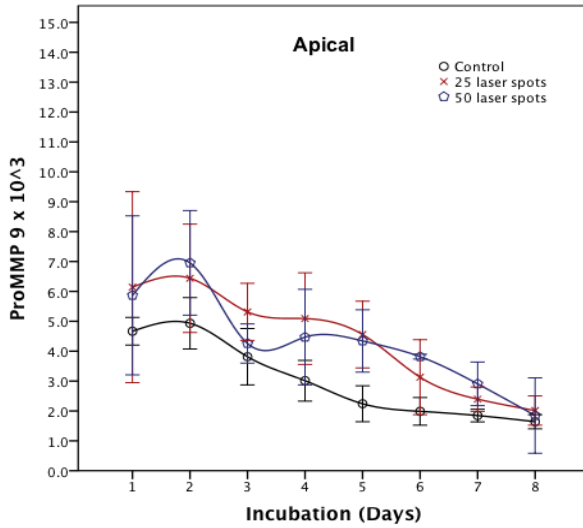
There is a similar decreasing trend noted for ProMMP9 in both apical and basal ends for both lasered and control samples although lasered samples have higher levels of MMP release.

There is increase in release of ProMMP2 post laser . Apically, it was noted that there is a peak release at day 4 post, whilst basally, the release had a stable peak which remained between days 3 to 5 post laser. The levels of increased ProMMP 2 release remained elevated even by Day 9 of incubation (end of experiment).

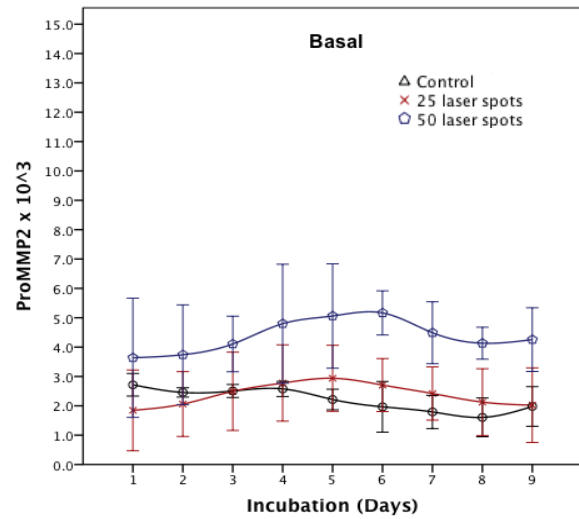
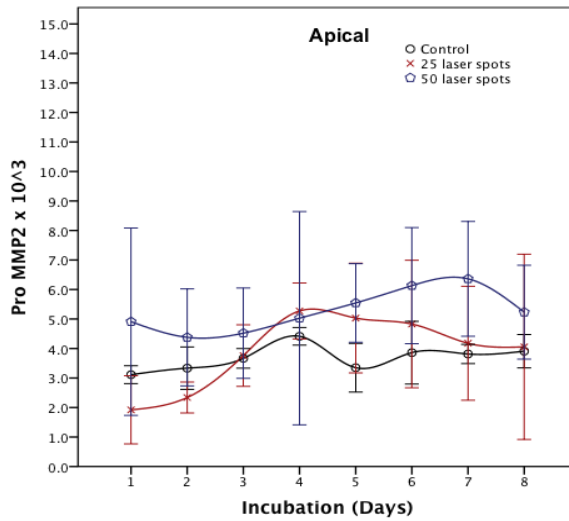
Post laser, there is increase in Active-MMP2 noted in lasered samples both apically and basally. The levels remain elevated by end of experiment (Day 9/Day 7 post laser). Apical sample had a peak release which was approximately twice that of basal release. This could be because of possible modulation in the interphotoreceptor matrix and time taken for diffusion through the choroid on the basal side.

Figure 4.5 MMP profiles of porcine explant culture post laser in varying number of laser shots

ProMMP9



ProMMP 2



Active-MMP 2

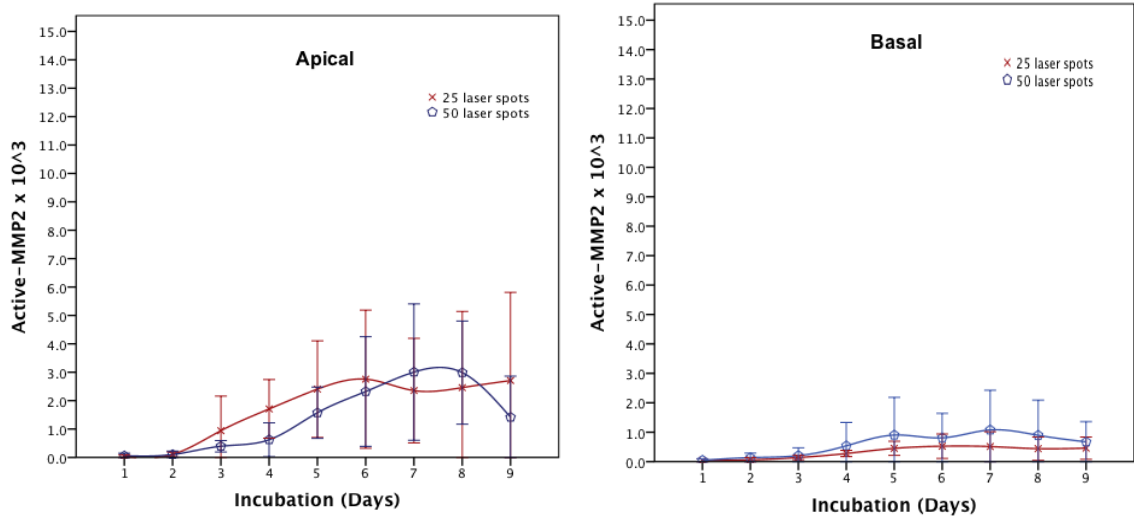


Figure 4.5 represent the MMP (Pro MMP 9, 2 and Active MMP 2) release profile of 25 versus 50 laser shots (n=4, n=4) as compared to control samples (n=4). Active-MMP9 was not plotted as it was not released in this experimental series. Graphs are plotted as lasered samples against controls (legend within graph) over a series of 9 days in both directions.

Means of graphs and the respective SEM was plotted (as above). Laser was applied at 48 hours and media was collected 24 hours post laser from D3.

Pro MMP9 shows a decreasing trend for both lasered samples and control in both compartments. Lasered samples had higher levels of ProMMP 9 in both directions. There was higher release of Pro MMP 2 from lasered samples with 50 laser spots as compared to 25 laser spots in both directions.

Comparing active-MMP2 release, there was a higher release of active-MMP2 in the samples with 50 laser spots as compared to 25 laser spots in both apical and basal compartments. In the basal compartment, it was noted that there is approximately twice the level of active-MMP 2 levels with 50 laser spots as compared to 25 spots. Release of active-MMP2 started from D3 (D1 post laser) and remained elevated by end of experimental incubation period in both lasered samples.

Figure 4.6 Levels of active-MMP2 basal release with different number of laser spots.

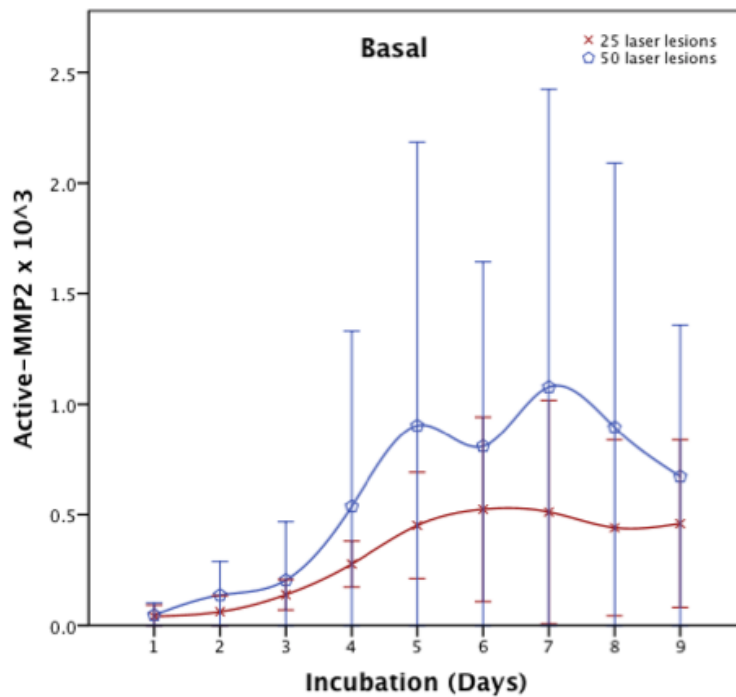


Figure 4.7 Total quantity of active-MMP2 release at Day 7 of incubation

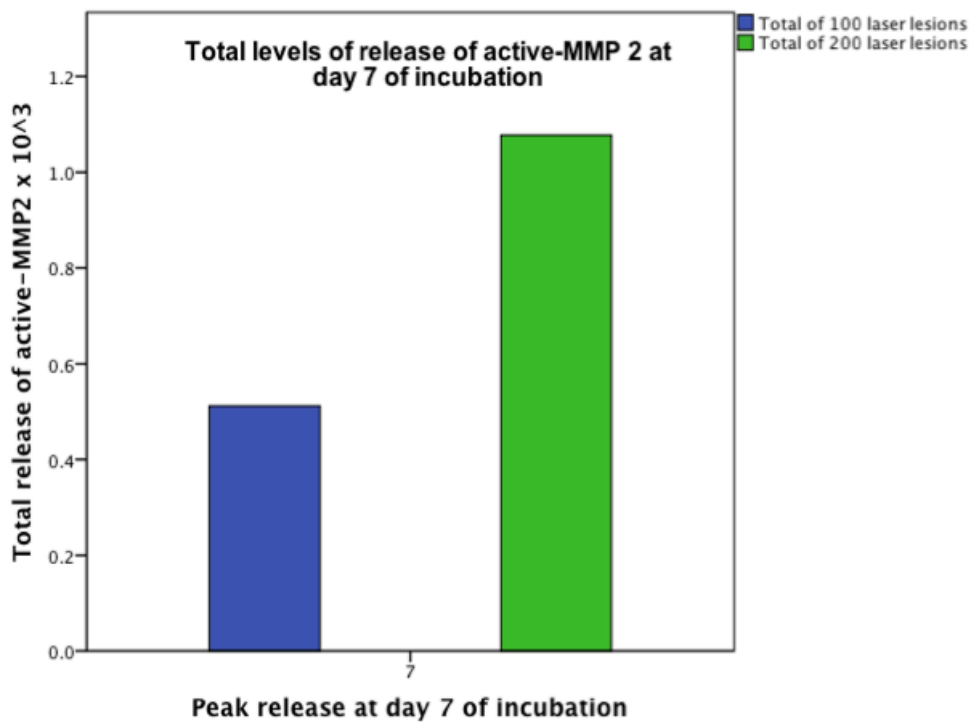


Figure 4.6 and 4.7 shows that higher number of laser lesions release higher levels of active-MMP2 on the basal end.

4.3.2 Description of Histology of Laser Lesion at End of Incubation Period

Histological examination for the laser lesion was undertaken at day 10 of incubation. The laser lesion was identified by the loss of RPE cells. The current histology did not show a discrete pattern of RPE cell death. There was also no multi-layering of RPE cells as expected for this period of wound healing.

There were areas of lifting of the RPE cells adjacent to the laser lesion, which may suggest either possible extension of laser injury to the periphery or poor RPE health at day 10 of incubation. Although the latter was less likely because of intact RPE layer in other areas not lasered.

There were areas of decreased intensity of staining extending beyond the RPE, into the BrM and choroidal capillaries. This suggest possible extension into the outer retina. (Figure 4.8)

Figure 4.8 Histology of laser lesion at day 10 of incubation/ day 8 post laser

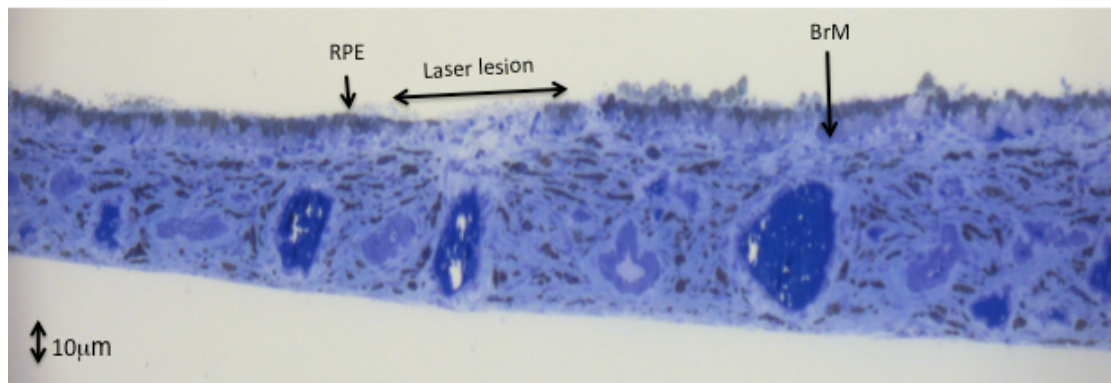


Figure 4.8 shows histology of porcine RPE-BrM-choroid explant culture at day 10 post incubation. The above histology was taken from a sample of 0.15mJ laser lesion. Note the crater created by the laser lesion with loss of RPE cells. Contrary to the postulated mechanisms of action of the 2RT laser, the current histology does not show a discrete pattern of RPE cell death. There were areas of decreased intensity of staining extending beyond the RPE, into the BrM and choroidal capillaries. This suggest possible extension into the outer retina.

4.4 Discussion

The results from this experimental series have several significant findings and implications. First, laser increased the levels of both pro MMP 9 and 2 as compared to laser under our organ culture conditions. Second, there was increase in active-MMP2 from day 3 of incubation (D1PL), which remained elevated beyond end of experimental incubation period. Third, this increase in MMP release was noted in both apical and basal compartments of the organ culture. More importantly, comparing the impact of varying number of laser spots on MMP release, the current results demonstrate that there was higher release of proMMP 2 and active-MMP2 in both apical and basal ends in samples with the higher number of laser spots. In the basal end, there was approximately twice the level of active-MMP2 release in 50 lasered spots as compared to 25 spots.

In the current experiment, it was noted that there was lower quantity of active-MMP2 release as compared to pro MMP2. This is because activation of MMP2 happens in stepwise fashion from ProMMP2. The activation mechanism for pro-MMP2 was previously found to be mediated by 2 molecules of transmembrane enzyme MMP-14, and TIMP2, on the basolateral surface of the RPE. The first MMP14 molecule will bind to TIMP2 and form a ternary complex with pro-MMP2. A second MMP14 molecule then cleaves this complex to release active MMP2. (Alcazar et al., 2007, Strongin et al., 1995, Smine and Plantner, 1997, Butler et al., 1998)

In this study, the levels of Pro MMP 9 show a decreasing trend and there was an absence of active-MMP9. This result replicated previous findings of increase active MMP 2 post laser in explant culture by Treumer et al. (Zhang et al., 2012, Treumer et al., 2012) The current result was in contrast with Zhang et al, where there was an increased Active-MMP 9 in aged human sample. (Zhang et al., 2012) The differences in the results maybe attributed species differences of the experimental explant sample. In our prior chapter, the difference in MMP profile between porcine and human explant culture had been demonstrated. In porcine explant culture controls, there was neither release of activated MMP2 nor 9, whilst in aged human samples, there was release of Active-MMP2. Some investigators have correlated the increase in pro MMP 9 with AMD in plasma samples. (Chau et al., 2007) This brings about the question of balance of risk of the activity of MMP 9, considering MMP9, being a powerful gelatinase, causes

massive increases of hydraulic conductivity, especially in the elderly (as compared to Active-MMP2); however, in overloaded doses, may tip to cause a negative feedback response to increase anti VEGF from the RPE. That mentioned, one should bare in mind that human BrM contains active-MMP9 and together with active MMP2 is responsible for turning over the matrix of the membrane. Also the results of Ahir et al showed that aged Bruch's contain abnormal constituents that are the substrates of active MMP9. Despite the presence of active MMP9, the control population does not show neovascularization.(Ahir et al., 2002) It is hence, the unregulated synthesis of active MMP9 that results in a problem.

MMP activity was found to be increased in both apical and basal directions of the RPE. Deposits from ageing, have been found to lie external to the RPE basally (Basal linear deposits) and within the BrM (Basal laminar deposits), hence, the basal directional release of active-MMP2 would be necessary for 'cleaning' up the debris to improve transport across the BrM. Having a basolateral release of MMP was not surprising as this was a known activity even amongst other epithelial cells. For example, in mammary epithelial cells and aortic endothelial cells, MMP secretion had been found to be mainly from the basolateral surfaces.(Unemori et al., 1990, Talhouk et al., 1991) That said, in this study, we have found MMP release in the apical surface. These results concur with Treumer et al and Zhang et al, using porcine and human RPE-BrM explant models respectively. Some investigators have hypothesized the role of MMPs in the turnover rate of the interphotoreceptor matrix (IPM) which was required to maintain health of the photoreceptor cells.(Padgett et al., 1997, Plantner et al., 1998b) MMPs and TIMPs have been found in the IPM and were suggested to clear old IPM for the daily synthesis of new components as well as for digesting photoreceptor outer segment tips for preparation of phagocytosis by RPE. Hence, the apical release of MMP can be explained by 2 theories; first, during the process of removal of the retina from the RPE, the tightly attached photoreceptor cell outer segments with the accompanying inter photoreceptor matrix may remain and inherent MMP may diffuse out during the time course of the experiment. However, this may not explain the increase of active-MMP with time post laser. Besides, there was no active-MMP in our controls. Hence, this explanation is unlikely. The more likely theory could be that the RPE releases MMP bidirectionally physiologically for 1. extracellular matrix turnover in the

interphotoreceptor matrix, 2. extracellular matrix turnover of the BrM. Thus, laser induced a bidirectional effect on the RPE migratory release of active-MMP which had a direct impact on rejuvenating health of the photoreceptor cells and an indirect impact through clearing of the BrM for increased transportation. It was also noted that basal chamber had quantitatively lower levels of release than the apical chamber. This could be explained by the slower diffusion of MMPs through the choroidal layer.

In this study, higher number of laser spots was shown to secrete higher levels of activated MMP2 in both directions, and this was more clearly defined in the basal compartment. The levels of active-MMP2 release was approximately twice for samples with 50 laser spots as compared to 25 laser spots. It is important to note this change as it is the basal end MMP activity that is critical to effect on the BrM which lies on the basal end of RPE cells. In this experiment, it was assumed that there was negligible effects from the energy differences in the range between 0.10 to 0.15mJ based on the previous finding of equivocal diameter of laser damage. Hence, the current profile of MMP release can be wholly attributed to the differences between laser spots. As mentioned earlier, the level of MMP release was highly dependent upon the volume of RPE injury and this may be achieved by either laser energy or number of laser spots. Thus, the ideal scenario would be to use the lowest possible laser energy (ie, 0.1 to 0.15mJ) with a larger number of laser spots for maximal effect. In this experiment, it was shown that higher number of laser spots resulted in higher release of MMP.

The histological data was expected to show a multi-layered RPE layer at day 9 post incubation (day 7 post laser) across the laser lesion with no extension of damage beyond the RPE. However, as shown in Figure 4.8, the current results showed disintegrate migration of discrete RPE cells in the laser lesion. The histological images show extension of the laser impact to beyond the BrM. The histological results may be interpreted 2 ways. The results may indicate a complete wipe out of the RPE cell in the center, which concurs with the flat mount results in chapter 2 or as complete RPE cell death from poor survival rates in explant cultures which had previously been shown by Treumer et al to be limited to 5 days. (Treumer et al.) The latter was less likely because the surrounding RPE cells appeared to still be relatively healthy.

The current results are critical as it indicates a more profound biochemical effect with higher number of laser spots. This has significant clinical implications. At 3 nanosecond time domain and Q switched, it was presumed from prior laser studies that the mechanism of action of the current 2RT laser causes micro cavitation effects with a limited extension of damage. Lund et al had previously shown that variation of laser spot sizes had limited effects in the ultra short pulse duration with micro cavitation mechanism of action. Hence, the only variability for changes in this case would be either laser energy or number of laser spots. In theory, a higher level of activity of MMP 2 may result in increases in hydraulic conductivity. However, a higher release of active-MMP2 can only presumably happen should there be a larger proportion of RPE cell migration. From the flat mount histological experiment in chapter 2, it was found that with a higher laser energy ($>0.25\text{mJ}$) there was a larger zone of damage, hence, it would be reasonable to assume that high energy levels may also result in higher MMP release. However, considering that there was disappointingly no discrete beam distribution, a higher laser energy would cause secondary damage from apoptosis of the photoreceptor cells. Thus, it seems the only way to circumvent this issue would be to use as low an energy as possible and to increase the number of laser spots. However, if the discontinuous beam configuration were intact, then there would be a higher release of MMPs per laser lesion, which in effect will negate the need for larger number of laser spots.

In this study, it has been established that the 2RT in the nanosecond time domain did cause release in MMP in porcine eyes and this was dependent on number of laser spots. This indicated that a larger total volume of RPE injury resulted in a quantitatively higher release of MMP. In particular, this study had demonstrated that at the lowest possible energy of 0.1mJ for this laser, there was sufficient impact to the RPE to cause a release of active-MMP.

In this study, there were a good number of lasered samples and controls. A standardised modified using chamber was used which allowed the differentiation of measurements of MMP in medium in apical and basal sides. It also allowed a standardised area of exposure of explant to medium and facilitate calculation of concentrated levels of medium with the volume chamber. It could perhaps be useful to repeat the experiment with high energy and low number of shots and vice versa. For example, it would be useful to repeat the

experiment with 3 or 4 explants at 0.1, 0.15, 0.20, 0.25mJ and 25 laser spots, 50 spots and 75 spots each to fully define the treatment thresholds for this laser.

4.5 Conclusions

In conclusion, the current data showed that laser may be a plausible modality to manipulate the extracellular protease profile that would be beneficial in rejuvenating the retina. Higher number of laser spots resulted in higher release of activated MMP 2 and the levels of MMP2 activity is sustained beyond day 9 of incubation on the basal end. This could have an implication for the design of clinical trials.

With the results, it was then vital to investigate the impact of varying levels of MMP activity on increasing transport across the BrM.

Chapter 5. The effect of exogenously applied MMPs on hydraulic conductivity across the Aged Bruch's membrane.

5.1 Introduction

The previous chapter established that the 2RT laser increased the levels of active-MMP in a directional and time-dependent sequence. The results have also shown that the profile of MMP release was dependent on the number of laser spots. Thus, it would be crucial to determine the impact of different levels of MMP activity on hydraulic conductivity in the aged BrM.

The neural retina undergoes a very high rate of oxidative metabolism as compared to other tissues in the body, hence requiring a sophisticated transport support system to provide it with the necessary nutrients and waste removal from release of the free radicals generated in this process. (Cohen and Noell, 1960, Ahmed et al., 1993, BS, 1983) For decades, it was known that the rate limiting anatomical structures for transport were the blood retinal barriers between the endothelial cells of retinal capillaries in the inner retina and the single layer RPE cells in the outer retina.(Cunha-Vaz et al., 1966, Foulds, 1990) more recently, Hussain et al have demonstrated the contribution of the inner collagenous layer of the BrM to resistance in the aged population. (Starita et al., 1997)

The BrM is a complex acellular pentalaminar structure made up of collagenous and elastic fibers which sits between the RPE and choroid layer. Although not a cause of the ageing retina, the BrM itself had been found to host a wealth of changes secondary to aging and itself compromises further downstream effects of the ageing macular. Structurally, it was known that the BrM increases from 2um in thickness in the first decade of age to 7um by the 10th decade.(A, 1985, Sarks, 1976b, Ramrattan et al., 1994b). Furthermore, Marshall and Bird have previously found an increase in lipid content in the inner collagenous layer of the BM, hence introducing a hydrophobic barrier amongst aged eyes.(Bird and Marshall, 1986) Furthermore, these changes were found to be more pronounced in the macula as compared to the periphery. Clinical evidence correlated these changes to a decreased rate of visual pigments recycling (Eisner et al., 1987, Coile and Baker, 1992, Sandberg and Gaudio, 1995) and delayed visual adaptation of receptors both in normal ageing and early AMD. From various experimental data, the formation of dysfunctional collagen from

AGEs and ALEs crosslinking play a significant role in causing this resistance and decrease in transportation function across the BrM with age. Hussain et al have developed a 'pore' model which explained the transportation pathways across the Bruch's membrane and Starita et al had demonstrated that the layer of highest resistance across the BrM which increased exponentially with age. Earlier experiments have also demonstrated age related decrease in hydraulic conductivity and molecular transport. (Starita et al., 1997)

Biochemical data from experiments by the same team also found increased sequestration of latent MMPs in aged BrM. As mentioned in the Introduction chapter, MMPs are one of the two groups of extracellular proteases, which function to regulate extracellular matrix in the human body. With a sequestration of latent MMPs, there is less availability for conversion into its active form for matrix regulation. Furthermore, preliminary studies conducted by Ahir et al have found addition of both activated MMP 2 and 9 to increase hydraulic conductivity across BrM. In these experiments, a more pronounced effect with activated MMP 9 was found in aged eyes whilst that of MMP 2 was more significant in eyes of younger donor age group. (Ahir et al., 2002) This implied that MMP activation play a crucial role in regulating turnover of the extracellular matrix of the BrM, which had important implications for a structurally and biochemically compromised aged Bruch's.

The abnormalities of the regulatory coupling of degradation and synthesis can cause structural and functional changes to the BrM.

In the earlier chapter, it was established that the 2RT nanosecond laser resulted in release of MMP in porcine RPE-BrM choroid explant culture and there was a higher quantity of active-MMP release with larger RPE volume damage. Given that previous pilot study have indicated that active-MMP9 resulted in larger improvements of hydraulic conductivity as compared to active-MMP2, it may be appropriate to refer to active-MMP9 as the 'emergency' enzyme and active-MMP2 as the 'maintenance' enzyme. At the first instance, it would be crucial to determine the impact of changes from the 'maintenance' enzyme on the functional capacities across the aged BrM. As such, commercially available active-MMP2 in different levels was chosen as the exogenous MMP added in this experiment. Thus, in the following experiment, the main objectives were to

1. assess the effect of MMP 2 activity (if any) on hydraulic conductivity across

the aged BrM; and 2. to determine the impact of different levels of MMP2 activity on hydraulic conductivity across the aged BrM.

5.2 Methods and materials

5.2.1 Preparation of Human Bruch's-Choroid sample

44 human eyes from 22 donors aged 34 to 80 years of age were used.(UK Transplant Support Service, Moorfields Lion Eye Bank, London, UK). Donor eyes were obtained and used in accordance with the provisions of the Declaration of Helsinki for research involving human tissue. Whole globes were dissected in a Petri dish lined with filter paper (Grade 50; Whatman, Maidstone, UK), moistened with phosphate-buffered saline, (PBS, composition: NaCl, 90 g; NaH₂PO₄, 13.65 g; and KH₂PO₄.2H₂O, 2.43 g dissolved in distilled water with final volume adjusted to 1 L [pH 7.4]; Sigma-Aldrich, Poole, UK) containing 100 U/mL penicillin and 100µg/mL streptomycin. The anterior portion of the eye was carefully removed by a circumferential incision at the pars plana, and the cornea, together with the lens, iris, and vitreous, were discarded. The posterior globe was inspected for any evidence of subretinal blood, extensive drusen, or irregular pigmentation of the RPE or any gross disease of the retina, and those exhibiting any abnormal appearance were discarded. The neural retina was gently peeled away from the underlying RPE and cut at the optic nerve head. One single sample was obtained from the macular of each eyecup with an 8-mm trephine (Stiefel Laboratories, Buckinghamshire, UK). The RPE was carefully brushed away with a fine sable-hair brush, and the Bruch's membrane-choroid complex was gently teased away from the underlying sclera.

The isolated preparation was mounted between the two halves of a Perspex modified Ussing chamber. Both surfaces were rinsed several times with PBS. Altogether, 44 macular samples of Bruch's-choroid from 44 eyes of 22 donors age ranged 34 to 79 years were used.

5.2.2 Activation of MMP

Commercial human pro MMP2 (Sigma-M9070) was used for this experiment. ProMMP2 was prepared as an enzyme stock solution (100 μ g/mL) using Tris-buffer. Enzyme stock is diluted with buffer into 1:1000, 1:500, 1:200, 1:100 and 1:50 concentrations of ProMMP2.

Table 5.1 Dilution and concentration of active-MMP2

Dilution:	MMP2 concentration: μg/ml
1:50	2
1:100	1
1:200	0.5
1:500	0.2
1:1000	0.1

Pro MMP2 was activated with APMA in DMSO to give a concentration of 1mM APMA. The solution is incubated at 37 ° C for 2 hours.

An initial gelatin zymography (methodology as described in chapter 3) with range of MMP concentration was done to check that the commercial protocol activated the ProMMP2 solution in varying concentrations defined above. Quantification of Pro MMP2 and active-MMP2 levels is performed as described previously and normalized against prior zymography results (chapter 3 and 4). (Figure 5.1)

A comparison between zymographic densitometric quantity and concentration of MMP was made semi-quantitatively. This will allow cross comparison of previous zymographic results in terms of densitometric quantity by conversion to concentration of MMP. (Figure 5.2)

Figure 5.1 Representative zymogram of APMA activated MMP2 in varying concentrations

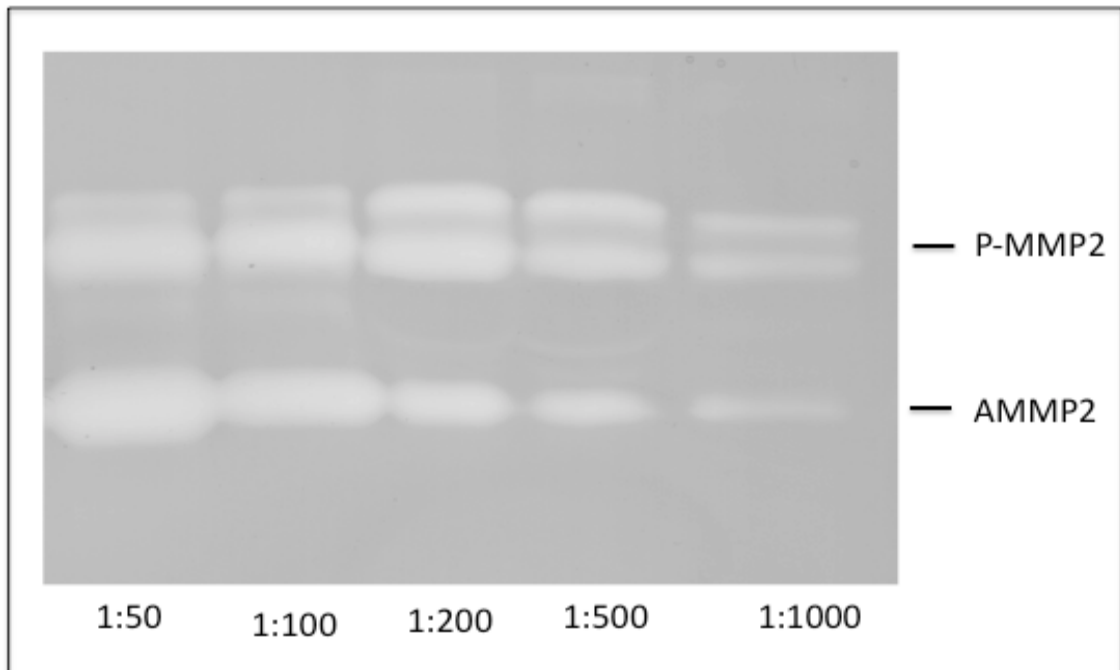


Figure 5.1 shows the representative zymogram of Active-MMP2 post APMA activation of varying concentrations of commercially available ProMMP2 (Sigma). Note the decreasing levels of Active-MMP2 with decreasing levels of proMMP2 concentration.

Figure 5.2 Graph comparing MMP densitometric quantity with concentration of active MMP2.

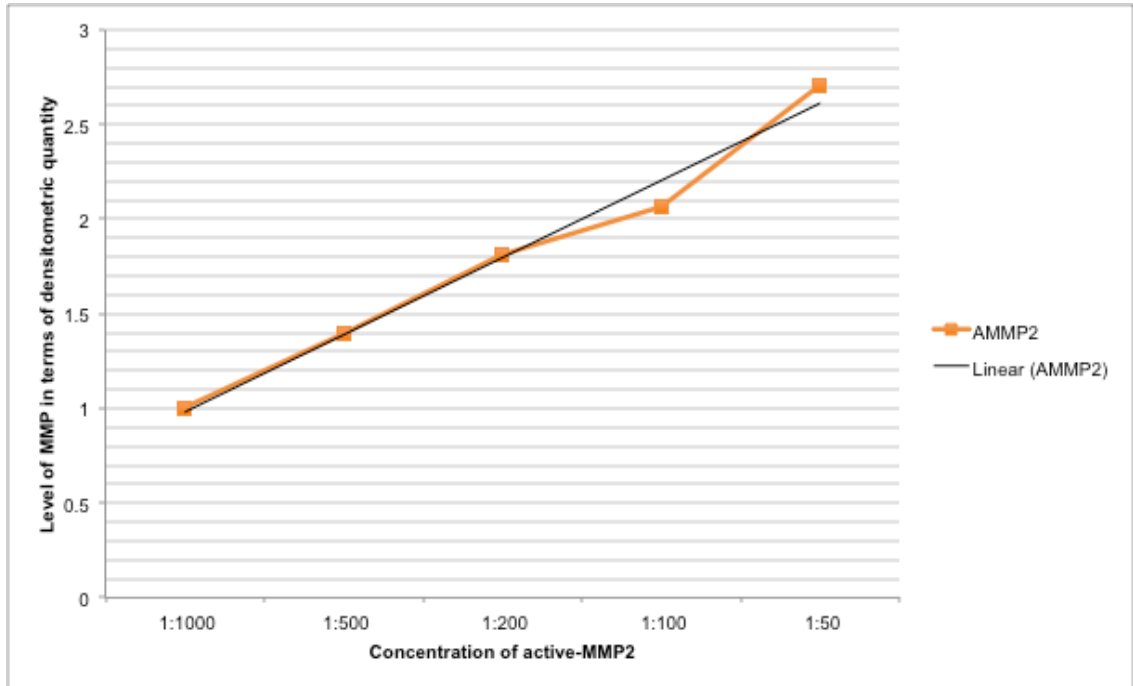


Figure 5.2 shows a graph comparing the levels of MMP in terms of densitometric quantification with the actual concentration of enzymes. (Refer to table 5.1 for concentration in $\mu\text{g/mL}$)

5.2.3 Measurement of hydraulic conductivity

Filter-mounted Bruch's-choroid tissue samples were secured in the Ussing chamber. Both compartments were flushed three times with PBS before being slowly filled to avoid any air bubbles. The compartment appositional to the Bruch's membrane surface was then coupled to a reservoir of PBS.

This arrangement allowed the hydraulic conductivity of the sample to be determined. Briefly, pressure was applied to the Bruch's membrane surface by the PBS reservoir at a fixed height of 220 mm, which applied a constant pressure of 2156 Pa. Once the tissue was under pressure, if a hole was present in the membrane, it became readily apparent because of the speed of movement of fluid into the apical chamber and such samples were discarded. Of the samples collected, fewer than five discs were found to have holes. Intact samples were allowed to equilibrate for 30 to 60 minutes under constant pressure. To measure the fluid outflow, fluid from the Bruch's membrane surface was pipetted and weighed every 15 minutes for 60 minutes, after which time, the Ussing chamber was disconnected and both compartments were washed with PBS. This provided the baseline hydraulic conductivity of the preparation.

The HC was calculated as follows:

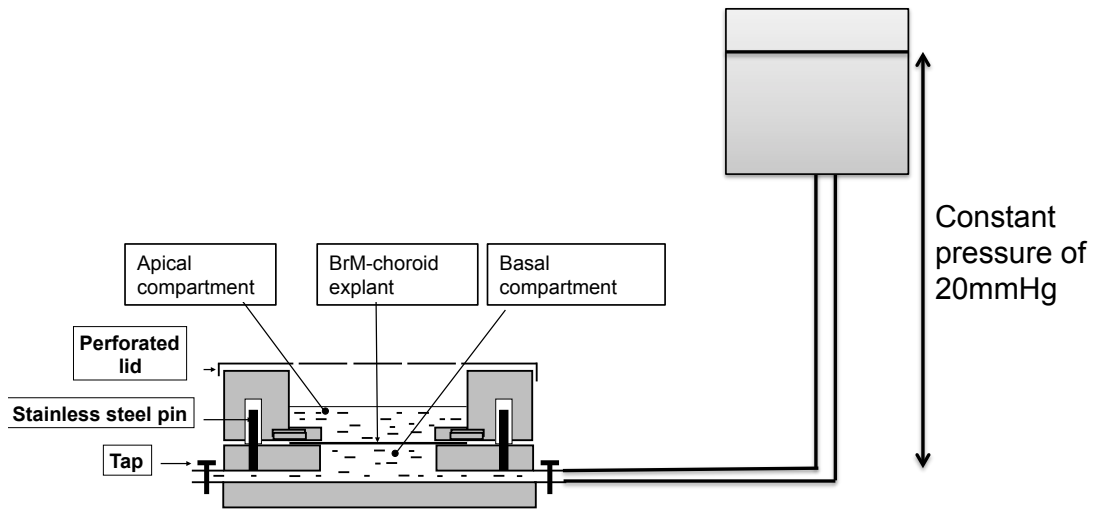
$$HC = \frac{\text{Flow/Unit area}}{\text{Pressure}}$$

Where Flow is referred to as volume collected as a measure of time per second.

Thereafter, activated MMP2 would be added on the apical surface (Bruch's membrane surface) of the chamber and incubated for 18 hours. 60 minutes was chosen as the time for HC measurements as per prior published experiment by Ahir et al (Ahir 2005) using 60 minutes for HC measurements and 18 hour incubation period.

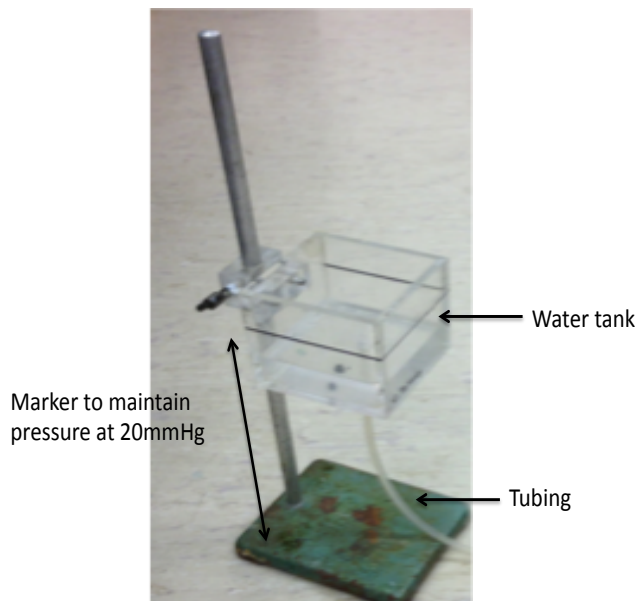
Post incubation, the same procedure would be repeated to measure the HC. Change in HC was calculated as HC minus baseline HC of tissue sample.

Figure 5.3 Schematic diagram of modified Ussing chamber for measurements of HC



Modified Ussing chamber for determination of static hydraulic conductivity. This model consists of a water tank placed at a standard height and attached to a rubber tubing which divides into 5 smaller tubings, each attached to a modified ussing chamber.

Figure 5.4 Photographic diagram of Ussing chamber water tank



5.3 Results

5.3.1 Baseline Hydraulic Conductivity

Baseline hydraulic conductivity of a total of 44 macular samples from 22 donor eyes aged 34 to 79 years of age were measured and plotted against the hydraulic conductivity in age-matched regression curve as measured by Starita et al previously. (Figure 5.5) In this experimental subset, it was noted that all except two donor samples (both aged 55 years) were higher than the expected measurements of hydraulic conductivity within 2 standard deviations.

Figure 5.5 Baseline Hydraulic Conductivity of samples

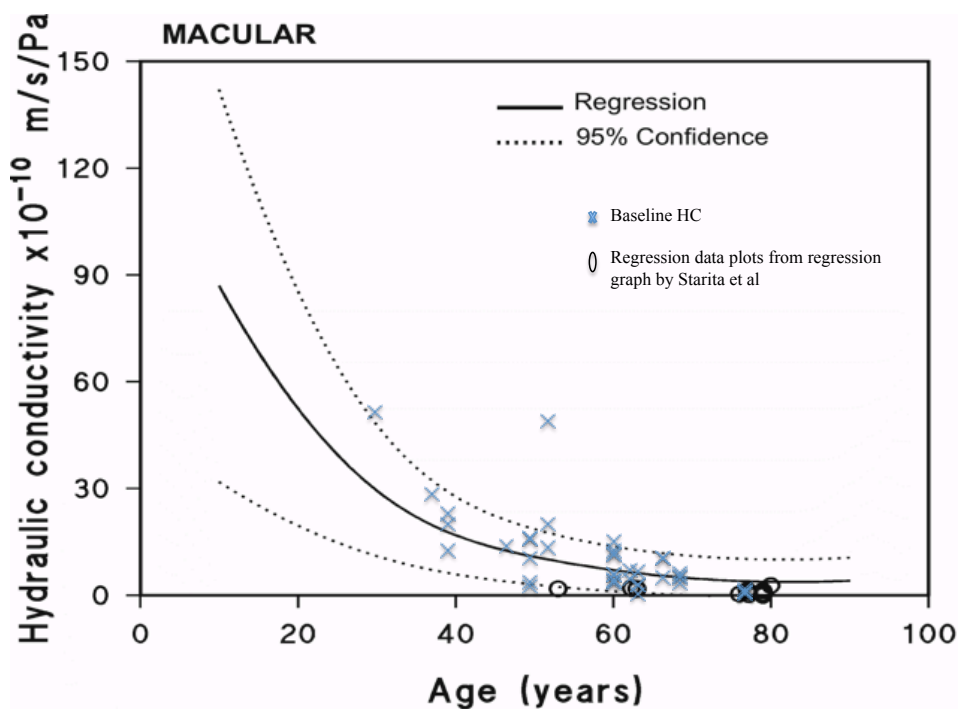


Figure 5.5 shows the distribution of the baseline HC in the current experiment with donor age ranging between 34 to 79 years. (n=44) The HC were measured against the age related standards measured by Starita et al, as shown in the regression model.

Other than 2 samples (both donor age 55 years) which are out of the range of HC, the others were within the normal range, age-matched.

5.3.2 Change in Hydraulic Conductivity

The current results showed an increase in hydraulic conductivity after addition of active-MMP2 (Figure 5.6a).

Further analysis of samples in the graded level of activity of MMP2 showed that younger donor aged samples were susceptible to increases in HC even with minimum levels of active-MMP2 added, but changes in the aged donor samples (>65years) were only quantifiable with addition of higher levels of active MMP2. (Figure 5.6b)

The ratio of change in HC was increased with the addition of a higher level of active MMP2. (Figure 5.7). The ratio of change with addition of 0.1 μ g/mL of ActiveMMP2 ranged between 0 to 3.32, of which only 1sample had a ratio change above 1.5. At 0.2 μ g/mL of activeMMP2 added, the ratio of change was between 1.20 to 1.85. At higher levels of activeMMP2 added, higher increases of ratio change were noted, particularly in the elderly (>60 to 2.55; whilst at 1 μ g/mL was 1.27 to 3.3. At 2 μ g/mL active-MMP2 added, the ratio change increased further to 1.80 to 3.82.

A linear plot was obtained which showed difference in the younger and older age group in terms of increases in ratio of HC change with active-MMP2 concentration. Mean donor age of the 44 samples was 63 years, as such, analysis was done for the young age group, taken as age below 63 year and the older age group, taken as above or equal to 63 years. From the graph in Figure 5.7, the results showed that there was a greater change in HC in the older age group with higher doses of active-MMP2 added. The linear regression model obtained for the samples with donor age less than 63 years of age was not statistically significant. The linear regression model for samples with the older donors had a calculated $R^2=0.196$, but was statistically significant.

Figure 5.6a Plot of pre and post HC with addition of varying dosage of Active-MMP-2

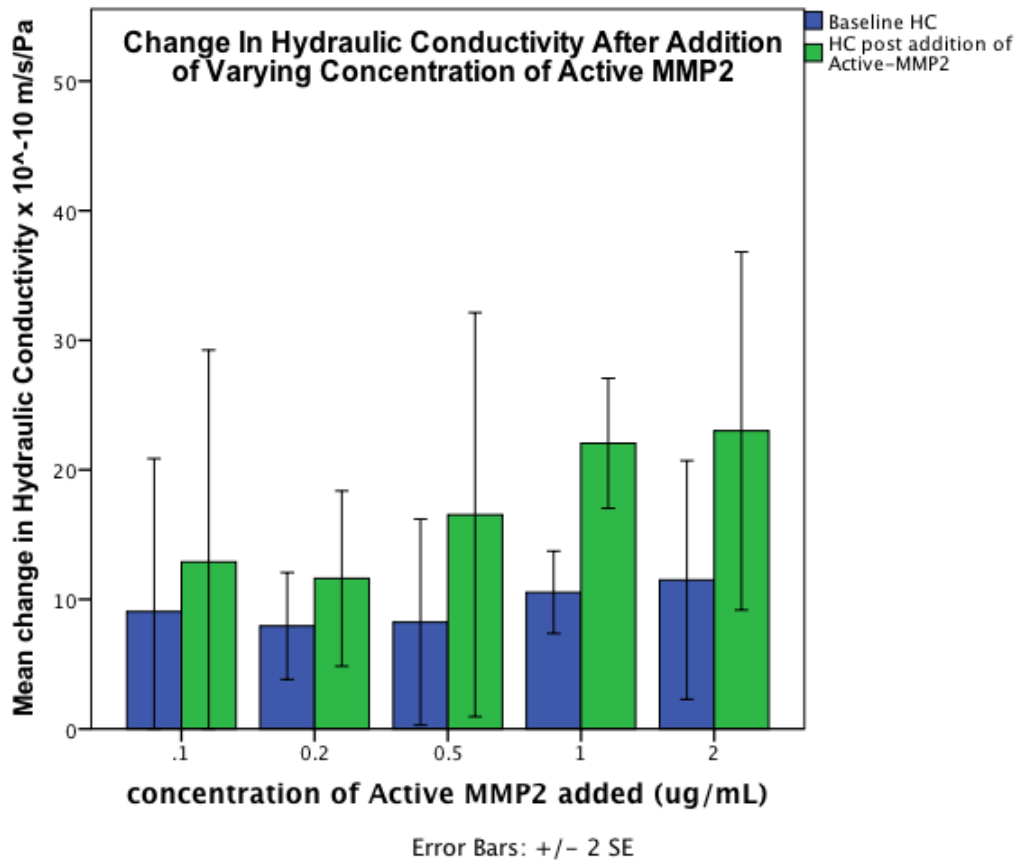
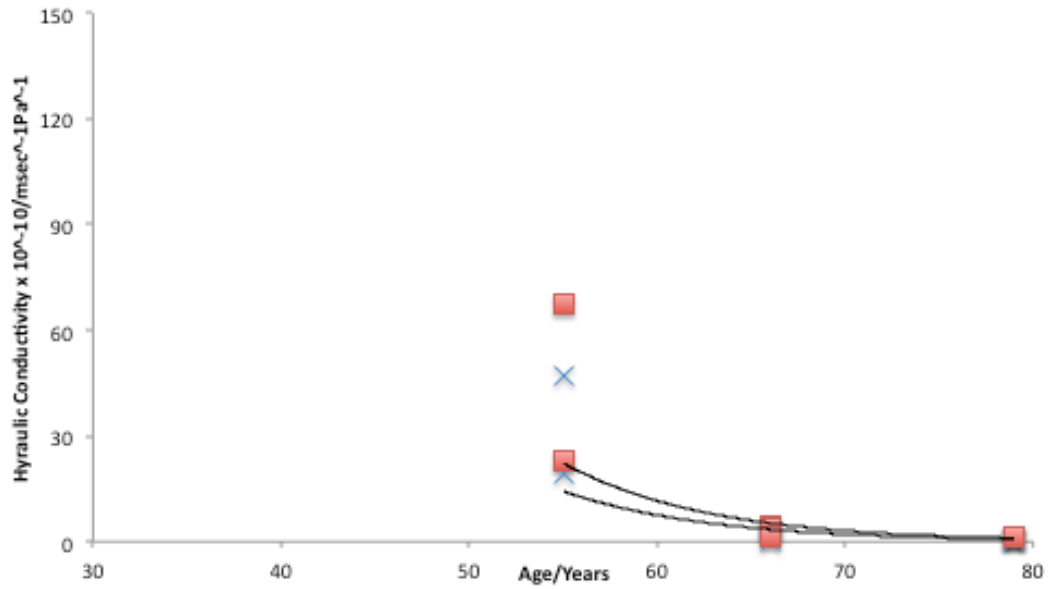
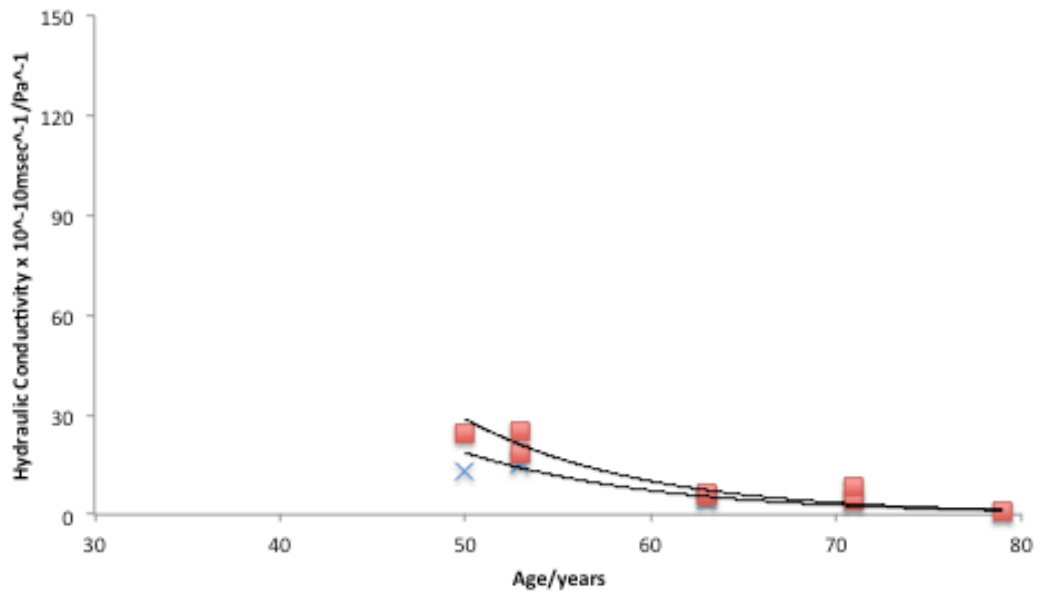


Figure 5.6b Change in HC versus concentration of Active-MMP2

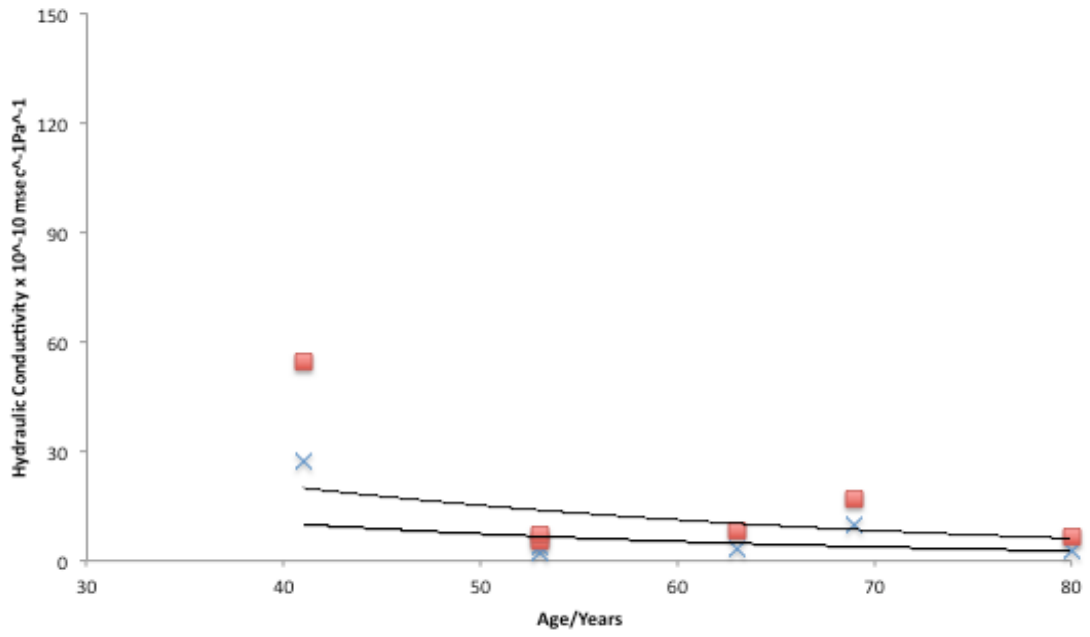
HC Pre and post addition of 0.1ug/mL Active-MMP2



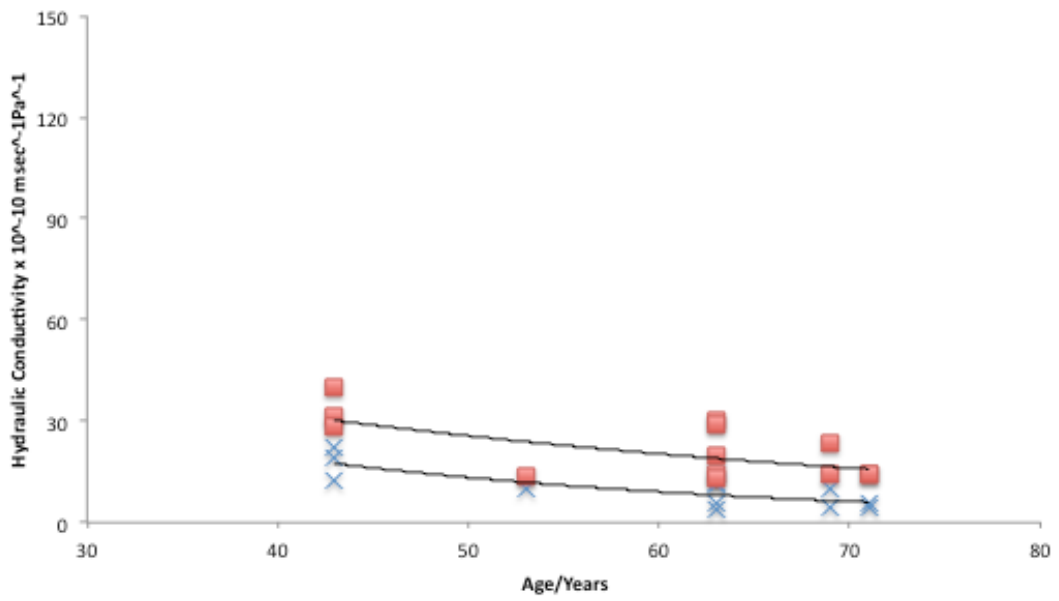
HC pre and post addition of 0.2ug/mL Active-MMP2



HC Pre and post addition of 0.5ug/mL Active-MMP2



HC Pre and post addition of 1ug/mL Active-MMP2



HC Pre and post addition of 2 μ g/mL Active-MMP2

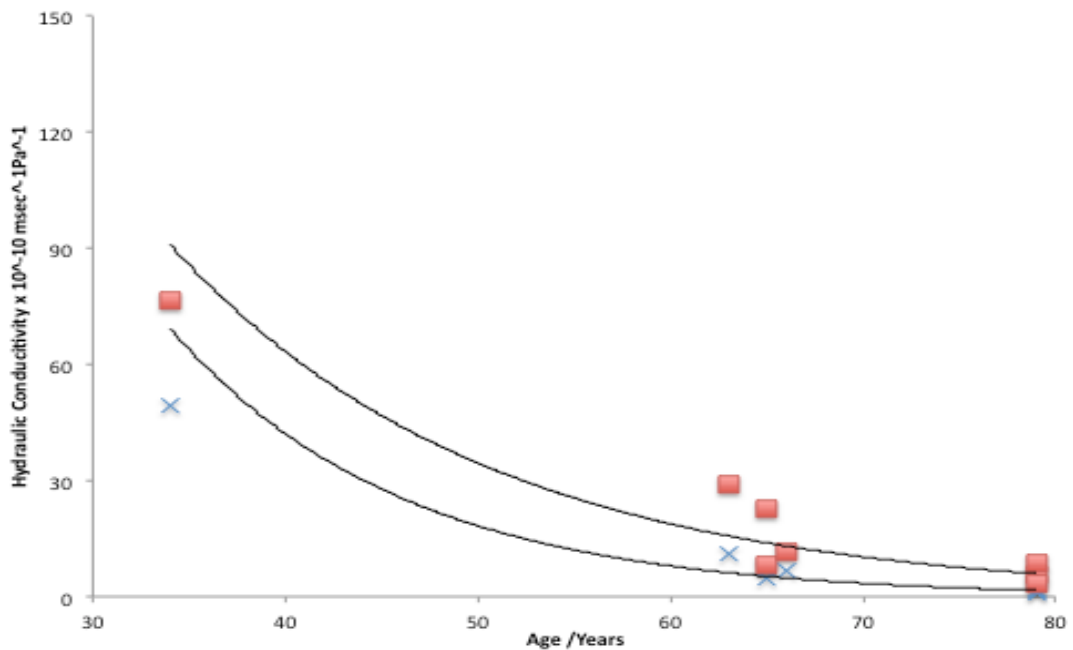


Figure 5.6a demonstrates the pre and post HC upon addition of varying levels of active MMP2 (0.1 to 2 μ g/mL) with age as compared to the regression model for age-related HC by Starita et al. Note the increase in HC after addition of activated MMP2. Increase in HC was noted to be dose-dependent.

Figure 5.6b shows a series of plots of HC pre and post addition of graded levels of activated MMP2 in the macular. With addition of 0.1 and 0.2 μ g/mL of activated MMP2, increases in HC was only noted in the younger donor age group. In the older donor aged samples, there was minimal increase in HC. With addition of 0.5, 1 and 2 μ g/mL of activated MMP2, there was higher increases of HC. The increase of HC was found to be both dose and age-dependent.

Figure 5.7 Linear plot of ratio of change in HC versus concentration of active MMP2 in young and older age group

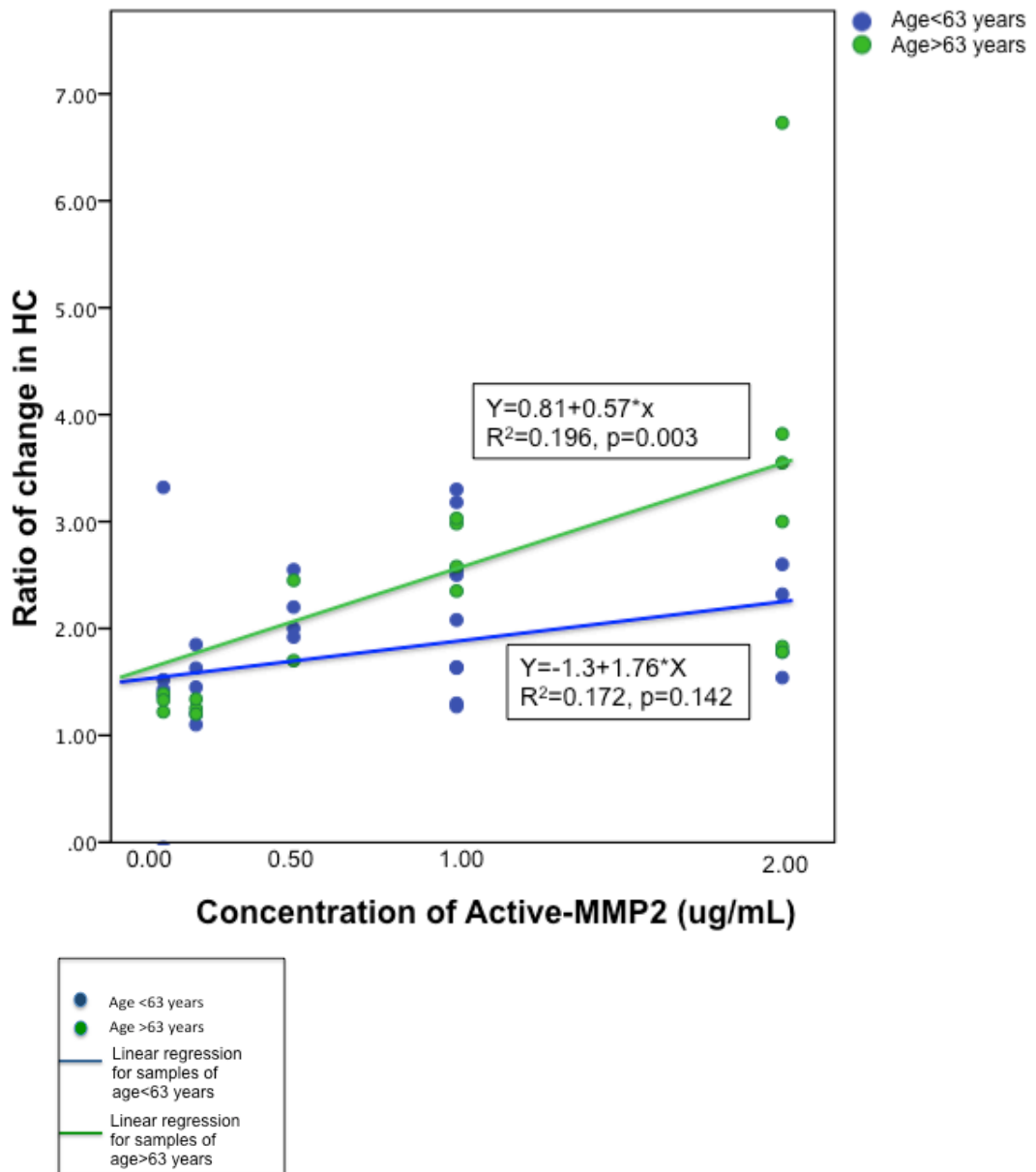


Figure 5.7 shows that in the older donor age samples, there was more pronounced increases in HC (ratio of change) with addition of higher doses of active-MMP2, as compared to the younger age group. Regression model was performed for each of the 2 groups. The linear regression model was not significant for samples <63 years of age. The linear regression model was significant for samples >63 years of age, although the $R^2 = 0.196$.

5.4 Discussion

Results from the prior experiment have shown that higher number of laser spots were associated with a greater increase in active-MMP2. Given that the main action of MMP activity was to clear debris in the extracellular matrix within the BrM, the release of active-MMP in the basal end would be of greater value in this instance. The results from chapter 4 seem to indicate that the increase in levels of active MMP2 on the basal end was proportional to the number of laser spots (ie, 50 laser spot samples had a mean release of twice the levels of active-MMP2 as compared to 25 laser spots).

Starita et al previously demonstrated a correlation between the quantity of lipids and the decline of hydraulic conductivity in the elderly population.(Starita et al., 1996a) In vitro experiments from the same team have previously found that hydraulic conductivity and taurine (and all other amino acids) transport were compromised across the BrM with age.(Hillenkamp et al., 2006) Pilot studies by Ahir et al have also found that the addition of activated MMP from RPE cell culture increases hydraulic conductivity.(Ahir et al., 2002) In this experimental subset, the age-defined baseline hydraulic conductivity was comparable to prior results at the age range that have been used. (Ahir et al., 2002) There were 2 main findings from the current results: 1. A minimal increase in activity of MMP 2 was required before there was any noticeable effect on the older aged donor samples; and 2. activity of MMP 2 on BrM was both age and dose dependent. Hence, it may be assumed from the results that age plays a major role in the debris clearing effect by MMP activity.

The use of an intact Bruch's-choroid sample had been justified previously with several studies. First, Starita et al had previously shown that the removal of choroidal fibres post-mounting of the explant sample did not result in changes to HC. Also, the same team had demonstrated that the greatest resistance to transport was located in the inner collagenous layer of the BM using excimer laser removal of adjacent layers. (Starita et al., 1997)Furthermore, in experiments conducted by Hillenkamp et al using young bovine eyes and aged human BrM, the authors have concluded that despite age related changes in the choroid, the choroidal layer itself played minimal role in the transport in aging retina. (Hillenkamp et al., 2006)In addition, there were several benefits of keeping the current BrM-choroid explant sample. First, there was thus far, limited literature in the technical success in isolation of BrM. Microdissection

resulted in formation of holes and tears whilst, although Schutt and Holz previously successfully used excimer laser to debulk most of choroidal tissue, they were not able to isolate the Bruch's without structural damage. (Schutt and Holz, 2002) Second, there was a lack of identifiable anatomical border because the posterior border of the BM expands to form intercapillary border of the choriocapillaries. (Olver ARVO poster 1990) Taken into totality, there would be further benefits to use BrM-choroid explant as a system.

There exist several in vitro methods for measuring fluid transport across the Bruch's membrane. Hydraulic conductivity could be measured from a static pressure (as per current experiment) or at various pressures and a flow-pressure profile (dynamic) obtained. Hussain et al had previously shown that in rigid membranes (BrM), both these profiles are linear and pressure-independent, whilst in non rigid membranes (Descemet's and basement membrane of lens capsule), which undergo compression with raised pressure, (Fisher, 1982, Fisher, 1987b), the differences in pressure would result in a nonlinear flow-pressure plot. Preliminary experiments by Hussein et al with BrM using both young and old human BrM sample did not observe signs of compression over a large pressure range. Hence, a linear and/or static pressure measurement would suffice to obtain accuracy of results in this experiment. (A.A Hussain, 2004)

Gelatinase A and B (MMP 2 and 9) regulates the activity of Collagen type IV, V, laminin, fibronectin. (Birkedal-Hansen et al., 1993) In the ageing Bruch's, investigators have found increase in dysfunctional collagen and type IV collagen lining the focal infoldings of basal membrane lining choriocapillaries in aged donors. Further more, increased laminin was found in drusen. There was found to be an increase in striated denatured collagen in both inner and outer collagenous layers of BrM and can be attributed to the increased in crosslinking with AGE and advanced lipoxidation products. Hence, the current results which show that the increasing HC from increased addition of active-MMP in aged Bruch's may be a function of increased degradation of the inherent nature of structural changes involved in an aged BrM. However, it is important to keep in mind that this was an artificially designed invitro experiment which was aimed to mimic a 'life' scenario by addition of activated MMP 2. The gelatinase scenario in an elderly outer retina is far more complex with TIMP and other MMP involvement. In this study, the focus had been on MMP 2 which is a

maintenance enzyme and had been found to have less exaggerated effects in previous studies. Nonetheless, it was still important to determine the impact of this enzyme on the aged BrM.

In this study, several major conclusions may be drawn. First, this study had shown that the older age group would require a higher level of MMP activity to increase its hydraulic conductivity, and second, a minimal level of MMP activity was required before any effect on hydraulic conductivity was noted.

Scientifically, our prior porcine eye laser experiment showed that higher RPE volume injury resulted in higher active-MMP 2 release and this experiment showed that higher levels of MMP2 activity increases HC to a greater extent, particularly in the elderly population. Several theories may account for this phenomena, first, it may well be that aged Bruch's with a higher content of debris would require a higher quantity of MMP activity to enhance its hydraulic conductivity for any rejuvenative effect; however, the results can also be explained by the fact that diffusional status is severely compromised in elderly subjects, and that since active-MMP2 had to move into the membrane via diffusional processes before it can act, and hence, higher levels of active MMP2 are required to achieve results. Perhaps, in the second scenario, incubations should then be prolonged to allow entry of sufficient quantities of these enzymes. Whichever of the two theories, certainly, the results show that higher levels of MMP2 activity is required to enhance transport across the Bruch's membrane, and this is especially so in the elderly population.

Although it must be kept in mind that different species were used in experimental models in chapter 4 and 5, direct comparisons can still be made between the results from the 2 chapters. The following calculations were simplified for comparative and estimation purposes. In a real-life situation, the mathematics behind the biochemical release and physical remodeling of the ECM in BrM for transport would be far more complex. In chapter 4, 50 laser spots at very low laser energy (0.1 to 0.15mJ) released approximately 0.1 μ g/mL of active-MMP2 in the basal compartment. From this chapter, a minimum level of 0.5 μ g/mL concentration of active-MMP2 was required before any effect was noted on hydraulic conductivity in the older age group. Hence, the number of laser spots required for sufficient impact on hydraulic conductivity would have to be in excess of 50 laser spots, and to be exact, a calculated number of 88 laser spots (Please refer to figure 5.2). Furthermore, based on the results, the release

of active-MMP2 is calculated to be 2ng/mL per laser lesion. Ultimately, there is a requirement to produce a database, which will allow future prediction of the potential volume of MMP release per unit laser insults.

Given the current results, it would be reasonable to design a clinical trial laser protocol with the use of minimal laser energy, with a larger number of laser spots.

5.5 Chapter conclusion

Several conclusions can be drawn from the current results. First, the findings suggest that the older population would require a higher concentration of active-MMP2 to improve transport across the BrM. In addition, active-MMP2 release from the 2RT laser would require an approximate of at least 88 laser spots to increase the hydraulic conductivity in the elderly population.

In part 1 of the thesis, laboratory experiments were designed to determine the beam profile of the 2RT laser and to evaluate the impact of this nanosecond laser on the RPE-BrM choroid explant in terms of biological release of MMP and its consequential effect on the transport across the BrM. First, in terms of the laser design, the laser was not found to have a viable speckled beam distribution which was initially designed to prevent secondary laser damage. Second, in terms of the biochemical impact of the laser on RPE-BrM organ culture, it may be concluded that the nanosecond 2RT laser increased the activity of MMPs which in turn increased the fluid transport across the BrM in a dose-dependent fashion. It would be essential to translate the current results into clinical research and determine if similar effects would be noted in human subjects and if so, to assess the efficacy of the laser in retarding the onset and/or progression of early AMD; and to determine the impact of the ultrashort pulse of the laser clinically.

Part 2

Chapter 6. Efficacy and safety of retinal rejuvenation using Ellex 2RT laser in age-related maculopathy (RETILASE trial)- background to investigation plan

6.1 Summary of Investigation plan

Part 1 of this thesis has addressed several problems identified. In summary, the following findings were apparent:

1. The 2RT laser in the current form does not have a viable discontinuous beam profile;
2. Active-MMP2 levels were increased with the application of the 2RT laser on RPE-BrM choroid explant culture;
3. Levels of active-MMP2 increase was a function of dose of laser (ie, number of laser spots), and was time and direction-dependent;
4. Addition of active-MMP2 increased hydraulic conductivity across the human BrM;
5. This increase in hydraulic conductivity was both age and dose-dependent (active-MMP2).

Having established the above findings, it was then important to evaluate the impact of the 2RT laser in human subjects, as a prophylactic treatment modality for preventing or retarding onset of AMD.

This sole purpose of this chapter was to evaluate the clinical study design as to allow some understanding of the clinical parameters set for further evaluation of the data (chapter 7 and 8).

The full title of the King's College Hospital/Moorfields Eye Hospital trial was called "Laser prophylaxis to prevent AMD" with the working title of "RETILASE trial" was designed to assess the efficacy and safety of the 2RT laser in improving visual function in patients diagnosed with early AMD. The RETILASE trial itself was a blinded randomized clinical trial over 24 months, however, this

thesis only evaluates the findings at 6 and 12 months due to time constraints for submission of thesis which was prior to the end of trial.

During the process of the clinical trial protocol design, the company was involved as the laser sponsor as this was the first clinical trial conducted in the UK for the 2RT laser in early AMD. At time of protocol design and start of trial, the laser was not CE marked for AMD, as such, this protocol was subject to approval by ethics and MHRA. The design of the clinical protocol was limited by constraints demanded by the commercial company which included the type of patients recruited, laser treatment protocol and the 6 monthly follow up regime. The following highlights an abbreviated version of the clinical trial protocol for the purposes of discussion and scientific evaluation of this thesis. The full clinical protocol can be found under the Appendix.

Table 6.1 Summary of RETILASE investigation plan

Title	Efficacy and safety of retinal rejuvenation with Ellex 2RT laser in age related maculopathy (RETILASE trial).
Objectives	To determine the efficacy and safety of Ellex 2RT laser in improving visual function and retinal morphology amongst patients with age related maculopathy.
Study Design	<p>A blinded randomized controlled trial to evaluate the efficacy and safety of Ellex 2RT compared to standard care in patients with age-related maculopathy.</p> <p>After informed consent, patients underwent baseline examinations of best corrected visual acuity, contrast sensitivity, microperimetry and flicker sensitivity. Structural changes was assessed by OCT, 2- field retina colour photographs, autofluorescence and fundus fluorescein angiography. Follow up visits was at 6 and 12 months.</p>
Planned Sample Size	80 patients – randomized 1:1 to treatment versus no treatment group.
Patient selection	Patients of either gender aged 55 or above with large drusen ($\geq 125\mu$) in at least one eye (AREDS simple severity grade 2 to 3). Best corrected visual acuity in the study eye was between 50 to 90 ETDRS letters.
Treatment protocols	<p>1) Treatment one: Ellex 2RT, 400μm diameter spot, 2 rings of concentric subthreshold laser spots applied at 2000μm (5 ½ spots sizes out from the fovea) and 2800μm (7 ½ spot sizes out from the fovea). So a total of at least 25 spots was applied.</p> <p>OR</p> <p>2) Standard care (No treatment but observed regularly).</p> <p>Treatment was performed by the principal investigators of each site. Other than the principal investigators, patients and all other investigators were blinded to randomized arm.</p>

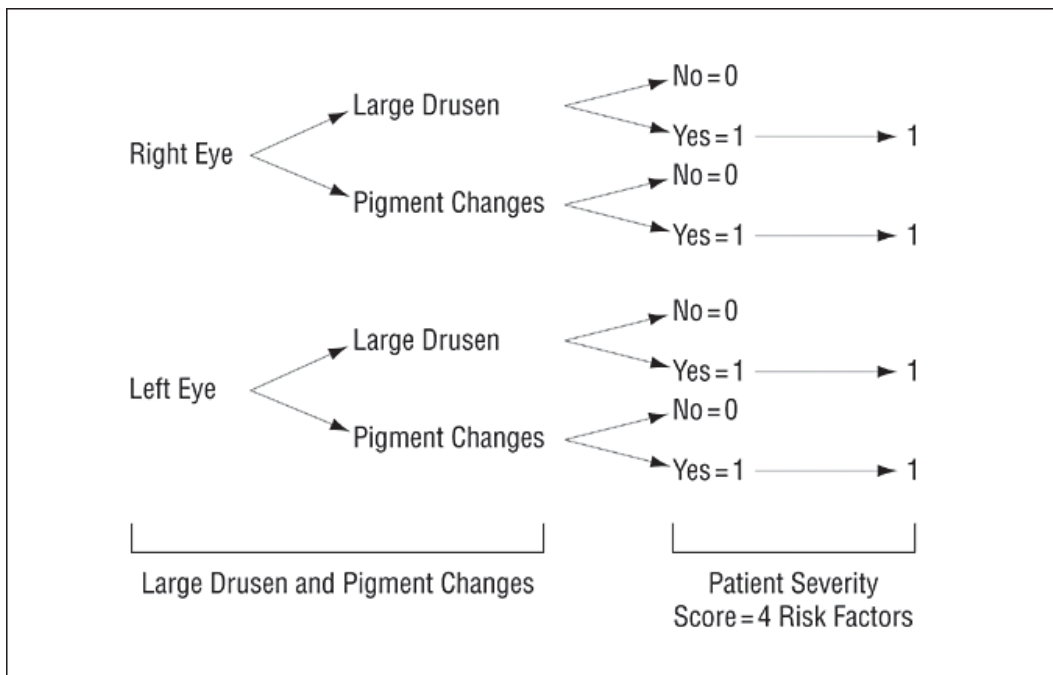
<p>Clinical Outcome Measures</p>	<p>Comparison of the outcomes of Ellex 2RT compared to observation (standard care) will be done on the following parameters at 12 months:</p> <p>Efficacy analyses:</p> <ol style="list-style-type: none"> 1. Primary outcome: Mean change in visual acuity at 12 months. 2. Secondary outcomes: <ol style="list-style-type: none"> a. Mean change in visual acuity at 12 months. b. Mean change in contrast sensitivity, microperimetry and flicker sensitivity at 6 and 12 months. c. Changes in fundus morphology as measured by optical coherence tomography, colour fundus photographs at 6 and 12 months. <p>Safety analyses by comparing the following between the two arms:</p> <ol style="list-style-type: none"> 1. Proportion of patients developing CNV at 12 months. 2. Proportion of patients developing retinal atrophy as measured by autofluorescence and OCT at 12 months 3. Proportion of patients who lost more than 15 ETDRS letters at 12 months. 4. Proportion of patients who lost more than 30 ETDRS letters at 12 months. 5. Any other complications observed at 12 months.
----------------------------------	--

6.2 Background to design of RETILASE trial

6.2.1 Introduction

Age Related Macular Degeneration (AMD) is the leading cause of blindness in the elderly in the western society. In the United Kingdom, an estimated 608, 213 people have been diagnosed with AMD. This number is expected to increase to 755, 867 by the end of the next decade. This attributes to 22.5% of the ageing population. (Minassian et al., 2011) Clinically, “dry” or early AMD is characterised by large drusen and RPE pigmentary changes that can progress to an advanced stage, geographic atrophy. “Wet” or neovascular AMD, another manifestation of advanced disease, is characterised by choroidal neovascularisation (CNV). Clinical classification of early AMD such as the AREDS simplified severity scale (Table 6.2) based on photographic assessment of drusen size and pigment changes in the macula.

Table 6.2 AREDS simplified severity scale grading table



6.2.2 The International grading of age related maculopathy

The progression of the disease is monitored by classifying the morphological changes in the fundus as per International Classification (IC) grading system:

Standard circles for grading ARM related fundus changes. Circles should be reduced on a transparent sheet according to the fundus camera used so that they are 1/24, 1/12, 1/8.6, 1/6 and 1/3 disk diameter. This results in an approximate diameter of the fundus of 63, 125, 175, 250 and 500 μm .

C0: differentiates small from large drusen

C1 and C2: measuring area of hyper or hypopigmentation of RPE

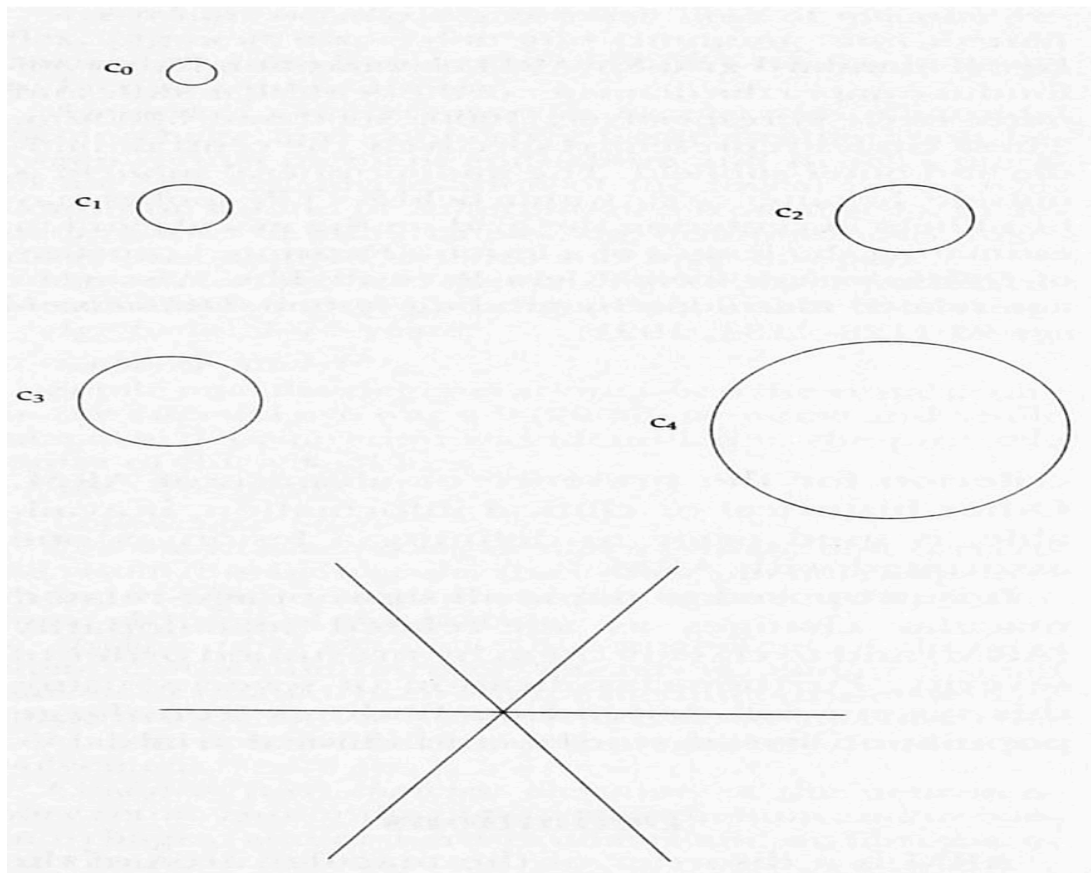
C2: minimum area of geographic atrophy

C3 and C4: geographic atrophy and neovascularization

Spokes: locating centre point and estimating size of lesion.

Figure 6.1 Pictorial demonstration of druse size grading, International Classification

Grading of Drusen



Drusen morphology. Grade highest present within outer circle.

- 0) absent
- 1) questionable
- 2) hard drusen (<C1, 125um)
- 3) intermediate, soft drusen (>C0_<C1; >63um<125gm)
- 4) large, soft distinct drusen (>C1, 125um)
- 5) large, soft indistinct drusen (>C1, 125gin)
- 5a) crystalline/calcified/glistening 5b) semisolid 5c) sero granular
- 7) cannot grade, obscuring lesions
- 8) cannot grade, photo quality

Number of drusen

- 0) absent
- 1) questionable
- 2) 1-9
- 3) 10-19
- 4) >20
- 7) cannot grade, obscuring lesions
- 8) cannot grade, photo quality

Drusen size

- 1) <Co (<63um)
- 2) >C0<C1 (>63um,<125um)
- 3) >C1<C2 (>125um, <175um)
- 4) >C2<C3 (>175um,<250um)
- 5) >C3(>250um)
- 7) cannot grade, obscuring lesions
- 8) cannot grade, photo quality

Main location of drusen

Drusen may not be central to indicated subfield, but may be more to periphery.

- 1) outside outer circle (mid-peripheral subfield)
- 2) in outer subfield
- 3) in middle subfield
- 4) in central subfield
- 4a) outside fovea (center point)
- 4b) in fovea
- 7) cannot grade, obscuring lesions
- 8) cannot grade, photo quality

Area covered by drusen in subfield

- 1) <10% 2)<25% 3)<50% 4) >50%

7) cannot grade, obscuring lesions 8) cannot grade, photo quality

Hyper and Hypopigmentation of the Retina

Hyperpigmentation

0) absent

1) questionable

2) present <Co (<63um)

3) present >Co(>63um)

7) cannot grade, obscuring lesions

8) cannot grade, photo quality

Hypopigmentation

0) absent

1) questionable

2) present <Co (<63 um)

3) present >Co(>63um)

7) cannot grade, obscuring lesions

8) cannot grade, photo quality

Main location hyper / hypopigmentation.

This may not be central to indicated subfield, but may be more to periphery. Choose most central location.

1) outside outer circle (mid-peripheral subfield)

2) in outer subfield

3) in middle subfield 4) in central subfield

4a) outside fovea (center point)

4b) in fovea

7) cannot grade, obscuring lesions

8) cannot grade, photo quality

Neovascular AMD

Presence

0) absent 1) questionable 2) present

7) cannot grade, obscuring lesions 8) cannot grade, photo quality

Typifying features

1) hard exudates 2) serous neuroretinal detachment 3) serous RPE detachment 4) hemorrhagic RPE detachment 5) retinal hemorrhage

5a) subretinal 5b) in plane of retina 5c) subhyaloid 5d) intravitreal

6) scar/glial/fibrous tissue

6a) subretinal 6b) preretinal

7) cannot grade, obscuring lesions 8) cannot grade, photo quality

Location. Choose most central location.

- 1) outside outer circle (mid-peripheral subfield) 2) in outer subfield
- 3) in middle subfield 4) in central subfield
- 4a) not underlying (in) fovea (center point)
- 4b) underlying (in) fovea
- 7) cannot grade, obscuring lesions 8) cannot grade, photo quality

Area covered

- 1) >C2<C3(>175um<250um) 2) >C3<C4(->250um<500um)
- 3) >C4 and < 1000um (-central circle of grid)
- 4) >1000um <3000um (-middle circle) 5) ->3000um <6000um (-outer circle)
- 6) >6000um
- 7) cannot grade, obscuring lesions 8) cannot grade, photo quality

Geographic Atrophy

Presence

- 0) absent 1) questionable 2) present: ->C2 7) cannot grade, 8) cannot grade, Location. Choose most central location.

- 1) outside outer circle (mid-peripheral subfield) 2) in outer subfield
- 3) in middle subfield 4) in central subfield
- 4a) not underlying (in) fovea (center point) 4b) underlying (in) fovea
- 7) cannot grade, obscuring lesions 8) cannot grade, photo quality

Area covered

- 1) >C1<C3(>175um<250um)
- 2) ->C3<C4(->250um<500um)
- 3) >C4 and < 1000um (central circle of grid)
- 4) >1000um and <3000um (-middle circle) 5) >3000um and <6000um (outer circle)
- 6) >6000um
- 7) cannot grade, obscuring lesions
- 8) cannot grade, photo quality

6.2.3 Summary of Current Clinical Understanding of Pathology of AMD

AMD is a degenerative disease that affects the outer neural retina, retinal pigment epithelium (RPE), Bruch's membrane (BrM), and the choroid. The clinical hallmark of the disease are the accumulation of yellow deposits called drusen in the fundus and this may be associated with hypo- and hyper-pigmented areas of RPE, the former signifying areas of RPE cell loss.(Sarks, 1976b) Since photoreceptors depend on the RPE and the choroidal circulation for nutrients as well as for the clearance of metabolic end-products, impairment of transport across BrM could contribute to abnormalities associated with late AMD. These may include photoreceptor dysfunction, atrophy, RPE detachment and sub-RPE neovascularisation (Vujosevic et al.)

6.2.4 Bruch's Membrane (BrM)

BrM is an important pentalaminar layer, located between the choriocapillaries and the RPE, contributing to the transport of nutrients and waste products into and out of the photoreceptor layer. BM thickness has been found to have a marginal increase with age. (Ramrattan et al., 1994b) A more significant observation is the build up of debris within this layer.(Grindle and Marshall, 1978)

Prior histological studies of aged BM have demonstrated the following:

1. Increases in collagen content and cross-linking(Newsome et al., 1987b, Karwatowski et al., 1995b)
2. Increased content and altered composition of proteoglycans has also been noted.(Kliffen et al., 1996a)
3. A higher total lipid content in BrM. (Fisher, 1987b) Lipid- and protein-rich debris has been found accumulating under the RPE and within BM. This contributes to the formation of focal (drusen) and diffuse (basal laminar and linear) deposits found in AMD.(Pauleikhoff et al., 1990, Green and Enger, 1993, Green, 1999a)

Taken in totality, this results in a structural disorganization of the collagen fibers and thinning as well as fragmentation of the elastic layer.(Hogan and Alvarado, 1967a, Spraul et al., 1999a)

There are several pieces of evidence for the contribution of metalloproteinases (MMPs) to the thickening of BrM, and hence, AMD.

First, both genetic and serum studies of inhibitors of MMPs (e.g. TIMP3) which is produced by the RPE, has been studied and found to have an increased in AMD patients compared to age matched controls.(Fariss et al., 1997a, Kamei and Hollyfield, 1999b) Higher levels of TIMP-3 may contribute to the thickening of BrM observed in AMD.

Also, whilst there is a known increase in inactive forms MMP 2 and 9 levels in the subretinal space as well as BrM of AMD, the accumulation of inactive forms of MMPs are hypothesized to be a consequence of remodeling of BrM in aged eyes.(Plantner et al., 1998b, Guo et al., 1999b) Increased deposition of collagen and other ECM components induces synthesis of MMPs; however, increased concentration of TIMPs or decreased porosity of BrM prevents its activation. Hence, from the gathered evidence, we postulate that BrM thickening is correlated to AMD and an inactivation of MMPs result in increased BrM thickening.

6.2.5 Ellex 2RT laser

The retinal rejuvenation therapy (Ellex 2RT) uses nanosecond duration pulses and a discontinuous beam energy distribution, which should not harm the photoreceptors (unlike previous conventional thermal lasers). It uses energy levels 500 times lower than current standard laser treatment. It was previously shown to be effective as an alternative to conventional laser in treatment of other retinal diseases such as diabetic macular edema (DMO).(Pelosini et al., 2013)

6.2.6 Prior research work

Preliminary laboratory work

Light sensitive cells of the human retina (photoreceptors) require high level of energy support and waste removal for optimal functioning. RPE is a single layer of epithelial cells which separates the photoreceptor layer from the choroid and controls many bi-directional support functions. RPE is attached to a basement membrane which is a matrix of collagen otherwise known as the BrM. This acts as a semi permeable barrier between the RPE cells and the choroids. Prior work by Professor John Marshall and Dr Ali Hussain and team has shown that debris within the BrM is a precursor of AMD with a resultant age related decreased hydraulic conductivity. (Hussain et al., 2010c, Kumar et al., 2010) Further work was done which explored treatment possibilities with migration of RPE cells across BM with an associated improvement in hydraulic conductivity. Ellex 2RT was shown to be able to induce a wound healing response in the RPE which induces migration and release of metalloproteinases (MMPs). (Guo et al., 1999b) This had a subsequent effect on improvement of transport across the BrM, with a postulated delay in onset of age related macular degeneration

Preliminary clinical work done with Ellex 2RT system.

Clinical results from a pilot study on Ellex 2RT for DME were presented at ARVO 2008. The results should be treated with caution as only 18 of the 29 patients completed the 6 months study. But the results showed that 43% of patients showed 2 or more lines gain in visual acuity and the central macular thickness decreased by more than 5% from baseline in 46% of patients. The laser lesions from the pilot study were shown to be completely subthreshold with no laser scars or any other complications. These results were subsequently published. (Pelosini et al., 2013)

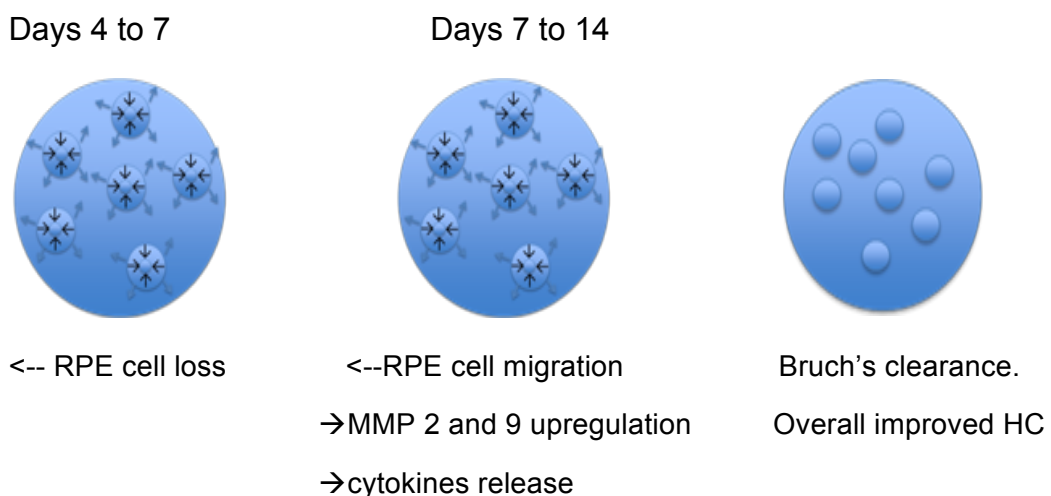
A second randomized controlled study was conducted on Ellex 2RT for DME was presented at ARVO 2010. The laser is currently undergoing clinical trials at CERA, Centre of Eye Research Australia. A 12 month report which includes 50 patients at 12 month follow up showed that the patients had a reduction in drusen. Drusen decreased in 70% of treated eyes. Using flicker and color thresholds, the trial showed these central visual functions improved in 38% of treated eyes. ((Guymer et al., 2014)

6.3 Theoretical Concepts for Delaying Ageing in the Outer Retina

In ageing and AMD, the accumulation of lipid- and protein-rich deposits in BM results in an overall thickening and a structural re-organisation of BM. (Ramrattan et al., 1994b) A consequent decrease in hydraulic conductivity and impairment of transport through BM may play a central role in the pathogenesis of AMD. So improvement of the hydraulic conductivity across the BrM should improve the transport to and from the choroid to the outer retina.

2RT is a nanosecond pulsed laser, which uses very low energy levels to produce limited effects that selectively target melanosomes within the RPE cells. This laser energy absorption by melanosomes within RPE cells causes microbubbles and cavitations to form, damaging a percentage of RPE cells within the laser spots without rupture of the cell membranes. The resultant effects are an upregulation of MMPs and cytokines and RPE cell migration. This should improve the hydraulic conductivity across BrM to and from photoreceptors and delay the progression of AMD in terms of reduction of clinical markers (dusen, pigment abnormality), improvement in visual function (visual acuity, color and contrast sensitivity and rod and cone recovery dynamics).

Figure 6.2 Pictorial demonstration of biochemical impact of nanosecond laser on the RPE



6.4 Objectives of RETILASE trial in reference to this thesis

To assess the efficacy and safety of retina rejuvenation therapy (Ellex 2RT) in patients with large drusen ($\geq 125 \mu\text{m}$) in at least one eye compared to standard care (no treatment). Comparison of the outcomes of Ellex 2RT compared to observation (standard care) was done on the following parameters at 6 and 12 months:

Efficacy analyses:

1. Primary outcome: Mean change in visual acuity at 12 months.
2. Secondary outcomes:
 - a. Mean change in visual acuity at 6 months.
 - b. Mean change in contrast sensitivity, microperimetry and flicker sensitivity at 6 and 12 months
 - c. Changes in fundus morphology as measured by optical coherence tomography, colour fundus photographs at 6 and 12 months

Safety analyses will be done by comparing the following between the two arms:

6. Proportion of patients developing CNV at 12 months
7. Proportion of patients developing retinal atrophy as measured by autofluorescence and OCT at 12 months
8. Proportion of patients who lost more than 15 ETDRS letters at 12 months.
9. Proportion of patients who lost more than 30 ETDRS letters at 12 months.
10. Any other complications observed at 12.

6.5 Study Design

6.5.1 Study Design

Plan of investigation and statistical power of the trial

This is a prospective randomized controlled trial that will compare the mean change in visual acuity at 12 months between the treatment group treated with Ellex 2RT and the observation group (standard care) in patients with age related maculopathy

Sample size (Statistical Power of the study of 80%)

A control sample of size 33, with a baseline ETDRS letters in the range 70-95, and 12 months ETDRS letters was used to provide estimates for the sample size calculation.

The mean score at baseline was 79.7, and the SD of the one year change from baseline EDTRS was 7.59. To be able to detect a difference of 5 EDTRS between arms, in the mean change from baseline to 12 months, based on t-test, at the 5% level of significance, and with an 80% power, would need 76 patients to be recruited. Allowing for 5% dropout the required sample size would be 80 patients, 40 in each arm using a 1:1 ratio. The data will be analysed using analysis of covariance which involves adjusting for baseline in order to increase the power and to provide narrower confidence intervals.

Patient Enrolment

It is expected that 90% of the patients will be recruited from Medical Retina Clinics in King's College Hospital and Moorfields Eye Hospital. The rest of the patients will be obtained from referrals from local optometrists and other ophthalmologists.

The local optometrists will be made aware of this study and patients with age related maculopathy will be informed about the study and referred to the screening clinics in the research department of both institutions. Suitable patients will be informed of the study verbally and by means of a Patient Information Sheet at the research clinics. Patients will be invited to attend a clinic dedicated to the study at both institutions after at least 24 hours. At this baseline visits written informed consent will be obtained from patients wishing to enter the study, prior to enrolment.

Withdrawal from Study

Patients have the right to withdraw from the study for any reason. The investigator also has the right to withdraw a patient at anytime due to failure to follow protocol, administrative or other reason.

Randomisation

Patients are randomised into 2 groups by means of an on-line computerised randomisation programme (randomization.com). The follow-up investigators will be masked of the randomization.

Patient Numbering

Each patient is uniquely identified by a unique study number. Once assigned to a patient, a number will not be reused.

6.6 Population

6.6.1 Inclusion Criteria

1. Patients of either sex aged 55 years or over
2. Diagnosis of age related maculopathy that meet the criteria of large drusen ($\geq 125 \mu$) in at least 1 eye.
3. Best corrected visual acuity in the study eye between 50 to 90 ETDRS letters at baseline visit.
4. Media clarity, pupillary dilation, and subject cooperation sufficient for adequate fundus photographs.
5. No previous macular laser therapy to study eye.
6. Written informed consent and willingness and ability to be followed up length of study.

6.6.2 Exclusion Criteria

1. Drusenoid PED, Choroidal neovascularisation and geographic atrophy in the study eye.
- 2.. Macular ischaemia (FAZ $> 1000\mu\text{m}$ in diameter or moderate perifoveal capillary loss in fluorescein angiogram).
3. Macular oedema of any cause such as wet AMD, diabetic macular oedema, pseudophakic macular oedema or taut posterior hyaloid.
4. Co-existent ocular disease that in the investigator's discretion would lead to decrease visual acuity by 3 lines or more by end of 12 months.
5. No coexistent choroidal neovascularization or geographic atrophy in either eye.
6. History of thermal lasers or treatment with intravitreal antiVEGF agents or steroids for any retinal conditions in the study eye.
7. Participation in an investigational trial within 30 days of randomisation that involved treatment with any drug including those that has not received regulatory approval at the time of study entry.
8. Anticipated major ocular surgery (including cataract extraction) for the period of the trial.
9. Amblyopia in study eye.
10. Known allergy to fluorescein dye or to any component of the study drug

11. Pregnancy at baseline and the patient will be withdrawn from the study if she becomes pregnant during the course of the study.

6.7 Summary of study assessments

Table 6.3 Summary of RETILASE study assessments

Time	Screening	#6 months post entry	#12 months post entry
Informed consent	X		
Ophthalmic history	X	X	X
Medical history	X	x	X
Visual acuity	X	x	X
Contrast sensitivity	X	x	X
Microperimetry	X	x	X
Flicker sensitivity	X	x	X
Ophthalmic examination	X	x	X
2 field photographs	X	x	X
Autofluorescence	X	x	X
Fluorescein angiography ^{\$}	X		
OCT	X	x	X
Randomisation	X		
Treatment	X		

\$ at physician's discretion in all other visits- if choroidal neovascularisation is suspected

Detailed protocol of study assessments can be found in complete RETILASE protocol in appendix. However, several assessments will be highlighted here.

Assessment of Visual acuity

The subjective refraction was performed at 6m using a Snellen chart with the room lights on. Following refraction the best VAs were measured at 4m using ETDRS Chart I for the right eye and Chart 2 for the left eye in a dark room. Both eyes were refracted at the baseline visit and at 12 months.

The VA in the non-study eye were measured as outlined above and the score recorded on the score sheet. If, at one of the follow-up visits, the VA in the non-study eye differs by two lines or more from the VA found at the initial visit, the eye would be refracted as well, and the VA measurement repeated.

At the baseline visit, the initial VA were measured with the patient wearing his/her own distance glasses or unaided (if patient doesn't have distance glasses), using ETDRS Chart RJChart3. At all follow-up visits the previous study refraction were used with the fellow eye lightly patched with a tissue.

Assessment of Contrast Sensitivity

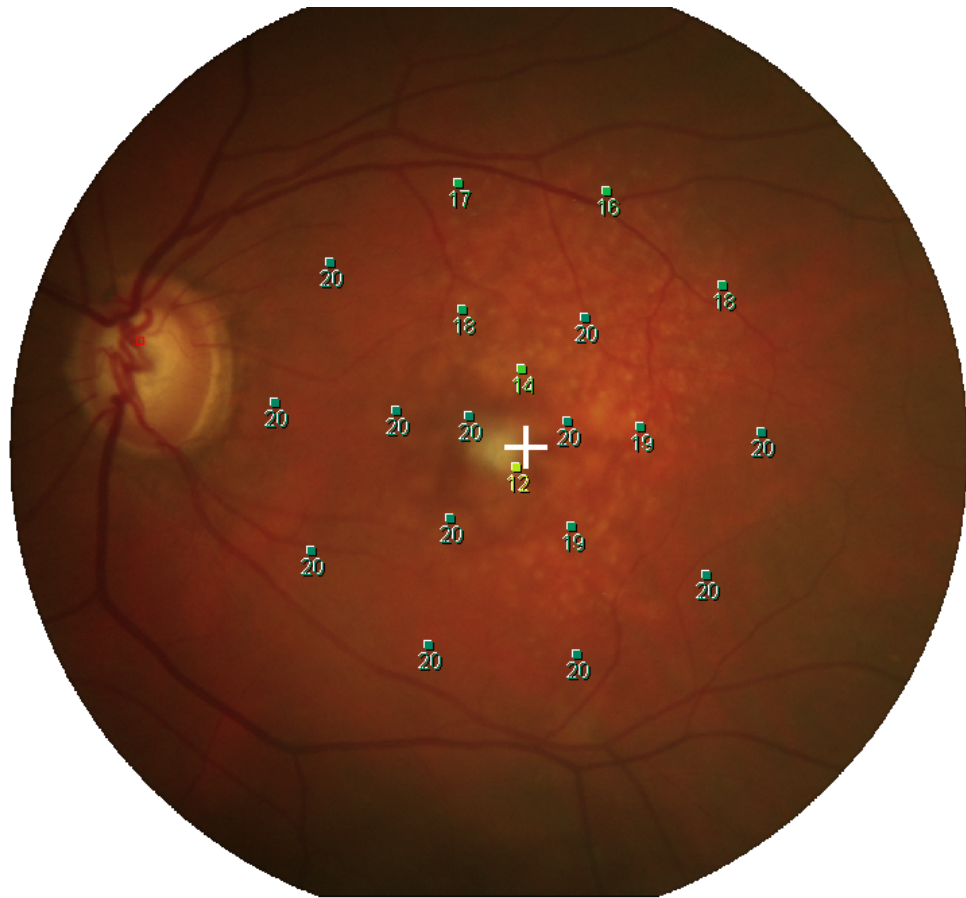
Contrast sensitivity measurements were performed using the Pelli-Robson chart (Clement Clarke Inc., Columbus, OH) at a distance of 1 m and chart luminance of 80 to 120 cd/m². The right eye will be tested followed by the left eye on charts 1 and 2, respectively, with +0.75 D added to the patient's refraction. The patients were asked to name each letter on the chart, starting with the high-contrast letters on the upper left-hand corner and reading horizontally across the entire line. As low-contrast letters could take some time to appear, the patients were given instructions to keep looking and not give up too soon. The optometrist would then circle each letter read correctly and cross out each letter read incorrectly, with letters not attempted left unmarked. The test would be stopped when the patient failed to correctly identify two or more letters in a triplet. The letter-by-letter scoring will be used.

Assessment of Microperimetry

Microperimetry was performed using the Nidek MP 1 (Nidek Technologies, Padova, Italy) device. This instrument allowed the examiner to view the fundus on the computer monitor while it is imaged in real time by an infrared (IR) fundus camera (768 x 576 pixels resolution; 45° field of view). Fixation target and stimuli were projected on to the liquid crystal display (LCD) within the MP1 for the subject to view. The examiner could also view the stimulus and fixation target as part of the IR image on the computer monitor.

The study eye was tested whilst the contralateral eye was patched during the test. Pupils were dilated with one drop each of tropicamide 1% and phenylephrine 2.5% at least 15 minutes prior to microperimetry. Microperimetry was performed by an experienced examiner. The examination was conducted in a darkened room. The following parameters were used: a fixation target consisting of red ring, 1° in diameter; white, monochromatic background at 4 apostilb (asb), stimulus size Goldman III, with 200 milliseconds projection time; and a customized radial grid of 20 stimuli covering the central 10° (centred on the fovea), 2° apart (outer stimuli). The starting stimulus light attenuation will be set at 10 dB. A 4-2-1 double-staircase strategy will be used with an automatic eye tracker that compensates for eye movements. Pretest training was performed, and a 5-minute mesopic visual adaptation was allowed before starting the test. The mean retinal sensitivity was evaluated within central 10°, covering approximately 3 mm of central retinal area on the OCT map. The "9 in 1 layout" printout page (or equivalent) produced by the Nidek MP1 software provides indices related to microperimetry performance, retinal sensitivity and fixation characteristics will be printed out and recorded. The duration of each microperimetry examination and the average eye motion speed (°/sec) will also be recorded as indicators of test performance. The change in fixation stability and retinal sensitivity were noted.

Figure 6.3 Microperimetry

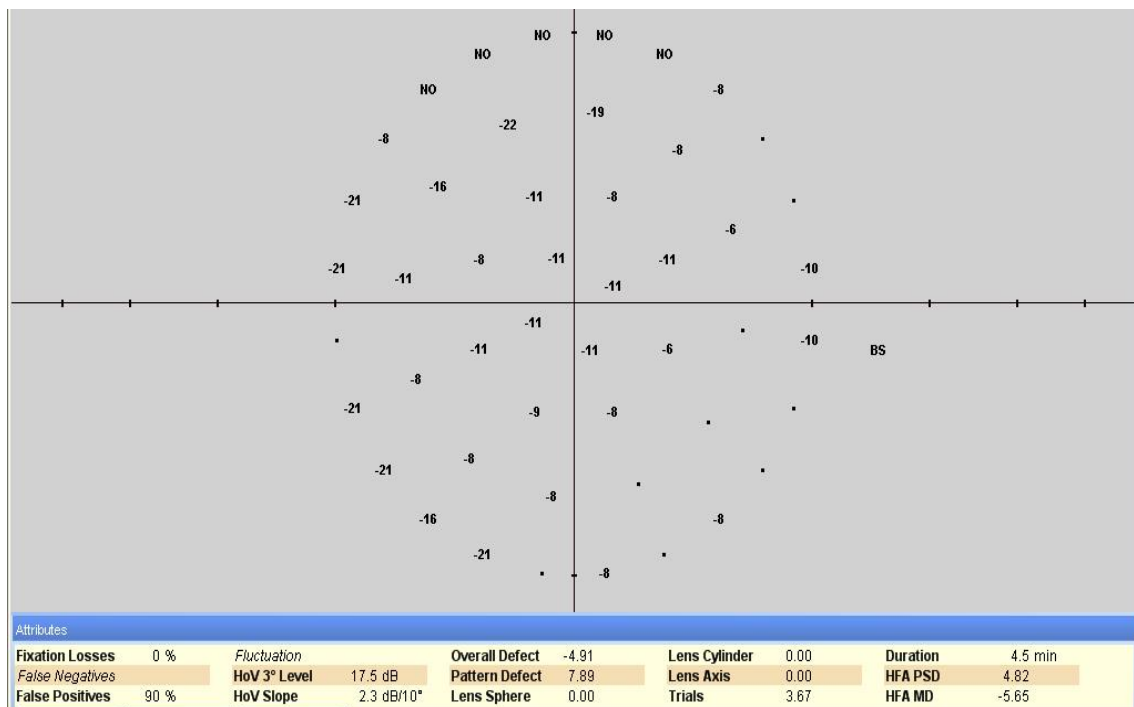


Test	Background	Fixation target	Reliability test	Pattern	Thresh. strategy	Stimulus	○
RETILASE	White	Single cross, 2 °	(0/3)	Follow-up (20)	4-2-1	Goldmann III (200 ms)	

Assessment of Flicker Perimetry

The Medmont perimeter was used to perform static and flicker visual field evaluation of the central 10°. The Macula pattern was used. Targets were 0.5° in diameter, with a maximum spot brightness of 320 cd/m² and was shown on a 3.2 cd/m² background. Spot presentation occurred for 200 ms in static perimetry and for 800 ms in flicker perimetry. Thresholding was achieved with a 6/3 dB staircase.

Figure 6.4 Flicker Perimetry



6.8 Treatment Regime

The Principal Investigators of each trial site performed the 2RT treatment.

Treatment spot size:	400 micron spot
Total number of laser spots per eye:	A total of at least 25 laser spots
Energy range:	70 – 120mJ/cm ²
Energy setting:	Energy increased while applying test nasal mid-peripheral area until a faintly visible spot is observed. Reduce the energy to 70% of this setting then apply the grid pattern
Contact lens:	Area Centralis 1:1 laser contact lens (or equivalent)

Treatment Protocol:

1. Treatment one: Ellex 2RT, 400µm diameter spot, 2 rings of concentric subthreshold laser spots applied, at 2000µm (5 ½ spots sizes out from the fovea) and 2800µm (7 ½ spot sizes out from the fovea). So a total of at least 25 spots will be applied.

OR

2. No treatment or observation (standard care)

Chapter 7

RETILASE results I. Efficacy Evaluation of RETILASE trial

7.1 Introduction

The background to the clinical trial protocol design and the important aspects of the clinical trial protocol such as inclusion/exclusion criteria, follow up regime, assessments as well as treatment regime have been highlighted. The following chapter examines the impact of the 2RT laser on visual function in patients with early AMD.

The primary objective of the RETILASE trial was to determine if the 2RT nanosecond laser is a viable option to delay onset of AMD. Secondly, the trial aimed to investigate the extent of the laser damage, in a group of patients with early AMD.

Part 1, chapter 3 to 5 of this thesis demonstrated the release of active-MMP in invitro RPE-BrM choroid explants. Furthermore, the laboratory studies have correlated the addition of activated MMPs to the increase in hydraulic conductivity across the BrM in an age-dependent fashion. The current laboratory results have found that a higher level of active MMP was required for the same increase in hydraulic conductivity in the older age donor explant cultures as compared to the young. With these earlier encouraging results, it would be prudent to ascertain the efficacy of this laser in rejuvenating the retina in the elderly human subjects.

It must be stressed that this laser was theoretically designed to delay or reverse ageing changes in the outer retina and thereby possibly delay or retard the manifestations of AMD. Due to ethical constraints, the trial was designed to treat subjects with early AMD and no advanced AMD in fellow eye. Ideally, efficacy measures should have included measurements in changes of BrM or changes in transport across the outer retina, however, the only available device that allows intricate measurements of changes were the focal flash recovery or fundus reflectometer which were not available. Hence, the treatment response was monitored using devices that enabled a quantitative measurement of the health of the photoreceptor cells. These included the measurements of visual acuity, contrast sensitivity, microperimetry and flicker perimetry.

This chapter will focus on evaluating the efficacy of the 2RT laser in 'rejuvenating' the aged retina.

7.2 Baseline characteristics of trial participants

7.2.1 Data Sets Analysed

At the onset of this result section, it should be emphasized that the RETILASE trial was suspended in 30 May 2012. The reason for suspension was due to concerns with regards to autofluorescent changes post laser in treated patients. The principal investigators of the trial, upon review of the clinical data collected at 6 with independent data monitoring committee (made up of 2 external consultants and an independent statistician) felt that the autofluorescent changes on FAF suggests that the laser energy applied was not subthreshold as previously conceived. (Discussion to follow in next chapter).

A total of 23 patients have been recruited. 18 patients were recruited from KCH, 5 patients from MEH. Altogether, there were 11 treated cases and 12 controls. All 23 patients completed both 6 and 12 months follow up. Two controls had conversion to wet AMD in the non study eye. By contrast, no cases converted to advanced AMD in the treated eyes.

7.2.2 Baseline Characteristics

A total of 23 patients have been recruited into this study. Mean age of our patients was 72 ± 8 years. 65% of the study cohort were females and 35% were male. Of the 23 patients recruited, 2 were of Indian ethnicity (9%) and the rest were Caucasians (91%).

Of the 23 patients, 11 patients had been treated with 2RT laser according to protocol regime and 12 were controls. The mean age of the cases at time of recruitment were 70 ± 10 years whilst that of controls was 75 ± 6 years. There was one case of Indian ethnicity in each case/control group.

Overall baseline VA of study cohort was 81.26 ± 5.09 EDTRS letters, and baseline contrast sensitivity was 34.57 ± 1.90 letters, baseline MP1 at 4 degrees was 15.60 ± 3.65 dB, at 12 degrees was 14.64 ± 3.88 dB, and baseline flicker perimetry was 2.16 ± 1.79 dB.

Mean baseline VA for cases was 78.64 ± 4.52 letters, whilst that for controls was 83.67 ± 4.48 letters. It should be noted that there was a problem apparent

with the randomization as from table 7.1, the control group had better VA than the treatment group. This randomization process was outside the control of the investigators. The difference between the groups for contrast sensitivity was equivocal. Baseline mean MP1 at 4 degrees was 16.02 ± 2.70 dB and for controls 14.83 ± 4.40 dB, whilst the baseline mean MP1 at 12 degrees was 14.18 ± 2.91 dB for cases and 15.06 ± 4.69 dB for controls. For flicker perimetry, the baseline was -2.35 ± 2.11 dB for cases and -1.98 ± 1.50 dB for controls.

Table 7.1a Baseline characteristics of study cohort

	Total No. of Patients (N)	Mean age/ years	Ethnicity, Caucasian /%	Ethnicity, Indian /%	Ethnicity, Africo-carribean /%
Controls	12	75+/-6	92	8	0
Cases	11	70+/-10	91	9	0

Table 7.1b Baseline measurements of study cohort

	Total No. of Patients (N)	VA/ ETDRS letters	Contrast Sensitivity/ letters	MP1 (4 Deg/dB)	MP1(12 Deg/dB)	FP/dB
Controls	12	83.67+/-4.48	34.83+/-2.88	14.83+/-4.40	15.06+/-4.69	-1.98+/-1.50
Cases	11	78.64+/-4.52	34.27+/-3.04	16.02+/-2.70	14.18+/-2.91	-2.35+/-2.11

7.2.3 Morphology of AMD status of patients recruited

Of the 23 early AMD patients recruited, there were 7(30%) patients classified under the AREDS group 2 and 16(70%) in the AREDS group 3. In accordance to the IC classification, this translated into 6(26%) patients in the early group and 17 (74%) in the intermediate group.

Of the patient cohort, 3 presented with pseudodrusen and 20 had conventional hard and soft , confluent drusen.

Of the cases, 3 (27%) were classified as AREDS 2 and 8 (73%) were AREDS 3, whilst using the IC, 2 (18%) were in the early stages and 9(82%) in the intermediate stages. There was 1 patient with pseudodrusen.

In the control group, there were 4 (33%) patients classified as AREDS 2 and early IC classification and 8 (67%) patients classified as AREDS 3 and intermediate stage of IC classification.

Table 7.2a Morphological profile of study cohort

AREDS	No. (n=23)	IC	No. (n=23)	Pseudodrusse	No. (n=23)
1	0	Early	6	Yes	3
2	7	Intermediate	17	No	20
3	16	Late	0		

Table 7.2b Morphological profile of cases cohort

AREDS	No. (n=11)	IC	No. (n=11)	Pseudodrusse	No. (n=11)
1	0	Early	2	Yes	1
2	3	Intermediate	9	No	10
3	8	Late	0		

Table 7.8c AMD Morphological profile of control cohort

AREDS	No. (n=12)	IC	No. (n=12)	Pseudodrusse	No. (n=12)
1	0	Early	4	Yes	2
2	4	Intermediate	8	No	10
3	8	Late	0		

7.3 Methods of Analysis of efficacy

7.3.1 Mean change in VA, Contrast Sensitivity, Microperimetry, Flicker Perimetry

SPSS vers 19.0 was used for the statistics of this study. The mean and standard deviation of the entire study cohort was calculated at baseline for VA, contrast sensitivity, microperimetry and flicker perimetry. Means of controls and cases were calculated at baseline, 6 months and 12 months and change from baseline at 6 and 12 months were calculated for the above outcome measures.

Correlation was done using nonparametric testing (Mann Whitney Tests) between controls and cases at 6 and 12 months. $P < 0.05$ was considered significant.

7.3.2 Changes in Fundus Morphology

Changes in fundus morphology post laser amongst cases were qualified using clinical measures by the AREDS and IC classification. In particular, the following in terms of percentage change were tabulated: 1. Drusen morphology (ie, from soft confluent drusen to hard drusen); 2. Change in drusen size (larger to smaller) ; 3. Change in drusen number ; 4. change in area of drusen; 5. Change in IC classification; 6. Change in AREDS classification. Comparison between changes in control group and cases were analyzed using the Fischer's exact test. P value < 0.05 was considered significant.

Figure 7.1 is a pictorial description of the method of measuring drusen size and area.

Table 7.9 AREDS classification

Age-Related Eye Disease Study Age-related Macular Degeneration Levels Defined for Eyes	
AMD Level	Criteria
1	Drusen maximum size \leq circle C-0 (63 μ m diameter) and total area \leq circle C-1 (125 μ m diameter)
2	Presence of one or more of the following: (a) Drusen maximum size \leq circle C-0 but $>$ circle C-1 (b) Drusen total area \leq circle C-1 (c) Retinal pigment epithelial pigment abnormalities consistent with AMD, defined as one or more of the following in the central or inner subfields: (1) Depigmentation present (2) Increased pigment \leq circle C-1 (3) Increased pigment present and depigmentation at least questionable
3	Presence of one or more of the following: (a) Drusen maximum size \leq circle C-1 (b) Drusen maximum size \leq circle C-0 and total area \leq circle I-2 and type is soft indistinct (c) Drusen maximum size \leq circle C-0 and total area \leq circle O-2 and type is soft distinct (d) Geographic atrophy within grid but none at center of macula
4 (Advanced)	Presence of one or more of the following: (a) Geographic atrophy in central subfield with at least questionable involvement of center of macula (b) Evidence of neovascular AMD (1) Fibrovascular/serous pigment epithelial detachment (2) Serous (or hemorrhagic) sensory retinal detachment (3) Subretinal/subretinal pigment epithelial hemorrhage (4) Subretinal fibrous tissue (or fibrin) (5) Photocoagulation for AMD

Adapted from AREDS Report 6

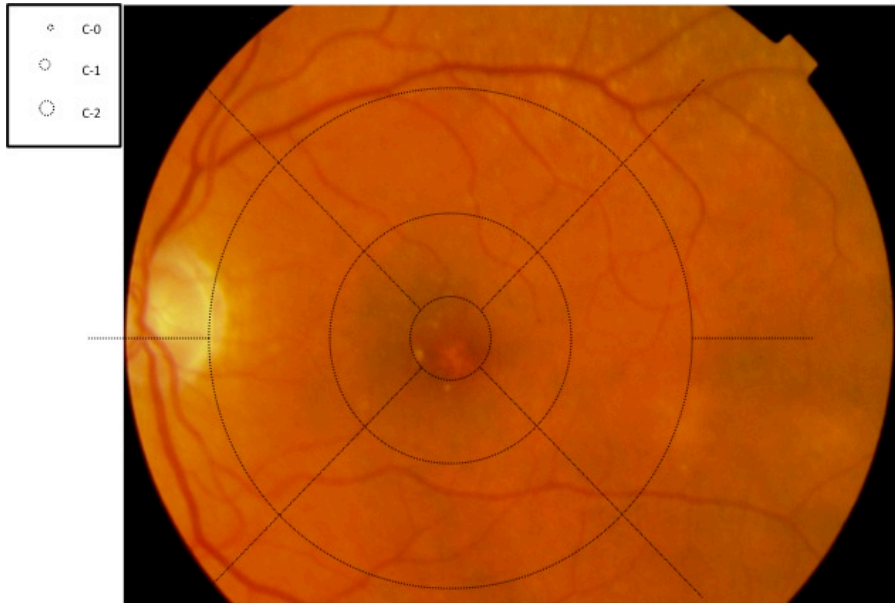
The classification proposed in the ‘International Classification’

Method of druse measurement

Drusen are deposits between the RPE and Bruch’s membrane with a yellowish-whitish appearance on fundus photographs, Drusen appearance, ranges from small round, spots in the plane of the retinal pigment epithelium to large deposits that have that often become confluent with adjacent drusen. The following drusen features are evaluated within the grid (below):

1. Drusen presence/maximum size: maximum size (based on diameter, or if elliptical, longest dimension) by comparing them with circles C-0 (1/24 disc diameter), C-1 (1/12 disc diameter), and C-2 (1/6 disc diameter), nominally 63 μ m, 125 μ m, and 250 μ m, respectively.
2. Morphology of drusen: Hard/soft drusen: drusen are placed in either a hard or soft category on the basis of uniformity of density (color) from center to periphery, sharpness of edges, and thickness: those with decreasing density from center to periphery and fuzzy edges are placed in the soft-indistinct category; those with uniform density, sharp edges, and a solid, thick appearance in the soft-distinct category; and those with sharp edges but without a solid, thick, nodular appearance in the hard category.
3. Total number of drusen: Drusen (all types) number within the grid is calculated manually in each of the subfields and added together. Confluent drusen are considered one drusen if the edges of the druse are not well defined.
4. Total area of drusen: Drusen area within the grid: total area covered by drusen is estimated by mentally moving together all definite drusen and comparing this composite area with those of standard circles and to the standard disk. Three areas are graded separately: the central subfield, the central zone, and the area within the grid.
5. Reticular drusen: yellowish material that looks like soft drusen arranged in ill-defined networks of broad interlacing ribbons.

Figure 7.1 Photographic demonstration of measurement of druse size using AREDS maculopathy grading grid



The Age-Related Eye Disease Study maculopathy grading grid, affixed to the photograph of left eye of one of the recruited patients at baseline. The grid is composed of three circles concentric with the center of the macula and four radial lines in the 1:30, 4:30, 7:30, and 10:30 meridians. The radius of the inner circle corresponds to 1/3 disc diameter in the fundus of an average eye, the radius of the middle circle to 1 disc diameters, and the radius of the outer circle to 2 disc diameters, yielding areas of 4/9 disc diameter, 4 disc diameters, and 16 disc diameters, respectively. Nominally these distances are referred to as 500 μ m, 1500 μ m, and 3000 μ m, respectively, in accordance with longstanding clinical convention, even though a more accurate estimate of the average disc diameter is 1800 to 2000 μ m. Thus, the grid defines nine subfields: central; inner superior, inner nasal, inner inferior, and inner temporal; and outer superior, outer nasal, outer inferior, and outer temporal. Two segments of a horizontal line project from the outermost circle so that the grid can be aligned with the horizontal meridian of the fundus as it is centered over the macula.

7.4 Results

7.4.1 Visual acuity outcome

6 months outcome

Comparison of change at 6 months in VA was made between controls and cases. A difference between baseline VA of 5.03 between the 2 study groups was noted but this was not found to be statistically significant.

At 6 months, the mean VA of controls 83.33 \pm 3.73 ETRDS letters, with a change from baseline of -0.33 \pm 3.28 ETRDS letters, the mean VA of cases was 83.73 \pm 5.20 ETRDS letters, which was an increase of 5.09 \pm 5.67 ETRDS letters, p=0.023.

In the control group, 1 (8%) subject had more than 5 letter improvements and no subjects had more than 10 letter improvements. 1 (8%) subject had more than 5 letter drop from baseline.(Figure 7.3a)

From Figure 7.3b, at 6 months, there were 8 subjects with VA improvements as compared to baseline. 4 (36%) subjects had more than 5 ETRDS letter improvements, of which 1 (9%) subject had more than 15 letters improvements and 2 (18%) subjects had between 10 to 14 letters improvements.

No subjects had more than 5 letters drop. In the subjects with more than 5 ETRDS letter improvements, 3 out of 4 of these subjects had baseline VA < 77 letters, whilst 1 had baseline VA of 85 letters.

From Figure 7.2 and 7.3b, a definite trend of VA improvements at 6 months post laser treatment was noted amongst cases.

12 months VA outcome (Primary outcome)

At 12 months (primary outcome), the change in VA from baseline for cases as compared to controls was 1.73 ± 5.00 letters versus -0.25 ± 4.29 letters, $P=0.449$.

Of the controls, 1(8%) had more than 5 letter improvement and 2(17%) had more than 5 letters drop in VA.

Of the 11 subjects treated with laser, 7 showed improvements in VA. 4 of these 7 cases (36%) had more than 5 letter improvements but none had more than 10 letter improvements. 1 (10)% of patients had a 5 letter drop in VA.

As compared to 6 months, the VA improvements decreased from 5.09 ± 5.67 to 1.73 ± 5.00 letters at 12 months.(Figure 7.2, 7.3b)

Table 7.4a RETILASE: MEAN VA baseline, 6 and 12 months

VA		N	Mean	SD	SEM
BASELINE	Control	12	83.67	4.48	1.29
	Case	11	78.64	4.52	1.36
VA 6 MONTHS	Control	12	83.33	3.73	1.08
	Case	11	83.73	5.20	1.57
VA 12 MONTHS	Control	12	83.42	5.52	1.59
	Case	11	80.82	4.49	1.35

Table 7.4b RETILASE: MEAN change of VA 6 and 12 months

Change VA		N	Mean	SD	SEM	Pvalue
VA change 6 MONTHS	Control	12	-0.33	3.28	0.95	
	Case	11	5.09	5.67	1.71	0.023
VA change 12 MONTHS	Control	12	-0.25	4.29	1.24	
	Case	11	1.73	5.00	1.51	0.449

Figure 7.2 Mean VA, cases versus controls

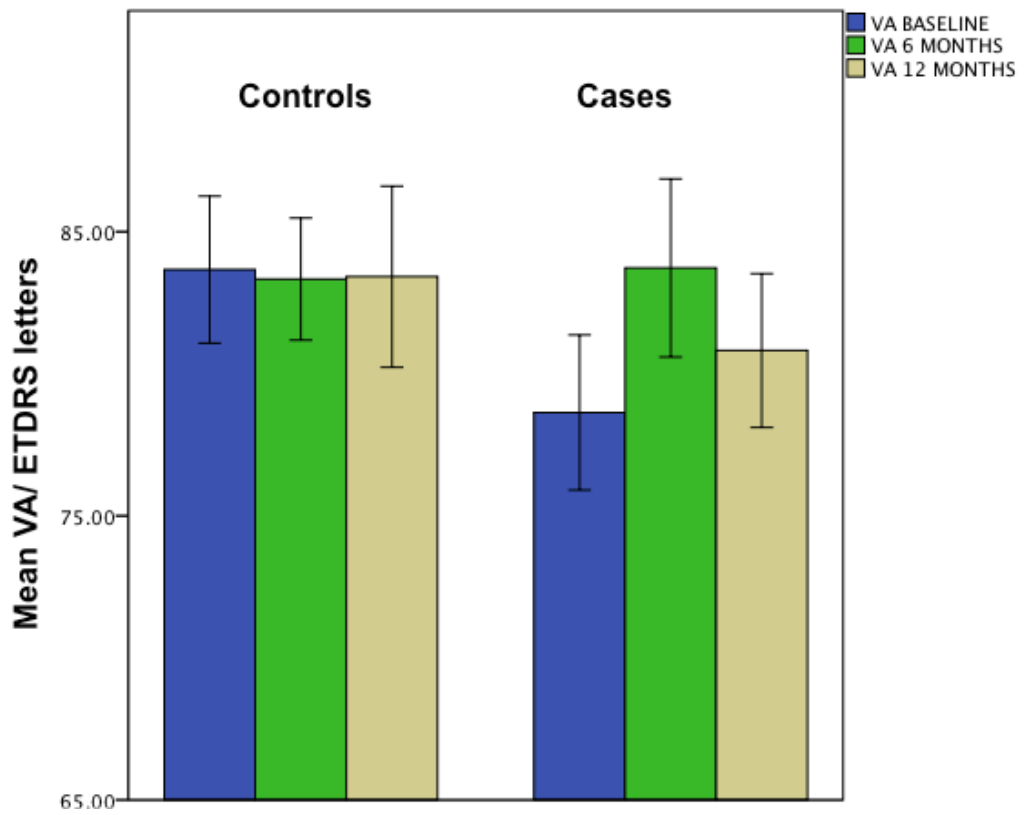


Figure 7.3a Individual plot of change in VA, controls

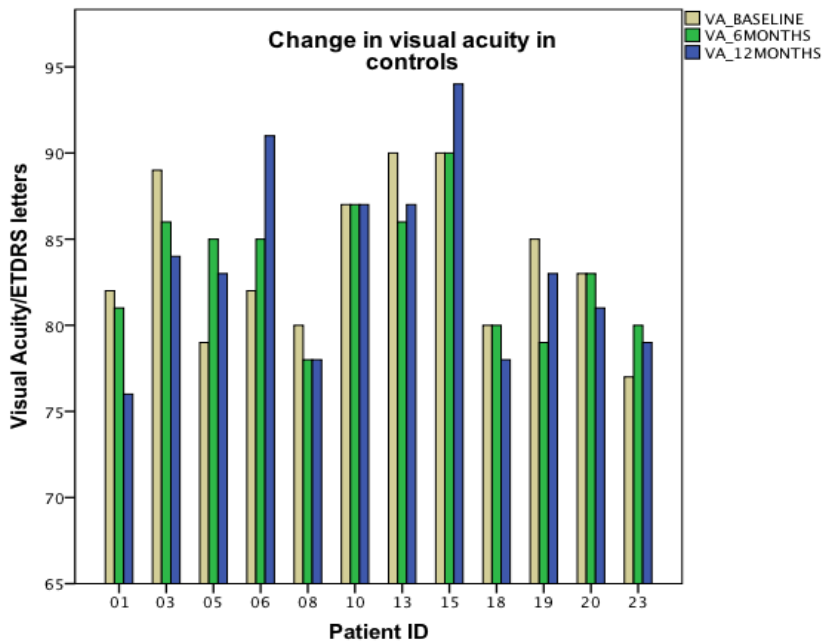


Figure 7.3b Individual plot of change in VA, cases

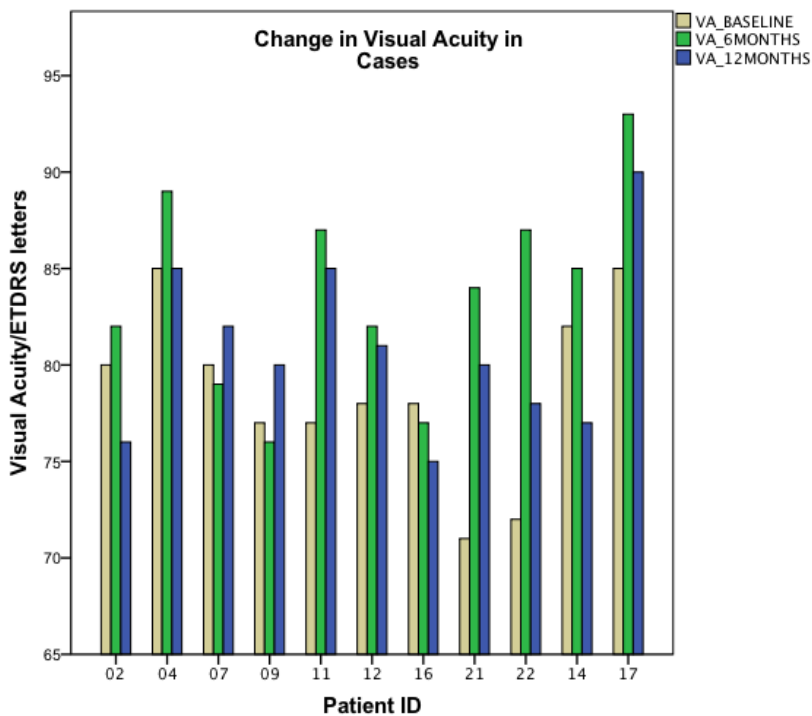


Figure 7.3 a and b shows the individual subject plot of change in VA from baseline to 6 and 12 months. A trend of increase in VA post laser treatment amongst cases at 6 months was noted. 8 of 11 subjects had improvements in VA post laser at 6 months. Of these, 7 of 11 subjects showed prolonged VA improvements at 12 months.

7.4.2 Contrast Sensitivity

The baseline, 6 months and 12 months difference between cases and controls in contrast sensitivity was equivocal. There were no statistically significant changes at 6 and 12 months. No definite patterns nor trends were noted from the individual patient plot as per Figure 7.4a,b.

Table 7.5a RETILASE: Mean Contrast Sensitivity baseline, 6 and 12 months

CONTRAST SENSITIVITY		N	Mean	SD	SEM
CONTRAST BASELINE	Control	12	34.83	2.89	0.83
	Case	11	34.27	3.04	0.92
CONTRAST 6 MONTHS	Control	12	34.17	3.43	0.99
	Case	11	34.18	2.89	0.87
CONTRAST 12 MONTHS	Control	12	35.67	3.42	0.99
	Case	11	34.91	4.13	1.25

Table 7.5b RETILASE: Change in Contrast Sensitivity 6 and 12 months

CHANGE CONTRAST		N	Mean	SD	SEM	Pvalue
Contrast change 6 MONTHS	Control	12	-0.67	1.78	0.51	0.428
	Case	11	-0.09	2.66	0.80	
Contrast change 12 MONTHS	Control	12	0.83	2.92	0.84	0.928
	Case	11	0.64	3.36	1.01	

Figure 7.2a Individual plot of change in CS, controls

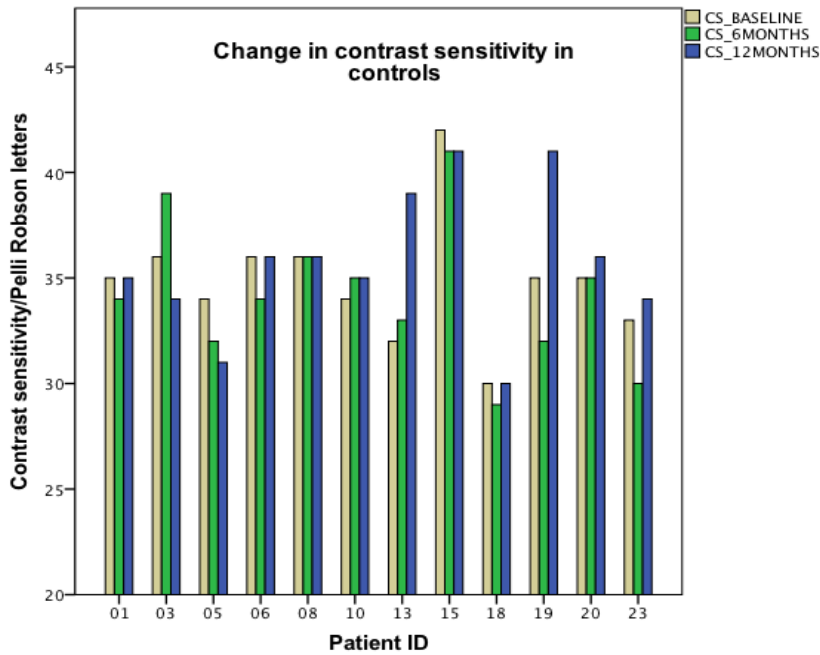
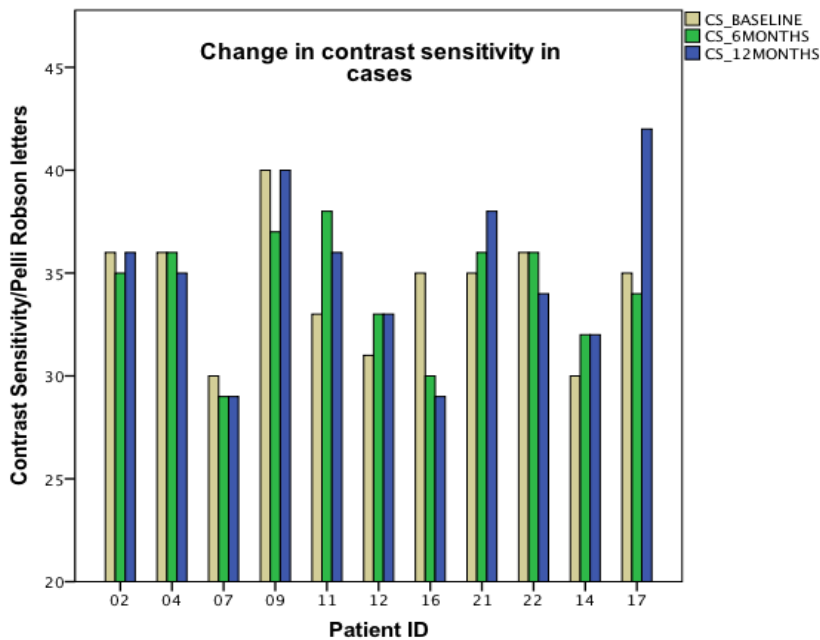


Figure 7.4b Individual plot of change in CS, cases



Figures 7.4a and b shows change in contrast sensitivity of controls and cases at baseline, 6 and 12 months. No significant changes at 6 and 12 months were noted.

7.4.3 Microperimetry

Functional changes can be interpreted as either improvements to the photoreceptors as an effect of treatment or defects from laser damage. In this study, functional changes was analyzed using microperimetry by assessing

1. Stability of fixation;
2. Means at central 4 degrees;
3. Changes at central 4 degrees;
4. Means at central 12 degrees and;
5. Changes at central 12 degrees.

In all controls and cases, recruited subjects demonstrated central and stable fixation at all microperimetric measurements at baseline, 6 and 12 months.

Means for MP1 at central 4 degrees for controls were noted to have slight improvements at 12 months. Baseline MP1 at 4 degrees was 14.83 ± 4.40 dB which improved to 15.10 ± 4.84 dB and 16.52 ± 2.36 dB at 6 and 12 months respectively.

3 of 12 (25%) and 2 of 12 (17%) subjects had more than 2.00dB microperimetric defect from baseline at 6 and 12 months. The results were however not statistically significant.

In contrast, at central 4 degrees, the mean for cases was 16.02 ± 2.70 dB at baseline, 15.80 ± 3.00 dB at 6 months and decreased to 14.61 ± 3.43 dB at 12 months. (Table 7.10, 7.11) Changes between baseline, 6 and 12 months were both not clinically and statistically significant.

At 6 months, 2 of 11 (18%) subjects had more than -2.00dB changes from baseline.(Figure 7.5b) At 12 months, 3 of 11 cases had more than -2.00dB changes as compared to baseline. (Figure 7.5b)

At paracentral 12 degrees, the mean baseline, 6 and 12 month microperimetry for controls were 15.06+/-4.68, 14.25 +/- 4.67 and 15.81 +/-3.16 respectively, whilst that of cases were 14.18+/- 2.91 dB, 13.51 +/-4.07 and 13.55+/- 3.55 respectively.

Mean changes in the control arm was -0.81+/-3.02 dB at 6 months which showed slight increase to -0.39+/-2.09 dB at 12 months, $p>0.05$. For cases, the mean changes at both 6 and 12 months were equivocal (-0.67+/-1.86 dB versus -0.64+/-2.03 dB). (Table 7.7a,b)

Mean changes between cases and controls at paracentral 12 degrees were neither clinically nor statistically significant.

Looking at individual patient plot profile, there was apparent pattern of improvements in the controls at 12 months, 4 degrees (6 patients improved for controls versus 2 for cases 12 months). However, this may be related to the 'non-randomization' process of the recruited subjects. (Figures 7.5a,b; 7.6a,b)

Table 7.6a RETILASE: Microperimetry Analysis at 4 degrees, Baseline, 6 and 12 months

MICROPERIMETRY (4)		N	Mean	SD	SEM
MP 1 (4)/dB	Control	12	14.83	4.40	1.269
	Case	11	16.02	2.70	0.815
MP 1(4) /dB 6 MONTHS	Control	12	15.10	4.84	1.398
	Case	11	15.80	3.00	0.906
MP1 (4) /dB 12 MONTHS	Control	11	16.52	2.36	0.711
	Case	11	14.61	3.43	1.035

Table 7.6b RETILASE: Change in microperimetry at 4 degrees at 6 and 12 months

MICROPERIMETRY CHANGE		N	Mean	SD	SEM	P value
Change MP1(4) /dB 6MONTHS	Control	12	0.271	2.642	.763	0.608
	Case	11	-0.227	3.163	.954	
Change MP1(4)/dB 12MONTHS	Control	11	0.610	2.592	.781	0.133
	Case	11	-1.41	3.169	.955	

Figure 7.3a Individual plot of change in MP1 at 4 degrees, controls

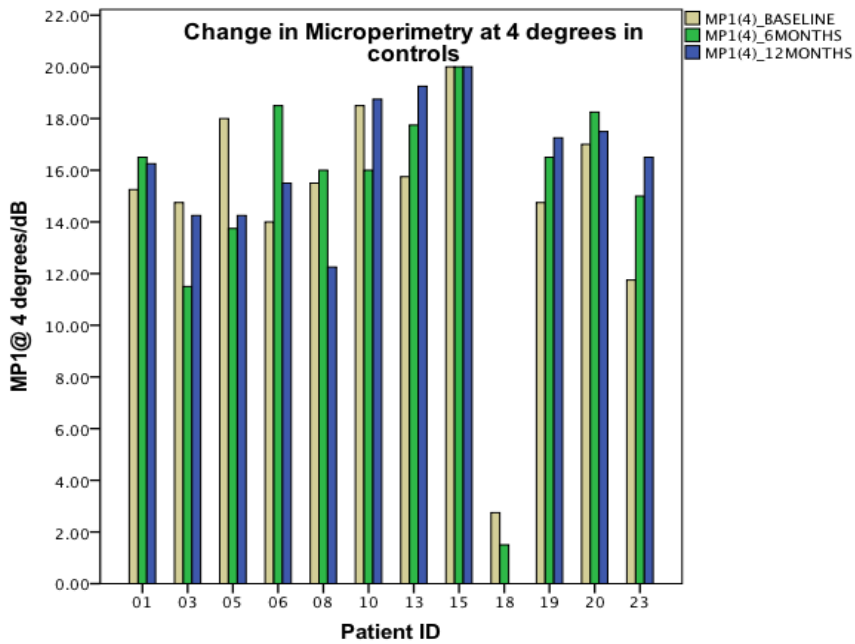


Figure 7.4b Individual plot of change in MP1 at 4 degrees, cases

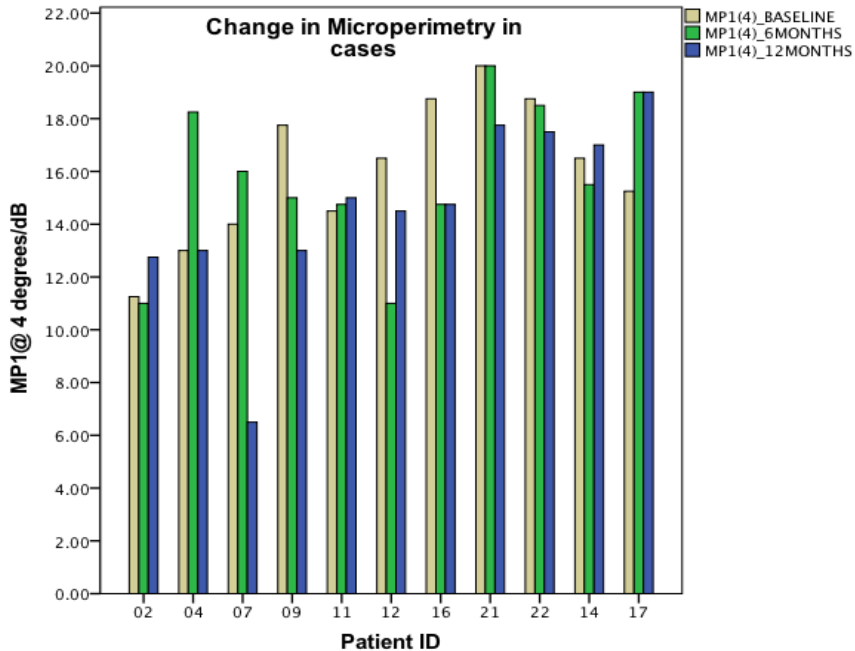


Figure 7.5a, b shows the graphs of changes at 6 and 12 months of individual subjects. In the control arm, 6 subjects showed improvements at 12 months compared to 2 in cases. However, the poor randomization process may account this for.

Table 7.7a RETILASE: Microperimetry analysis at 12 degrees, baseline, 6 and 12 months

MICROPERIMETRY (12)		N	Mean	SD	SEM
MP 1(12) /dB	Control	12	15.06	4.69	1.352
	Case	11	14.18	2.91	0.878
MP1(12)/dB 6 MONTHS	Control	12	14.25	4.67	1.358
	Case	11	13.51	4.07	1.229
MP1(12)/dB 12 MONTHS	Control	11	15.81	3.16	0.953
	Case	11	13.55	3.55	1.070

Table 7.7b RETILASE: Change in microperimetry at 12 degrees, 6 and 12 months

Microperimetry change		N	Mean	SD	SEM	P value
Change MP1(12)/dB 6MONTHS	Control	12	-0.81	3.02	.871	0.833
	Case	11	-0.67	1.86	.560	
Change MP1(12) /dB 12 MONTHS	Control	11	-0.39	2.09	.629	0.748
	Case	11	-0.64	2.03	.612	

Figure 7.6a Individual plot of change in MP1 at 12 degrees, controls

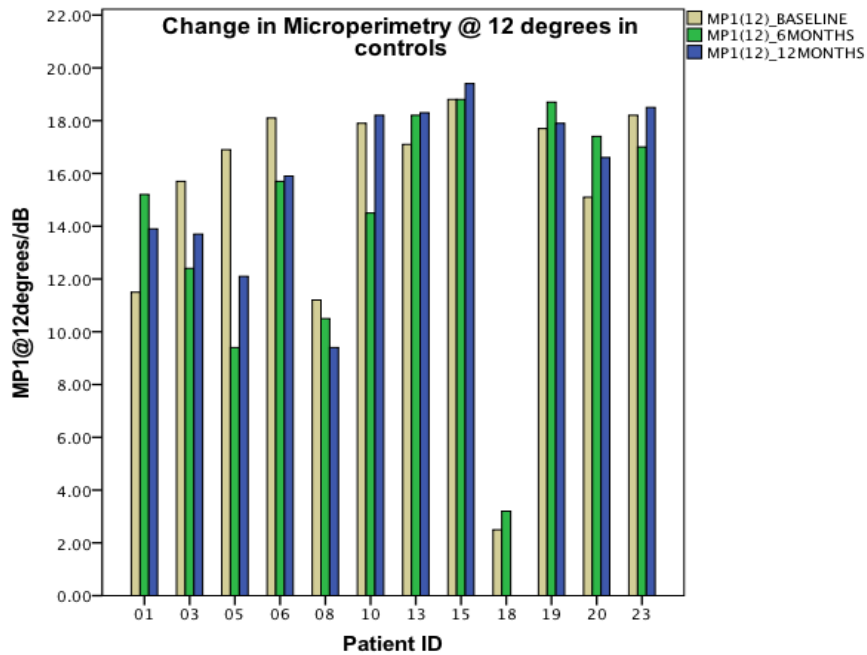


Figure 7.6b Individual plot of change in MP1 at 12 degrees, cases

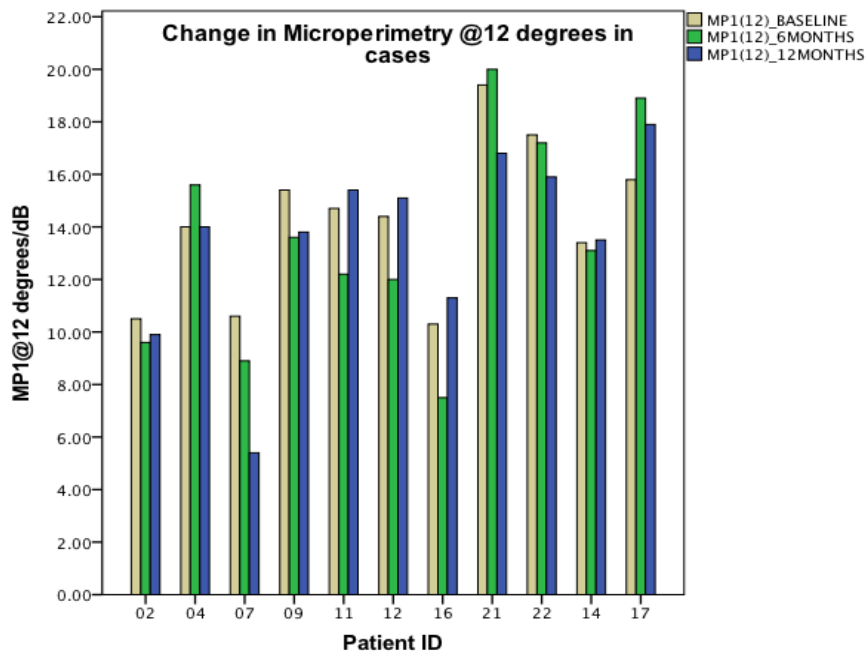


Figure 7.6a and b shows individual patient plot of microperimetric analysis at the 12 degrees paracentral macular region at baseline, 6 and 12 months for cases and controls respectively. No obvious patterns of changes in microperimetry were noted in both cases and controls.

7.4.4 Flicker Perimetry

Flicker perimetric results showed minimal improvements for both controls and cases at 6 and 12 months. For controls, the mean change at 6 months was +0.28 \pm 2.195 dB and +0.20 \pm 2.908 dB at 12 months.

For cases, at baseline, the mean change at 6 months was +0.37 \pm 2.59 dB and +0.73 \pm 2.57dB at 12 months.

Differences between controls and cases were not statistically significant. From the plots in 7.7a, b, no definite trends can be elucidated.

Table 7.8a RETILASE: Flicker perimetry analysis at baseline, 6 and 12 months

FLICKER PERIMETRY		N	Mean	SD	SEM
BASELINE	Control	12	-1.98	1.50	0.432
	Case	11	-2.35	2.11	0.636
6 MONTHS	Control	12	-1.70	2.26	0.651
	Case	11	-1.98	2.36	0.711
12 MONTHS	Control	12	-1.78	3.05	0.881
	Case	11	-1.62	2.40	0.724

Table 7.8b RETILASE: change in Flicker perimetry

FLICKER CHANGE		N	Mean	SD	SEM	P value
6MONTHS	Control	12	+0.28	2.20	0.634	0.833
	Case	11	+0.37	2.60	0.782	
12 MONTHS	Control	12	+0.20	2.91	0.834	0.347
	Case	11	+0.74	2.57	0.774	

Figure 7.7a Individual plot of change in Flicker perimetry for controls

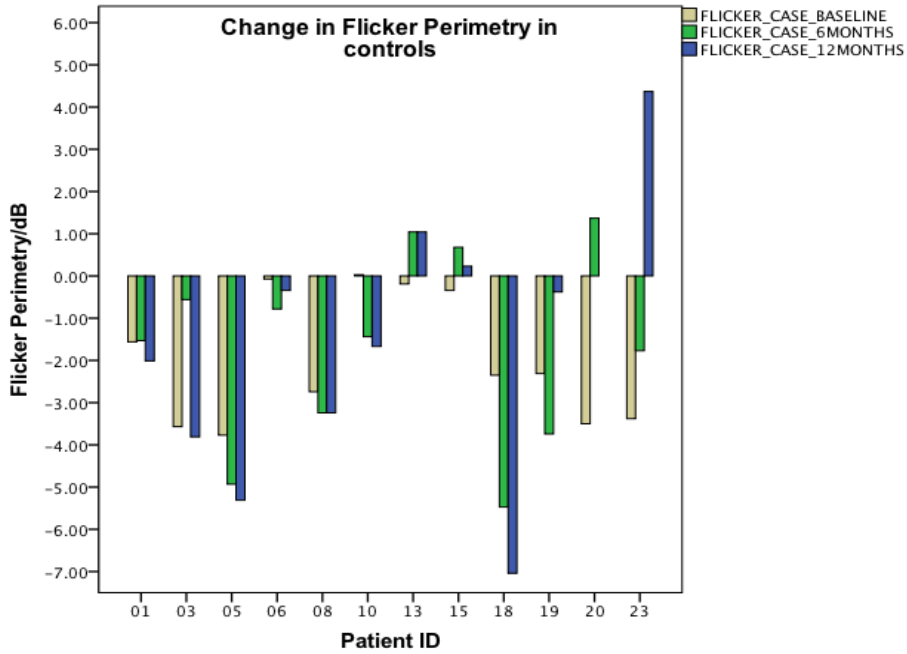


Figure 7.7b Individual plot of change in Flicker perimetry, cases

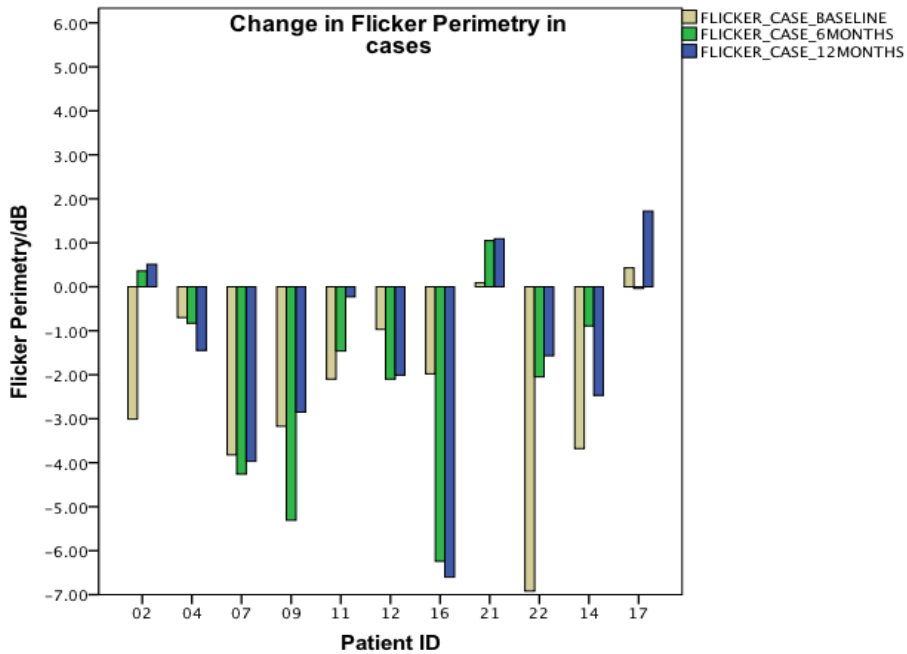


Figure 7.7 a and b shows changes in flicker perimetric analysis for controls and cases at baseline, 6 and 12 months. No definite trends were noted in either controls or cases.

7.4.5 Changes in Fundus Morphology

Post laser, at 6 months, 3 cases showed changes in drusen morphology, whilst 5 had decrease in drusen size (as compared to 2 in controls arm). 5 cases had a decrease in number of drusen and location of drusen. In terms of classification, 2 cases improved from AREDS 3 to AREDS 2, and 3 from the intermediate to early groups using the IC classification.

At 12 months, 2 of 11 of cases showed a change in drusen morphology, whilst 4 versus 3 cases and controls had decrease in drusen size. 2 cases had decrease in drusen number and 5 demonstrated change in drusen location. Only 1 case had changed from intermediate to early group under IC classification, whilst 2 cases improved from AREDS 3 to AREDS 2. 2 controls had worsening in classification status from AREDS 2 to 3, and 3 controls from early to intermediate AMD under the IC classification.

Using the Fisher-exact test, comparison of morphological change in drusen at 6 and 12 months between controls and cases did not yield statistical significance.

Table 7.9a RETILASE: Morphological change in drusen at 6 months

	Morph-ology	Size (p=0.069)	Number (p=0.069)	Location	Area	Change in IC	Change in AREDS
Con-trols, (n=12)	6	2	2	6	3	2	1
Cases (n=11)	3	5	5	5	4	3	2

Table 7.9b RETILASE: Morphological change in drusen at 12 months

	Morp-hology	Size	Number	Location	Area of	Change in IC	Change in AREDS
Controls (n=12)	4	3	1	6	5	3	2
Cases (n=11)	2	4	2	5	3	2	1

7.5 Statistical/analytical issues

In the analysis of the current dataset, few statistical issues were identified.

First the study was suspended and hence the number of patients recruited was 25% of target of a calculated sample size of 80 patients. Although the number of cases versus controls was almost equal, it was difficult to get a statistically valuable significance in view of the small numbers in each group.

Second, we have found a statistically significant improvement in visual acuity at 6 months in cases. However, the baseline VA was lower in this subgroup compared to controls. Despite the early suspension of the study, there was clearly a poor randomization process in this study. Randomization was based on a computer software (assigned to Kings College Hospital, London, UK, Clinical Trial Unit) which allocates each recruited patient in accordance to high and low VA to the case and control group randomly.

Also, the study design did not account for variability in refraction, and each patient underwent refraction by single optometrist once.

Third, we have used the first generation Nidek MP 1 which did not incorporate an SLO-tracking system. Hence, it was prone to subjective technician error from poor recognition of veins/arteries. Hence, the comparison of follow up tests may not yield accurate results. Furthermore, no repeated testing was performed and the results may be subject to an improved learning effect. This also applies to flicker perimetry.

Also, the point-to-point measurement of microperimetric defect may not have incorporated areas where the laser was applied. The means of results tabulated from the means of 4 readings from an individual at 4 and 12 degrees respectively and then averaged amongst the 11 cases and 12 controls. Studies have shown the association between structural changes in early AMD such as druse and pigmentation and microperimetric defects at individual lesions. (Midea et al., 2007) The averaging of results will negate effect of abnormal results of individual regions or areas. Hence, graphs has been plotted to show the individual patient trend in microperimetric change at 4 and 12 degrees respectively to give an approximate gauge of the status of central retinal function of individual patient.

7.6 Discussion

There were 2 aims of this trial, first to determine the efficacy of 2RT in delaying or renovating ageing changes in the outer retina, with the hope that if present, such changes could delay the onset of AMD; and second, to determine the safety of the 2RT laser. The term 'efficacy' used here was defined as the effect of the laser on visual function and 'safety' was defined as proportion of patients that converted to advanced AMD or losing vision post laser. In the context of this PhD, further detailed analysis was done (for example, evaluating changes in AMD morphology) to get more valuable scientific results. At this preliminary stage of using the 2RT on human subjects, it was also vital to ascertain the impact of the laser on the retina and this would be discussed in the next chapter.

As mentioned earlier in the introduction chapter, the main purpose of laser was to rejuvenate the retina at the stage of physiological ageing, however, the ethical limits of this clinical trial only permitted the recruitment of patients with signs of early AMD, ie, drusen or pigmentary changes. Hence, the results of the RETILASE trial could be interpreted as either an improvement in the status of AMD or macular function and defects attributable to laser damage.

The RETILASE trial demonstrated several important findings:

First, there was trend of visual acuity improvements post 2RT laser in early AMD patients at 6 months. This trend was noted to be both clinically and statistically significant. However, the trial showed that the visual effects were short lasting, as the VA improvements returned almost to baseline at 12 months.

Second, the results did not yield statistically and clinically significant changes in visual function tests such as microperimetric analysis and flicker perimetry.

There were no obvious trends of change noted amongst cases in either visual function tests. The current results were different to Guymer and team in Melbourne who found improvements in flicker perimetry. This may be attributed to the small number of cases analyzed. (Pelosini et al., 2013, Guymer et al., 2013)

The current results were surprising considering the good baseline visual acuity in our study cohort. A 5 letter increase in this baseline visual acuity may be considered clinically significant considering the possible ceiling effect of visual improvements in this visual bracket. This improvement in visual acuity was

coupled with changes in drusen morphology, number and individual druse size, although there were no significant changes in the overall drusen area and the respective classification gradings. Visual acuity measurements in early AMD subjects are usually 20/20 or within the normal range. Hence, VA measurements have not been known to be a sensitive indicator of change in this disease subset, especially since only 44% of normal cone complement is required for a normal vision.(Midena et al., 2010) Such improvements in VA post laser treatment amongst subjects with normal VA may suggest improvements in cone function from perhaps the increased nutritional support from increased transport across the BrM.

It may be argued that the difference in visual outcome could be because of the lower baseline VA for cases group as compared controls, although this was not found to be statistically significant. To account for this difference in baseline VA, a graph of individual patient changes was plotted to determine a trend in VA change post laser at 6 and 12 months.

In the RETILASE study, there was no noticeable trend in contrast sensitivity over 1 year in both cases and controls. This trial has used the Pelli Robson contrast sensitivity chart which contains 16 triplets of 4.9x4.9cm letters. At the test distance (1metre), these letters gives a spatial frequency of 1 to 2 cycles per degree and there is same contrast within each set of 3 letters. Every letter on the chart decreases the scoring results by 0.05 log units. In most publications for contrast sensitivity studies, the units of measurements were noted to be in log units, however, the RETILASE trial protocol was designed to tabulate data in number of letters. That said, reliability studies performed earlier on found a significant change in contrast sensitivity score to be 0.30log units or 6 letters.(Elliott et al., 1990) As such, the current results in the trial did not yield both statistical and clinical significance. Results for contrast sensitivity in early AMD has been controversial. Sjostrand and Frisen in 1977 first found decreases in high and intermediate frequencies across early AMD, whereas Loshin and White in 1984 found decreases in contrast sensitivity across all frequencies.(Sjostrand and Frisen, 1977, Loshin and White, 1984) Brown and Lovie-Kithchin found depressed contrast sensitivity across all frequencies in patients with early AMD as compared to normal, but at all eccentricities including the fovea, although a greater loss was noted in higher frequencies spectrum.(Brown and Lovie-Kithchin, 1989) In a review by Professor

Chakravarthy analyzing results from various studies, they concluded that contrast sensitivity was not a good prognostic indicator for progression of AMD.(Hogg and Chakravarthy, 2006)

In this small population, there was no conversion to advanced AMD at 1 year. However, it must be considered that the rate of progression of early AMD ranges from 0.5% to 50 in 5 years.(Ferris et al., 2013) In a small subset of patients followed up, it is not surprising that there is 0% of conversion to advanced AMD in the study eye. Hence, the current results must be interpreted with caution.

Microperimetry was measured at central 4 and paracentral 12 degrees in this clinical study. Studies have shown the decrease in perimetric means in the central 0 to 5 degrees as compared to outer eccentricities.(Parisi et al., 2007) These findings were coupled with histological evidence of parafoveal rod death and decreased density of photoreceptors noted even in early AMD patients.(Curcio et al., 1996, Owsley et al., 2000) In this study, firstly, the mean microperimetric analysis was higher than findings in other studies. (15.60 at 4 degrees and 14.64 at 12 degrees as compared to 5.83 and 6.43 dB in central and paracentral retina)(Parisi et al., 2007) but lower than the normal age-matched population as determined in a normative study by Sabates et al.(Sabates et al., 2011) This could be because of the earlier stages of early AMD in this current patient cohort as compared to previous studies. Second, in keeping with the current knowledge of age related changes in photoreceptor cells in different eccentricities, the mean microperimetric analysis for both cases and controls at baseline were noted to be lower at the central 4 degrees as compared to 12 degrees. However, there was no observable trend of improvements at 6 or 12 months in both cases and controls. The current results were taken as means of 4 individual points in each of the annular ring of 4 and 12 degrees and as such, any individual points of defects secondary to druse or pigmentary changes may be averaged out. This is because the deposits from druse will cause a loss of contact between photoreceptors and RPE and hence discrete photoreceptor cell loss. The concept as introduced earlier in this thesis is based on the previous findings that deposits are found diffusely in the BrM, causing a hydrophobic layer and decreased nutrient load to photoreceptor cells.(Chen et al., 1992) Thus, in theory, there should be a diffuse decrease in

macular function even in very early stages of AMD before visualization of any clinical hallmarks of AMD.

Flicker sensitivity has been used in research previously as a measure of early AMD. However, the results have not been convincing. Flicker sensitivity is based on the theory on adding stress to photoreceptor cells by increasing metabolic demand from the flicker. In the RETILASE study, there was no obvious pattern or trend discernable both in cases and controls.

It would have been ideal to grade total drusen area on not only on CFP on our study cases, however, in our study cohort, there were few patients with countable drusen to determine a viable outcome. Another novel option would be to determine drusen volume on OCT and/or BrM thickness. However, current OCT technology has a X-Y axis of maximum resolution of $7\mu\text{m}$, which first would not be reliable and accurate in determining the Bruch's as it is on an average in the elderly age group without advanced AMD between 5 to $7\mu\text{m}$. Also, considering the anatomy of druse to be between RPE and inner collagenous layer of Bruch's, without defining the base of drusen, it would be impossible to accurately determine drusen volume.

Given the concoction of all the various ways to analyze improvement in visual function and retinal morphology post 2RT last, it appears that the only objective result obtained is the improvements in visual acuity at 6 months amongst cases.

7.7 Conclusions

In conclusion, despite the small number of participants in this clinical trial, the results suggest a possible benefit of using the nanosecond laser technology as a therapy. The clinical elements has drawn the following conclusions:

1. Randomization process in this trial has compromised the validity of the results;
2. The results showed benefit at 6 months which tailed off by 12 months, which imply that repeat lasers can possibly be required.

Further larger scale trial and dose escalation studies are required to define the laser parameters for maximal effects.

Chapter 8

RETILASE Results II. Safety of the 2RT laser in patients with early AMD

8.1 Introduction

In the last chapter, the 6 and 12 months visual function data of the RETILASE trial data was analyzed. Despite the small numbers, there was a positive trend in visual improvements post laser treatment at 6 months. Analysis undertaken in this chapter aimed to determine the 'safety' of the 2RT laser as a prophylactic therapy in AMD. The analysis of 'safety outcome' as per the original RETILASE trial protocol (chapter 6) was based on the measurements of the following between the cases and controls:

1. Proportion of patients developing CNV at 12 months.
2. Proportion of patients developing retinal atrophy as measured by autofluorescence and OCT at 12 months
3. Proportion of patients who lost more than 15 ETDRS letters at 12 months.
4. Proportion of patients who lost more than 30 ETDRS letters at 12 months.
5. Any other complications observed at 12 months.

However, due to the early termination of the study, this analysis would not yield any sensible results. In fact, none of the subjects that underwent laser developed any of the above.

Despite this, it was still crucial to evaluate the impact of the nanosecond laser on the retina, particularly as no studies had yet undertaken a detailed clinical analysis of the use of the 2RT laser in human subjects. As such, analysis in this chapter was undertaken to define the structural and functional impact of the laser in human subjects with early AMD.

8.2 Methods of Analysis of Safety

Analysis attempted in this chapter evaluated the clinical imaging obtained during the study for structural and functional changes post laser. Images obtained from FAF (Heiderlberg, Germany), OCT (Spectralis, Heiderlberg) and CFP (Topcon) were analyzed for any structural changes, whilst functional changes were assessed using the Microperimetry (Nidek, MP1) According to the protocol, our 23 recruited patients had at least baseline, 6 months and 12 months clinical imaging acquired. However, in the interim leading to suspension of the study, some patients were recalled for monitoring purposes. Altogether, 2 patients had further 1 month follow and 2 patients had further 3 month follow up images taken.

8.2.1 Fundus Autofluorescence

Parameters of the FAF images obtained were in accordance to the RETILASE trial protocol. (Appendix)

FAF changes were analyzed both qualitatively. FAF images were obtained from the Heiderlberg software on the FAF machines and saved as JPEG images.

Saved images were imported into image J(NIH) for viewing and analysis.

Changes were described as hypo or hyperfluorescence. Hypofluorescence was defined as reduction of normal fluorescence whilst hyperfluorescence was defined as increase of normal fluorescence.

6 and 12 month images were compared to baseline images to identify changes due to laser.

8.2.2 Optical Coherence Tomography

Parameters of the OCT images obtained using the Spectralis OCT machine can be found in the RETILASE trial protocol. (Appendix)

OCT images were initially viewed on the Spectralis machine and exported as a series of JPEG images. Saved images were imported into image J(NIH).

To compare changes noted on FAF images and corresponding OCT, FAF images were overlaid on the infra-red segment of the spectralis OCT scan using the overlay modality on image J(NIH). (Figure 8.2) Both FAF images and the infra-red scans were both taken at 40 degrees field of view mode. FAF

image was adjusted to align the retinal vasculature between the 2 images. This method can only give an approximate alignment of corresponding location. Each line scan of the 49 OCT scans were analysed for approximate corresponding changes to laser lesions noted on FAF. When grading images, it was noted that segmentation of outer retina is currently impossible as the highest resolution of OCT is in the range of 10-14 μ m (despite claims of a 3 μ m resolution as noted in investigator's brochure from Heidelberg). Hence, the analysis presumed and grouped structures as a complex such as the RPE-BrM complex. (Figure 8.3) In particular, structural defects were graded in accordance to the following:

Changes to neurosensory layer

1. Disruption of presumed IS/OS junction
2. Disruption of presumed ELM
3. Increased reflectivity of INL

Changes to outer retina

4. Changes to RPE-Bruch's membrane complex
5. Increased transmission to choriocapillaries

OCT Changes corresponding to hyper and hypofluorescent areas on FAF were described separately.

Figure 8.1 OCT and infra-red image obtained from Spectralis

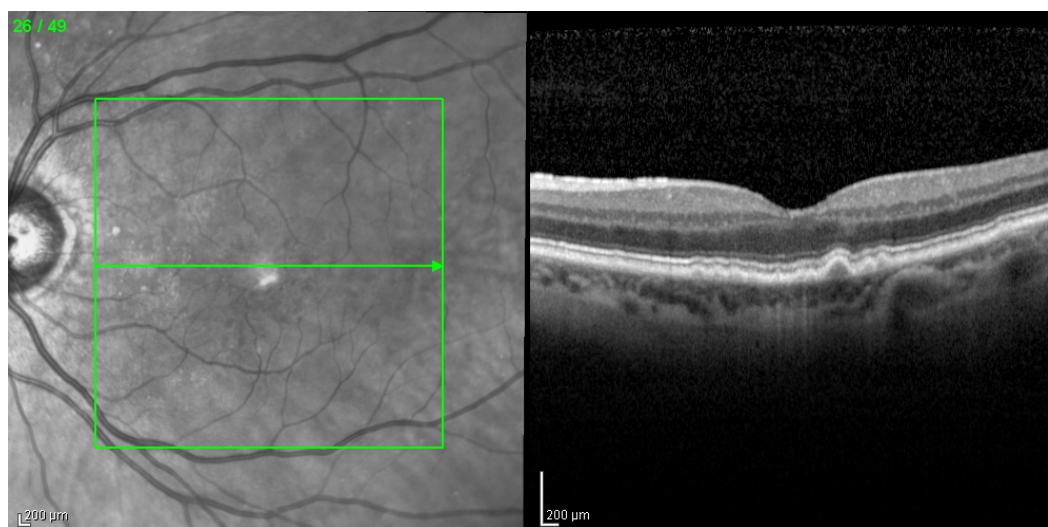
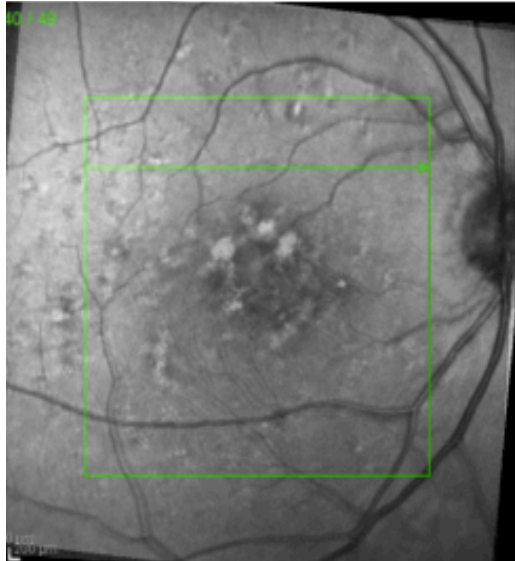
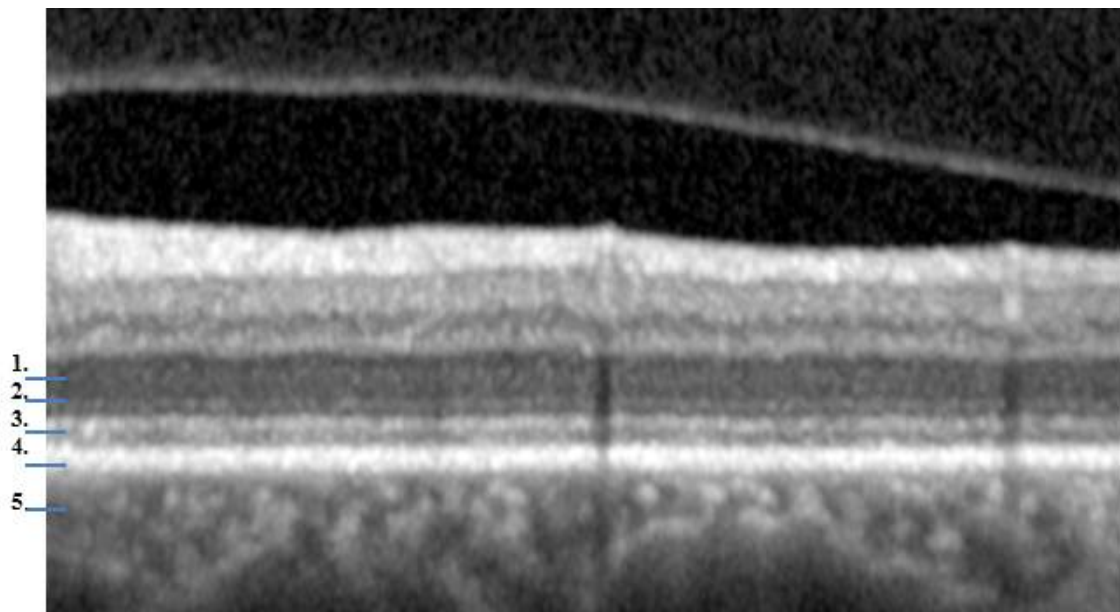


Figure 8.2 FAF and infrared overlay



Overlay of FAF and infra-red image of OCT.

Figure 8.3 Presumed OCT anatomical layers as defined in this thesis (Magnified image)



1 = outer nuclear layer; 2= external limiting membrane; 3 = interface of the inner and outer segments of the photoreceptor layer (IS-OS); 3 = outer segment-RPE interdigitation (COST); and 4 = RPE/Bruch membrane complex; 5= Choroidal thickness.

8.2.3 Color Fundus Photography

FAF images were taken at 40 degrees field of view, whilst CFP images in this study were taken at 30 degrees.

Hence, laser lesions on CFP were recognized and compared to FAF changes by approximating its location in terms of proximity to the different retinal vasculature.

CFP images were saved as JPEG and imported into image J(NIH). Using known scales, diameter of individual laser lesions were measured using the semi-automated 'analyze', 'measure' function on image J.

Corresponding laser lesion on FAF were described for the visibility of laser lesion on CFP, size and association with pigmentation.

8.2.4 Microperimetry

Functional changes post laser were measured across individual laser lesion.

This analysis was undertaken in 2 ways. First, means of perimetric changes at 4 degrees and 12 degrees respectively for each of the types of laser lesion as recognized on FAF were tabulated (assuming that there would be different patterns of laser lesions). In this thesis, a term 'global functional defect', which 'means overall effect from laser' was coined to refer to this.

Second, perimetric changes at 6 and 12 months across individual laser lesions were tabulated.

It was noted that the location of test-retest reliability using this MP1 system (NAVIS software, 1.72, Nidek Technologies) did not correspond in many of the follow up images, although an exact proportion was not calculated here. Hence, to ensure accurate tabulation of results, 2 main criteria must be met.

First, to ensure measurements were taken at the correct target, distance between the nasal 12 degree MP 1 target was measured from the optic disc at baseline. Similar measurements were taken at the exact location for the 6 and 12 month MP 1 images. Only images with exact corresponding distances were analyzed.

Second, to determine corresponding perimetric results across individual laser lesion, the 'overlay' technique using image J (NIH) was used. By comparing images of FAF and the MP1, only perimetric stimulus that corresponded exactly with laser lesions were tabulated. (Figure 8.4)

Figure 8.4 Demonstration of MP1 analysis

Figure 8.4a

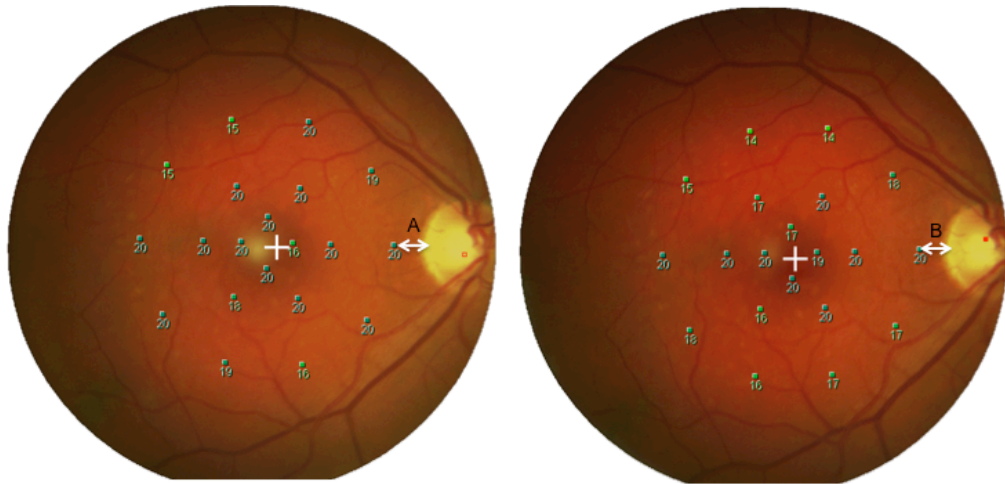


Figure 8.4b



Laser lesion with corresponding perimetric measurement

Figure 8.4a,b demonstrates the analysis of functional changes across individual laser lesion using the Microperimetry system (MP1, Nidek Technologies). 2 criterias must be met for the analysis. 1. MP1 images to be compared must have the stimulus directed at exact point-to-point location, ie, all 20 points on MP1 must be taken at the same location. For example, in Figure 8.4a, the distance from nasal edge of optic disc to stimulus must be same in both comparing images. (Distance of $A=B$)
Figure 8.4b shows overlaid FAF and MP1 images. Individual points of perimetric measurements were taken only if they were directly corresponding to laser lesion.

8.3 Summary of Results of Safety Analysis

Due to constraints of the design of the clinical trial, images were obtained mainly at 6monthly intervals for 12months. Hence, the results and following images were at most reflections of possible temporal changes at 6 months and beyond. In the following, it was not possible to assess the dynamic wound recovery process.

Although there were mainly 6 monthly follow up images for 12 months, during the recall period, additional follow up images, one of which extended to an 18-month period had been taken and analyzed. Of the cases analyzed, only 1 was of Indian ethnicity, others were Caucasian with average pigmentation of the patients, 7 had 0.1mJ of energy per laser spot, 2 had 0.3mJ, 1 had 0.17mJ and 1 had 0.19mJ. Number of laser shots ranged between 52 to 102 shots.

8.3.1 Changes on Fundus Autofluorescence

FAF laser lesions were described as hyperfluorescent or hypofluorescent. Inferring from Marshall's findings on the zones of laser damage on the RPE, laser lesions undergo dynamic changes with time as per figure 8.5a. In the early or acute phase post laser, there is a whorl of disintegrated RPE structure from laser damage in the center (zone 1), RPE migration in surrounding zone (zone 2) and distinct shrinkage of cells in the periphery (zone 3), (figure 8.5b). With recovery, the laser damage center area decreases with a larger zone of migrating RPE. The size of laser lesion was notably reduced. Complete laser recovery involved complete wound healing with reestablishment of single amelanotic RPE layer.

3 Distinct types of laser lesion patterns on FAF were observed. These patterns corresponded to the changes described above at different time points. This indicated a varying severity of laser damage and recovery which might have been laser dose dependent. These laser lesion patterns were broadly classified into the following (Table 8.1, Figure 8.6)

Figure 8.7 shows a full fields FAF demonstrating the effect of varying energy levels on the uptake on FAF. Suprathreshold laser lesions were noted at 12 months as hyperfluorescent type I pattern with evidence of zone 1, 2 and 3 laser damage, whilst threshold lesion were comparable to hyperfluorescent type II lesion with evidence of zone 1 and 2 and subthreshold lesions (70% of threshold, as per protocol) were noted as hypofluorescent laser lesion.

Of the 11 subjects treated, 6 presented with mainly the first pattern (hyperflorescent type I laser lesion), 3 with mainly the second pattern (hyperflorescent type II lesion); and 2 subjects had hypoflorescent laser lesions. The 3 types of FAF patterns did not demonstrate a direct relation to visual effect but when compared with MP1 changes at 12 degrees: type II and III showed improvements at 12 months, as compared to group I. (further described below)

Figure 8.5a Recovery of RPE damage post laser

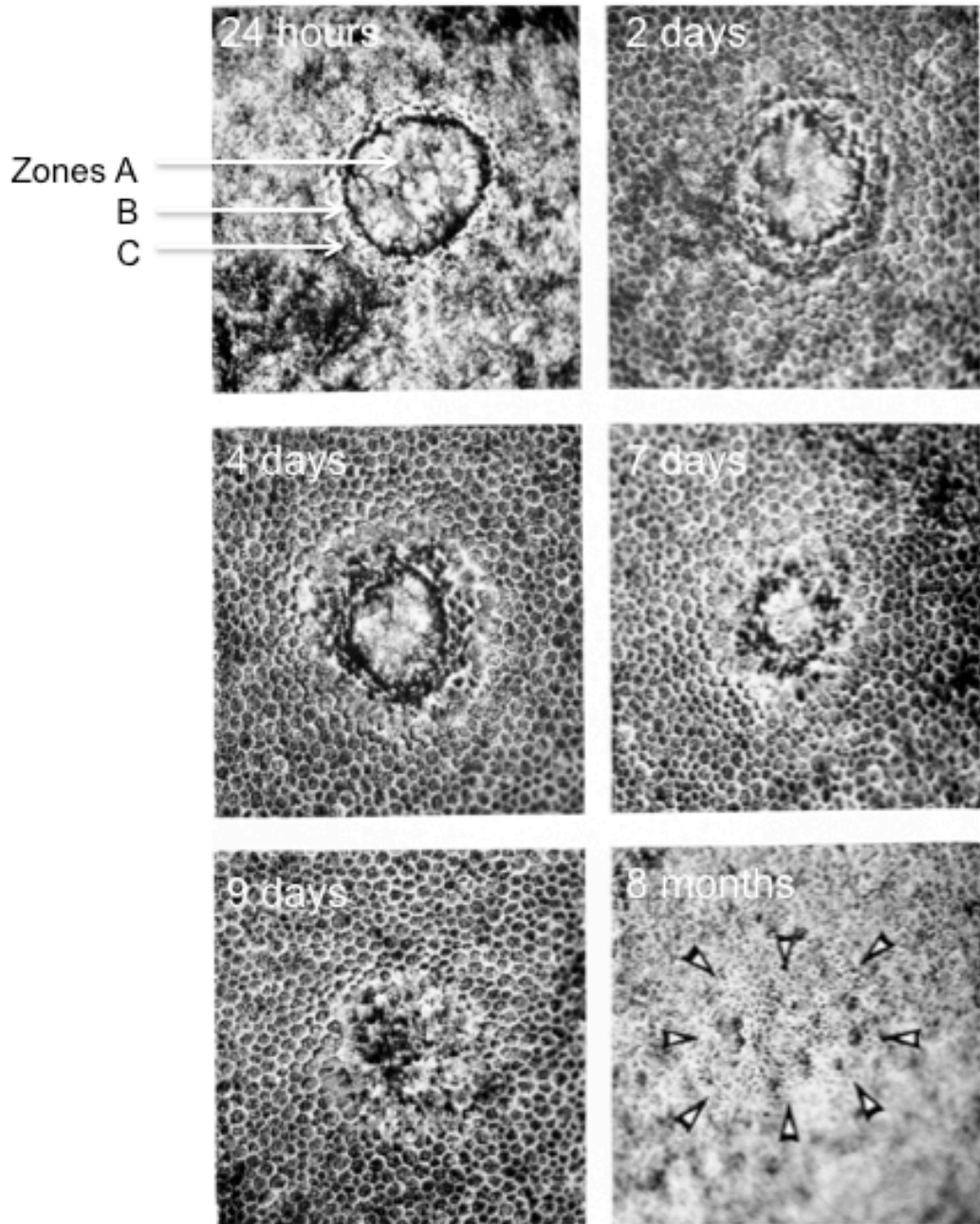


Figure 8.5a shows the temporal recovery of RPE laser damage in different time series. Zone A is the zone of highest energy from the incident laser beam with degenerate RPE cells in the center; Zone B shows a ring of pigmentation and zone C shows an area of hyperfluorescence from shrinkage of cells and oedema in the periphery. From day 2, zone A becomes smaller. Note that from day 4, the ring of pigmentation disappears and is replaced by a few layers of pigmented cells, which represents cell migration. This layer increases in size with the recovery period. (Marshall 1967)

Figure 8.5b Dynamic Process of RPE laser lesion recovery

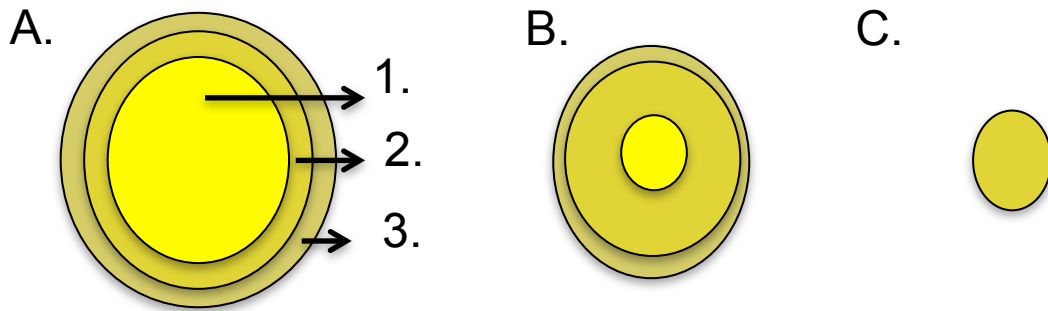


Figure 8.5b , A to C shows the dynamic process of RPE wound healing post laser induced injury. Arrows point 1. Illustrates zone of laser damage and was seen as hyperfluorescence on FAF; 2. shows zone of RPE migration which was noted as rim of less intense hyperfluorescence on FAF and zone 3. demonstrates cell shrinkage and ‘pulling away’ which was seen as intensely dark hypofluorescence on FAF.

A. shows the initial or acute phase where there was centre laser damage with surrounding migrating RPE cells and shrinkage in the periphery.

B. shows mid-recovery of laser lesion with larger zone of migrating RPE cells and smaller laser lesion.

C. shows recovery of laser lesion with complete zone of single layer of amelanotic RPE cells. The zones of recovery are similar to the flat mount histology of RPE laser damage in figure 8.5a with increase in RPE migration with increasing recovery period.

Table 8.1 FAF classification of 2RT laser lesions

Classification	Description
Hyperfluorescent type I	Visible areas of zone 1 + 2 + 3.
Hyperfluorescent type II	Visible areas of zone 1+ 2 only
Hypofluorescent	Visible areas of zone 2 only

Figure 8.6 A-C FAF classification of laser lesions

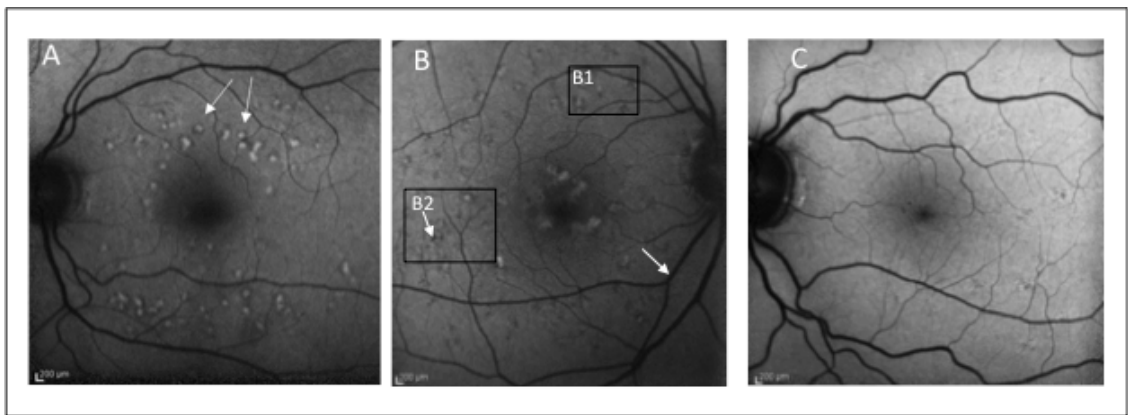


Figure A to C depicts patterns of FAF post laser.

A: Hyperfluorescent type I laser lesion

B: Hyperfluorescent type II laser lesion

C: Hypofluorescent laser lesion

Figure 8.7 Full fields FAF image at 15 months post laser

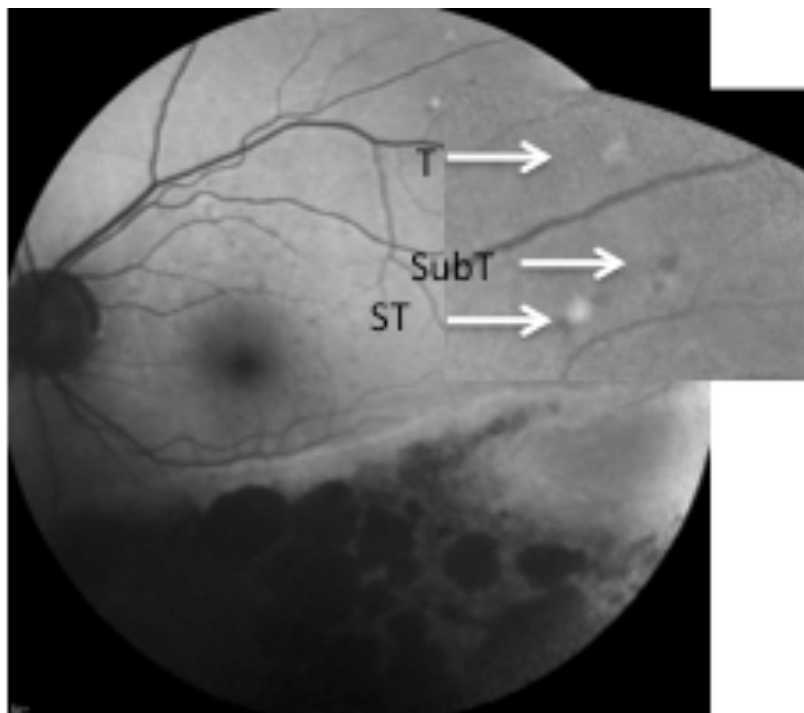


Figure 8.7 shows a fullfields FAF image taken at 15 months post laser. T: threshold lesion; SubT: Subthreshold lesion with laser energy at 70% of threshold energy; ST: suprathreshold lesion

8.3.2 Optical Coherence tomography

FAF superimposed on OCT allowed an approximate analysis of individual laser lesion. There were notable differences in OCT patterns in each of the different FAF groups.

All laser lesions showed effects limited to the RPE-BrM complex at 6 months. There were no involvement of the INL nor CC and no loss of photoreceptor cell layers (ie, ELM, IS/OS layer). Main changes were described as a focal elevation of the RPE-BrM complex which appeared intensely florescent.

Differences between the types of laser lesions can be described in terms of the depth of the focal elevation of the RPE-BrM complex.

Laser lesions in type I showed focal the elevations of the RPE-Bruch's membrane complex with a larger depth. These lesions have a 'dome-shape' which decreased in size with time. Hyperflorescent oval lesions were noted above some laser lesions. These were similar to lesions previously described by Duker et al as pigment migration. Furthermore, there were few defects noted in the presumed IS/OS junction and if so, these changes recovered by 12 months. There was no involvement of the INL nor CC. There were no obvious signs of atrophy. Although in the single patient with Indian ethnicity, there was 'scalloping' of the inner retina, which worsened at 12 months. There was no notable coinciding hypoflorescence on FAF, however the functional change on MP1 for this particular lesion was not mapped. (Figure 8.10a)

The OCT changes for type II was subtler, with a smaller depth of the focal elevation whose appearance was better described as 'ripples' of the RPE-Bruch's membrane layer. These changes decreased in size at 12 months. (Figure 8.10b)

Hypoflorescent laser lesions were either not visible or showed mild 'ripples' at 6 months (smaller depth than hyperflorescent lesions) which again decreased in size or disappeared by 12 months. (Figure 8.10c)

8.3.3 Color Fundus Photography

In FAF type I classification, laser lesions were noted as pale laser marks with or without central pigmentation at 6 months. 4 of the 6 patients had lesions with central pigmentation at 6 months, some of which disappeared by 12 months. The lesions remained stable in size at 12 months (266 to 269 μ m). It is of note that the mean of laser lesion size was smaller than the 400 μ m spot size of the laser beam.

In type II lesions, smaller laser lesions were noted at 6 months which decreased in size at 12 months (159 μ m vs 129 μ m). None of the lesions showed pigmentation.

In hypofluorescent laser lesions, no visible laser lesions were noted on CFP.

Figure 8.8 Comparison of laser lesion on CFP and FAF



Figure 8.9 Evolution of laser scars on CFP

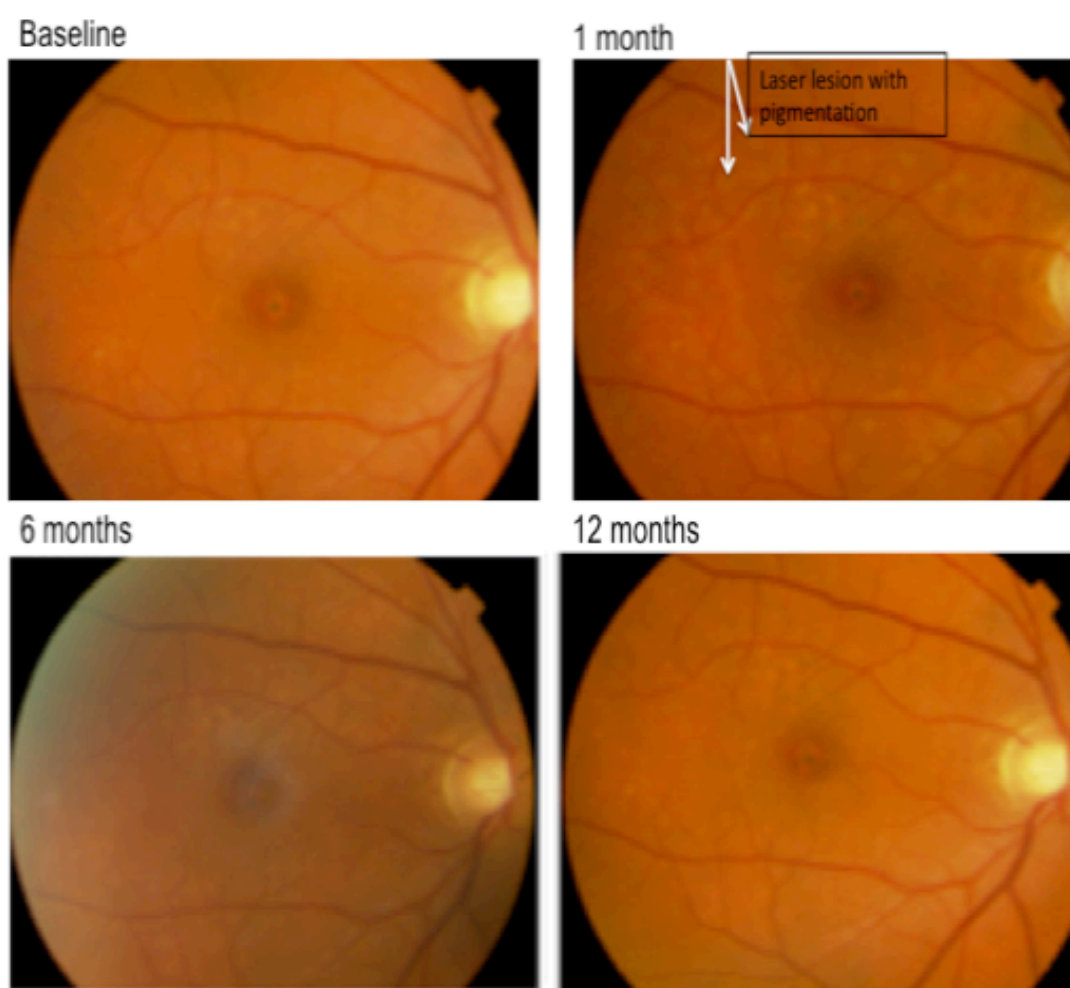
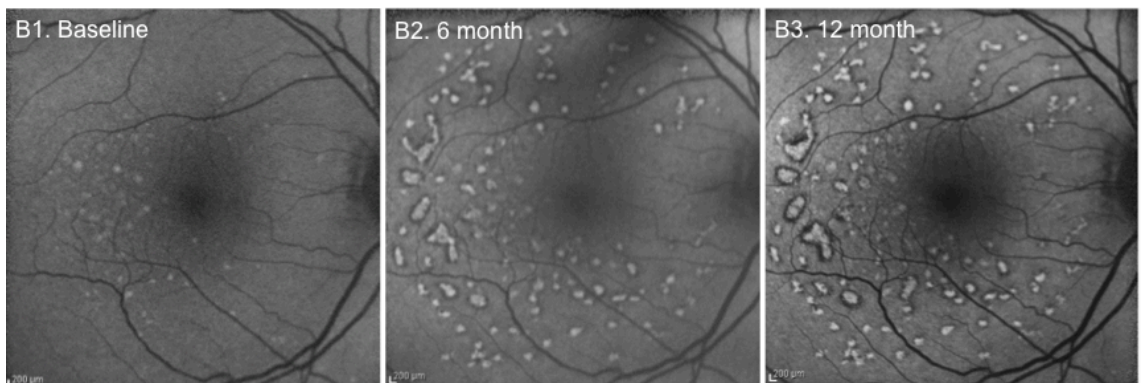


Figure 8.9 shows color fundus photographs of patient with type I laser lesion at baseline, 1, 6 and 12 months. At one month, some laser lesions had central pigmentation. By 6 months, pigmentation disappeared. There was a decrease in size and number of visible laser lesions. At 12 months, size of individual laser lesion decreased further.

Table 8.2 RETILASE: Mean diameter of laser lesion on CFP

FAF classification	No. of laser lesions measured, 6 months	Mean of laser lesions at 6months +/- SD/μm	No. of laser lesions measured, 12 months	Mean of lesions at 12 months +/- SD/μm
Type I	91	265.98+/- 88.15	91	269.55+/- 105.66
Type II	33	159.58+/- 38.55	28	129.18+/- 34.86

Figure 8.10a Example of Hyperfluorescent type I laser lesion



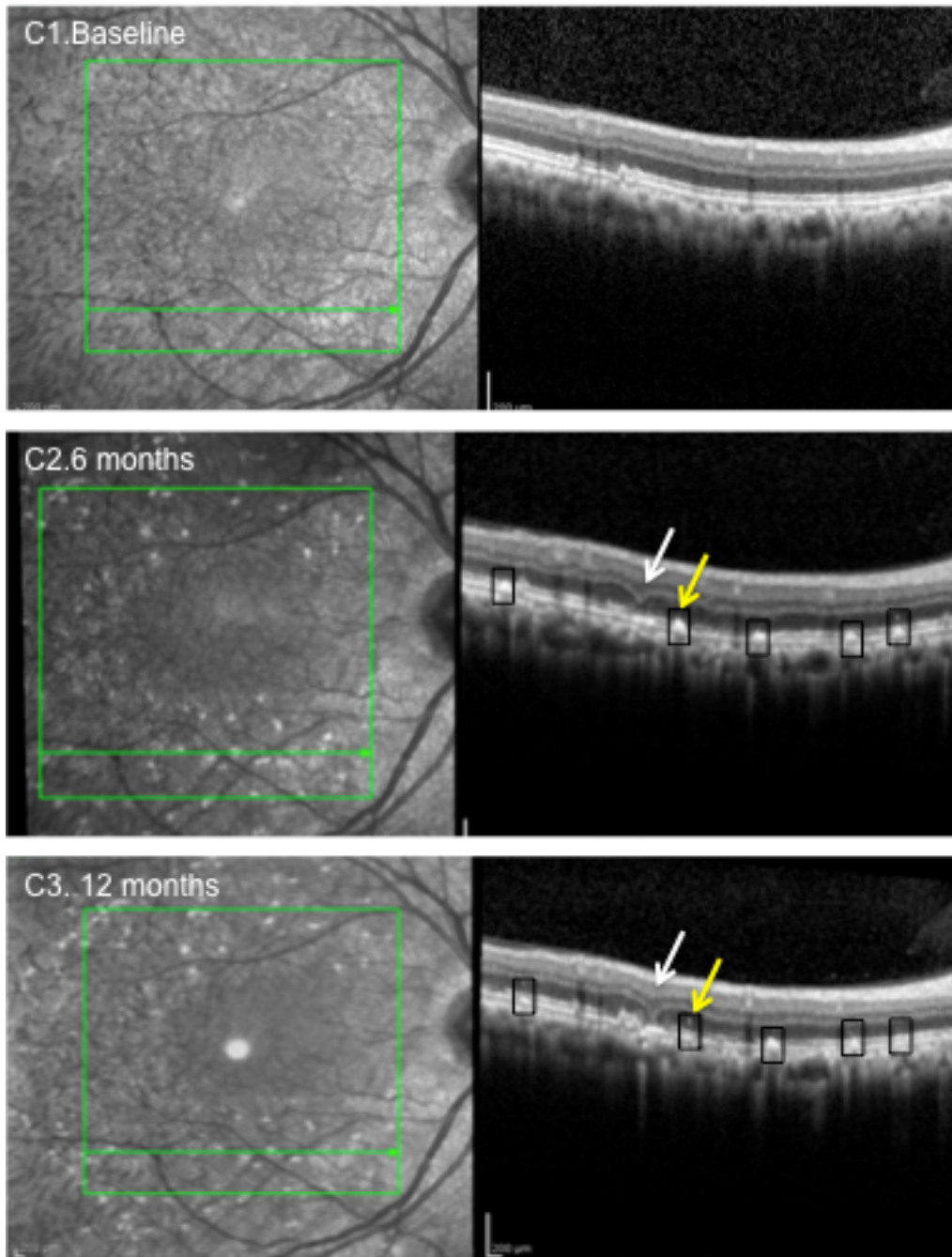


Figure 8.10a shows the CFP, FAF and OCT images of hyperfluorescent type I laser lesions.

Figures labeled A,B,C shows temporal sequence post laser at baseline, 1 month, 6 months and 12 months respectively. This patient is of Indian ethnicity and has confluent soft druse on fundus examination at baseline.

A1-3 shows 1. decrease in drusen load over time and 2. pale laser lesion which becomes smaller over time. (White arrow points to laser lesion)

FAF shows hyperfluorescent laser uptake of various shapes and sizes. Note increase of hypofluorescent rim over time

C1-3 shows infrared image on right and OCT on left. Infra-red shows hyperfluorescent laser lesion.

Note the involvement of inner nuclear layer without FAF changes of atrophy. (white arrow) Also note the hyperfluorescent discrete lesion above a laser lesion which has decreased in size by month 12 (yellow arrow). Boxed areas are laser lesions which show a decrease in size both axially and laterally with time.

Figure 8.10b Example of hyperflorescent type II laser lesion



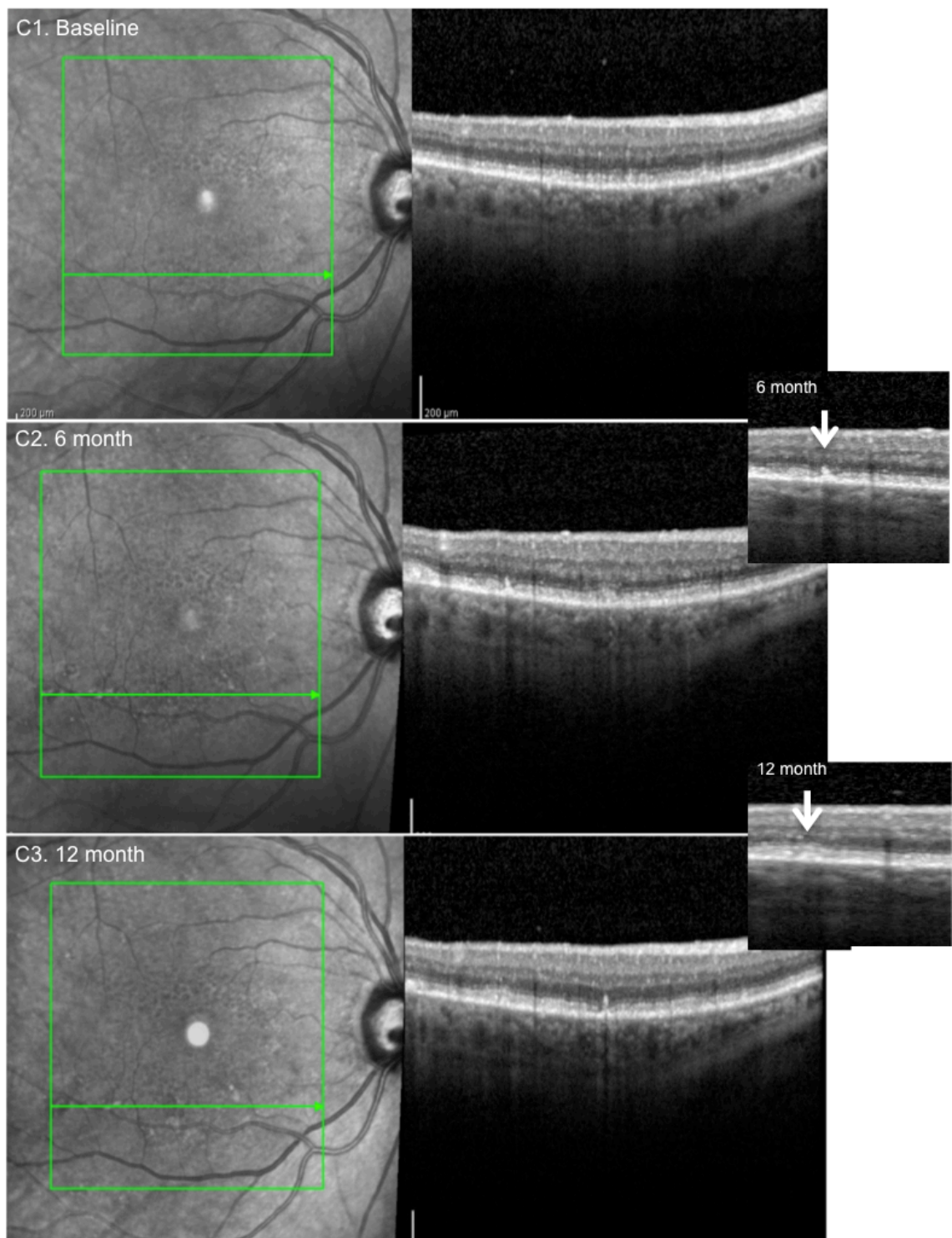
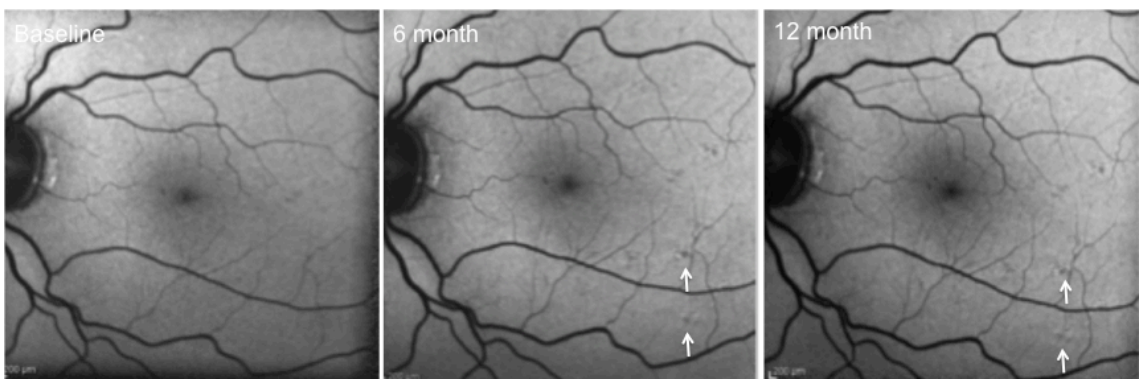


Figure 8.10b shows CFP, FAF and OCT of type II hyperfluorescent laser lesions. A2-3 shows faint laser lesions (arrow). Not all laser lesions on FAF showed up on CFP. B2 shows laser lesion on FAF at 6 months. Note the comparatively thicker rim of hypofluorescence (as compared to type I laser lesions). C2-3 shows laser lesion as hyperfluorescence on the infrared images. Note the hyperintense thickening or 'rippling' of the RPE-BrM complex (magnified image) at 6 months. This hyperintense thickening decreased in size at 12 months.

Figure 8.10c Example of hypofluorescent laser lesion



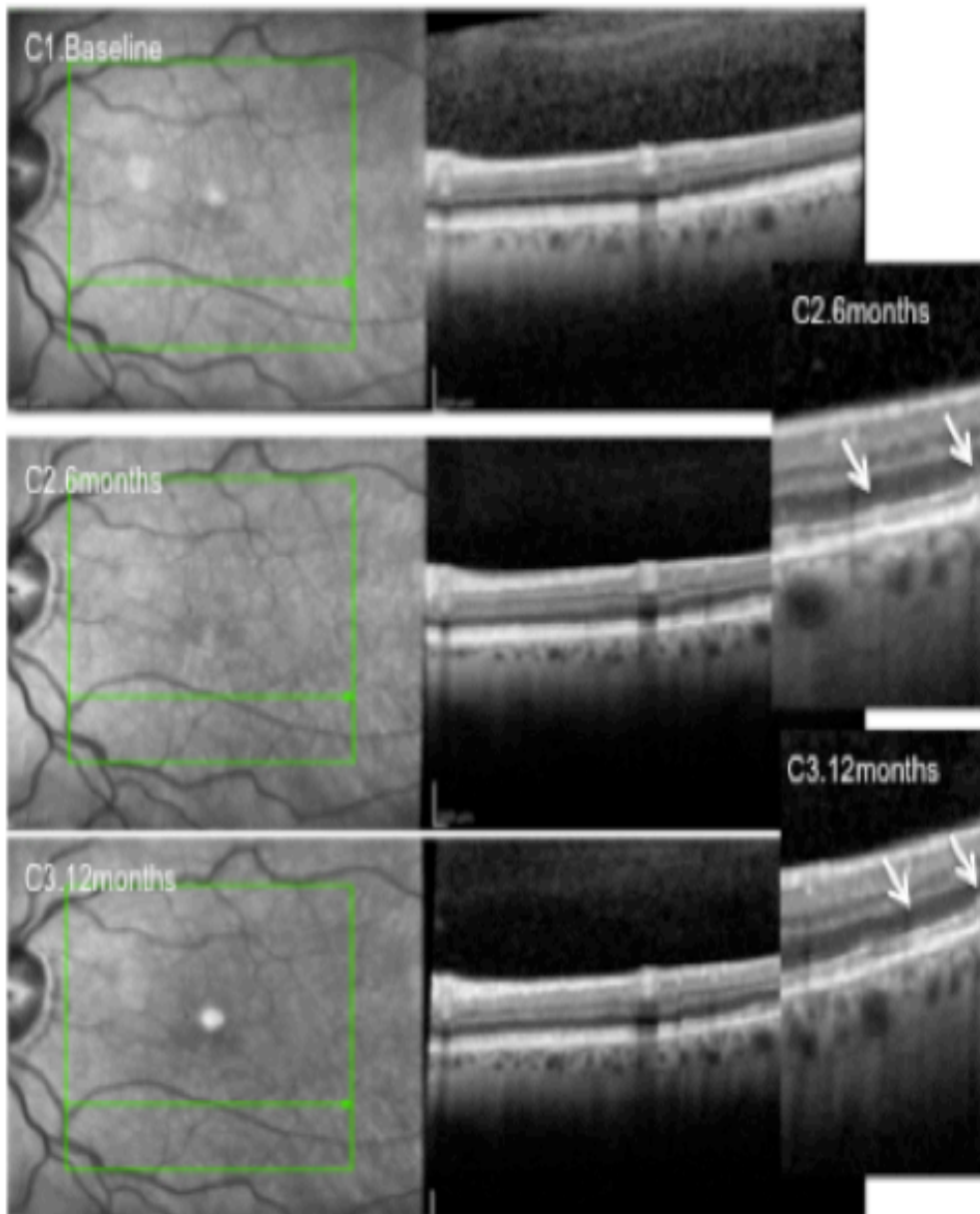


Figure 8.10c shows the CFP, FAF and OCT images of hypofluorescent laser lesions. A1-3 did not show any obvious laser lesions. B1-3 FAF image shows laser lesion uptake as hypofluorescence. Arrow pointing to laser lesion. C1-2, infrared did not show any change at 6 months. No obvious OCT structural changes was noted at 6 months.

8.3.4 Microperimetric analysis of laser lesions

Type I hyperfluorescent laser lesions were found to have “global functional defect” at 12 months at both 4 and 12 degrees. However, type II lesions showed improvements in function at 12 months only at 12 degrees, $+1.27 \pm 0.74$, $p < 0.05$. Hypofluorescent laser lesion also showed mild improvements at 12 months at 12 degrees. Although this was statistically significant, it was not clinically significant, $+0.40 \pm 0.42$, $P < 0.05$. (Table 8.2a,b)

Tabulating data from individual laser lesions, type I lesions showed significant defects at 12 months, -0.86 ± 2.74 , $p < 0.05$. Type II and hypofluorescent patterns were found to have functional improvements both at 6 and 12 months, of which type II lesions demonstrated greater improvements quantitatively. ($+2.64 \pm 2.29$ vs $+1.00 \pm 2.83$ at 6 months) and ($+2.80 \pm 1.81$ vs $+0.70 \pm 2.67$ at 12 months) (Table 8.3)

Table 8.3a RETILASE: change in MP1 at 4 degrees for laser lesions

	N (no. patient)	MP1 baseline	MP1 6 months	MP1 12 months	MP1 Change 6month	MP1 change 12 month
Hyperflorescent I	6	15.79+/- 3.52	16.46+/- 3.23	13.42+/- 4.10	+0.67+/- 2.71	-2.38+/- 3.28
Hyperflorescent II	3	16.17+/- 2.27	16.17+/- 2.45	16.25+/- 2.39	0+/-3.88	+0.08+/- -3.89
Hypoflorescent	2	16.50+/- 0.00	13.25+/- 3.18	15.75+/- 1.77	-2.75+/- 2.48	-0.75+/- 1.77
P value					0.254	0.604

Table 8.3b RETILASE: change in MP1 at 12 degrees for laser lesions

	N (no. patient)	MP1 baseline	MP1 6 months	MP1 12 months	MP1 Change 6month	MP1 change 12 month
Hyperflorescent I	6	14.57+/- 3.61	14.15+/- 4.34	12.63+/- 4.27	-0.42+/- 1.34	-1.93+/- 1.84
Hyperflorescent II	3	13.60+/- 2.91	12.87+/- 5.73	14.87+/- 3.33	+0.93+/- 3.25	+1.27+/- 0.74
Hypoflorescent	2	13.90+/- 0.71	12.55+/- 0.78	14.30+/- 1.13	-1.35+/- 1.49	+0.40+/- 0.42
P value					0.591	0.018

Table 8.4 Individual laser lesion MP1 defect

	N (no. lesion)	MP1 baseline	MP1 6 months	MP1 12 months	MP1 Change 6month	MP1 change 12 month
Hyper- florescent I	n=20(6months); n=14(12months)	13.25+/- 5.37	13.25+/- 5.29	14.57+/- 4.11	+0.5+/- 3.36	-0.86+/- 2.74
Hyper- florescent II	n=11(6months); n=10(12months)	13.73+/- 5.48	16.36+/- 6.15	16.10+/- 4.28	+2.64+/- 2.29	+2.80+/- 1.81
Hypo- florescent	n=10 (6, 12 months)	14.4+/- 1.58	15.4+/- 2.80	15.1+/- 2.56	+1.00+/- 2.83	+0.70+/- 2.70
P value					0.056	0.008

8.4 Discussion

In this study, different noninvasive retinal clinical imaging modalities such as FAF, OCT, CFP and Microperimetry were used to identify both structural and functional changes post laser. The analysis of the current data was a reflection of the static wound healing process at 6 and 12 months, which may well implicate the longer-term prognosis of laser effects. However, the current results did not allow a definition of the temporal-dynamic wound healing process because of the study design.

Based on observations of laser changes on FAF, laser lesions were classified into 3 patterns: 1. hyperflorescent type I; 2. Hyperflorescent type II and 3. Hypoflorescent type-lesions.

Hyperflorescent type I lesions showed variable degree of damage on the photoreceptor cells, as demonstrated structurally and functionally. This indicates overtreatment of subjects. Type II laser lesions demonstrated partial wound healing with a less exaggerated damage profile. There was no involvement of photoreceptor cells. Hypoflorescent laser lesions were probably ideal and could have represented almost complete healing at 6 months.

This classification reflects the differential wound healing response, which gives an indication of the severity of the initial impact of laser upon the individual subjects.

From the OCT data, it was observed that most changes were focal to the RPE-Bruch's membrane complex. There was limited extension beyond the IS/OS junction and into the choriocapillaries. Previous histological evidence using cw argon laser of monkey and human retina demonstrated necrosis of RPE and lifting of RPE from BrM with subsequent budding, migration and proliferation of RPE cells to form multi-layered RPE in area of laser irradiation 7 days post treatment.(Marshall and Mellerio, 1967, Marshall and Mellerio, 1968) There was evidence of intrusion into the choroidal layers. In an animal model that underwent selective RPE photocoagulation, the initial wound healing histological results were similar to those described above. This suggests all retinal lasers, regardless of time domain, undergo a similar wound healing process.(Framme et al., 2008) Thus, the OCT changes observed in the current results could be a reflection of the histological changes observed previously, with 'thickening of RPE-BrM complex' represents part of the healing process which led to the formation of a multilayered RPE structure.

Previous studies have shown that autofluorescence noted on FAF was from the lipofuscin within RPE as a byproduct of phagocytosis of photoreceptors. In general, fundus autofluorescence changes may be described as hyper or hypofluorescent. Previous studies with conventional lasers, patterned lasers and selective retinal therapy(SRT) have found laser lesions to be immediately hypofluorescent and then hyperfluorescent and back to hypofluorescent over a period of 1 week to 15 months. (Midena et al., 2007, Vujosevic et al., 2010) This was presumed to be RPE atrophy because of irreversible denaturation of photoreceptor cells.

In the case of the hyperfluorescence noted after the 2RT laser, an alternative explanation may be suggested. The current observations may be because of increased metabolic activity from the wound healing process which resulted in increased turnover and higher quantity of lipofuscin formation. This increased lipofuscin levels were noted as hyperfluorescence on FAF.

Conventional lasers were found to become hypofluorescent with time with corresponding atrophic changes. This was not noted in the data set over a 12 month period in this study.

Microperimetric analysis on individual laser lesions have found minimal defects in type I lesions, but improvements in type II and hypofluorescent lesions. It was noted that type II lesions had greater perimetric improvements than hypofluorescent lesions. This reason for this is unknown but may be explained if type II lesions had sufficient energy to cause a larger impact than hypofluorescent lesion but limited enough not to result in over-treatment as in type I lesions.

It was noted that in this study, the energy laser levels have been limited to within a small range, hence, such changes can only be accounted for by the differences in individual and intra-individual melanin and perhaps lipofuscin content, the latter exaggerated in this subgroup of patient profile.

There was a single patient with extension between inner retina and outer retina on OCT which extended beyond 12 months. There was no corresponding FAF hypofluorescence to suggest atrophy. This changes may be explained as a gliotic change instead of atrophy as previously described by Tso et al or longer term atrophic changes where FAF changes would become obvious over years.(Wallow and Tso, 1973a) This was the only patient in this study subset of Indian ethnicity and it was noted that almost his entire macular was covered

with soft confluent druse. This suggests that first the level of melanin and second, the impact of lipofuscin plays a crucial role in energy absorption and subsequent impact of these selective modern lasers.

The full fields image with peripheral laser test shots of supra threshold, threshold and subthreshold energy demonstrated the impact of energy levels with FAF changes, with suprathreshold as hyperfluorescence with rim of hypofluorescence and subthreshold as hypofluorescence. Hence, in the same light, the FAF changes may be secondary to varying levels of laser energy absorption.

The design of this laser with the speckled beam profile initially aimed to prevent secondary death of photoreceptor cells. The large spot size of the nanosecond laser was designed to circumvent the problem of narrow therapeutic index from ultra-short pulsed lasers. Although results from chapter 2 did not find a 'speckled' laser beam configuration, the current data did not demonstrate gross structural nor functional defects even with the presumed overtreated subjects (ie, type I laser lesions).

Several caveats were identified in the analysis of this study. First, the study had a very small sample size and majority of the laser energy and number of laser spots applied was within the same range. Analysis was attempted but failed to show an association between laser spot numbers, laser energy, laser lesion pattern and VA. Hence, it was not possible to determine the effects of varying laser energy and/or number of laser spots in this pilot study. Also, the study did not have a huge variation in ethnicity to account for the changes secondary to pigmentation. More importantly, other than the few images obtained during 1 and 3 month from subject recall, most of the earliest images were acquired at the 6th month when most of the effects of laser would have settled. It would have been ideal to determine changes acutely at 24 hours, 3 days, 1 week, 1 month and every 3-month thereafter where the laser healing process may be properly monitored.

Table 8.5 Classification of Q switched nanosecond laser changes based on FAF findings

FAF classification	Structural changes			Functional Changes
	OCT	CFP	Infra-red	Micro-perimetry
Hyperflorescent type I	At 6 months, thickening of RPE-Bruch's membrane complex noted which decreases with time. Variable disruption of IS/OS junction. No involvement beyond IS/OS junction.	Pale laser lesion with or without central pigmentation, which is stable in size at 12 months.	Hyperflorescent laser lesion.	Functional defect in laser lesion noted at 12 months.
Hyperflorescent type II	At 6 months, 'mild thickening' of RPE-Bruch's membrane complex. No involvement of IS/OS junction. At 12 months, changes become less obvious.	Variable uptake of pale laser lesion. Laser scar smaller in size than type I. Absence of pigmentation. Lesion decrease in size at 12 months.	Laser lesions noted as hyper-florescence.	Improvements in function both at 6 and 12 months.
Hypoflorescent	At 6 months, either no change or mild 'rippling' at RPE-Bruch's membrane complex with no involvement of IS/OS junction. Changes no longer apparent at 12 months.	No visible laser lesion.	No visible lesion	Functional improvements in individual laser lesions at 6 and 12 months.

Table 8.6 FAF classification and implications

FAF Classification	IMPLICATIONS
Hyperflorescent type I	<ol style="list-style-type: none"> 1. Laser wound healing effects may be prolonged. Damage mainly limited to RPE ,with variable effects on IS/OS. 2. Wound healing effects may be prolonged. 3. Threshold of damage limited by inter and intra patient variability. 4. May result in functional defects long term in highly pigmented patients. <p>Suggest Gross Laser overtreatment</p>
Hyperflorescent type II	<p>Milder response than type I with faster wound healing response and improvements in function.</p> <p>Mild laser overtreatment</p>
Hypoflorescent lesion	<p>Mild response, damage limited to RPE with no effects on IS/OS.</p> <p>Ideal laser treatment</p>

8.5 Conclusions

In summary, the above results demonstrated that the nanosecond laser technology has a limited damage profile. The results indicate that

1. The current laser energy settings led to over-treatment of most patients with prolonged RPE wound recovery period, although no clinically significant functional defects were found over a 12 month period.
2. The beam profile was not discontinuous in nature, which concurred with results from chapter 2.

Hence, it would be necessary to lower the laser settings and address the beam profile for optimal use in human subjects.

Chapter 9. Discussion

9.1 Discussion

The main purpose of this thesis was to determine the potential of the 2RT (3 nanosecond, 400 μ m, speckled laser beam) as a rejuvenative therapy to reverse the ageing of the outer retina, thereby retarding the onset of AMD. Several problems identified at the beginning of this thesis have been addressed through a series of laboratory and clinical studies. In summary, the following findings may be concluded from this thesis:

In laboratory studies undertaken,

1. The unique laser beam configuration was evaluated and found not to have a speckled beam profile;
2. The 2RT laser does cause increase in levels of active-MMP2 in a porcine explant culture model in both a time and directional-dependent response;
3. Higher levels of active-MMP2 were released with a larger number of laser spots;
4. Active-MMP2 increases hydraulic conductivity across the BrM in an age and dose-dependent fashion.

From the clinical studies, the following were concluded:

1. Application of the 2RT laser results in a short-term improvement in vision. This indicates that repeat laser may be required.
2. The laser in its current settings were too high and caused over treatment of subjects;
3. Despite this, the structural defects were limited and there were no gross functional defects. This indicates that although there was no 'speckled' beam profile, there was also limited secondary laser damage.

The following will discuss the findings from the laboratory and clinical studies in this thesis. Earlier in the introduction, the problem of choosing a sensitive and easily available clinical device to follow up on patients with early AMD and good vision was identified. In the RETILASE trial, the team also encountered initial problems with choosing a viable primary outcome measure. Hence, although it was not within the remit of this thesis to evaluate the use of outcome measures for AMD, this problem is sufficiently important to warrant a short discussion in the following.

9.2 The Role of the 2RT Laser in Rejuvenating the Aged Outer Retina

Laboratory studies have shown that the nanosecond laser application resulted in increased levels of active-MMP 2 in both the apical and basal end of the RPE BrM choroid explant. The release of active-MMP2 peaked at day 4 post laser and remained elevated beyond 9 days post laser. Furthermore, there was higher release of active-MMP2 with higher number of laser spots. Current findings concurred with the results from Treumer et al who also used porcine RPE-Bruch's explant.(Treumer et al., 2012) However, the current results differed from Zhang et al who demonstrated release of active-MMP 9 in addition to active-MMP2 in aged human RPE-Bruch's explant culture.(Zhang et al., 2012) This could be because of species differentiation between porcine and human eyes. A less likely reason could be that the porcine eyes were taken from young pigs, although this point has not being proven. Previous experiments have shown that active-MMP 9 resulted in higher levels of increases in hydraulic conductivity than active-MMP 2 in aged BrM.(Ahir et al., 2002) On the other hand, clinical studies have found association between MMP 9 and neovascularization, although these studies did not differentiate between pro and active-MMP9.(Chau et al., 2007) Hence, it may be postulated that there is a spectrum of MMP activity in terms of directional release, topographical and quantity of which one end results in rejuvenative therapy and the other as a precursor to AMD.

The series of studies involving explant cultures in this thesis extended beyond 7 days. Previous studies have demonstrated that the RPE layer forms its full layer with intact tight junction by 7 days post laser. Other invitro explant study also shown that the optimal period of explant incubation was 5 days. Histology from the control experiments have shown a possible lifting of the RPE from the BrM at day 7 of incubation, which may indicate cell death. Hence, although there had been conclusive evidence of raised active-MMP levels beyond 9 days in the laboratory experiments, the exact levels of enzyme quantity may be subject to question. Repeat experiments using in-vivo models may be a solution. In the current experimental set up, it was not possible to measure the transepithelial resistance of the RPE-BrM explant because the electrical probes which was designed in this using chamber were placed in the upper and lower chamber,

first would measure trans resistance across RPE, BrM, choroid and the filter membrane which gets clogged up with debris within days. Despite this, the current results with the increase of MMPs with laser and stabilization of MMP levels with controls does indicate that the RPE cells are intact. In this study, laser was applied on day 3 post initiation of culture, which aims to allow stabilization of the explant culture. Hence, it can be safely concluded that the release of active-MMP2 is an effect of laser.

Findings from chapter 5 have shown that the impact of MMP on hydraulic conductivity increases was both age and dose dependent. This suggested that the elderly population would require higher dose of the laser application for any effect. This may be achieved by either higher laser energy or a larger number of laser spots. Given that the current histological and clinical data results seemed to indicate that this laser energy was insufficiently low, it would be only wise to increase dosage of active-MMP release via increasing number of laser spots using lowered energy levels. From the experiments, the release of active-MMP2 per laser lesion in the range of 0.10 to 0.15mJ was calculated to be 2ng/mL. Unfortunately, in the current laser prototype, there was a failure in the speckled beam configuration. In theory, should the speckled beam configuration be functioning, there would be further release of active-MMP per laser lesion, hence, decreasing the need for a large number of laser spots.

The key concept here would be to define the 'balance' between the wound healing period of the laser lesion, maximal beneficial transport improvements and the appropriate balance from increased laser energy such as to prevent secondary apoptosis of the photoreceptor cells.

Thus, from the laboratory data, it was concluded that the 2RT laser in the nanosecond domain increased levels of activated MMP. This increase in active-MMP2 resulted in improvements in hydraulic conductivity across the BrM in a dose-related fashion, thereby forming part of the basis of which Gass first observed the decrease in drusen post laser.

Translating the laboratory results to human subjects, several important findings were noted.

Unfortunately, in the clinical trial, the study was terminated early and the remaining recruited subjects appeared to have undergone a randomization process, which for some reason seemed to have failed. Despite this, the current data found improvements in visual acuity in treated eyes at 6 months. This data

was not ever noted in previous laser AMD studies nor the study conducted by Guymer and team in Melbourne.

There had been difficulties defining the primary endpoint for the clinical trial, considering that patients with early AMD generally retain good vision. The first submission to ethics of the RETILASE trial protocol with flicker perimetry as the primary end point had resulted in ethics failure due to the lack in publications and common use of this device in the United Kingdom. The decision to use flicker perimetry then was made by the commercial firm due to the limited findings of flicker perimetry improvements in the study by the Melbourne team. Flicker perimetry is a relatively novel concept with minimal established data in regards to early AMD and being a continuous measurement, would require a calculated sample size in the range of 10,000 patients. Correspondence between international AMD experts at the Macular of Paris conference 2012, this very same issue was discussed and decided that visual acuity remains the best primary end point measurement at the moment. In this study, there was a short term improvement in visual acuity at 5.09 ± 5.67 ETDRS letters. This visual improvement was not sustained by 12 months. This suggested that the effect of laser was short term and a repeat treatment would be necessary. The results however were based on a very small sample size of patient because of early termination of recruitment. It was also noted that the baseline visual acuity of cases were lower than control which allowed for a larger improvements in visual acuity because of threshold effects with vision. Furthermore, due to constraints of the trial protocol, refraction was only done at every follow up visit, which might have been subject to further technical or subjective error. Despite this, as an initial study, the current results are encouraging and further explorative pilot dose escalation studies will need to be carried out.

Because of the small size of the RETILASE study and that the inclusion criteria was confined to patients with AREDS 2 and 3, there were only few patients that showed obvious decrease in drusen load. Most of the patients did not begin with a high drusen load to begin with.

The application of laser in the current study was limited by the lower threshold energy of 0.1mJ on the laser machine. Hence, 7 out of 11 of treated cases were at 0.1mJ, which did not allow calculation of dosing effect.

The main purpose of the use of the 2RT laser was to rejuvenate the aged outer retina. The main risk factor of AMD is ageing and it would be ideal to target

individuals at an earlier age (ie, in the 40s) when the hydraulic conductivity would have been compromised but before manifestations of signs of AMD. By doing so, the physiological process of ageing is retarded and the onset of AMD delayed. (Figure 9.1) Hence, the initial results from this thesis have demonstrated that the nanosecond laser was effective at preventing AMD by enhancing transport across the Bruch's membrane via the MMP pathway and this resulted in improvements of the visual outcome in affected patients. Thus, the 2RT laser is a potential therapeutic modality to rejuvenate the aged outer retina.

Figure 9.1 Demonstration of possible effects of rejuvenating the aged outer retina

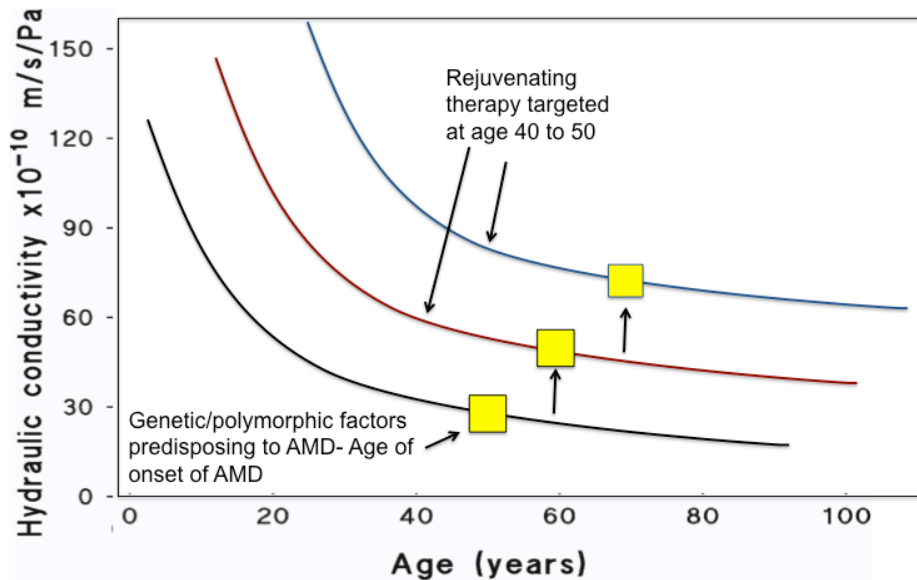


Figure 9.1 is a pictorial demonstration of the possible effect of rejuvenating the aged outer retina. By prophylactically renovating the process of physiological ageing of the macular, the HC has been shown to increase, thereby delaying the age of onset of AMD

9.3 Safety profile of the 2RT laser

The design of the 2RT laser was unique in that it was the first laser which functions as

1. a 3 nanosecond pulse laser,
2. it operates in the Q switched mode,
3. it has a speckled laser beam topography which targets discrete groups of RPE cells in a 400um beam spot size.

The combination of this unique design, if in the exact operational mode, was hypothesized to prevent both primary thermal damage to inner retina and secondary damage by photoreceptor apoptosis. The operational mode of the 2RT laser may be explained by figure 9.2. The 'cut off' threshold for speckling has been predetermined based on thermal relaxation time of the RPE. The peak energies above the 'cut off' as shown below would induce RPE cell death. At lower energies, a smaller number of peaks meet the 'cut off' and hence resulting in discrete groups of RPE cell death from the few energy peaks. From B, with higher laser energy, more individual peaks surpass the relaxation energy 'cut off', hence, resulting in a wider area of cell death. It must be noted that although Figure 9.2 was used in this instance to explain the operation of the 2RT laser, this figure, which was adapted from Wood et al, must be reviewed with caution for the following reasons. First, the image did not show discontinuous laser beam profile, ie, the 'dead' cells which appeared black were in groups of RPE cells death. Also, there were areas of dark green which was in between the 'black' and 'bright green' cells which indicated dead and living cells respectively. This could be due to poor experimental technique. Lastly, the 'cut off' zones demarcated in the figure did not correlate with the areas of RPE cell death or injury.

Based on current findings from the laser beam analysis and flat mount histology, it was concluded that the laser beam topography was likely set at too high an energy 'cut off', hence, resulting in an insufficiently separated spatial distance between the energy peaks and inadequate differential damage to RPE cells. (Figure 9.3)

Figure 9.2 Demonstration of speckling of 2RT laser beam

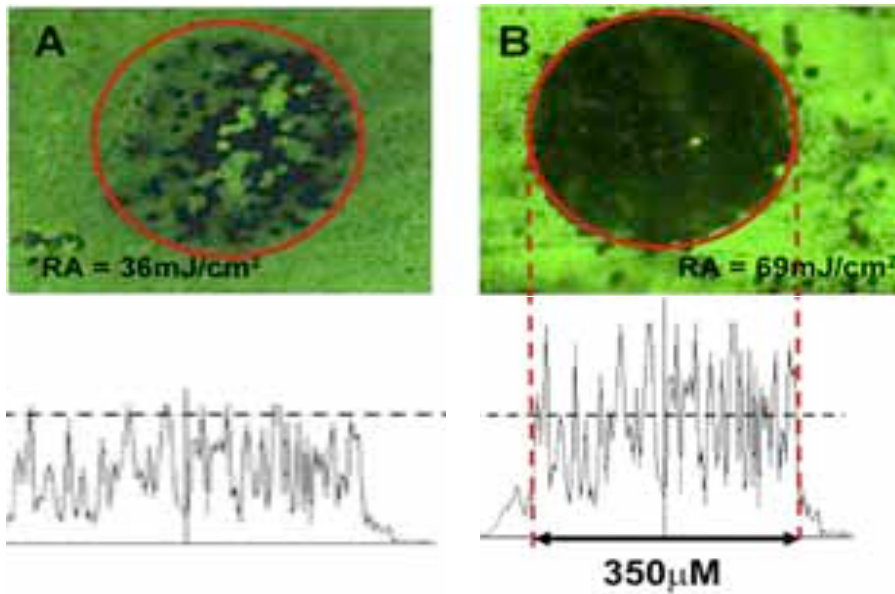


(Figure from J Wood et al)

Figure 9.3 Pictorial demonstration of impact of energy levels on speckling of 2RT laser beam

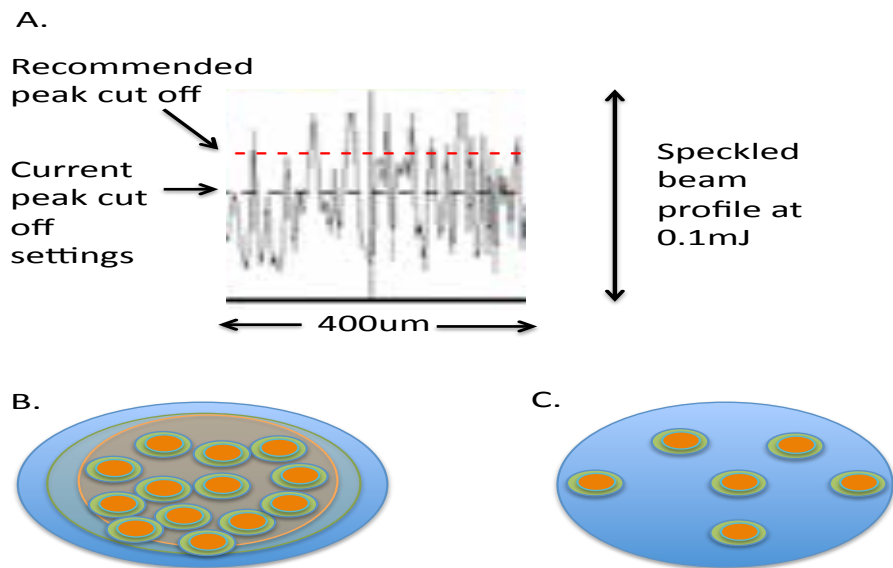


Figure A refers to speckled laser beam profile at 0.1 mJ. Current laser settings are too high, resulting in multiple peaks and multiple groups of RPE damage, which coalesce into a gaussian like beam damage (B.). A lower beam cut off will result in few peaks, figure C, with well separated and discrete RPE damage.

The structural and functional impact of the 2RT laser on human subjects was also evaluated using various clinical imaging modalities such as the FAF, OCT, CFP and microperimetry. The study protocol was designed with limited information from Guymer and team and the commercial company, Ellex. Then, most of the subjects in Melbourne have undergone laser treatment with energy levels 0.3mJ with no adverse effects. Hence, an energy level with an arbitrary 30% below peripheral threshold lesion energy was taken as the laser treatment protocol. ED 50 studies on porcine eyes subsequently indicate that a better estimate of visual damage was closer to 0.22mJ. That said, the lowest energy range on the laser machine was 0.1mJ, and it would not have been possible to turn the energy even lower for most of the subjects treated.

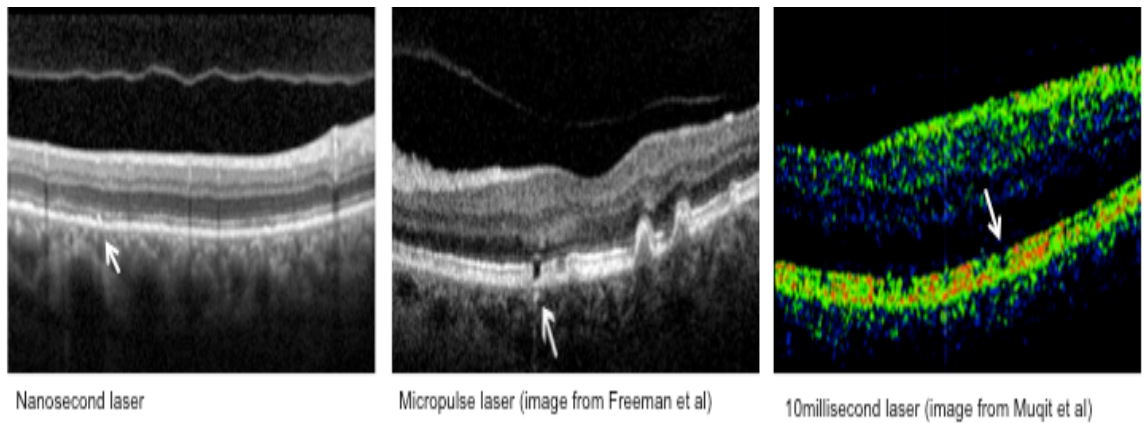
The advent of the OCT has allowed virtual invivo analysis of the human retina. In the RETILASE trial, the Spectralis OCT was used (Heidelberg Germany). Previous study by Marshall et al has demonstrated the agreement of OCT analysis and histology in the neurosensory layer, but the segmentation of outer retina still proves contradictory.(Chauhan and Marshall, 1999) In the study and based on prior histological knowledge, it can only be assumed the hyper-reflective bands in the outer retina is part of the IS/OS-ellipsoid layer, followed by the RPE-Bruch's membrane layer and the choroid. The purpose of using the OCT in the study was to evaluate damage both in the direction of the inner and the outer retina.

The fundus autofluorescence fluoresces with fluorophores, in particular, the lipofuscin which is contained within the RPE. This imaging modality allowed the analysis of laser impact on the RPE layer. Both the flicker and microperimetric testing investigated the functional effect of laser on the photoreceptor cells. In the RETILASE study, there were interesting results and a distinctive pattern associated with wound recovery. Laser lesions were classified based on observations on FAF into hyper and hypofluorescence patterns and hyperfluorescent lesions were further sub classified based on the stage of wound recovery. Given the clinical data, the current laser settings of the 2RT laser was safe as compared to conventional laser with limited damage profile, but still too high to accommodate variations between inter and intra individual melanin and/or lipofuscin contents. This resulted in what was described as overtreatment of several subjects.

Unfortunately, as mentioned, the sample size of this study was too small to allow calculation in terms of laser energy and spot numbers. Based on the findings, the ideal pattern may be that of hyperfluorescent type II laser lesion which demonstrated improvements in function on microperimetric analysis and limited damage to the RPE.

Subthreshold lasers have gained interest in the last 5 years. There are several lasers in the market currently which uses the concept of 'selective photothermolysis'. The following table summarizes the damage profile of the 'newer age' lasers in humans using a variety of clinical imaging modalities. The cw millisecond wave laser(PASCAL) has the most severe effect with immediate changes extending to the outer nuclear layer on OCT. Over long term, both micropulse laser and cw millisecond laser(PASCAL) demonstrate atrophic laser lesion with disruption of photoreceptor cells.(Muqit et al., 2010a, Mojana et al., 2011) The working mechanism of action and wound healing process of these lasers compared to the Q switched 2RT laser is clearly different. Whilst FAF findings were similar during the initial phase, ie, both were hyperfluorescent at 3 months, earlier CW argon type lasers became hypofluorescent over time with corresponding atrophy. This was further shown in a recent human histopathological study which showed extension of PASCAL laser (20millisecond) into the inner retina and further extension into the outer retina with RPE atrophy and disorganization of choriocapillaries.(Paulus et al., 2013)

Figure 9.4 Damage profile of lasers in mili to nanosecond time domain on OCT



Nanosecond laser has limited damage on the RPE, with no involvement of IS/OS nor choroid. Note the atrophic area on Micropulse laser with increased transmission to choroid. Both images were taken on Spectralis OCT. 10ms laser shows similar atrophy to micropulse. OCT taken on Fourier domain OCT.

Table 9.1 Clinical assessment of laser damage in varying laser time domains

Time-Domain	Pulse	Laser	Clinical Imaging			Functional assessment
			FAF	OCT	CFP	
Milli-second	CW, patterned laser	Pascal (Muqit et al., 2009, Muqit et al., 2010a, Muqit et al., 2010b)	Hyper-florescent at 1 week to 3 months.	Increased optical reflectivity within OPL and defect at level of the IS/OS and upper surface of RPE immediately post laser. 4 weeks post laser, the localised defects at the IS/OS but sparing of photoreceptors and RPE adjacent to either side of each burn.	Pale laser lesion which did not enlarge over time. Diameter of burns decreased with decreasing time domain up to 35%. (20 ms vs 100ms)	No published literature
Micro-second	Pulsed	Micro-pulse (IRIS Medical Oculight SLx))-subthreshold laser (Mojana et al., 2011) (Ohkoshi and Yamaguchi, 2010, Figueira et al., 2009, Vujosevic et al., 2010)	Hyper-florescent laser lesions at 3 months	Variable involvement of IS/OS, ONL (PRL).	Pale laser lesion	Improvements at 12 months at 4 and 12 degrees. Better preservation of mfERG. (as compared to conventional laser)

	Q-switched	SRT (Framme et al., 2009, Roeder et al., 1999, Roeder et al., 1992)	Hypo-florescent immediately post laser and remains hyper-florescent from 1 week to 15 months.	Variable thickening of RPE layer. No involvement of neuro-sensory layer.	-	Micro-perimetric changes detectable with higher number of pulses and energy (500 pulse and 100uJ vs 100 pulse and 70uJ).
Nano-second	Q-switched	2RT	Hypo-florescent laser lesion and hyper-florescent lesion which decreases in size over time.	Variable thickening of RPE layer. Recovery period between 6 months to beyond 18 months.	Pale laser lesion with or without central pigmentation. Decreases in size over time.	No significant defect on MP 1 in both DME and AMD patients.

The 2RT laser selectively targets the RPE cell likely through mechanical microbubble formation which results in microcavitation and disruption of individual RPE cells. Unlike conventional lasers, there was less disruption on the inner retina. In contrast to prior AMD laser prophylaxis trials, there was no increased rate of conversion in our AMD patients although the numbers were very small and were in the early stage of disease which in theory has a rate of conversion between 0.5 to 50% over 5 years.(Ferris et al., 2013) In the current study, there was a noticeable decrease in drusen load in some the few patients with a higher drusen load at baseline. However, there were no quantitative calculations of the proportionate decrease due to the small numbers. Previously, studies have been conducted and have failed to demonstrate both efficacy and safety of laser prophylaxis in AMD. The major clinical trials included the CNVPT ,CAPT and PTAMD (USA), DLS (Talhok et al.), and Nordic study.(Frennesson et al., 2009, Friberg et al., 2006, 2003, 2006) These trials were divided into either bilateral arm study (both eyes with early maculopathy) or unilateral eye study (fellow eye has exudative AMD). Common endpoints of the studies included change in BCVA, either continuous or proportional (number of lines improvements or decreased) and rates of CNV formation. Conclusions based on these studies have found increased rates of

CNV formation in the unilateral arm studies. Results for bilateral arm studies have however been equivocal. Olk et al and CNVPT have found increase with vision that is correlated with drusen decrease at 12 months, however PTAMD have found higher proportion of visual loss of > 2 lines amongst treated patients. Hence, the concept of laser prophylaxis of AMD was largely aborted. Subanalysis of the CNVPT study of the unilateral arm have found that higher intensity laser resulted in higher rates of CNV formation, most of which were occult in nature, at the site of laser application. Table 9.2 highlights the laser treatment parameters. It is noteworthy that most of the laser used in the previous trials were continuous wave in nature and were of significantly higher laser time domain as compared to our nanosecond laser technology. In theory, it may be argued that higher intensity laser burns resulted in higher rates of conversion to wet AMD, which was likely secondary to a break in BrM as a consequence of laser therapy. This is especially so in unilateral patients, where the eye may have higher levels of lipofuscin due to the more advanced stage of the disease. In this special group of patients, it is important to stress that most lipofuscin and melanin plays important role as laser energy scavenger and hence is exposed to higher laser impact than younger patients.

The RETILASE trial was a bilateral arm study. In addition to the main outcomes such as change in BCVA and rates of CNV conversion, we have measured the qualitative changes on OCT, FAF and functional defects on perimetric analysis using microperimetry and flicker perimetry. Guymer et al have shown improvements in flicker perimetry at 12 months in using the 2RT laser on bilateral AMD patients using 12 laser spots. No visual improvements were however reported.(Guymer et al., 2013) The use of flicker perimetry to determine cone functions is still debatable; hence, the results from the flicker perimetry must be interpreted with caution. Perimetry results were analyzed as improvements in a global function of the retina at 4 and 12 degrees and at individual laser lesions. Based on these results, the nanosecond laser did not demonstrate defects structurally and functionally. There was no comparison for the previous AMD trials for this subgroup of patients as these earlier studies did not incorporate these retinal imaging. Although the RETILASE trial had a very small sample size, the results are encouraging and may prove to circumvent the previous problems in prior studies.

Table 9.10 Laser protocols used in prior laser-drusen studies

	Laser type	Spots	Spot size (μm)	Time (seconds)	Intensity
CNVPT	Argon green	20	100	0.1	Grey/white
DLS	Green/yellow	12	200	0.2	Faint uptake
PTAMD	810-nm diode	48	125	0.2	Sub-threshold
CAPT	Argon green	60	100	0.1	Barely visible
Frennesson (Nordic)	Argon green	100	200	0.05	Sub-threshold/ barely visible
RETILASE	Nd: YAG (doubled frequency)	>55	400 μm (speckled beam)	3ns	Subthreshold

Table 9.3 Summary of study design and outcome of laser-drusen studies

Ref	Laser	Treatment protocol	Study Design Bilateral/unilateral study Follow up period Outcome measurements	Results/ Conclusion
Olk 1999 (basis for PTAM D)	810nm, diode, sub-threshold and minimally threshold lesions.	48 laser spots, 125 µm size. 4 concentric circles outside the FAZ in a scatter or grid pattern between 750 µm and 2250 µm from the center of the FAZ	24 months follow up. Bilateral and unilateral arm. Outcome measures: <ul style="list-style-type: none"> • Reduction of drusen • Change in visual acuity • Rate of CNV development 	At 24 months, 11.4% of treated patients had >2 lines improvements of VA. 62% treated eyes showed reduction in drusen in threshold lesion at 12 months and 65% for subthreshold lesion at 18 months.
PT-AMD 2006	810nm diode sub-threshold laser	48 laser spots, extrafovea, 125 µm diameter. Single treatment	Total of 36 months follow up. Unilateral eye study Outcome measures: <ul style="list-style-type: none"> • Development of CNV • Change in BCVA. 	Increased rates of CNV at 1year (15.5% vs 1.4% controls). Treated eyes showed higher rates of VA loss of more than 3 lines at 3 and 6 months.
CNVP T 1999 (basis for CAPT)	Argon laser 0.1s, 100µm	Multiple, 100µm laser spots, 750µm from fovea	12 months outcome. Bilateral and Unilateral eye study. Primary outcome: <ul style="list-style-type: none"> • Change in visual acuity Secondary outcome: <ul style="list-style-type: none"> • Change in contrast threshold • Change in critical print size 	At 12 months, laser-treated eyes with 50% or more drusen reduction had visual acuity improvements (1-2lines) and less losses in visual acuity Similar improvements were noted for contrast threshold but not critical print size. Increased rates of CNV for unilateral arm,
CAPT 2006	Argon laser 0.1s, 100µm spot size	Initial treatment of 60 barely visible burns in a grid pattern within an annulus between 1500 and	5 year follow up. Bilateral eye study Primary outcome: <ul style="list-style-type: none"> • Change in visual Acuity Secondary outcome: <ul style="list-style-type: none"> • Incidence of complications of 	20.5% of treated eyes and 20.5% of controls had > 3 lines visual loss from baseline at 5 years. No difference in occurrence of wet or dry AMD at 5

		2500 microns from the fovea Repeated treatment at 12 months if 10 or more large drusen remained in the treated eye within 1500 microns of the foveal center	AMD <ul style="list-style-type: none"> Changes in contrast threshold and critical print size for reading 	years. Results for contrast threshold and critical print size were insignificant. Concluded no clinically significant benefits of laser photocoagulation.
Drusen Laser study (DLS 2003)	Argon laser, 0.2s, 200µm	12 burns;4 burns 750 µm from the center of the fovea at 12, 3, 6, and 9 o'clock, and 8 burns, 1500 µm from the center of the fovea at 12, 1:30, 3, 4:30, 6, 7:30, 9, and 10:30 o'clock.	36 months follow up Unilateral and bilateral study. <ul style="list-style-type: none"> BCVA Development of CNV 	Unilateral group, vision loss occurred 28.8%of patients in laser vs 19.7% (not significant) Incidence of CNV was 29.7% vs 17.65%. Bilateral group, vision loss 8.3% of laser-treated patients vs 13.9% (not significant) CNV developed in 11.6% vs 6.8%. Concluded that laser is not beneficial in unilateral arm treatment.
Frenneson 2009	Argon, 0.05s, 200µm spot size	Scattered on and between drusen in the posterior pole. Subthreshold/ barely visible	Follow up 3.7 years Bilateral and Unilateral arms Outcome measures: <ul style="list-style-type: none"> Change in BCVA Rate of CNV development 	More CNVs in treated group in unilateral arm; VA reduced from baseline although not different from controls in both arms. Laser treatment not beneficial nor harmful, not recommended.
RETI-LASE	Doubled frequency Nd:YAG, 400µm spot size(speckled beam)	>55 laser spots in 2 annulus 500µm from fovea	24 months Unilateral arm Primary outcome: <ul style="list-style-type: none"> Change in BCVA Secondary outcome: <ul style="list-style-type: none"> Rates of CNV formation Changes on FAF/OCT/MP1/ flicker perimetry 	6 months increase mean vision of 1 line in treated patients. No conversion to CNV at 12 months. (11 treated patients) MP 1 did not show laser defects at 4 and 12 degrees.

9.4 Evaluation of tools to monitor early AMD

Histological studies have shown changes in the photoreceptors to choroidal capillaries prior to clinical onset of AMD. These changes include the decrease in rod and cone density, especially in the macular, thickening of the Bruch's membrane, lipoid-proteinaceous deposits sub-RPE or within the inner collagenous layers of the BrM and thinning of the choroidal capillaries.

Transportation studies have also found age-dependent demise in hydraulic conductivity and amino acid transport across the BrM. Currently, the diagnosis of early AMD is based on the identification of clinical hallmarks such as drusen and/or pigmentary abnormalities which are observed on clinical slit lamp ophthalmoscopy or color fundus photography. AMD classifications (AREDS, IC) are largely based on these clinical markers as risk of developing late stages of AMD such as geographic atrophy or choroidal neovascularization (Dry or Wet AMD).

Given that age-related changes mentioned above occur on a continual basis, the concept of aging macular is vital in introducing a preventative measure prior to the onset of clinical changes. Currently, there is a paucity of available modalities to first ascertain the diagnosis of very early aging macular or age related macular degeneration and to monitor its progression. A good assay for clinical application must be sensitive and specific, reproducible, easy to use and economically viable for community diagnosis and monitoring purposes.

Assays to evaluate status of early AMD can be broadly categorized into 2 groups: structural and functional. Structural assays include imaging modalities which allows static visualization of structures and follow up in time for quantification and/or qualification of changes such as number of size of druse, change in RPE layer, thickening of BrM, quantification of photoreceptors. The recent years have seen huge progress in retinal imaging modalities. There are 3 main imaging modalities for the diagnosis of AMD, but mainly used in identifying the wet or dry AMD. First, fluorescein angiography(FFA) , remains the current gold standard of diagnosis which enables diagnosis via the visualization of leakage and staining concept of retinal vessels and tissues. Second, the indocyanine green (ICG), which uses the SLO technology enhances clarity of the deep, ill defined 'occult or sub RPE' CNV. It also enables differentiation of the etiology of CNV such as polypoidal choroidal vasculopathy and chorioretinal anastomosis can be made.(Yannuzzi et al., 1992, Hyvarinen and Flower, 1980)

Recently, investigators have found corresponding features on OCT and FFA which suggests the use of OCT as a noninvasive tool to diagnose neovascular AMD. (Mathew et al., 2014) OCT has allowed detection of subretinal and intraretinal fluid from CNV as well as the identification of various types of drusen in early AMD. (Huang et al., 1991, Schlanitz et al., 2010, Freeman et al., 2010, Leuschen et al., 2013) In the very early stages of AMD, FFA and ICG would play minimal roles. Several authors such as Soubrane et al and Coscas et al has published in depth review articles and books on OCT features in AMD.(Coscas et al., 2004, Coscas, 2009) As the OCT is a relatively young technology with limited histo-pathological references, the numerous features described in current literature remains as inferences to the histopathology of disease states.(Stopa et al., 2008, Toth et al., 1997)

The advent of OCT has provided useful information of the anatomical microstructure of the retina using the anteroposterior scans.(Huang et al., 1991) As an imaging modality itself, OCT has progressed tremendously, from the conventional(time domain TD OCT) to the modern day spectral domain(SD OCT) with a much higher resolution and better clarity from reduced noise levels and added advantage of faster image acquisition, hence allowing 3D compilation or mapping, patient eye motion tracking, as well as RPE segmentation, added advantage of combination modalities such as angiography/autofluorescence/microperimetry.(Coscas, 2009, Alam et al., 2006, Menke et al., 2006) Using OCT, we are able to both qualify and quantify the drusen deposits. Although the identification of drusen is relatively easy with other imaging modalities, with the high resolution SD OCT, clinicians are able to address several issues and qualify drusen in an unprecedented way. On OCT, soft drusen are recognized as an elevation of the RPE with a moderately reflective drusen cavity. There is minimal posterior shadowing associated with it. SD OCT also demonstrates better visibility of reticular drusen, as a thickened band and undulations of the RPE with no altered outer nuclear layer. Khanifar et al has evaluated and found 17 different types of drusen based on the shape, size, heterogeneity as well as internal reflectivity.(Khanifar et al., 2008) Other than drusen, the surrounding presumed RPE band, IS/OS interface, external limiting membrane as well as outer nuclear layer has been noted to be thinned. Johnson et al has demonstrated both structural and functional photoreceptor changes over drusen in postmortem eyes. These include change in

photoreceptor cell density, gene expression and synapses over drusen. (Johnson et al., 2003, Johnson et al., 2005) Shuman et al studied the neurosensory retina abnormalities in sites relative to drusen in early AMD and found a decreased thickening of PRL over drusen, suggesting a focal degenerative process with postulated eventual progress to visual loss, even in early stage AMD. (Schuman et al., 2009) Other qualitative changes noted in relation to drusen include the absence of photoreceptor outer segment, disruption of the photoreceptor inner segment/outer segment junction, hyper-reflective foci adjacent and over drusen, all of which were presumed anatomy defined by other investigators. (Schuman et al., 2009, Coscas, 2009) With further advancements to the latest SD OCT, which has a high axial resolution of 5 μm , high intensity and high speed acquisition, accounting for patient motion effects and hence decreases artifacts, several authors have continued the pursuit of drusen quantification, now in terms of even more specific drusen area and volume. There were up to 5 studies previously published on quantifying drusen using OCT using RPE segmentation. There are 2 issues with this technique, first, as mentioned several times in this thesis, there is a poor correlation between the presumed OCT structures currently defined by the ophthalmic community and the its true anatomy simply because of the x-y resolution current OCT technology has (Figure 9.5). Second, much focus has been put on drusen to define progress of AMD, laser prophylaxis studies of AMD also included drusen quantification as an outcome measure for determining effect of therapy. However, as per this thesis, it must be stressed that drusen is a late downstream consequence, which should not be taken as a target for progression or change. The ability to measure BrM thickness would have been ideal. BrM is at approximately 7 μm in thickness in early stages of AMD and would not have been identifiable on the current OCT technology. A confocal coronal scan OCT enables en-face evaluation of the BrM, but this is not currently commercially available. A recent development of the Swept-source OCT uses a short cavity-swept laser (vs. a super-luminescent diode used in SD-OCT) to achieve superior acquisition rates at a longer wavelength (1,060 nm), hence enabling the imaging of discrete photoreceptor cells. Using this OCT, investigators has also demonstrated thinning of choriocapillaries in relation to pseudoregular druse. (Ueda-Arakawa et al., 2014) Enhanced depth

imaging (EDI)-OCT also allows better visualization of the choroid.(Spaide, 2009, Coscas et al., 2012, Querques et al., 2012)

Figure 9.5 Pictorial demonstration of imaging resolution as compared to anatomical structure

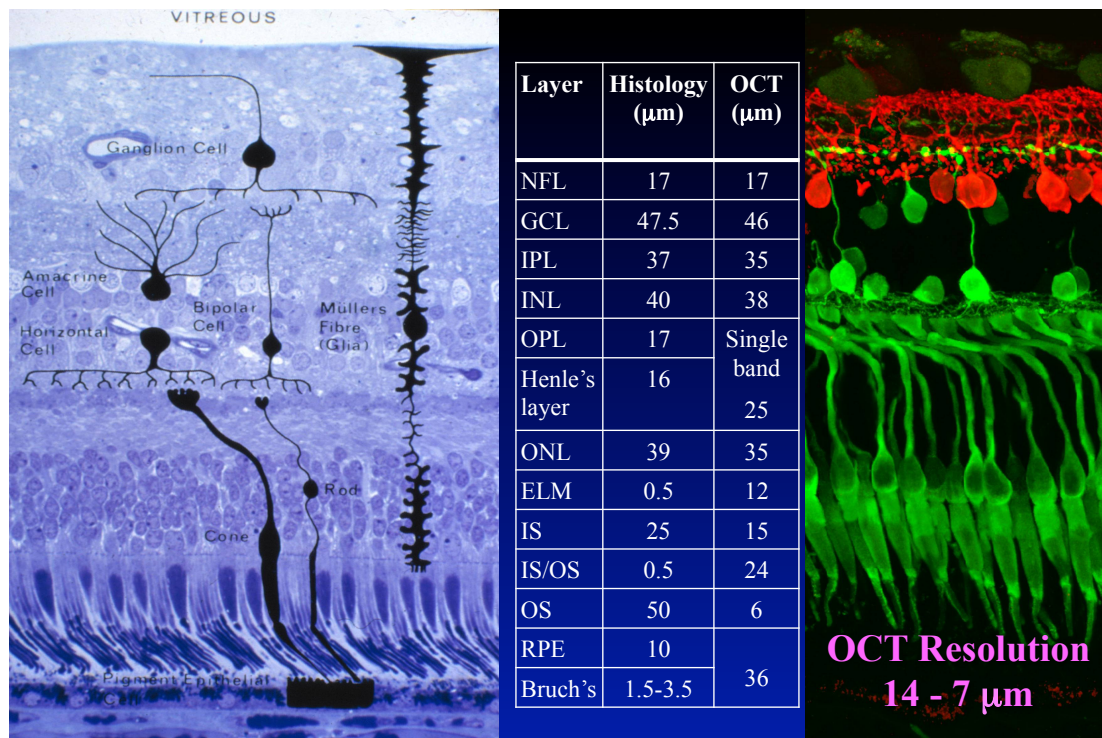


Figure 9.5 Pictorial demonstration of resolution of OCT as compared to anatomical structure of the retina

Lipofuscin which fluorescence with short wavelength light accumulates in RPE cells with age.(Sugino et al., 2014) FAF emits light in the 500- to 750-nm range (peak~630 nm). Lipofuscin signal mainly arises from the RPE, and the loss of FAF is associated with loss of RPE. FAF has been shown to be helpful in identifying severity in early AMD but again this focuses on later stages of early AMD with clinical identification of druse and pigmentary abnormalities. (Bindewald et al., 2005, Midea et al., 2007)

Adaptive optics scanning laser ophthalmoscopy (AOSLO) as a technology is gaining popularity in recent years due to its ability to identify rods and cones and RPE.(Obata and Yanagi, 2014, Muthiah et al., 2014, Lombardo et al., 2013, Rossi et al., 2013) Adaptive optics allows a lateral image resolution of 2 µm, hence allowing visualization of individual cone photoreceptors.(Liang et al., 1997, Roorda et al., 2002, Talcott et al., 2011) The use of AOSLO enables

visualization of individual cells but does not give further useful information regarding the health of the rods/cones and the photodynamics or integration between the photoreceptors-RPE-BrM.

The second category of assay involves the functional assessments of rods/cones in relation to early AMD or aging macular. This involves static and dynamic measurements of rod/cone functions using psychophysical tests. Static analysis involves the functional capacity of rods and cones and its post receptor elements, whilst dynamic analysis involves evaluation of the integration of PRL-RPE-BrM complex, ie, regeneration of photopigment in photoreceptor layer. These tests range from the vision function tests such as visual acuity, color vision, contrast sensitivity to the more intricate tests such as microperimetry, flicker perimetry to dark adaptation, pigment densitometry and photostress tests.

Visual acuity measurement is a simple assessment which can be used in a daily clinical setting. However, VA testing gives minimal information on retinal function in early AMD due to first, the wide range of variability of the test and second, involves cortical processing in the higher order.(Dimitrov et al., 2011, Siderov and Tiu, 1999) The Beaver Dam Eye Study shows minimal letter loss in early AMD, hence, although convenient and economically viable, is not a highly sensitive nor specific test for early AMD.(Klein et al., 1995) Furthermore, there is a coefficient of repeatability of 12 letters in prior studies.(Aslam et al., 2014, Patel et al., 2008)

Contrast sensitivity have been found to be decreased in early AMD. The coefficient of repeatability is approximately 7 letters.(Aslam et al., 2014, Patel et al., 2009) Reduced foveal contrast sensitivity, have been demonstrated in patients with early AMD.(Stangos et al., 1995)

Color thresholds especially in the blue-yellow (titan) spectra have been shown to be affected in AMD patients in accordance to Kollner's rule and allows for early diagnosis.(Hart, 1987, Bowman, 1980, Arden and Wolf, 2004, Holz et al., 1995, Frennesson et al., 1995) Professor Arden has developed a computerized system integrating color thresholds with contrast thresholds, hence, maximizing the ability to detect functional losses from the disease.

Conventional perimetry shows a good relation to drusen and pigmentary changes, but the quantification of retinal thresholds over time is difficult with the older system.(Sunness et al., 1995) A new SLO-implemented perimeter has

overcome this problem.(Midea et al., 2004) Repeatability of microperimetry is found to be 4.2dB in the macular region.(Cideciyan et al., 2012) Flicker perimeter is based on the use of increasing the metabolic needs of retinal tissue, hence, causing compensatory retinal vascularization and oxygen tension. In patients with outer retina pathology, the compensatory mechanisms may be overstretched and result in functional deficiencies.(Feigl et al., 2007, Formaz et al., 1997, Shakoor et al., 2006) Studies have found flicker sensitivity to be impaired in patients with early AMD.(Phipps et al., 2004) In particular Dimitrov et al have also found flicker measurements to be more sensitive than color threshold measurements. Thus far, there are no repeatability studies published for flicker perimetry.(Dimitrov et al., 2011)

Electrophysiological tests have been found to be able to measure the degree of impairment based on the integration of the BrM-RPE-PRL. These tests are highly specialized and expensive and limited to tertiary centers. Examples include dark adaptation and photostress test of cones. Recovery dynamics have been found to be compromised in AMD patients.(Sloane et al., 1988, Cheng and Vingrys, 1993, Owsley et al., 2001, Owsley et al., 2007, Bartlett et al., 2004, Haimovici et al., 2002) Exaggerated results were found in rods as compared to cones, signifying a further compromise of rods as compared to cones, especially in relation to age-related rod loss and marginal cone loss in healthy population.(Curcio et al., 1993, Jackson and Owsley, 2000) Hence, in monitoring purposes of early AMD post treatment in clinical trials, dynamic psychophysical tests may be a superior assay.

Several of the techniques discussed have been used to monitor the progression of AMD in the RETILASE study. The primary outcome of the study was visual acuity at 12 months. There was an increase of approximately 5 letters at 6 months in cases. According to known data from repeatability studies, this would not be clinically significant due to the large variability inherent in this measurement technique. However, the progression rate of change of VA in early AMD was shown to be 2 letters in the population based Beaver Dam eye study. This would indicate that our current results does have clinical value as a potential therapeutic intervention, but would require larger scale studies with longer term follow up. In the RETILASE study, there are 2 components to consider in analyzing the results, first, the change in AMD pathophysiology post laser treatment, second the structural change from laser. The use of the

Spectralis SD OCT allowed a gross evaluation of the structural damage from laser in time, but was not able to analyze the intricate changes in BrM as expected based on the earlier laboratory results.

Functional analysis used in the RETILASE included static threshold studies such as microperimetry and flicker perimetry. It was difficult in this instance to ascertain whether the current changes were secondary to progression of AMD or laser changes. It would have been useful to include dynamic studies in subsequent studies to evaluate ability to monitor the photoreceptor status over time to give an objective interpretation of photoreceptor function post treatment. An ideal device would be the Optos designed fundus reflectometer, which allows measurements of rhodopsin, and the density of rhodopsin, and its rate of regeneration as well as its distribution. Unfortunately, this device is currently only available for research. In the design of RETILASE, there was limitation in funding and electrophysiological analysis were not included.

9.5 Conclusions and future direction

In conclusion, there were several salient findings from this thesis,

1. The 2RT laser in the current prototype did not have a viable speckled beam configuration. In theory, this may lead in secondary laser damage. However, the clinical results did not show any involvement of the photoreceptor cells both structurally and functionally.

2. Although the beam profile had proven disappointing, studies have found that the 2RT laser in its nanosecond domain does result in release of active-MMPs in porcine explant cultures. Pilot studies in this thesis prove that higher volume of RPE injury increases quantity of active-MMPs and this increase in volume of RPE injury may be achieved by increasing number of laser spots.

3. Laboratory studies in this thesis correlated the activity of MMPs with improvements in hydraulic conductivity across the human BrM. In particular, the older donor age appeared to require higher doses of MMPs for any improvements in hydraulic conductivity as compared to the younger donor subsets. Translated into clinical terms, this means that older aged population would require a higher volume of MMPs to clear debris in the outer retina for any transport improvements. MMPs are released by RPE migration and the 2RT laser is a plausible modality to cause RPE injury. By increasing number of laser spots, the total volume of RPE injury or effective circumference for RPE migration could be increased for total increase in MMP release.

Lastly, results from the RETILASE trial suggested possible short term benefits of visual improvements. However, the data also indicated the need for repeat treatment. The laser in its current form causes gross over-treatment in human subjects and would need to be adjusted in terms of 1. lowering the energy level threshold, 2. Increasing the speckled beam profile. This could be done by adding twisted optical fibers to limit transmission. Twisting the optical fibers creates differences in depth of radiation transmission, hence reducing the proportion of radiation that is able to pass through.

A discontinuous laser beam and discontiguous RPE cell injury limits secondary laser damage and increases the effective circumference for RPE migration.

With this, the quantity of active-MMP release per laser lesion would be higher, and less number of laser spots would be required for treatment.

There were several limitations in the design of studies undertaken in this thesis.

First, the definitive laser-MMP release studies were done on porcine explant

cultures. It would be crucial to repeat these studies in human explants and to increase the number of sample sizes with a broad range of donor age. Second, although there were a good number of sample sizes (n=44) in the hydraulic conductivity study in chapter 5, most of the samples were in the age group over 60 years of age. Hence, the study was biased in the sense there was a disproportionate percentage of younger donor BrM.

More importantly, results of the RETILASE trial at 24 months and beyond would allow determination of the longer term impact of the 2RT laser on human subjects. A laser dose escalation study with careful inclusion of assessments such as fundus densitometer and flash recovery ERG in the future will yield important and conclusive information on the 2RT treatment to prevent AMD. As established, this thesis has hopefully set the direction for future studies to be conducted. At this stage, it is still juvenile to conclude that laser is the ultimate preventative therapy for AMD. Perhaps combination therapy of multivitamins and laser will prove to be beneficial.

The use of laser as a prophylactic therapy in AMD has been a 'black hole' in the ophthalmic community at large due to the results of the prior studies. It is necessary to re-educate ophthalmologists on the causes of failure and re-introduce the current concept of debris clearance of the BrM and the safety of the current novel concept nanosecond laser with the results of this thesis.

In conclusion, although the 2RT laser is superior to conventional lasers in terms of its damage profile, the laser in its current state is still considered inadequate because of a non-viable 'speckled beam' and insufficiently low energy levels. Despite this, the concept of the 2RT laser has been proven in this thesis to play a potential role in rejuvenating transport in the aged outer retina.

References

1985. Photocoagulation for diabetic macular edema. Early Treatment Diabetic Retinopathy Study report number 1. Early Treatment Diabetic Retinopathy Study research group. *Archives of ophthalmology*, 103, 1796-806.
1993. Antioxidant status and neovascular age-related macular degeneration. Eye Disease Case-Control Study Group. *Archives of ophthalmology*, 111, 104-9.
2003. Laser treatment in fellow eyes with large drusen: updated findings from a pilot randomized clinical trial. *Ophthalmology*, 110, 971-8.
2006. Laser treatment in patients with bilateral large drusen: the complications of age-related macular degeneration prevention trial. *Ophthalmology*, 113, 1974-86.
- A, B. (ed.) 1970. *Ocular circulation*, St Louis: The C.V. Mosby Co.
- A, M. J. A. L. 1985. *The special pathology of the ageing macula. In Retinal Degeneration: experimental and Clinical studies.*
- A.A HUSSAIN, C. S., J MARSHALL 2004. *In Focus on Macular Degeneration Research: Transport Characteristics of Ageing Human Bruch's Membrane: Implications for Age-Related Macular Degeneration (AMD)*, Nova Science Publishers Inc.
- ABDELSALAM, A., DEL PRIORE, L. & ZARBIN, M. A. 1999. Drusen in age-related macular degeneration: pathogenesis, natural course, and laser photocoagulation-induced regression. *Survey of ophthalmology*, 44, 1-29.
- AHIR, A., GUO, L., HUSSAIN, A. A. & MARSHALL, J. 2002. Expression of metalloproteinases from human retinal pigment epithelial cells and their effects on the hydraulic conductivity of Bruch's membrane. *Investigative ophthalmology & visual science*, 43, 458-65.
- AHMED, J., BRAUN, R. D., DUNN, R., JR. & LINSSENMEIER, R. A. 1993. Oxygen distribution in the macaque retina. *Investigative ophthalmology & visual science*, 34, 516-21.
- AL-HUSSAINI, H., KAM, J. H., VUGLER, A., SEMO, M. & JEFFERY, G. 2008. Mature retinal pigment epithelium cells are retained in the cell cycle and proliferate in vivo. *Molecular vision*, 14, 1784-91.
- AL., S. 1959. *Infrared and optical masers.*, New york, NY, Columbia University Press.
- ALAM, S., ZAWADZKI, R. J., CHOI, S., GERTH, C., PARK, S. S., MORSE, L. & WERNER, J. S. 2006. Clinical application of rapid serial fourier-domain optical coherence tomography for macular imaging. *Ophthalmology*, 113, 1425-31.
- ALCAZAR, O., COUSINS, S. W. & MARIN-CASTANO, M. E. 2007. MMP-14 and TIMP-2 overexpression protects against hydroquinone-induced oxidant injury in RPE: implications for extracellular matrix turnover. *Investigative ophthalmology & visual science*, 48, 5662-70.
- ALEXANDER, J. P., BRADLEY, J. M., GABOUREL, J. D. & ACOTT, T. S. 1990. Expression of matrix metalloproteinases and inhibitor by human retinal pigment epithelium. *Investigative ophthalmology & visual science*, 31, 2520-8.
- ALEXANDER, J. P., SAMPLES, J. R., VAN BUSKIRK, E. M. & ACOTT, T. S. 1991. Expression of matrix metalloproteinases and inhibitor by human trabecular meshwork. *Investigative ophthalmology & visual science*, 32, 172-80.
- ALLIANCE FOR AGING RESEARCH, A. P., ALLIANCE FOR EYE AND VISION RESEARCH (AEVR) (ed.) 2011. *The Silver Book Vision Loss Volume III Chronic Disease and Medical Innovation in an aging Nation, Cost of Vision Loss, Age-A Major Risk Factor Section, Age Related Macular Degeneration.*
- ALM, A. & BILL, A. 1973. Ocular and optic nerve blood flow at normal and increased intraocular pressures in monkeys (*Macaca irus*): a study with

- radioactively labelled microspheres including flow determinations in brain and some other tissues. *Experimental eye research*, 15, 15-29.
- ANDERSON, R. R. & PARRISH, J. A. 1983. Selective photothermolysis: precise microsurgery by selective absorption of pulsed radiation. *Science*, 220, 524-7.
- APTE, S. S., MATTEI, M. G. & OLSEN, B. R. 1994. Cloning of the cDNA encoding human tissue inhibitor of metalloproteinases-3 (TIMP-3) and mapping of the TIMP3 gene to chromosome 22. *Genomics*, 19, 86-90.
- ARDEN, G. B. & WOLF, J. E. 2004. Colour vision testing as an aid to diagnosis and management of age related maculopathy. *The British journal of ophthalmology*, 88, 1180-5.
- ASHTON, N., WARD, B. & SERPELL, G. 1954. Effect of oxygen on developing retinal vessels with particular reference to the problem of retrolental fibroplasia. *The British journal of ophthalmology*, 38, 397-432.
- ASLAM, T., MAHMOOD, S., BALASKAS, K., PATTON, N., TANAWADE, R. G., TAN, S. Z., ROBERTS, S. A., PARKES, J. & BISHOP, P. N. 2014. Repeatability of visual function measures in age-related macular degeneration. *Graefe's archive for clinical and experimental ophthalmology = Albrecht von Graefes Archiv fur klinische und experimentelle Ophthalmologie*, 252, 201-6.
- ASTON-MOURNEY, K., ZRAIKA, S., UDAYASANKAR, J., SUBRAMANIAN, S. L., GREEN, P. S., KAHN, S. E. & HULL, R. L. 2013. Matrix metalloproteinase-9 reduces islet amyloid formation by degrading islet amyloid polypeptide. *The Journal of biological chemistry*, 288, 3553-9.
- AUGOOD, C., CHAKRAVARTHY, U., YOUNG, I., VIOQUE, J., DE JONG, P. T., BENTHAM, G., RAHU, M., SELAND, J., SOUBRANE, G., TOMAZZOLI, L., TOPOUZIS, F., VINGERLING, J. R. & FLETCHER, A. E. 2008. Oily fish consumption, dietary docosahexaenoic acid and eicosapentaenoic acid intakes, and associations with neovascular age-related macular degeneration. *The American journal of clinical nutrition*, 88, 398-406.
- BACOVA, B., RADOSINSKA, J., KNEZL, V., KOLENOVA, L., WEISMANN, P., NAVAROVA, J., BARANCIK, M., MITASIKOVA, M. & TRIBULOVA, N. 2010. Omega-3 fatty acids and atorvastatin suppress ventricular fibrillation inducibility in hypertriglyceridemic rat hearts: implication of intracellular coupling protein, connexin-43. *Journal of physiology and pharmacology : an official journal of the Polish Physiological Society*, 61, 717-23.
- BANDYOPADHYAY, M. & ROHRER, B. 2012. Matrix metalloproteinase activity creates pro-angiogenic environment in primary human retinal pigment epithelial cells exposed to complement. *Investigative ophthalmology & visual science*, 53, 1953-61.
- BARTLETT, H., DAVIES, L. N. & EPERJESI, F. 2004. Reliability, normative data, and the effect of age-related macular disease on the Eger Macular Stressometer photostress recovery time. *Ophthalmic & physiological optics : the journal of the British College of Ophthalmic Opticians*, 24, 594-9.
- BASOV NG, P. A. 1954. Application of molecular rays to radiospectroscopic studies of the rotational spectra of molecules. *Zh Eksp Teor Fiz Pis'ma*, 27, 431-438.
- BAYNES, J. W. 2001. The role of AGEs in aging: causation or correlation. *Experimental gerontology*, 36, 1527-37.
- BINDEWALD, A., BIRD, A. C., DANDEKAR, S. S., DOLAR-SZCZASNY, J., DREYHAUPT, J., FITZKE, F. W., EINBOCK, W., HOLZ, F. G., JORZIK, J. J., KEILHAUER, C., LOIS, N., MLYNSKI, J., PAULEIKHOFF, D., STAURENGHI, G. & WOLF, S. 2005.

- Classification of fundus autofluorescence patterns in early age-related macular disease. *Investigative ophthalmology & visual science*, 46, 3309-14.
- BIRD, A. C. 1992. Bruch's membrane change with age. *The British journal of ophthalmology*, 76, 166-8.
- BIRD, A. C., BRESSLER, N. M., BRESSLER, S. B., CHISHOLM, I. H., COSCAS, G., DAVIS, M. D., DE JONG, P. T., KLAVER, C. C., KLEIN, B. E., KLEIN, R. & ET AL. 1995. An international classification and grading system for age-related maculopathy and age-related macular degeneration. The International ARM Epidemiological Study Group. *Survey of ophthalmology*, 39, 367-74.
- BIRD, A. C. & MARSHALL, J. 1986. Retinal pigment epithelial detachments in the elderly. *Transactions of the ophthalmological societies of the United Kingdom*, 105 (Pt 6), 674-82.
- BIRKEDAL-HANSEN, H., MOORE, W. G., BODDEN, M. K., WINDSOR, L. J., BIRKEDAL-HANSEN, B., DECARLO, A. & ENGLER, J. A. 1993. Matrix metalloproteinases: a review. *Critical reviews in oral biology and medicine : an official publication of the American Association of Oral Biologists*, 4, 197-250.
- BLUMENKRANZ, M. S., RUSSELL, S. R., ROBEY, M. G., KOTT-BLUMENKRANZ, R. & PENNEYS, N. 1986. Risk factors in age-related maculopathy complicated by choroidal neovascularization. *Ophthalmology*, 93, 552-8.
- BOK, D. 1970. The distribution and renewal of RNA in retinal rods. *Investigative ophthalmology*, 9, 516-23.
- BOK, D. 1985. Retinal photoreceptor-pigment epithelium interactions. Friedenwald lecture. *Investigative ophthalmology & visual science*, 26, 1659-94.
- BORLAND, R. G., BRENNAN, D. H., MARSHALL, J. & VIVEASH, J. P. 1978. The role of fluorescein angiography in the detection of laser-induced damage to the retina: a threshold study for Q-switched, neodymium and ruby lasers. *Experimental eye research*, 27, 471-93.
- BOWBYES, J., HAMILTON, A. M., KOHNER, E. M. & MARSHALL, J. 1973. The effect of the argon laser on the retina. *The Journal of physiology*, 231, 70P.
- BOWMAN, K. J. 1980. The relationship between color discrimination and visual acuity in senile macular degeneration. *American journal of optometry and physiological optics*, 57, 145-8.
- BRINKMANN, J. N. R. 2005. Boiling nucleation on melanosomes and microbeads transiently heated by nanosecond and microsecond laser pulses. *J. Biomed. Opt.*, 10.
- BROWN, B. & LOVIE-KITCHIN, J. E. 1989. Temporal summation in age-related maculopathy. *Optometry and vision science : official publication of the American Academy of Optometry*, 66, 426-9.
- BROWN, D. M., KAISER, P. K., MICHELS, M., SOUBRANE, G., HEIER, J. S., KIM, R. Y., SY, J. P. & SCHNEIDER, S. 2006. Ranibizumab versus verteporfin for neovascular age-related macular degeneration. *The New England journal of medicine*, 355, 1432-44.
- BROWN, D. M., MICHELS, M., KAISER, P. K., HEIER, J. S., SY, J. P. & IANCHULEV, T. 2009. Ranibizumab versus verteporfin photodynamic therapy for neovascular age-related macular degeneration: Two-year results of the ANCHOR study. *Ophthalmology*, 116, 57-65 e5.
- BS, W. (ed.) 1983. *The intermediary metabolism of the retina: Biochemical and functional aspects*; American Academy of Ophthalmology.
- BUTLER, G. S., BUTLER, M. J., ATKINSON, S. J., WILL, H., TAMURA, T., SCHADE VAN WESTRUM, S., CRABBE, T., CLEMENTS, J., D'ORTHO, M. P. & MURPHY, G. 1998. The TIMP2 membrane type 1 metalloproteinase "receptor" regulates

- the concentration and efficient activation of progelatinase A. A kinetic study. *The Journal of biological chemistry*, 273, 871-80.
- CALDWELL, R. B., BARTOLI, M., BEHZADIAN, M. A., EL-REMESSY, A. E., AL-SHABRAWAY, M., PLATT, D. H., LIOU, G. I. & CALDWELL, R. W. 2005. Vascular endothelial growth factor and diabetic retinopathy: role of oxidative stress. *Current drug targets*, 6, 511-24.
- CAO, L., WANG, H., WANG, F., XU, D., LIU, F. & LIU, C. 2013. Abeta-induced senescent retinal pigment epithelial cells create a proinflammatory microenvironment in AMD. *Investigative ophthalmology & visual science*, 54, 3738-50.
- CARDINAULT, N., ABALAIN, J. H., SAIRAFI, B., COUDRAY, C., GROLIER, P., RAMBEAU, M., CARRE, J. L., MAZUR, A. & ROCK, E. 2005. Lycopene but not lutein nor zeaxanthin decreases in serum and lipoproteins in age-related macular degeneration patients. *Clinica chimica acta; international journal of clinical chemistry*, 357, 34-42.
- CHARBEL ISSA, P., CHONG, N. V. & SCHOLL, H. P. 2011. The significance of the complement system for the pathogenesis of age-related macular degeneration - current evidence and translation into clinical application. *Graefe's archive for clinical and experimental ophthalmology = Albrecht von Graefes Archiv fur klinische und experimentelle Ophthalmologie*, 249, 163-74.
- CHAU, K. Y., SIVAPRASAD, S., PATEL, N., DONALDSON, T. A., LUTHERT, P. J. & CHONG, N. V. 2007. Plasma levels of matrix metalloproteinase-2 and -9 (MMP-2 and MMP-9) in age-related macular degeneration. *Eye*, 21, 1511-5.
- CHAUHAN, D. S. & MARSHALL, J. 1999. The interpretation of optical coherence tomography images of the retina. *Investigative ophthalmology & visual science*, 40, 2332-42.
- CHEN, J. C., FITZKE, F. W., PAULEIKHOFF, D. & BIRD, A. C. 1992. Functional loss in age-related Bruch's membrane change with choroidal perfusion defect. *Investigative ophthalmology & visual science*, 33, 334-40.
- CHENG, A. S. & VINGRYS, A. J. 1993. Visual losses in early age-related maculopathy. *Optometry and vision science : official publication of the American Academy of Optometry*, 70, 89-96.
- CHIDLOW, G., SHIBEEB, O., PLUNKETT, M., CASSON, R. J. & WOOD, J. P. 2013. Glial cell and inflammatory responses to retinal laser treatment: comparison of a conventional photocoagulator and a novel, 3-nanosecond pulse laser. *Investigative ophthalmology & visual science*, 54, 2319-32.
- CHIHARA, E. & NAO-I, N. 1985. Resorption of subretinal fluid by transepithelial flow of the retinal pigment epithelium. *Graefe's archive for clinical and experimental ophthalmology = Albrecht von Graefes Archiv fur klinische und experimentelle Ophthalmologie*, 223, 202-4.
- CHIU, C. J., HUBBARD, L. D., ARMSTRONG, J., ROGERS, G., JACQUES, P. F., CHYLACK, L. T., JR., HANKINSON, S. E., WILLETT, W. C. & TAYLOR, A. 2006. Dietary glycemic index and carbohydrate in relation to early age-related macular degeneration. *The American journal of clinical nutrition*, 83, 880-6.
- CHIU, C. J., MILTON, R. C., GENSLER, G. & TAYLOR, A. 2007. Association between dietary glycemic index and age-related macular degeneration in nondiabetic participants in the Age-Related Eye Disease Study. *The American journal of clinical nutrition*, 86, 180-8.
- CHIU, C. J., MILTON, R. C., KLEIN, R., GENSLER, G. & TAYLOR, A. 2009. Dietary compound score and risk of age-related macular degeneration in the age-related eye disease study. *Ophthalmology*, 116, 939-46.

- CHIU, C. J. & TAYLOR, A. 2011. Dietary hyperglycemia, glycemic index and metabolic retinal diseases. *Progress in retinal and eye research*, 30, 18-53.
- CHO, E., HANKINSON, S. E., ROSNER, B., WILLETT, W. C. & COLDITZ, G. A. 2008. Prospective study of lutein/zeaxanthin intake and risk of age-related macular degeneration. *The American journal of clinical nutrition*, 87, 1837-43.
- CHO, E., HUNG, S., WILLETT, W. C., SPIEGELMAN, D., RIMM, E. B., SEDDON, J. M., COLDITZ, G. A. & HANKINSON, S. E. 2001. Prospective study of dietary fat and the risk of age-related macular degeneration. *The American journal of clinical nutrition*, 73, 209-18.
- CHO, E., SEDDON, J. M., ROSNER, B., WILLETT, W. C. & HANKINSON, S. E. 2004. Prospective study of intake of fruits, vegetables, vitamins, and carotenoids and risk of age-related maculopathy. *Archives of ophthalmology*, 122, 883-92.
- CHONG, E. W., ROBMAN, L. D., SIMPSON, J. A., HODGE, A. M., AUNG, K. Z., DOLPHIN, T. K., ENGLISH, D. R., GILES, G. G. & GUYMER, R. H. 2009. Fat consumption and its association with age-related macular degeneration. *Archives of ophthalmology*, 127, 674-80.
- CHONG, N. H., KEONIN, J., LUTHER, P. J., FRENNESSON, C. I., WEINGEIST, D. M., WOLF, R. L., MULLINS, R. F. & HAGEMAN, G. S. 2005. Decreased thickness and integrity of the macular elastic layer of Bruch's membrane correspond to the distribution of lesions associated with age-related macular degeneration. *Am J Pathol*, 166, 241-51.
- CHRISTEN, W. G., GLYNN, R. J., CHEW, E. Y. & BURING, J. E. 2010. Vitamin E and age-related macular degeneration in a randomized trial of women. *Ophthalmology*, 117, 1163-8.
- CIDECIYAN, A. V., SWIDER, M., ALEMAN, T. S., FEUER, W. J., SCHWARTZ, S. B., RUSSELL, R. C., STEINBERG, J. D., STONE, E. M. & JACOBSON, S. G. 2012. Macular function in macular degenerations: repeatability of microperimetry as a potential outcome measure for ABCA4-associated retinopathy trials. *Investigative ophthalmology & visual science*, 53, 841-52.
- COHEN, L. H. & NOELL, W. K. 1960. Glucose catabolism of rabbit retina before and after development of visual function. *Journal of neurochemistry*, 5, 253-76.
- COILE, D. C. & BAKER, H. D. 1992. Foveal dark adaptation, photopigment regeneration, and aging. *Visual neuroscience*, 8, 27-39.
- COSCAS, F., COSCAS, G., QUERQUES, G., MASSAMBA, N., QUERQUES, L., BANDELLO, F. & SOUIED, E. H. 2012. En face enhanced depth imaging optical coherence tomography of fibrovascular pigment epithelium detachment. *Investigative ophthalmology & visual science*, 53, 4147-51.
- COSCAS, G. 2009. *Optical Coherence Tomography in Age-Related Macular Degeneration*.
- COSCAS, G., COSCAS, F., ZOURDANI, A. & SOUBRANE, G. 2004. [Optical coherence tomography and ARMD]. *Journal francais d'ophtalmologie*, 27, 3S7-30.
- CUNHA-VAZ, J. G., SHAKIB, M. & ASHTON, N. 1966. Studies on the permeability of the blood-retinal barrier. I. On the existence, development, and site of a blood-retinal barrier. *The British journal of ophthalmology*, 50, 441-53.
- CURCIO, C. A., MEDEIROS, N. E. & MILLICAN, C. L. 1996. Photoreceptor loss in age-related macular degeneration. *Investigative ophthalmology & visual science*, 37, 1236-49.

- CURCIO, C. A., MILLICAN, C. L., ALLEN, K. A. & KALINA, R. E. 1993. Aging of the human photoreceptor mosaic: evidence for selective vulnerability of rods in central retina. *Investigative ophthalmology & visual science*, 34, 3278-96.
- D, B. 1994. Retinal photoceptor disc shedding and pigment epithelial phagocytosis. In: Retina. In: S, R. (ed.). St Louis, USA: Mosby.
- DAVIS, M. D., GANGNON, R. E., LEE, L. Y., HUBBARD, L. D., KLEIN, B. E., KLEIN, R., FERRIS, F. L., BRESSLER, S. B. & MILTON, R. C. 2005. The Age-Related Eye Disease Study severity scale for age-related macular degeneration: AREDS Report No. 17. *Archives of ophthalmology*, 123, 1484-98.
- DELCOURT, C., CARRIERE, I., CRISTOL, J. P., LACROUX, A. & GERBER, M. 2007. Dietary fat and the risk of age-related maculopathy: the POLANUT study. *European journal of clinical nutrition*, 61, 1341-4.
- DELCOURT, C., CRISTOL, J. P., TESSIER, F., LEGER, C. L., DESCOMPS, B. & PAPOZ, L. 1999. Age-related macular degeneration and antioxidant status in the POLA study. POLA Study Group. Pathologies Oculaires Liees a l'Age. *Archives of ophthalmology*, 117, 1384-90.
- DELLA, N. G., CAMPOCHIARO, P. A. & ZACK, D. J. 1996. Localization of TIMP-3 mRNA expression to the retinal pigment epithelium. *Investigative ophthalmology & visual science*, 37, 1921-4.
- DH., S. 1988. Interaction mechanisms of laser radiation with ocular tissues. In: *First International Symposium on Laser Biological Effects and Exposure Limits: Lasers et Normes de Protection*. Paris: Commissariat a l'Energie Atomique De'partement de Protection Sanitaire, Service de Documentation, 64-83.
- DICHTL, W., DULAK, J., FRICK, M., ALBER, H. F., SCHWARZACHER, S. P., ARES, M. P., NILSSON, J., PACHINGER, O. & WEIDINGER, F. 2003. HMG-CoA reductase inhibitors regulate inflammatory transcription factors in human endothelial and vascular smooth muscle cells. *Arteriosclerosis, thrombosis, and vascular biology*, 23, 58-63.
- DIMITROV, P. N., ROBMAN, L. D., VARSAMIDIS, M., AUNG, K. Z., MAKEYEVA, G. A., GUYMER, R. H. & VINGRYS, A. J. 2011. Visual function tests as potential biomarkers in age-related macular degeneration. *Investigative ophthalmology & visual science*, 52, 9457-69.
- DOREY, C. K., WU, G., EBENSTEIN, D., GARSD, A. & WEITER, J. J. 1989. Cell loss in the aging retina. Relationship to lipofuscin accumulation and macular degeneration. *Investigative ophthalmology & visual science*, 30, 1691-9.
- EDSALL, D. J. L. D. R. F. S. W. H. P. R. 1997. Variation of retinal ED50 with exposure duration for near-IR sources. *Proc. SPIE*, 2974.
- EISNER, A., FLEMING, S. A., KLEIN, M. L. & MAULDIN, W. M. 1987. Sensitivities in older eyes with good acuity: eyes whose fellow eye has exudative AMD. *Investigative ophthalmology & visual science*, 28, 1832-7.
- ELLIOTT, D. B., SANDERSON, K. & CONKEY, A. 1990. The reliability of the Pelli-Robson contrast sensitivity chart. *Ophthalmic & physiological optics : the journal of the British College of Ophthalmic Opticians*, 10, 21-4.
- EMI, K., PEDERSON, J. E. & TORIS, C. B. 1989. Hydrostatic pressure of the suprachoroidal space. *Investigative ophthalmology & visual science*, 30, 233-8.
- FARISS, R. N., APTE, S. S., OLSEN, B. R., IWATA, K. & MILAM, A. H. 1997a. Tissue inhibitor of metalloproteinases-3 is a component of Bruch's membrane of the eye. *The American journal of pathology*, 150, 323-8.

- FARISS, R. N., APTE, S. S., OLSEN, B. R., IWATA, K. & MILAM, A. H. 1997b. Tissue inhibitor of metalloproteinases-3 is a component of Bruch's membrane of the eye. *Am J Pathol*, 150, 323-8.
- FEENEY-BURNS, L., BERMAN, E. R. & ROTHMAN, H. 1980. Lipofuscin of human retinal pigment epithelium. *American journal of ophthalmology*, 90, 783-91.
- FEENEY-BURNS, L. & ELLERSIECK, M. R. 1985. Age-related changes in the ultrastructure of Bruch's membrane. *American journal of ophthalmology*, 100, 686-97.
- FEENEY-BURNS, L., HILDERBRAND, E. S. & ELDRIDGE, S. 1984. Aging human RPE: morphometric analysis of macular, equatorial, and peripheral cells. *Investigative ophthalmology & visual science*, 25, 195-200.
- FEIGL, B., BROWN, B., LOVIE-KITCHIN, J. & SWANN, P. 2007. Functional loss in early age-related maculopathy: the ischaemia postreceptor hypothesis. *Eye*, 21, 689-96.
- FERRIS, F. L., 3RD, WILKINSON, C. P., BIRD, A., CHAKRAVARTHY, U., CHEW, E., CSAKY, K. & SADDA, S. R. 2013. Clinical classification of age-related macular degeneration. *Ophthalmology*, 120, 844-51.
- FIGUEIRA, J., KHAN, J., NUNES, S., SIVAPRASAD, S., ROSA, A., DE ABREU, J. F., CUNHA-VAZ, J. G. & CHONG, N. V. 2009. Prospective randomised controlled trial comparing sub-threshold micropulse diode laser photocoagulation and conventional green laser for clinically significant diabetic macular oedema. *The British journal of ophthalmology*, 93, 1341-4.
- FINNEY, D. J., ED. 1952. Probit Analysis. *Cambridge, England, Cambridge University Press*.
- FIOTTI, N., PEDIO, M., BATTAGLIA PARODI, M., ALTAMURA, N., UXA, L., GUARNIERI, G., GIANANTE, C. & RAVALICO, G. 2005. MMP-9 microsatellite polymorphism and susceptibility to exudative form of age-related macular degeneration. *Genetics in medicine : official journal of the American College of Medical Genetics*, 7, 272-7.
- FISHER, R. F. 1982. The water permeability of basement membrane under increasing pressure: evidence for a new theory of permeability. *Proceedings of the Royal Society of London. Series B, Containing papers of a Biological character. Royal Society*, 216, 475-96.
- FISHER, R. F. 1987a. The influence of age on some ocular basement membranes. *Eye (Lond)*, 1 (Pt 2), 184-9.
- FISHER, R. F. 1987b. The influence of age on some ocular basement membranes. *Eye*, 1 (Pt 2), 184-9.
- FORMAZ, F., RIVA, C. E. & GEISER, M. 1997. Diffuse luminance flicker increases retinal vessel diameter in humans. *Current eye research*, 16, 1252-7.
- FOULDS, W. S. 1990. The choroidal circulation and retinal metabolism--an overview. *Eye*, 4 (Pt 2), 243-8.
- FRAMME, C., SCHUELE, G., KOBUCH, K., FLUCKE, B., BIRNGRUBER, R. & BRINKMANN, R. 2008. Investigation of selective retina treatment (SRT) by means of 8 ns laser pulses in a rabbit model. *Lasers in surgery and medicine*, 40, 20-7.
- FRAMME, C., SCHUELE, G., ROIDER, J., BIRNGRUBER, R. & BRINKMANN, R. 2004. Influence of pulse duration and pulse number in selective RPE laser treatment. *Lasers in surgery and medicine*, 34, 206-15.
- FRAMME, C., SCHUELE, G., ROIDER, J., KRACHT, D., BIRNGRUBER, R. & BRINKMANN, R. 2002. Threshold determinations for selective retinal

- pigment epithelium damage with repetitive pulsed microsecond laser systems in rabbits. *Ophthalmic surgery and lasers*, 33, 400-9.
- FRAMME, C., WALTER, A., PRAHS, P., REGLER, R., THEISEN-KUNDE, D., ALT, C. & BRINKMANN, R. 2009. Structural changes of the retina after conventional laser photocoagulation and selective retina treatment (SRT) in spectral domain OCT. *Current eye research*, 34, 568-79.
- FREEMAN, S. R., KOZAK, I., CHENG, L., BARTSCH, D. U., MOJANA, F., NIGAM, N., BRAR, M., YUSON, R. & FREEMAN, W. R. 2010. Optical coherence tomography-raster scanning and manual segmentation in determining drusen volume in age-related macular degeneration. *Retina*, 30, 431-5.
- FRENNESSON, C., NILSSON, U. L. & NILSSON, S. E. 1995. Colour contrast sensitivity in patients with soft drusen, an early stage of ARM. *Documenta ophthalmologica. Advances in ophthalmology*, 90, 377-86.
- FRENNESSON, C. I., BEK, T., JAAKKOLA, A. & NILSSON, S. E. 2009. Prophylactic laser treatment of soft drusen maculopathy: a prospective, randomized Nordic study. *Acta ophthalmologica*, 87, 720-4.
- FRIBERG, T. R., MUSCH, D. C., LIM, J. I., MORSE, L., FREEMAN, W. & SINCLAIR, S. 2006. Prophylactic treatment of age-related macular degeneration report number 1: 810-nanometer laser to eyes with drusen. Unilaterally eligible patients. *Ophthalmology*, 113, 622 e1.
- FRIEDMAN, E. 2004. Update of the vascular model of AMD. *The British journal of ophthalmology*, 88, 161-3.
- G., M.-S. 1960. *Light coagulation*, St Louis, CV Mosby Company.
- GLENN, J. V., MAHAFFY, H., WU, K., SMITH, G., NAGAI, R., SIMPSON, D. A., BOULTON, M. E. & STITT, A. W. 2009. Advanced glycation end product (AGE) accumulation on Bruch's membrane: links to age-related RPE dysfunction. *Investigative ophthalmology & visual science*, 50, 441-51.
- GOLDBERG, J., FLOWERDEW, G., SMITH, E., BRODY, J. A. & TSO, M. O. 1988. Factors associated with age-related macular degeneration. An analysis of data from the first National Health and Nutrition Examination Survey. *American journal of epidemiology*, 128, 700-10.
- GORDON JP, Z. H., TOWNES CH 1954. Molecular microwave oscillator and new hyperfine structure in the microwave spectrum of Nh3. . *Phys Rev*, 95, 282-284.
- GRANADO, F., OLMEDILLA, B. & BLANCO, I. 2003. Nutritional and clinical relevance of lutein in human health. *The British journal of nutrition*, 90, 487-502.
- GREEN, W. R. 1999a. Histopathology of age-related macular degeneration. *Molecular vision*, 5, 27.
- GREEN, W. R. 1999b. Histopathology of age-related macular degeneration. *Mol Vis*, 5, 27.
- GREEN, W. R. & ENGER, C. 1993. Age-related macular degeneration histopathologic studies. The 1992 Lorenz E. Zimmerman Lecture. *Ophthalmology*, 100, 1519-35.
- GREEN, W. R. & KEY, S. N., 3RD 1977. Senile macular degeneration: a histopathologic study. *Transactions of the American Ophthalmological Society*, 75, 180-254.
- GRINDLE, C. F. & MARSHALL, J. 1978. Ageing changes in Bruch's membrane and their functional implications. *Transactions of the ophthalmological societies of the United Kingdom*, 98, 172-5.

- GROSS, J. & LAPIERE, C. M. 1962. Collagenolytic activity in amphibian tissues: a tissue culture assay. *Proceedings of the National Academy of Sciences of the United States of America*, 48, 1014-22.
- GUO, L., HUSSAIN, A. A., LIMB, G. A. & MARSHALL, J. 1999a. Age-dependent variation in metalloproteinase activity of isolated human Bruch's membrane and choroid. *Invest Ophthalmol Vis Sci*, 40, 2676-82.
- GUO, L., HUSSAIN, A. A., LIMB, G. A. & MARSHALL, J. 1999b. Age-dependent variation in metalloproteinase activity of isolated human Bruch's membrane and choroid. *Investigative ophthalmology & visual science*, 40, 2676-82.
- GUYMER, R. H., BRASSINGTON, K. H., DIMITROV, P., MAKEYEVA, G., PLUNKETT, M., XIA, W., CHAUHAN, D., VINGRYS, A. & LUU, C. D. 2013. Nanosecond-laser application in intermediate AMD: 12-month results of fundus appearance and macular function. *Clinical & experimental ophthalmology*.
- GUYMER, R. H., BRASSINGTON, K. H., DIMITROV, P., MAKEYEVA, G., PLUNKETT, M., XIA, W., CHAUHAN, D., VINGRYS, A. & LUU, C. D. 2014. Nanosecond-laser application in intermediate AMD: 12-month results of fundus appearance and macular function. *Clinical & experimental ophthalmology*, 42, 466-79.
- GUYMER, R. H., CHIU, A. W., LIM, L. & BAIRD, P. N. 2005. HMG CoA reductase inhibitors (statins): do they have a role in age-related macular degeneration? *Survey of ophthalmology*, 50, 194-206.
- HAGEMAN, G. S., LUTHER, P. J., VICTOR CHONG, N. H., JOHNSON, L. V., ANDERSON, D. H. & MULLINS, R. F. 2001. An integrated hypothesis that considers drusen as biomarkers of immune-mediated processes at the RPE-Bruch's membrane interface in aging and age-related macular degeneration. *Progress in retinal and eye research*, 20, 705-32.
- HAIMOVICI, R., OWENS, S. L., FITZKE, F. W. & BIRD, A. C. 2002. Dark adaptation in age-related macular degeneration: relationship to the fellow eye. *Graefe's archive for clinical and experimental ophthalmology = Albrecht von Graefes Archiv fur klinische und experimentelle Ophthalmologie*, 240, 90-5.
- HALE, I. L., FISHER, S. K. & MATSUMOTO, B. 1991. Effects of retinal detachment on rod disc membrane assembly in cultured frog retinas. *Investigative ophthalmology & visual science*, 32, 2873-81.
- HANDA, J. T., VERZIJL, N., MATSUNAGA, H., AOTAKI-KEEN, A., LUTTY, G. A., TE KOPPELE, J. M., MIYATA, T. & HJELMELAND, L. M. 1999. Increase in the advanced glycation end product pentosidine in Bruch's membrane with age. *Investigative ophthalmology & visual science*, 40, 775-9.
- HART, W. M., JR. 1987. Acquired dyschromatopsias. *Survey of ophthalmology*, 32, 10-31.
- HELLER, J. & BOK, D. 1976. Transport of retinol from the blood to the retina: involvement of high molecular weight lipoproteins as intracellular carriers. *Experimental eye research*, 22, 403-10.
- HERRON, W. L., RIEGEL, B. W., MYERS, O. E. & RUBIN, M. L. 1969. Retinal dystrophy in the rat--a pigment epithelial disease. *Investigative ophthalmology*, 8, 595-604.
- HILLENKAMP, J., HUSSAIN, A. A., JACKSON, T. L., CUNNINGHAM, J. R. & MARSHALL, J. 2004. The influence of path length and matrix components on ageing characteristics of transport between the choroid and the outer retina. *Investigative ophthalmology & visual science*, 45, 1493-8.
- HILLENKAMP, J., HUSSAIN, A. A., JACKSON, T. L., CUNNINGHAM, J. R. & MARSHALL, J. 2006. Effect of taurine and apical potassium concentration on

- electrophysiologic parameters of bovine retinal pigment epithelium. *Experimental eye research*, 82, 258-64.
- HJELMELAND, L. M., CRISTOFOLLO, V. J., FUNK, W., RAKOCZY, E. & KATZ, M. L. 1999. Senescence of the retinal pigment epithelium. *Molecular vision*, 5, 33.
- HOGAN, M. J. & ALVARADO, J. 1967a. Studies on the human macula. IV. Aging changes in Bruch's membrane. *Archives of ophthalmology*, 77, 410-20.
- HOGAN, M. J. & ALVARADO, J. 1967b. Studies on the human macula. IV. Aging changes in Bruch's membrane. *Arch Ophthalmol*, 77, 410-20.
- HOGG, R. E. & CHAKRAVARTHY, U. 2006. Visual function and dysfunction in early and late age-related maculopathy. *Progress in retinal and eye research*, 25, 249-76.
- HOLZ, F. G., GROSS-JENDROSKA, M., ECKSTEIN, A., HOGG, C. R., ARDEN, G. B. & BIRD, A. C. 1995. Colour contrast sensitivity in patients with age-related Bruch's membrane changes. *German journal of ophthalmology*, 4, 336-41.
- HOLZ, F. G., PAULEIKHOFF, D., KLEIN, R. & BIRD, A. C. 2004. Pathogenesis of lesions in late age-related macular disease. *Am J Ophthalmol*, 137, 504-10.
- HOLZ, F. G., SHERAIDAH, G., PAULEIKHOFF, D. & BIRD, A. C. 1994. Analysis of lipid deposits extracted from human macular and peripheral Bruch's membrane. *Archives of ophthalmology*, 112, 402-6.
- HUANG, D., SWANSON, E. A., LIN, C. P., SCHUMAN, J. S., STINSON, W. G., CHANG, W., HEE, M. R., FLOTTE, T., GREGORY, K., PULIAFITO, C. A. & ET AL. 1991. Optical coherence tomography. *Science*, 254, 1178-81.
- HUNT, R. C., FOX, A., AL PAKALNIS, V., SIGEL, M. M., KOSNOSKY, W., CHOUDHURY, P. & BLACK, E. P. 1993. Cytokines cause cultured retinal pigment epithelial cells to secrete metalloproteinases and to contract collagen gels. *Investigative ophthalmology & visual science*, 34, 3179-86.
- HUSSAIN, A. A., LEE, Y. & MARSHALL, J. 2010a. High molecular-weight gelatinase species of human Bruch's membrane: compositional analyses and age-related changes. *Invest Ophthalmol Vis Sci*, 51, 2363-71.
- HUSSAIN, A. A., LEE, Y., ZHANG, J. J. & MARSHALL, J. 2011. Disturbed matrix metalloproteinase activity of Bruch's membrane in age-related macular degeneration. *Investigative ophthalmology & visual science*, 52, 4459-66.
- HUSSAIN, A. A., ROWE, L. & MARSHALL, J. 2002. Age-related alterations in the diffusional transport of amino acids across the human Bruch's-choroid complex. *Journal of the Optical Society of America. A, Optics, image science, and vision*, 19, 166-72.
- HUSSAIN, A. A., STARITA, C., HODGETTS, A. & MARSHALL, J. 2010b. Macromolecular diffusion characteristics of ageing human Bruch's membrane: implications for age-related macular degeneration (AMD). *Exp Eye Res*, 90, 703-10.
- HUSSAIN, A. A., STARITA, C., HODGETTS, A. & MARSHALL, J. 2010c. Macromolecular diffusion characteristics of ageing human Bruch's membrane: implications for age-related macular degeneration (AMD). *Experimental eye research*, 90, 703-10.
- HUSSAIN, A. A., STARITA, C., MARSHALL, J. 1999. Molecular Weight size exclusion limit and diffusional status of ageing human Bruch's membrane. *ARVO Abstract. Invest Ophthalmol. Vis. Sci.*
- HYVARINEN, L. & FLOWER, R. W. 1980. Indocyanine green fluorescence angiography. *Acta ophthalmologica*, 58, 528-38.
- JACKSON, G. R. & OWSLEY, C. 2000. Scotopic sensitivity during adulthood. *Vision research*, 40, 2467-73.

- JENNINGS, P. E., MACEWEN, C. J., FALLON, T. J., SCOTT, N., HAINING, W. M. & BELCH, J. J. 1991. Oxidative effects of laser photocoagulation. *Free radical biology & medicine*, 11, 327-30.
- JOHNSON, P. T., BROWN, M. N., PULLIAM, B. C., ANDERSON, D. H. & JOHNSON, L. V. 2005. Synaptic pathology, altered gene expression, and degeneration in photoreceptors impacted by drusen. *Investigative ophthalmology & visual science*, 46, 4788-95.
- JOHNSON, P. T., LEWIS, G. P., TALAGA, K. C., BROWN, M. N., KAPPEL, P. J., FISHER, S. K., ANDERSON, D. H. & JOHNSON, L. V. 2003. Drusen-associated degeneration in the retina. *Investigative ophthalmology & visual science*, 44, 4481-8.
- KAISER, R. S., BERGER, J. W., MAGUIRE, M. G., HO, A. C. & JAVORNIK, N. B. 2001. Laser burn intensity and the risk for choroidal neovascularization in the CNVPT Fellow Eye Study. *Archives of ophthalmology*, 119, 826-32.
- KAMEI, M. & HOLLYFIELD, J. G. 1999a. TIMP-3 in Bruch's membrane: changes during aging and in age-related macular degeneration. *Invest Ophthalmol Vis Sci*, 40, 2367-75.
- KAMEI, M. & HOLLYFIELD, J. G. 1999b. TIMP-3 in Bruch's membrane: changes during aging and in age-related macular degeneration. *Investigative ophthalmology & visual science*, 40, 2367-75.
- KARWATOWSKI, W. S., JEFFRIES, T. E., DUANCE, V. C., ALBON, J., BAILEY, A. J. & EASTY, D. L. 1995a. Preparation of Bruch's membrane and analysis of the age-related changes in the structural collagens. *Br J Ophthalmol*, 79, 944-52.
- KARWATOWSKI, W. S., JEFFRIES, T. E., DUANCE, V. C., ALBON, J., BAILEY, A. J. & EASTY, D. L. 1995b. Preparation of Bruch's membrane and analysis of the age-related changes in the structural collagens. *The British journal of ophthalmology*, 79, 944-52.
- KAUSHIK, S., WANG, J. J., FLOOD, V., TAN, J. S., BARCLAY, A. W., WONG, T. Y., BRAND-MILLER, J. & MITCHELL, P. 2008. Dietary glycemic index and the risk of age-related macular degeneration. *The American journal of clinical nutrition*, 88, 1104-10.
- KHANIFAR, A. A., KOREISHI, A. F., IZATT, J. A. & TOTH, C. A. 2008. Drusen ultrastructure imaging with spectral domain optical coherence tomography in age-related macular degeneration. *Ophthalmology*, 115, 1883-90.
- KILLINGSWORTH, M. C. 1987. Age-related components of Bruch's membrane in the human eye. *Graefes Arch Clin Exp Ophthalmol*, 225, 406-12.
- KINNUNEN, K., PETROVSKI, G., MOE, M. C., BERTA, A. & KAARNIRANTA, K. 2012. Molecular mechanisms of retinal pigment epithelium damage and development of age-related macular degeneration. *Acta ophthalmologica*, 90, 299-309.
- KLEIN, R., KLEIN, B. E. & LINTON, K. L. 1992. Prevalence of age-related maculopathy. The Beaver Dam Eye Study. *Ophthalmology*, 99, 933-43.
- KLEIN, R., WANG, Q., KLEIN, B. E., MOSS, S. E. & MEUER, S. M. 1995. The relationship of age-related maculopathy, cataract, and glaucoma to visual acuity. *Investigative ophthalmology & visual science*, 36, 182-91.
- KLIFFEN, M., MOOY, C. M., LUIDER, T. M., HUIJMANS, J. G., KERKVLIELT, S. & DE JONG, P. T. 1996a. Identification of glycosaminoglycans in age-related macular deposits. *Archives of ophthalmology*, 114, 1009-14.
- KLIFFEN, M., MOOY, C. M., LUIDER, T. M., HUIJMANS, J. G., KERKVLIELT, S. & DE JONG, P. T. 1996b. Identification of glycosaminoglycans in age-related macular deposits. *Arch Ophthalmol*, 114, 1009-14.

- KORSHUNOV, S. S., SKULACHEV, V. P. & STARKOV, A. A. 1997. High protonic potential actuates a mechanism of production of reactive oxygen species in mitochondria. *FEBS letters*, 416, 15-8.
- KROLL, A. J. & MACHEMER, R. 1969. Experimental retinal detachment and reattachment in the rhesus monkey. Electron microscopic comparison of rods and cones. *American journal of ophthalmology*, 68, 58-77.
- KUMAR, A., EL-OSTA, A., HUSSAIN, A. A. & MARSHALL, J. 2010. Increased sequestration of matrix metalloproteinases in ageing human Bruch's membrane: implications for ECM turnover. *Investigative ophthalmology & visual science*, 51, 2664-70.
- KUNDAIKER, S., HUSSAIN, A. A. & MARSHALL, J. 1996. Component characteristics of the vectorial transport system for taurine in isolated bovine retinal pigment epithelium. *The Journal of physiology*, 492 (Pt 2), 505-16.
- L'ESPERANCE, F. A., JR. 1966a. Clinical comparison of xenon-arc and laser photocoagulation of retinal lesions. *Archives of ophthalmology*, 75, 61-7.
- L'ESPERANCE, F. A., JR. 1966b. Xenon arc versus laser photocoagulation. *International ophthalmology clinics*, 6, 335-50.
- L'ESPERANCE, F. A., JR. 1969. The treatment of ophthalmic vascular disease by argon laser photocoagulation. *Transactions - American Academy of Ophthalmology and Otolaryngology. American Academy of Ophthalmology and Otolaryngology*, 73, 1077-96.
- LEBRUN, L. & JUNTER, G. A. 1993. Diffusion of sucrose and dextran through agar gel membranes. *Enzyme and microbial technology*, 15, 1057-62.
- LEIBOWITZ, H. M., KRUEGER, D. E., MAUNDER, L. R., MILTON, R. C., KINI, M. M., KAHN, H. A., NICKERSON, R. J., POOL, J., COLTON, T. L., GANLEY, J. P., LOEWENSTEIN, J. I. & DAWBER, T. R. 1980. The Framingham Eye Study monograph: An ophthalmological and epidemiological study of cataract, glaucoma, diabetic retinopathy, macular degeneration, and visual acuity in a general population of 2631 adults, 1973-1975. *Surv Ophthalmol*, 24, 335-610.
- LEUSCHEN, J. N., SCHUMAN, S. G., WINTER, K. P., MCCALL, M. N., WONG, W. T., CHEW, E. Y., HWANG, T., SRIVASTAVA, S., SARIN, N., CLEMONS, T., HARRINGTON, M. & TOTH, C. A. 2013. Spectral-domain optical coherence tomography characteristics of intermediate age-related macular degeneration. *Ophthalmology*, 120, 140-50.
- LI, J., LIU, Y., WEI, J. Q., WANG, K., CHEN, L. X., YAO, X. S. & QIU, F. 2012. Isolation and identification of phase 1 metabolites of curcuminoids in rats. *Planta medica*, 78, 1351-6.
- LIANG, J., WILLIAMS, D. R. & MILLER, D. T. 1997. Supernormal vision and high-resolution retinal imaging through adaptive optics. *Journal of the Optical Society of America. A, Optics, image science, and vision*, 14, 2884-92.
- LOMBARDO, M., LOMBARDO, G., SCHIANO LOMORIELLO, D., DUCOLI, P., STIRPE, M. & SERRAO, S. 2013. Interocular symmetry of parafoveal photoreceptor cone density distribution. *Retina*, 33, 1640-9.
- LONGO, G. M., XIONG, W., GREINER, T. C., ZHAO, Y., FIOTTI, N. & BAXTER, B. T. 2002. Matrix metalloproteinases 2 and 9 work in concert to produce aortic aneurysms. *The Journal of clinical investigation*, 110, 625-32.
- LOSHIN, D. S. & WHITE, J. 1984. Contrast sensitivity. The visual rehabilitation of the patient with macular degeneration. *Archives of ophthalmology*, 102, 1303-6.
- MAINSTER, M. A. 1986. Wavelength selection in macular photocoagulation. Tissue optics, thermal effects, and laser systems. *Ophthalmology*, 93, 952-8.

- MARES-PERLMAN, J. A., FISHER, A. I., KLEIN, R., PALTA, M., BLOCK, G., MILLEN, A. E. & WRIGHT, J. D. 2001. Lutein and zeaxanthin in the diet and serum and their relation to age-related maculopathy in the third national health and nutrition examination survey. *American journal of epidemiology*, 153, 424-32.
- MARSHALL, G. E., KONSTAS, A. G., REID, G. G., EDWARDS, J. G. & LEE, W. R. 1992. Type IV collagen and laminin in Bruch's membrane and basal linear deposit in the human macula. *The British journal of ophthalmology*, 76, 607-14.
- MARSHALL, G. E., KONSTAS, A. G., REID, G. G., EDWARDS, J. G. & LEE, W. R. 1994. Collagens in the aged human macula. *Graefe's archive for clinical and experimental ophthalmology = Albrecht von Graefes Archiv fur klinische und experimentelle Ophthalmologie*, 232, 133-40.
- MARSHALL, J. 1970. Thermal and mechanical mechanisms in laser damage to the retina. *Investigative ophthalmology*, 9, 97-115.
- MARSHALL J, H. A., STARITA C, MOORE DJ AND PATMORE A. (ed.) 1988. *Ageing and Bruch's membrane*. In *Retinal Pigment Epithelium: Function and Disease*, New York: Oxford University Press.
- MARSHALL, J., HAMILTON, A. M. & BIRD, A. C. 1975. Histopathology of ruby and argon laser lesions in monkey and human retina. A comparative study. *The British journal of ophthalmology*, 59, 610-30.
- MARSHALL, J. & MELLERIO, H. J. 1968. Histology of retinal lesions produced with Q-switched lasers. *Experimental eye research*, 7, 225-30.
- MARSHALL, J. & MELLERIO, J. 1967. Histology of the formation of retinal laser lesions. *Experimental eye research*, 6, 4-9.
- MATHEW, R., PEFKIANAKI, M., KOPSACHILIS, N., BRAR, M., RICHARDSON, M. & SIVAPRASAD, S. 2014. Correlation of fundus fluorescein angiography and spectral-domain optical coherence tomography in identification of membrane subtypes in neovascular age-related macular degeneration. *Ophthalmologica. Journal internationale d'ophtalmologie. International journal of ophthalmology. Zeitschrift fur Augenheilkunde*, 231, 153-9.
- MATSUMOTO, M., YOSHIMURA, N. & HONDA, Y. 1994. Increased production of transforming growth factor-beta 2 from cultured human retinal pigment epithelial cells by photocoagulation. *Investigative ophthalmology & visual science*, 35, 4245-52.
- MAURICE, D. M., SALMON, J. & ZAUBERMAN, H. 1971. Subretinal pressure and retinal adhesion. *Experimental eye research*, 12, 212-7.
- MCCLUNG, F. J. A. H., R.W 1962. Giant optical pulsations from ruby. *Journal of Applied Physics*, 33, 828-829.
- MENKE, M. N., SATO, E., VAN DE VELDE, F. J. & FEKE, G. T. 2006. Combined use of SLO microperimetry and OCT for retinal functional and structural testing. *Graefe's archive for clinical and experimental ophthalmology = Albrecht von Graefes Archiv fur klinische und experimentelle Ophthalmologie*, 244, 634-8.
- MERI, S. & PANGBURN, M. K. 1994. Regulation of alternative pathway complement activation by glycosaminoglycans: specificity of the polyanion binding site on factor H. *Biochemical and biophysical research communications*, 198, 52-9.
- MEYER-SCHWICKERATH, G. 1954. Lichtkoagulation. Eine methode zur Behandlung und Verhütung der Netzhaut- ablosung. . *Graefes ArchivfurOphthalmologie*, 156, 2-34.
- MICHIKAWA, T., ISHIDA, S., NISHIWAKI, Y., KIKUCHI, Y., TSUBOI, T., HOSODA, K., ISHIGAMI, A., IWASAWA, S., NAKANO, M. & TAKEBAYASHI, T. 2009. Serum

- antioxidants and age-related macular degeneration among older Japanese. *Asia Pacific journal of clinical nutrition*, 18, 1-7.
- MIDENA, E., RADIN, P. P., PILOTTO, E., GHIRLANDO, A., CONVENTO, E. & VARANO, M. 2004. Fixation pattern and macular sensitivity in eyes with subfoveal choroidal neovascularization secondary to age-related macular degeneration. A microperimetry study. *Seminars in ophthalmology*, 19, 55-61.
- MIDENA, E., VUJOSEVIC, S. & CAVARZERAN, F. 2010. Normal values for fundus perimetry with the microperimeter MP1. *Ophthalmology*, 117, 1571-6, 1576 e1.
- MIDENA, E., VUJOSEVIC, S., CONVENTO, E., MANFRE, A., CAVARZERAN, F. & PILOTTO, E. 2007. Microperimetry and fundus autofluorescence in patients with early age-related macular degeneration. *The British journal of ophthalmology*, 91, 1499-503.
- MILLER, H., MILLER, B., ISHIBASHI, T. & RYAN, S. J. 1990. Pathogenesis of laser-induced choroidal subretinal neovascularization. *Investigative ophthalmology & visual science*, 31, 899-908.
- MINASSIAN, D. C., REIDY, A., LIGHTSTONE, A. & DESAI, P. 2011. Modelling the prevalence of age-related macular degeneration (2010-2020) in the UK: expected impact of anti-vascular endothelial growth factor (VEGF) therapy. *The British journal of ophthalmology*, 95, 1433-6.
- MISHIMA, K., HANDA, J. T., AOTAKI-KEEN, A., LUTTY, G. A., MORSE, L. S. & HJELMELAND, L. M. 1999. Senescence-associated beta-galactosidase histochemistry for the primate eye. *Investigative ophthalmology & visual science*, 40, 1590-3.
- MIYAMOTO, Y. & DEL MONTE, M. A. 1994. Na(+)-dependent glutamate transporter in human retinal pigment epithelial cells. *Investigative ophthalmology & visual science*, 35, 3589-98.
- MJ, H. 1971. *Histology of the human retina. An Atlas and textbook*, Philadelphia, WB Saunders Co.
- MOJANA, F., BRAR, M., CHENG, L., BARTSCH, D. U. & FREEMAN, W. R. 2011. Long-term SD-OCT/SLO imaging of neuroretina and retinal pigment epithelium after subthreshold infrared laser treatment of drusen. *Retina*, 31, 235-42.
- MOORE, D. J. & CLOVER, G. M. 2001a. The effect of age on the macromolecular permeability of human Bruch's membrane. *Investigative ophthalmology & visual science*, 42, 2970-5.
- MOORE, D. J. & CLOVER, G. M. 2001b. The effect of age on the macromolecular permeability of human Bruch's membrane. *Invest Ophthalmol Vis Sci*, 42, 2970-5.
- MOORE, D. J., HUSSAIN, A. A. & MARSHALL, J. 1995a. Age-related variation in the hydraulic conductivity of Bruch's membrane. *Investigative ophthalmology & visual science*, 36, 1290-7.
- MOORE, D. J., HUSSAIN, A. A. & MARSHALL, J. 1995b. Age-related variation in the hydraulic conductivity of Bruch's membrane. *Invest Ophthalmol Vis Sci*, 36, 1290-7.
- MOSELEY, H. & FOULDS, W. S. 1982. The movement of xenon-133 from the vitreous to the choroid. *Experimental eye research*, 34, 169-79.
- MUQIT, M. M., GRAY, J. C., MARCELLINO, G. R., HENSON, D. B., YOUNG, L. B., CHARLES, S. J., TURNER, G. S. & STANGA, P. E. 2009. Fundus autofluorescence and Fourier-domain optical coherence tomography

- imaging of 10 and 20 millisecond Pascal retinal photocoagulation treatment. *The British journal of ophthalmology*, 93, 518-25.
- MUQIT, M. M., GRAY, J. C., MARCELLINO, G. R., HENSON, D. B., YOUNG, L. B., PATTON, N., CHARLES, S. J., TURNER, G. S., DICK, A. D. & STANGA, P. E. 2010a. In vivo laser-tissue interactions and healing responses from 20- vs 100-millisecond pulse Pascal photocoagulation burns. *Archives of ophthalmology*, 128, 448-55.
- MUQIT, M. M., GRAY, J. C., MARCELLINO, G. R., HENSON, D. B., YOUNG, L. B., PATTON, N., CHARLES, S. J., TURNER, G. S. & STANGA, P. E. 2010b. Barely visible 10-millisecond pascal laser photocoagulation for diabetic macular edema: observations of clinical effect and burn localization. *American journal of ophthalmology*, 149, 979-986 e2.
- MURPHY, G. 2011. Tissue inhibitors of metalloproteinases. *Genome biology*, 12, 233.
- MURPHY, G. & CRABBE, T. 1995. Gelatinases A and B. *Methods in enzymology*, 248, 470-84.
- MUTHIAH, M. N., GIAS, C., CHEN, F. K., ZHONG, J., MCCLELLAND, Z., SALLO, F. B., PETO, T., COFFEY, P. J. & DA CRUZ, L. 2014. Cone photoreceptor definition on adaptive optics retinal imaging. *The British journal of ophthalmology*.
- NAGASE, H., ENGHILD, J. J., SUZUKI, K. & SALVESEN, G. 1990. Stepwise activation mechanisms of the precursor of matrix metalloproteinase 3 (stromelysin) by proteinases and (4-aminophenyl)mercuric acetate. *Biochemistry*, 29, 5783-9.
- NAGASE, H., VISSE, R. & MURPHY, G. 2006. Structure and function of matrix metalloproteinases and TIMPs. *Cardiovascular research*, 69, 562-73.
- NEGI, A. & MARMOR, M. F. 1986. Mechanisms of subretinal fluid resorption in the cat eye. *Investigative ophthalmology & visual science*, 27, 1560-3.
- NEWSOME, D. A., HEWITT, A. T., HUH, W., ROBEY, P. G. & HASSELL, J. R. 1987a. Detection of specific extracellular matrix molecules in drusen, Bruch's membrane, and ciliary body. *Am J Ophthalmol*, 104, 373-81.
- NEWSOME, D. A., HUH, W. & GREEN, W. R. 1987b. Bruch's membrane age-related changes vary by region. *Current eye research*, 6, 1211-21.
- OBATA, R. & YANAGI, Y. 2014. Quantitative analysis of cone photoreceptor distribution and its relationship with axial length, age, and early age-related macular degeneration. *PloS one*, 9, e91873.
- OHKOSHI, K. & YAMAGUCHI, T. 2010. Subthreshold micropulse diode laser photocoagulation for diabetic macular edema in Japanese patients. *American journal of ophthalmology*, 149, 133-9.
- OKADA, R., KAWAI, S., NAITO, M., HISHIDA, A., HAMAJIMA, N., SHINCHI, K., CHOWDHURY TURIN, T., SUZUKI, S., MANTJORO, E. M., TOYOMURA, K., ARISAWA, K., KURIYAMA, N., HOSONO, S., MIKAMI, H., KUBO, M., TANAKA, H. & WAKAI, K. 2012. Matrix metalloproteinase-9 gene polymorphisms and chronic kidney disease. *American journal of nephrology*, 36, 444-50.
- OPHTHALMOLOGISTS., T. R. C. O. 2012. Age-Related Macular Degeneration Guidelines for Management.
- OWEN, C. G., JARRAR, Z., WORMALD, R., COOK, D. G., FLETCHER, A. E. & RUDNICKA, A. R. 2012. The estimated prevalence and incidence of late stage age related macular degeneration in the UK. *The British journal of ophthalmology*, 96, 752-6.
- OWSLEY, C., JACKSON, G. R., CIDECIYAN, A. V., HUANG, Y., FINE, S. L., HO, A. C., MAGUIRE, M. G., LOLLEY, V. & JACOBSON, S. G. 2000. Psychophysical

- evidence for rod vulnerability in age-related macular degeneration. *Investigative ophthalmology & visual science*, 41, 267-73.
- OWSLEY, C., JACKSON, G. R., WHITE, M., FEIST, R. & EDWARDS, D. 2001. Delays in rod-mediated dark adaptation in early age-related maculopathy. *Ophthalmology*, 108, 1196-202.
- OWSLEY, C., MCGWIN, G., JR., JACKSON, G. R., KALLIES, K. & CLARK, M. 2007. Cone- and rod-mediated dark adaptation impairment in age-related maculopathy. *Ophthalmology*, 114, 1728-35.
- PADGETT, L. C., LUI, G. M., WERB, Z. & LAVAIL, M. M. 1997. Matrix metalloproteinase-2 and tissue inhibitor of metalloproteinase-1 in the retinal pigment epithelium and interphotoreceptor matrix: vectorial secretion and regulation. *Experimental eye research*, 64, 927-38.
- PAREKH, N., CHAPPELL, R. J., MILLEN, A. E., ALBERT, D. M. & MARES, J. A. 2007. Association between vitamin D and age-related macular degeneration in the Third National Health and Nutrition Examination Survey, 1988 through 1994. *Archives of ophthalmology*, 125, 661-9.
- PARISI, V., PERILLO, L., TEDESCHI, M., SCASSA, C., GALLINARO, G., CAPALDO, N. & VARANO, M. 2007. Macular function in eyes with early age-related macular degeneration with or without contralateral late age-related macular degeneration. *Retina*, 27, 879-90.
- PASCOLINI, D. & MARIOTTI, S. P. 2012. Global estimates of visual impairment: 2010. *The British journal of ophthalmology*, 96, 614-8.
- PATEL, P. J., CHEN, F. K., RUBIN, G. S. & TUFAIL, A. 2008. Intersession repeatability of visual acuity scores in age-related macular degeneration. *Investigative ophthalmology & visual science*, 49, 4347-52.
- PATEL, P. J., CHEN, F. K., RUBIN, G. S. & TUFAIL, A. 2009. Intersession repeatability of contrast sensitivity scores in age-related macular degeneration. *Investigative ophthalmology & visual science*, 50, 2621-5.
- PATZ, A., EASTHAM, A., HIGGINBOTHAM, D. H. & KLEH, T. 1953. Oxygen studies in retrolental fibroplasia. II. The production of the microscopic changes of retrolental fibroplasia in experimental animals. *American journal of ophthalmology*, 36, 1511-22.
- PAULEIKHOFF, D., HARPER, C. A., MARSHALL, J. & BIRD, A. C. 1990. Aging changes in Bruch's membrane. A histochemical and morphologic study. *Ophthalmology*, 97, 171-8.
- PAULUS, Y. M., KAUR, K., EGBERT, P. R., BLUMENKRANZ, M. S. & MOSHFEGHI, D. M. 2013. Human histopathology of PASCAL laser burns. *Eye*, 27, 995-6.
- PELOSINI, L., HAMILTON, R., MOHAMED, M., HAMILTON, A. M. & MARSHALL, J. 2013. Retina rejuvenation therapy for diabetic macular edema: a pilot study. *Retina*, 33, 548-58.
- PENFOLD, P. L., MADIGAN, M. C., GILLIES, M. C. & PROVIS, J. M. 2001. Immunological and aetiological aspects of macular degeneration. *Progress in retinal and eye research*, 20, 385-414.
- PEPPIN, G. J. & WEISS, S. J. 1986. Activation of the endogenous metalloproteinase, gelatinase, by triggered human neutrophils. *Proceedings of the National Academy of Sciences of the United States of America*, 83, 4322-6.
- PHIPPS, J. A., DANG, T. M., VINGRYS, A. J. & GUYMER, R. H. 2004. Flicker perimetry losses in age-related macular degeneration. *Investigative ophthalmology & visual science*, 45, 3355-60.
- PIERMAROCCHI, S., VARANO, M., PARRAVANO, M., ODDONE, F., SARTORE, M., FERRARA, R., SERA, F. & VIRGILI, G. 2011. Quality of Vision Index: a new

- method to appraise visual function changes in age-related macular degeneration. *European journal of ophthalmology*, 21, 55-66.
- PILKINGTON, S. M., WATSON, R. E., NICOLAOU, A. & RHODES, L. E. 2011. Omega-3 polyunsaturated fatty acids: photoprotective macronutrients. *Experimental dermatology*, 20, 537-43.
- PLANTNER, J. J., JIANG, C. & SMINE, A. 1998a. Increase in interphotoreceptor matrix gelatinase A (MMP-2) associated with age-related macular degeneration. *Exp Eye Res*, 67, 637-45.
- PLANTNER, J. J., SMINE, A. & QUINN, T. A. 1998b. Matrix metalloproteinases and metalloproteinase inhibitors in human interphotoreceptor matrix and vitreous. *Current eye research*, 17, 132-40.
- QUERQUES, G., QUERQUES, L., FORTE, R., MASSAMBA, N., COSCAS, F. & SOUIED, E. H. 2012. Choroidal changes associated with reticular pseudodrusen. *Investigative ophthalmology & visual science*, 53, 1258-63.
- RAMRATTAN, R. S., VAN DER SCHAFT, T. L., MOOY, C. M., DE BRUIJN, W. C., MULDER, P. G. & DE JONG, P. T. 1994a. Morphometric analysis of Bruch's membrane, the choriocapillaris, and the choroid in aging. *Invest Ophthalmol Vis Sci*, 35, 2857-64.
- RAMRATTAN, R. S., VAN DER SCHAFT, T. L., MOOY, C. M., DE BRUIJN, W. C., MULDER, P. G. & DE JONG, P. T. 1994b. Morphometric analysis of Bruch's membrane, the choriocapillaris, and the choroid in aging. *Investigative ophthalmology & visual science*, 35, 2857-64.
- REGILLO, C. D., BROWN, D. M., ABRAHAM, P., YUE, H., IANCHULEV, T., SCHNEIDER, S. & SHAMS, N. 2008. Randomized, double-masked, sham-controlled trial of ranibizumab for neovascular age-related macular degeneration: PIER Study year 1. *American journal of ophthalmology*, 145, 239-248.
- REIDY, D. M. A. 2010. *Annual Evidence Update on Age related macular degeneration-future sight loss*.
<http://www.library.nhs.uk/Eyes/ViewResource.aspx?resID=377527>
 [Online].
- REIN, D. B., ZHANG, P., WIRTH, K. E., LEE, P. P., HOERGER, T. J., MCCALL, N., KLEIN, R., TIELSCH, J. M., VIJAN, S. & SAADDINE, J. 2006. The economic burden of major adult visual disorders in the United States. *Archives of ophthalmology*, 124, 1754-60.
- RENKIN, E. M. 1954. Filtration, diffusion, and molecular sieving through porous cellulose membranes. *The Journal of general physiology*, 38, 225-43.
- ROBMAN, L., VU, H., HODGE, A., TIKELLIS, G., DIMITROV, P., MCCARTY, C. & GUYMER, R. 2007. Dietary lutein, zeaxanthin, and fats and the progression of age-related macular degeneration. *Canadian journal of ophthalmology. Journal canadien d'ophtalmologie*, 42, 720-6.
- ROIDER, J., BRINKMANN, R., WIRBELAUER, C., LAQUA, H. & BIRNGRUBER, R. 1999. Retinal sparing by selective retinal pigment epithelial photocoagulation. *Archives of ophthalmology*, 117, 1028-34.
- ROIDER, J., MICHAUD, N. A., FLOTTE, T. J. & BIRNGRUBER, R. 1992. Response of the retinal pigment epithelium to selective photocoagulation. *Archives of ophthalmology*, 110, 1786-92.
- ROORDA, A., ROMERO-BORJA, F., DONNELLY III, W., QUEENER, H., HEBERT, T. & CAMPBELL, M. 2002. Adaptive optics scanning laser ophthalmoscopy. *Optics express*, 10, 405-12.
- ROSSI, E. A., RANGEL-FONSECA, P., PARKINS, K., FISCHER, W., LATCHNEY, L. R., FOLWELL, M. A., WILLIAMS, D. R., DUBRA, A. & CHUNG, M. M. 2013. In vivo

- imaging of retinal pigment epithelium cells in age related macular degeneration. *Biomedical optics express*, 4, 2527-39.
- SABATES, F. N., VINCENT, R. D., KOULEN, P., SABATES, N. R. & GALLIMORE, G. 2011. Normative data set identifying properties of the macula across age groups: integration of visual function and retinal structure with microperimetry and spectral-domain optical coherence tomography. *Retina*, 31, 1294-302.
- SAID, A. H., RAUFMAN, J. P. & XIE, G. 2014. The role of matrix metalloproteinases in colorectal cancer. *Cancers*, 6, 366-75.
- SANCHEZ, M. C., LUNA, J. D., BARCELONA, P. F., GRAMAJO, A. L., JUAREZ, P. C., RIERA, C. M. & CHIABRANDO, G. A. 2007. Effect of retinal laser photocoagulation on the activity of metalloproteinases and the alpha(2)-macroglobulin proteolytic state in the vitreous of eyes with proliferative diabetic retinopathy. *Experimental eye research*, 85, 644-50.
- SANDBERG, M. A. & GAUDIO, A. R. 1995. Slow photostress recovery and disease severity in age-related macular degeneration. *Retina*, 15, 407-12.
- SANGIOVANNI, J. P., AGRON, E., MELETH, A. D., REED, G. F., SPERDUTO, R. D., CLEMONS, T. E. & CHEW, E. Y. 2009. {omega}-3 Long-chain polyunsaturated fatty acid intake and 12-y incidence of neovascular age-related macular degeneration and central geographic atrophy: AREDS report 30, a prospective cohort study from the Age-Related Eye Disease Study. *The American journal of clinical nutrition*, 90, 1601-7.
- SARKS, J. P., SARKS, S. H. & KILLINGSWORTH, M. C. 1988. Evolution of geographic atrophy of the retinal pigment epithelium. *Eye*, 2 (Pt 5), 552-77.
- SARKS, S. H. 1976a. Ageing and degeneration in the macular region: a clinicopathological study. *Br J Ophthalmol*, 60, 324-41.
- SARKS, S. H. 1976b. Ageing and degeneration in the macular region: a clinicopathological study. *The British journal of ophthalmology*, 60, 324-41.
- SARKS, S. H., ARNOLD, J. J., KILLINGSWORTH, M. C. & SARKS, J. P. 1999. Early drusen formation in the normal and aging eye and their relation to age related maculopathy: a clinicopathological study. *The British journal of ophthalmology*, 83, 358-68.
- SCHLANITZ, F. G., AHLERS, C., SACU, S., SCHUTZE, C., RODRIGUEZ, M., SCHRIEFL, S., GOLBAZ, I., SPALEK, T., STOCK, G. & SCHMIDT-ERFURTH, U. 2010. Performance of drusen detection by spectral-domain optical coherence tomography. *Investigative ophthalmology & visual science*, 51, 6715-21.
- SCHOLL, H. P., CHARBEL ISSA, P., WALIER, M., JANZER, S., POLLOK-KOPP, B., BORNCKE, F., FRITSCHKE, L. G., CHONG, N. V., FIMMERS, R., WIENKER, T., HOLZ, F. G., WEBER, B. H. & OPPERMANN, M. 2008. Systemic complement activation in age-related macular degeneration. *PloS one*, 3, e2593.
- SCHUMAN, S. G., KOREISHI, A. F., FARSIU, S., JUNG, S. H., IZATT, J. A. & TOTH, C. A. 2009. Photoreceptor layer thinning over drusen in eyes with age-related macular degeneration imaged in vivo with spectral-domain optical coherence tomography. *Ophthalmology*, 116, 488-496 e2.
- SCHUTT, F. & HOLZ, F. G. 2002. Microablation of choroidal tissue from Bruch's membrane using a 193nm excimer laser. *Experimental eye research*, 74, 155-7.
- SCHVEIGERT, D., VALUCKAS, K. P., KOVALCIS, V., ULYS, A., CHVATOVIC, G. & DIDZIAPETRIENE, J. 2013. Significance of MMP-9 expression and MMP-9 polymorphism in prostate cancer. *Tumori*, 99, 523-9.

- SEDDON, J. M., AJANI, U. A., SPERDUTO, R. D., HILLER, R., BLAIR, N., BURTON, T. C., FARBER, M. D., GRAGODAS, E. S., HALLER, J., MILLER, D. T. & ET AL. 1994. Dietary carotenoids, vitamins A, C, and E, and advanced age-related macular degeneration. Eye Disease Case-Control Study Group. *JAMA : the journal of the American Medical Association*, 272, 1413-20.
- SEDDON, J. M., ROSNER, B., SPERDUTO, R. D., YANNUZZI, L., HALLER, J. A., BLAIR, N. P. & WILLETT, W. 2001. Dietary fat and risk for advanced age-related macular degeneration. *Archives of ophthalmology*, 119, 1191-9.
- SHAKIB, M., RUTKOWSKI, P. & WISE, G. N. 1972. Fluorescein angiography and the retinal pigment epithelium. *American journal of ophthalmology*, 74, 206-18.
- SHAKOOR, A., BLAIR, N. P., MORI, M. & SHAHIDI, M. 2006. Chorioretinal vascular oxygen tension changes in response to light flicker. *Investigative ophthalmology & visual science*, 47, 4962-5.
- SHERAIDAH, G., STEINMETZ, R., MAGUIRE, J., PAULEIKHOFF, D., MARSHALL, J. & BIRD, A. C. 1993. Correlation between lipids extracted from Bruch's membrane and age. *Ophthalmology*, 100, 47-51.
- SIDEROV, J. & TIU, A. L. 1999. Variability of measurements of visual acuity in a large eye clinic. *Acta ophthalmologica Scandinavica*, 77, 673-6.
- SIMONELLI, F., ZARRILLI, F., MAZZEO, S., VERDE, V., ROMANO, N., SAVOIA, M., TESTA, F., VITALE, D. F., RINALDI, M. & SACCHETTI, L. 2002. Serum oxidative and antioxidant parameters in a group of Italian patients with age-related maculopathy. *Clinica chimica acta; international journal of clinical chemistry*, 320, 111-5.
- SJOSTRAND, J. & FRISEN, L. 1977. Contrast sensitivity in macular disease. A preliminary report. *Acta ophthalmologica*, 55, 507-14.
- SKULACHEV, V. P. 1996. Role of uncoupled and non-coupled oxidations in maintenance of safely low levels of oxygen and its one-electron reductants. *Quarterly reviews of biophysics*, 29, 169-202.
- SLINEY, D. H. 1999. Overview of Range of Mechanisms. *Laser induced damage in optical materials*, 3902, 2-19.
- SLINEY, D. H. A. M., J. 1992. Tissue specific damage to the retinal pigment epithelium: mechanisms and therapeutic implications. *Lasers Light Ophthalmol*, 5, 17-28.
- SLOANE, M. E., OWSLEY, C. & JACKSON, C. A. 1988. Aging and luminance-adaptation effects on spatial contrast sensitivity. *Journal of the Optical Society of America. A, Optics and image science*, 5, 2181-90.
- SMIDDY, W. E., FINE, S. L., QUIGLEY, H. A., DUNKELBERGER, G., HOHMAN, R. M. & ADDICKS, E. M. 1986. Cell proliferation after laser photocoagulation in primate retina. An autoradiographic study. *Archives of ophthalmology*, 104, 1065-9.
- SMINE, A. & PLANTNER, J. J. 1997. Membrane type-1 matrix metalloproteinase in human ocular tissues. *Current eye research*, 16, 925-9.
- SMITH, W., MITCHELL, P. & LEEDER, S. R. 2000. Dietary fat and fish intake and age-related maculopathy. *Archives of ophthalmology*, 118, 401-4.
- SMITH, W., MITCHELL, P. & ROCHESTER, C. 1997. Serum beta carotene, alpha tocopherol, and age-related maculopathy: the Blue Mountains Eye Study. *American journal of ophthalmology*, 124, 838-40.
- SPAIDE, R. F. 2009. Enhanced depth imaging optical coherence tomography of retinal pigment epithelial detachment in age-related macular degeneration. *American journal of ophthalmology*, 147, 644-52.

- SPRAUL, C. W., LANG, G. E., GROSSNIKLAUS, H. E. & LANG, G. K. 1999a. Histologic and morphometric analysis of the choroid, Bruch's membrane, and retinal pigment epithelium in postmortem eyes with age-related macular degeneration and histologic examination of surgically excised choroidal neovascular membranes. *Survey of ophthalmology*, 44 Suppl 1, S10-32.
- SPRAUL, C. W., LANG, G. E., GROSSNIKLAUS, H. E. & LANG, G. K. 1999b. Histologic and morphometric analysis of the choroid, Bruch's membrane, and retinal pigment epithelium in postmortem eyes with age-related macular degeneration and histologic examination of surgically excised choroidal neovascular membranes. *Surv Ophthalmol*, 44 Suppl 1, S10-32.
- STANGOS, N., VOUTAS, S., TOPOUZIS, F. & KARAMPATAKIS, V. 1995. Contrast sensitivity evaluation in eyes predisposed to age-related macular degeneration and presenting normal visual acuity. *Ophthalmologica. Journal internationale d'ophtalmologie. International journal of ophthalmology. Zeitschrift fur Augenheilkunde*, 209, 194-8.
- STARITA, C., HUSSAIN, A. A., PAGLIARINI, S. & MARSHALL, J. 1996a. Hydrodynamics of ageing Bruch's membrane: implications for macular disease. *Experimental eye research*, 62, 565-72.
- STARITA, C., HUSSAIN, A. A., PAGLIARINI, S. & MARSHALL, J. 1996b. Hydrodynamics of ageing Bruch's membrane: implications for macular disease. *Exp Eye Res*, 62, 565-72.
- STARITA, C., HUSSAIN, A. A., PATMORE, A. & MARSHALL, J. 1997. Localization of the site of major resistance to fluid transport in Bruch's membrane. *Investigative ophthalmology & visual science*, 38, 762-7.
- STOPA, M., BOWER, B. A., DAVIES, E., IZATT, J. A. & TOTH, C. A. 2008. Correlation of pathologic features in spectral domain optical coherence tomography with conventional retinal studies. *Retina*, 28, 298-308.
- STRONGIN, A. Y., COLLIER, I., BANNIKOV, G., MARMER, B. L., GRANT, G. A. & GOLDBERG, G. I. 1995. Mechanism of cell surface activation of 72-kDa type IV collagenase. Isolation of the activated form of the membrane metalloprotease. *The Journal of biological chemistry*, 270, 5331-8.
- SUBRAMANIAN, M. L., NESS, S., ABEDI, G., AHMED, E., DALY, M., FEINBERG, E., BHATIA, S., PATEL, P., NGUYEN, M. & HOURANIEH, A. 2009. Bevacizumab vs ranibizumab for age-related macular degeneration: early results of a prospective double-masked, randomized clinical trial. *American journal of ophthalmology*, 148, 875-82 e1.
- SUGINO, I. K., SUN, Q., CHEEWATRAKOOLPONG, N., MALCUIT, C. & ZARBIN, M. A. 2014. Biochemical Restoration of Aged Human Bruch's Membrane: Experimental Studies to Improve Retinal Pigment Epithelium Transplant Survival and Differentiation. *Developments in ophthalmology*, 53, 133-42.
- SUNNESS, J. S., SCHUCHARD, R. A., SHEN, N., RUBIN, G. S., DAGNELIE, G. & HASELWOOD, D. M. 1995. Landmark-driven fundus perimetry using the scanning laser ophthalmoscope. *Investigative ophthalmology & visual science*, 36, 1863-74.
- TABABAT-KHANI, P., BERGLUND, L. M., AGARDH, C. D., GOMEZ, M. F. & AGARDH, E. 2013. Photocoagulation of human retinal pigment epithelial cells in vitro: evaluation of necrosis, apoptosis, cell migration, cell proliferation and expression of tissue repairing and cytoprotective genes. *PloS one*, 8, e70465.
- TALCOTT, K. E., RATNAM, K., SUNDQUIST, S. M., LUCERO, A. S., LUJAN, B. J., TAO, W., PORCO, T. C., ROORDA, A. & DUNCAN, J. L. 2011. Longitudinal study of cone photoreceptors during retinal degeneration and in response to ciliary

- neurotrophic factor treatment. *Investigative ophthalmology & visual science*, 52, 2219-26.
- TALHOUK, R. S., CHIN, J. R., UNEMORI, E. N., WERB, Z. & BISSELL, M. J. 1991. Proteinases of the mammary gland: developmental regulation in vivo and vectorial secretion in culture. *Development*, 112, 439-49.
- TAYLOR, N. 2000. LASER: The inventor, the Nobel laureate, and the thirty year patent war. *New York: Simon & Schuster*.
- TH, M. 1960. Stimulated optical radiation in ruby. *Nature* 187, 493-494.
- TOTH, C. A., NARAYAN, D. G., BOPPART, S. A., HEE, M. R., FUJIMOTO, J. G., BIRNGRUBER, R., CAIN, C. P., DICARLO, C. D. & ROACH, W. P. 1997. A comparison of retinal morphology viewed by optical coherence tomography and by light microscopy. *Archives of ophthalmology*, 115, 1425-8.
- TOTH, M., CHVYRKOVA, I., BERNARDO, M. M., HERNANDEZ-BARRANTES, S. & FRIDMAN, R. 2003. Pro-MMP-9 activation by the MT1-MMP/MMP-2 axis and MMP-3: role of TIMP-2 and plasma membranes. *Biochemical and biophysical research communications*, 308, 386-95.
- TOTH, M., SOHAIL, A. & FRIDMAN, R. 2012. Assessment of gelatinases (MMP-2 and MMP-9) by gelatin zymography. *Methods in molecular biology*, 878, 121-35.
- TREUMER, F., KLETTNER, A., BALTZ, J., HUSSAIN, A. A., MIURA, Y., BRINKMANN, R., ROIDER, J. & HILLENKAMP, J. 2012. Vectorial release of matrix metalloproteinases (MMPs) from porcine RPE-choroid explants following selective retina therapy (SRT): towards slowing the macular ageing process. *Experimental eye research*, 97, 63-72.
- TRIESCHMANN, M., BEATTY, S., NOLAN, J. M., HENSE, H. W., HEIMES, B., AUSTERMANN, U., FOBKER, M. & PAULEIKHOFF, D. 2007. Changes in macular pigment optical density and serum concentrations of its constituent carotenoids following supplemental lutein and zeaxanthin: the LUNA study. *Experimental eye research*, 84, 718-28.
- UEDA-ARAKAWA, N., OOTO, S., ELLABBAN, A. A., TAKAHASHI, A., OISHI, A., TAMURA, H., YAMASHIRO, K., TSUJIKAWA, A. & YOSHIMURA, N. 2014. Macular choroidal thickness and volume of eyes with reticular pseudodrusen using swept-source optical coherence tomography. *American journal of ophthalmology*, 157, 994-1004.
- UGARTE, M., HUSSAIN, A. A. & MARSHALL, J. 2006. An experimental study of the elastic properties of the human Bruch's membrane-choroid complex: relevance to ageing. *The British journal of ophthalmology*, 90, 621-6.
- UNEMORI, E. N., BOUHANA, K. S. & WERB, Z. 1990. Vectorial secretion of extracellular matrix proteins, matrix-degrading proteinases, and tissue inhibitor of metalloproteinases by endothelial cells. *The Journal of biological chemistry*, 265, 445-51.
- VAN DER SCHAFT, T. L., MOOY, C. M., DE BRUIJN, W. C., ORON, F. G., MULDER, P. G. & DE JONG, P. T. 1992. Histologic features of the early stages of age-related macular degeneration. A statistical analysis. *Ophthalmology*, 99, 278-86.
- VAN LEEUWEN, R., BOEKHOORN, S., VINGERLING, J. R., WITTEMAN, J. C., KLAVER, C. C., HOFMAN, A. & DE JONG, P. T. 2005. Dietary intake of antioxidants and risk of age-related macular degeneration. *JAMA : the journal of the American Medical Association*, 294, 3101-7.
- VANDENLANGENBERG, G. M., MARES-PERLMAN, J. A., KLEIN, R., KLEIN, B. E., BRADY, W. E. & PALTA, M. 1998. Associations between antioxidant and zinc intake and the 5-year incidence of early age-related maculopathy in the Beaver Dam Eye Study. *American journal of epidemiology*, 148, 204-14.

- VRANKA, J. A., JOHNSON, E., ZHU, X., SHEPARDSON, A., ALEXANDER, J. P., BRADLEY, J. M., WIRTZ, M. K., WELEBER, R. G., KLEIN, M. L. & ACOTT, T. S. 1997. Discrete expression and distribution pattern of TIMP-3 in the human retina and choroid. *Current eye research*, 16, 102-10.
- VUJOSEVIC, S., BOTTEGA, E., CASCIANO, M., PILOTTO, E., CONVENTO, E. & MIDENA, E. 2010. Microperimetry and fundus autofluorescence in diabetic macular edema: subthreshold micropulse diode laser versus modified early treatment diabetic retinopathy study laser photocoagulation. *Retina*, 30, 908-16.
- WALLOW, I. H. 1984. Repair of the pigment epithelial barrier following photocoagulation. *Archives of ophthalmology*, 102, 126-35.
- WALLOW, I. H. & TSO, M. O. 1973a. Repair after xenon arc photocoagulation. 2. A clinical and light microscopic study of the evolution of retinal lesions in the rhesus monkey. *American journal of ophthalmology*, 75, 610-26.
- WALLOW, I. H. & TSO, M. O. 1973b. Repair after xenon arc photocoagulation. 3. An electron microscopic study of the evolution of retinal lesions in rhesus monkeys. *American journal of ophthalmology*, 75, 957-72.
- WANG, W., SCHULZE, C. J., SUAREZ-PINZON, W. L., DYCK, J. R., SAWICKI, G. & SCHULZ, R. 2002. Intracellular action of matrix metalloproteinase-2 accounts for acute myocardial ischemia and reperfusion injury. *Circulation*, 106, 1543-9.
- WEBER, B. H., VOGT, G., PRUETT, R. C., STOHR, H. & FELBOR, U. 1994. Mutations in the tissue inhibitor of metalloproteinases-3 (TIMP3) in patients with Sorsby's fundus dystrophy. *Nature genetics*, 8, 352-6.
- WEIKEL, K. A., TAYLOR, A. & CHIU, C. J. 2012. Nutritional modulation of age-related macular degeneration. *Molecular aspects of medicine*.
- WILSON, T. M., STRANG, R., WALLACE, J., HORTON, P. W. & JOHNSON, N. F. 1973. The measurement of the choroidal blood flow in the rabbit using 85-krypton. *Experimental eye research*, 16, 421-5.
- WINKLER, M. M., BRUENING, G. & HERSHEY, J. W. 1983. An absolute requirement for the 5' cap structure for mRNA translation in sea urchin eggs. *European journal of biochemistry / FEBS*, 137, 227-32.
- WOLBARSHT, M. L., FLIGSTEN, K. E. & HAYES, J. R. 1965. Retina: pathology of neodymium and ruby laser burns. *Science*, 150, 1453-4.
- WOLBARSHT, M. L. & LANDERS, M. B., 3RD 1980. The rationale of photocoagulation therapy for proliferative diabetic retinopathy: a review and a model. *Ophthalmic surgery*, 11, 235-45.
- WOOD, J. P., PLUNKETT, M., PREVIN, V., CHIDLOW, G. & CASSON, R. J. 2011. Nanosecond pulse lasers for retinal applications. *Lasers in surgery and medicine*, 43, 499-510.
- WYLER, A. R., ROBBINS, C. A. & KLEIN, S. 1979. Non-burst epileptic firing patterns of neurons in chronic epileptic foci. *Brain research*, 169, 173-7.
- YADAV, R. K. 2009. Definitions in laser technology. *Journal of cutaneous and aesthetic surgery*, 2, 45-6.
- YANNUZZI, L. A., SLAKTER, J. S., SORENSON, J. A., GUYER, D. R. & ORLOCK, D. A. 1992. Digital indocyanine green videoangiography and choroidal neovascularization. *Retina*, 12, 191-223.
- YOUNG, R. W. 1976. Visual cells and the concept of renewal. *Investigative ophthalmology & visual science*, 15, 700-25.

- YOUNG, R. W. & BOK, D. 1969. Participation of the retinal pigment epithelium in the rod outer segment renewal process. *The Journal of cell biology*, 42, 392-403.
- YOUNG, R. W. & BOK, D. 1970. Autoradiographic studies on the metabolism of the retinal pigment epithelium. *Investigative ophthalmology*, 9, 524-36.
- ZHANG, J. J., SUN, Y., HUSSAIN, A. A. & MARSHALL, J. 2012. Laser-mediated activation of human retinal pigment epithelial cells and concomitant release of matrix metalloproteinases. *Investigative ophthalmology & visual science*, 53, 2928-37.
- ZWENG, H. C., ROSAN, R. C., PEABODY, R. R. & SHUMAN, R. M. 1967. Experimental Q-switched ruby laser retinal damage. *Archives of ophthalmology*, 78, 634-40.

Presentations and publications

Publications

1. Treatments in early AMD

Optometry in Practice, Hospital Special Issue, 2012;13(3):115-122

2. The role of OCT in the diagnosis of early AMD

Presentations

1. Vectorial release of MMP post 2RT laser in porcine RPE-BrM explants culture

ARVO 2013 (poster)

2. Role of MMP activity in increasing hydraulic conductivity across the aged human Bruch's membrane

ARVO 2014 (poster)

Appendix

- I. Definition of terms and units in relation to laser technology
- II. RETILASE protocol
- III. Consent, Patient information sheet of RETILASE trial

I. Definition of terms and units in relation to laser technology

Laser: light amplification by the stimulated emission of radiation, is an instrument that generates a beam of light of a single wavelength or color that is both highly coherent (in phase) and collimated (parallel). (Yadav, 2009)

The following defines terms and units in accordance to ICNIRP guidelines (health physics 2013, 271). **Power**, is defined as rate of emission of energy from laser, (W). **Irradiance**, E , ($W m^{-2}$) is defined as surface exposure dose rate or power density (power on a unit surface area), whilst and **Radiant exposure**, H , ($J m^{-2}$), is defined as surface exposure dose from laser radiation. **Radiance**, L ($W m^{-2} sr^{-1}$) is term used to describe “brightness” of an extended source that gives rise to an image on the retina and when integrated over time, gives the **Radiance dose**, D , ($J m^{-2} sr^{-1}$).

Pulse is defined as the time of interaction between laser beam and given biological tissue, example, millisecond, microseconds, nanoseconds.

Q-switching is the creation of multiple very short pulses, for instance 1 to 100ns, within a defined time width, with extreme high peak powers per pulse.

Q stands for quality factor, the ratio of the energy stored in the optical resonant cavity to energy loss per cycle. The higher the quality factor, the lower the losses. This is used in Q-switching where energy is stored in the amplifying medium by optical pumping while the cavity Q is lowered to prevent the onset of laser emission. When a high cavity Q is restored, the stored energy is suddenly released in the form of a very short pulse of light. Example of this application include the 2RT nanosecond laser.

Transmission is defined as the simple passage of laser energy through a biologic tissue, whilst **Absorption** is the change of radiant energy to another form (heat energy) upon interaction with biological tissues.

Thermal effect is the generation of heat energy in absorbed and adjacent tissue post irradiation. **Thermal relaxation time** refers to dissipation time of target tissue to approximately 63% of the incident thermal energy.

Photoacoustic effect is the generation of rapidly moving waves in biological tissue, destroying melanin pigments post laser. **Mechanical effect**, used in the

context of this thesis, refers to the absorption of energy by melanosomes to cause microcavitation withinin RPE cells.

Thermomodulation refers to the ability of low-energy light to upregulate biological molecules without consequent injuries; whilst **Selective photothermolysis** is a novel concept defined as the localization of injury to specific targets. In retina research, Anderson and Parrish first defined localization of laser injury to the RPE, by manipulation of laser parameters such as wavelength, pulse duration and energy.

Radiometric					Photometric			
Term	Symbol	Lay definitions*	Defining equation	SI units and abbreviation	Term	Symbol	Defining equation	SI units and abbreviation
Radiant energy	Q_e	A measure of energy emitted	—	Joule (J)	Quantity of light	Q_v	$Q_v = \int \phi_v dt$	Lumen-second (lm/s) talbot
Radiant energy density	W_e		$W_e = \frac{dQ_e}{dV}$	Joule per cubic metre (J/m ³)	Luminous energy density	W_v	$W_v = \frac{dQ_v}{dV}$	Talbot per cubic metre (lm/m ³)
Radiant power (radiant flux)	$\phi_e P$		$\phi_e = \frac{dQ_e}{dt}$	Watt (W)	Luminous flux	ϕ_v	$\phi_v = 680 \times \int \frac{d\phi_e}{d\lambda} V(\lambda) d\lambda$	Lumen (lm)
Irradiance or radiant flux density	E_e	The rate at which energy falls on or passes through an area of surface (i.e. the dose rate)	$E_e = \frac{d\phi_e}{dA}$	Watt per square metre (W/m ²)	Illuminance (luminous density)	E_v	$E_v = \frac{d\phi_v}{dA}$	Lumen per square metre (lm/m ²)
Radiant intensity	I_e		$I_e = \frac{d\phi_e}{d\Omega}$	Watt per steradian (W/sr)	Luminous intensity (candle-power)	I_v	$I_v = \frac{d\phi_v}{d\Omega}$	Lumen per steradian (lm/sr) or candela (cd)
Radiance†	L_e	The "brightness" of a source	$L_e = \frac{d^2\phi_e}{d\Omega dA \cdot \cos\theta}$	Watt per steradian per square metre (W/sr · m ²)	Luminance†	L_v	$L_v = \frac{d^2\phi_v}{d\Omega \cdot dA \cdot \cos\theta}$	Candela per square metre (cd/m ²)
Radiant exposure	H_e	The term for dose in photobiology	$H_e = \frac{d\phi_e}{dA}$	Joule per square metre (J/m ²)	Light exposure	H_v	$H_v = \frac{dQ_v}{dA} = \int E_v dt$	Lux-second (lx/s)
Optical density‡	D_e	A measure of the inability to pass light	$D_e = -\log_{10}\tau_e$	Unit-less	Optical density‡	D_v	$D_v = -\log_{10}\tau_v$	Unit-less
—	—	—	—	—	Retinal illuminance, in trolands	E_t	$E_t = L_v \cdot S_p$	Troland (td) = luminance of cd/m ² times pupil area in mm ²

II. RETILASE protocol

Efficacy and safety of retinal rejuvenation using Ellex 2RT laser in age-related maculopathy (RETILASE trial)

ISRCTN No:

REC No: 11/EE/0171

Sponsor:

Name King's College Hospital NHS Foundation Trust
Contact: Dr Zoe Harris
Address: King's College Hospital, Denmark Hill, London SE5 9RS
Telephone: 020 3299 3841
Email z.harris@nhs.net

Chief Investigator:

Name: Miss Sobha Sivaprasad
Address: King's College Hospital, Denmark Hill, London SE5 9RS
Telephone: 020 3299 1297
Fax: 020 3299 4548
Email: Sobha.sivaprasad@nhs.net

Signatures:

Chief Investigator
Ms Sobha Sivaprasad

Date

Principal Investigator:

Mr Robin Hamilton
Consultant in Ophthalmology
Moorfields Eye Hospital
162, City Road
EC1V 2PD
Robin.hamilton@moorfields.nhs.uk

Scientific Advisor:

Prof John Marshall
Professor of Ophthalmology
Institute of Ophthalmology
11-43 Bath Street
EC 1V 9EL
Eye.marshall@googlemail.com

Sub Investigator:

Dr Ling Zhi Heng
Clinical Research Fellow
King's College Hospital &
Moorfields Eye Hospital
Email: xinglz@hotmail.com

Table of Contents

Table of Contents	310
1. Summary of protocol	312
2. Background	314
2.1 Introduction.....	314
2.2 The International grading of age related maculopathy	315
2.3 Pathology of AMD	319
2.4 Bruch’s membrane (BM)	319
2.5 Ellex 2RT laser	320
2.6 Prior Research Work	321
3. Scientific Hypothesis	322
4. Objectives	323
5. Study Purpose and Design	324
5.1 Study Rationale	324
5.2 Study Design	324
6. Population	325
6.1 Inclusion Criteria.....	325
6.2 Exclusion Criteria	325
7. Summary of study assessments	326
8. Detailed assessment Protocols	17
8.1 Visual function tests.....	17
8.2 Contrast sensitivity.....	19
8.3 Microperimetry	20
8.4 Flicker sensitivity.....	20
8.5 Autofluorescence.....	20
8.6 2-field color and macular stereo fundus photography.....	21
8.7 Fluorescein Fundus Angiogram (FFA).....	21
8.8 Spectral domain optical coherence tomography.....	22
9.Treatment Regime	333
10. Adverse Events	334
10.1 Adverse Events	334
10.2 Procedures for Recording and Reporting Adverse Events.....	334
11.Data Monitoring	336

11.1	Data collection.....	336
11.2	Data analysis of efficacy.....	336
11.3	Planned analysis	336
13.	Milestones and targets for the work.....	337
14.	Quality Assurance.....	337
15.	Publication policy.....	337
16.	Finance.....	337
17.	Signature of Chief Investigator	338
18.	References	Error! Bookmark not defined.

1. Summary of protocol

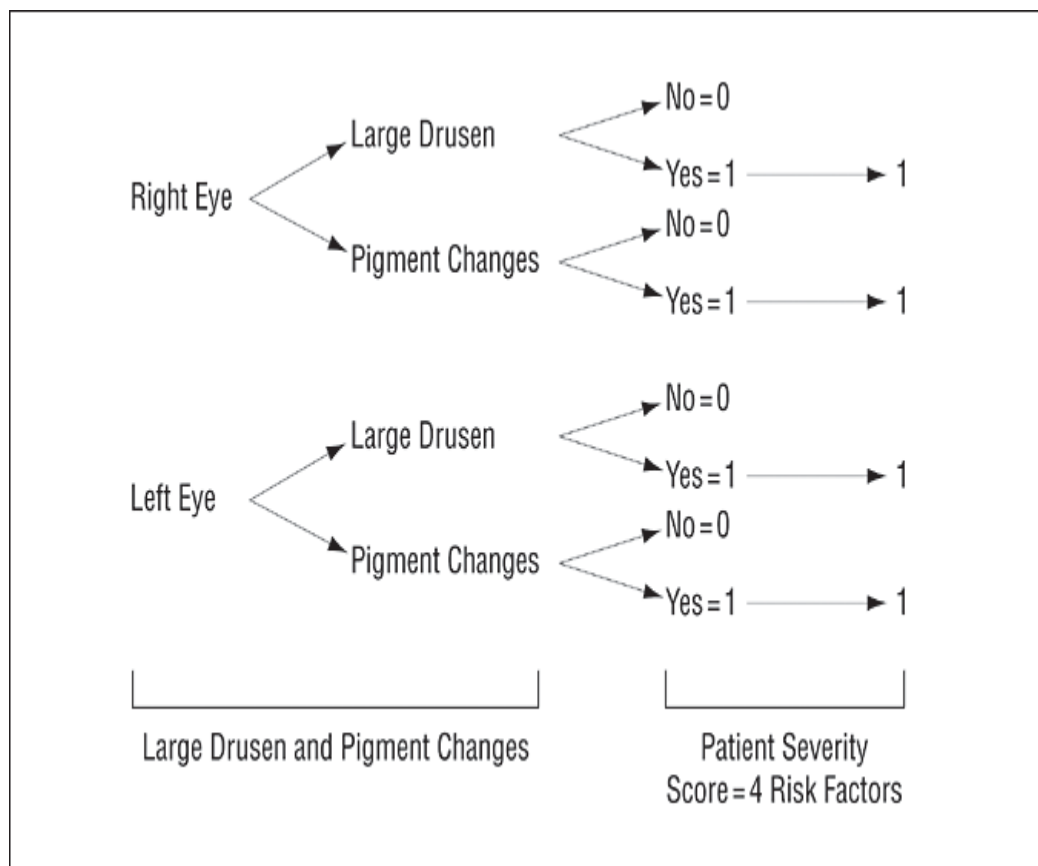
Title	Efficacy and safety of retinal rejuvenation with Ellex 2RT laser in age related maculopathy (RETILASE trial).
Objectives	To determine the efficacy and safety of Ellex 2RT laser in improving visual function and retinal morphology amongst patients with age related maculopathy.
Study Design	<p>A randomized controlled trial to evaluate the efficacy and safety of Ellex 2RT compared to standard care in patients with age-related maculopathy.</p> <p>After informed consent, patients will undergo baseline examinations of best corrected visual acuity, contrast sensitivity, microperimetry and flicker sensitivity. Structural changes will be assessed by OCT, 2- field retina colour photographs, autofluorescence and fundus fluorescein angiography. Follow up visits will be at 6, 12, 18 and 24 months.</p>
Planned Sample Size	80 patients – randomized 1:1 to treatment versus no treatment group.
Patient selection	Patients of either gender aged 55 or above with large drusen ($\geq 125\mu$) in at least one eye (AREDS simple severity grade 2 to 3). Best corrected visual acuity in the study eye must be between 50 to 90 ETDRS letters.
Treatment protocols	<p>3) Treatment one: Ellex 2RT, 400μm diameter spot, 2 rings of concentric subthreshold laser spots applied at 2000μm (5 ½ spots sizes out from the fovea) and 2800μm (7 ½ spot sizes out from the fovea). So a total of at least 25 spots will be applied.</p> <p>OR</p> <p>4) Standard care (No treatment but observed regularly).</p>
Clinical Outcome	Comparison of the outcomes of Ellex 2RT compared to

Measures	<p>observation (standard care) will be done on the following parameters at 12 and 24 months:</p> <p>Efficacy analyses:</p> <ol style="list-style-type: none"> 3. Primary outcome: Mean change in visual acuity at 12 months. 4. Secondary outcomes: <ol style="list-style-type: none"> d. Mean change in visual acuity at 24 months. e. Mean change in contrast sensitivity, microperimetry and flicker sensitivity at 12 and 24 months. f. Changes in fundus morphology as measured by optical coherence tomography, colour fundus photographs at 12 and 24 months. <p>Safety analyses by comparing the following between the two arms:</p> <ol style="list-style-type: none"> 11. Proportion of patients developing CNV confirmed by fluorescein angiography at 12 and 24 months 12. Proportion of patients developing retinal atrophy as measured by fluorescein angiography, autofluorescence and OCT at 12 and 24 months 13. Proportion of patients who lost more than 15 ETDRS letters at 12 and 24 months. 14. Proportion of patients who lost more than 30 ETDRS letters at 12 and 24 months. 15. Any other complications observed at 12 and 24 months.
----------	--

2. Background

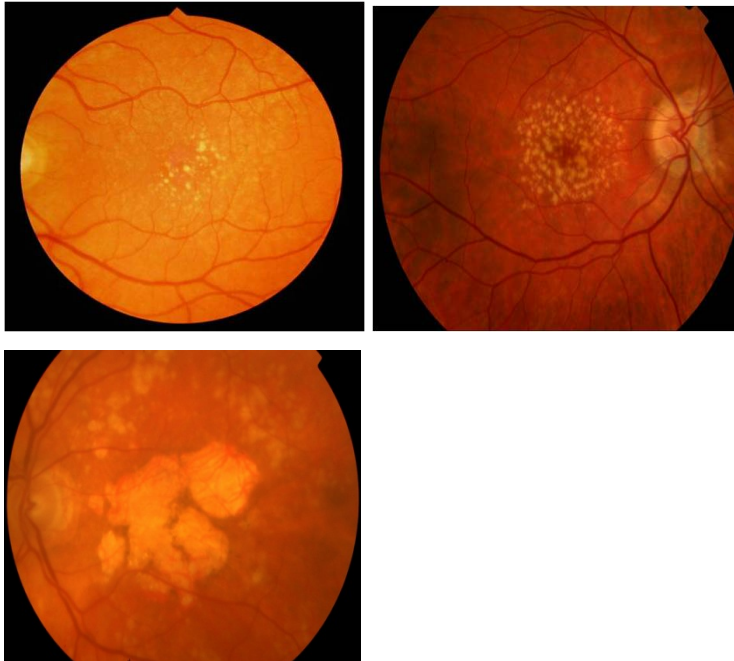
2.1 Introduction

Age Related Macular Degeneration (AMD) is the leading cause of blindness in the elderly in the western society.(Leibowitz et al., 1980, Klein et al., 1992) In the United Kingdom, an estimated 608, 213 people have been diagnosed with AMD. This number is expected to increase to 755, 867 by the end of the next decade. This attributes to 22.5% of the ageing population.(Reidy, 2010) Clinically, “dry” or early AMD is characterised by large drusen and RPE pigmentary changes that can progress to an advanced stage, geographic atrophy. “Wet” or neovascular AMD, another manifestation of advanced disease, is characterised by choroidal neovascularisation (CNV). Clinical classification of early AMD is based on AREDS simplified severity scale (see below) based on photographic assessment of drusen size and pigment changes in the macula [4].



Progression of AMD

Dry/Early AMD → Intermediate AMD → Advanced AMD
(multiple small or intermediate drusen) (extensive drusen or non central GA) (GA involving fovea or CNV)



2.2 The International grading of age related maculopathy

The progression of the disease is monitored by classifying the morphological changes in the fundus as per International Classification (IC) grading system: Standard circles for grading ARM related fundus changes. Circles should be reduced on a transparent sheet according to the fundus camera used so that they are 1/24, 1/12, 1/8.6, 1/6 and 1/3 disk diameter. This results in an approximate diameter of the fundus of 63, 125, 175, 250 and 500 μm .

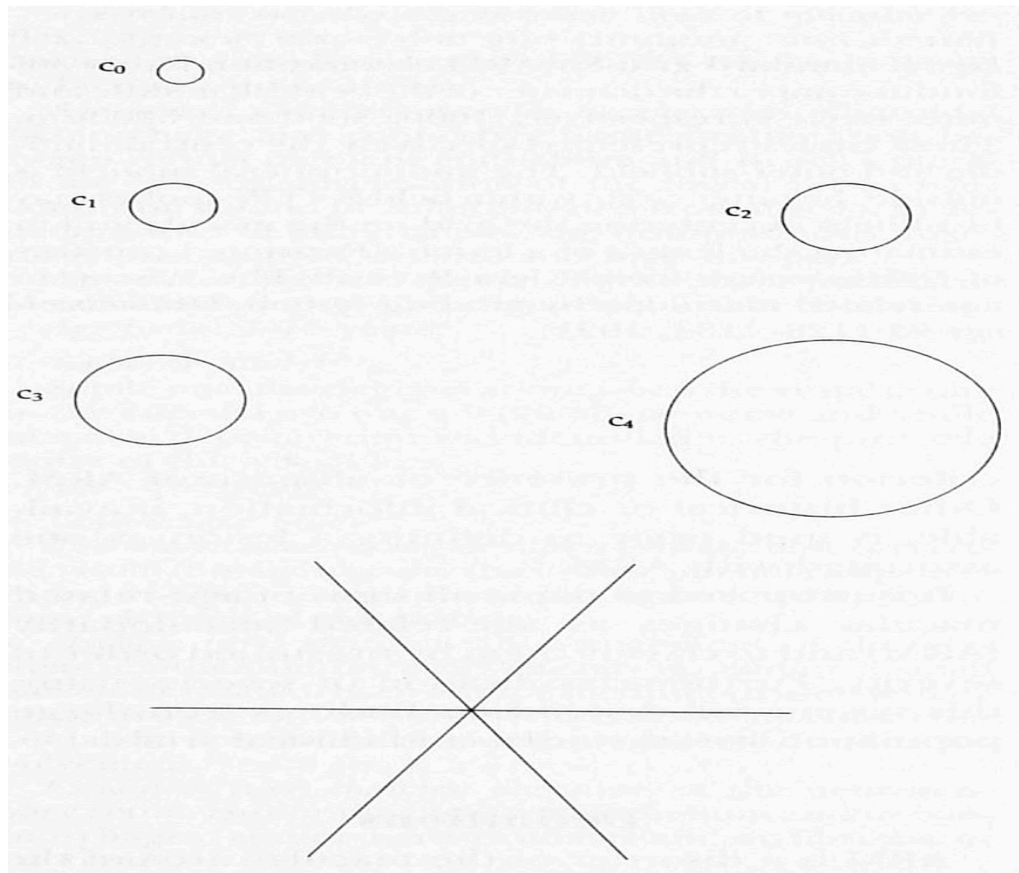
C0: differentiates small from large drusen

C1 and C2: measuring area of hyper or hypopigmentation of RPE

C2: minimum area of geographic atrophy

C3 and C4: geographic atrophy and neovascularization

Spokes: locating centre point and estimating size of lesion.



Grading of Drusen

Drusen morphology. Grade highest # present within outer circle.

- 0) absent
- 1) questionable
- 2) hard drusen (<C1, 125um)
- 3) intermediate, soft drusen (>C0_<C1; >63um<125gm)
- 4) large, soft distinct drusen (>C1, 125um)
- 5) large, soft indistinct drusen (>C1, 125gin)
- 5a) crystalline/calcified/glistening 5b) semisolid 5c) sero granular
- 7) cannot grade, obscuring lesions
- 8) cannot grade, photo quality

Number of drusen

- 0) absent
- 1) questionable
- 2) 1-9
- 3) 10-19

- 4) >20
- 7) cannot grade, obscuring lesions
- 8) cannot grade, photo quality

Drusen size

- 1) <Co (<63um)
- 2) >C0<C1 (>63um,<125um)
- 3) >C1<C2 (>125um, <175um)
- 4) >C2<C3 (>175um,<250um)
- 5) >C3(>250um)
- 7) cannot grade, obscuring lesions
- 8) cannot grade, photo quality

Main location of drusen

Drusen may not be central to indicated subfield, but may be more to periphery.

- 1) outside outer circle (mid-peripheral subfield)
- 2) in outer subfield
- 3) in middle subfield
- 4) in central subfield
- 4a) outside fovea (center point)
- 4b) in fovea
- 7) cannot grade, obscuring lesions
- 8) cannot grade, photo quality

Area covered by drusen in subfield

- 1) <10% 2)<25% 3)<50% 4) >50%
- 7) cannot grade, obscuring lesions 8)cannot grade, photo quality

Hyper and Hypopigmentation of the Retina

Hyperpigmentation

- 0) absent
- 1) questionable
- 2) present <Co (<63um)
- 3) present >Co(>63um)
- 7) cannot grade, obscuring lesions
- 8) cannot grade, photo quality

Hypopigmentation

- 0) absent
- 1) questionable
- 2) present <Co (<63 um)
- 3) present >Co(>63um)

7) cannot grade, obscuring lesions

8) cannot grade, photo quality

Main location hyper / hypopigmentation.

This may not be central to indicated subfield, but may be more to periphery.

Choose most central location.

1) outside outer circle (mid-peripheral subfield)

2) in outer subfield

3) in middle subfield 4) in central subfield

4a) outside fovea (center point)

4b) in fovea

7) cannot grade, obscuring lesions

8) cannot grade, photo quality

Neovascular AMD

Presence

0) absent 1) questionable 2) present

7) cannot grade, obscuring lesions 8) cannot grade, photo quality

Typifying features

1) hard exudates 2) serous neuroretinal detachment 3) serous RPE detachment

4) hemorrhagic RPE detachment 5) retinal hemorrhage

5a) subretinal 5b) in plane of retina 5c) subhyaloid 5d) intravitreal

6) scar/glial/fibrous tissue

6a) subretinal 6b) preretinal

7) cannot grade, obscuring lesions 8) cannot grade, photo quality

Location. Choose most central location.

1) outside outer circle (mid-peripheral subfield) 2) in outer subfield

3) in middle subfield 4) in central subfield

4a) not underlying (in) fovea (center point)

4b) underlying (in) fovea

7) cannot grade, obscuring lesions 8) cannot grade, photo quality

Area covered

1) >C2<C3(>175um<250um) 2) >C3<C4(->250um<500um)

3) >C4and < 1000um (-central circle of grid)

4) >1000um <3000um (-middle circle) 5) ->3000um <6000um (-outer circle)

6) >6000um

7) cannot grade, obscuring lesions 8) cannot grade, photo quality

Geographic Atrophy

Presence

0) absent 1) questionable 2) present: ->C2 7) cannot grade, 8) cannot grade,
Location. Choose most central location.

1) outside outer circle (mid-peripheral subfield) 2) in outer subfield

3) in middle subfield 4) in central subfield

4a) not underlying (in) fovea (center point) 4b) underlying (in) fovea

7) cannot grade, obscuring lesions 8) cannot grade, photo quality

Area covered

1) >C1<C3(>175um<250um)

2) ->C3<C4(->250um<500um)

3) >C4 and < 1000um (central circle of grid)

4) >1000um and <3000um (-middle circle) 5)>3000um and <6000um (outer circle)

6) >6000um

7) cannot grade, obscuring lesions

8) cannot grade, photo quality

2.3 Pathology of AMD

AMD is a degenerative disease that affects the outer neural retina, retinal pigment epithelium (RPE), Bruch's membrane (BM), and the choroid. The clinical hallmark of the disease are the accumulation of yellow deposits called drusen in the fundus and this may be associated with hypo- and hyper-pigmented areas of RPE, the former signifying areas of RPE cell loss.(Sarks, 1976a) Since photoreceptors depend on the RPE and the choroidal circulation for nutrients as well as for the clearance of metabolic end-products, impairment of transport across BM could contribute to abnormalities associated with late AMD. These may include photoreceptor dysfunction, atrophy, RPE detachment and sub-RPE neovascularisation (NV) (Sarks, 1976a, Killingsworth, 1987, Moore et al., 1995b, Starita et al., 1996b, Holz et al., 2004).

2.4 Bruch's membrane (BM)

BM is an important pentalaminar layer, located between the choriocapillaries and the RPE, contributing to the transport of nutrients and waste products into and out of the photoreceptor layer. BM thickness has been found to increase with age.(Ramrattan et al., 1994a) This increases the diffusion path length, coinciding with an inverse relationship with hydraulic conductivity across BM as well as macromolecules.(Moore and Clover, 2001b)

Prior histological studies of aged BM have demonstrated the following:

4. Increases in collagen content and cross-linking (Newsome et al., 1987a, Karwatowski et al., 1995a)
5. Increased content and altered composition of proteoglycans has also been noted.(Kliffen et al., 1996b)
6. A higher total lipid content in BM.(Moore and Clover, 2001b, Fisher, 1987a) Lipid- and protein-rich debris has been found accumulating under the RPE and within BM. This contributes to the formation of focal (drusen) and diffuse (basal laminar and linear) deposits found in AMD. (Pauleikhoff et al., 1990, Green and Enger, 1993, Green, 1999b)

Taken in totality, this results in a structural disorganization of the collagen fibres (Hogan and Alvarado, 1967b) and thinning as well as fragmentation of the elastic layer.(Spraul et al., 1999b, Chong et al., 2005)

There are several pieces of evidence for the contribution of metalloproteinases (MMPs) to the thickening of BM, and hence, AMD. MMPs are a family of enzymes called zinc- required endopeptidases which are associated with remodeling of the ECM.

First, both genetic and serum studies of inhibitors of MMPs (e.g. TIMP3) which is produced by the RPE, has been studied and found to have an increased in AMD patients compared to age matched controls.(Apte et al., 1994, Fariss et al., 1997b, Kamei and Hollyfield, 1999a) Higher levels of TIMP-3 may contribute to the thickening of BM observed in AMD.

Also, whilst there is a known increase in inactive forms MMP 2 and 9 levels in the subretinal space as well as BM of AMD (Plantner et al., 1998a, Guo et al., 1999a), the accumulation of inactive forms of MMPs are hypothesized to be a consequence of remodeling of BM in aged eyes. Increased deposition of collagen and other ECM components induces synthesis of MMPs; however, increased concentration of TIMPs or decreased porosity of BM prevents its activation. Hence, from the gathered evidence, we postulate that BM thickening is correlated to AMD and an inactivation of MMPs result in increased BM thickening.

2.5 Ellex 2RT laser

The retinal rejuvenation therapy (Ellex 2RT) uses nanosecond duration pulses, which do not harm the photoreceptors (unlike previous conventional thermal lasers). It uses energy levels 500 times lower than current standard laser

treatment. It was previously shown to be effective as an alternative to conventional laser in treatment of other retinal diseases such as diabetic macular edema (DME).[27]

2.6 Prior Research Work

Preliminary laboratory work

Light sensitive cells of the human retina (photoreceptors) require high level of energy support and waste removal for optimal functioning. RPE is a single layer of epithelial cells which separates the photoreceptor layer to the choroids and controls many bi-directional support functions. RPE is attached to a basement membrane which is a matrix of collagen otherwise known as the Bruch's membrane (BM). This acts as a semi permeable barrier between the RPE cells and the choroids. Prior work by Professor John Marshall and Dr Ali Hussain and team has shown that thickening of the BM is a precursor of AMD with a resultant age related decreased hydraulic conductivity.(Hussain et al., 2010a, Hussain et al., 2010b) Further work was done which explored treatment possibilities with migration of RPE cells across BM with an associated improvement in hydraulic conductivity. Ellex 2RT was shown to be able to induce a wound healing response in the RPE which induces migration and release of metalloproteinases (MMPs).(Guo et al., 1999a) This had a subsequent effect on improvement of transport across the Bruch's membrane, with a postulated delay in onset of age related macular degeneration

Preliminary clinical work done with Ellex 2RT system.

Clinical results from a pilot study on Ellex 2RT for DME were presented at ARVO 2008 [30] The results should be treated with caution as only 18 of the 29 patients completed the 6 months study. But the results showed that 43% of patients showed 2 or more lines gain in visual acuity and the central macular thickness decreased by more than 5% from baseline in 46% of patients. The laser lesions from the pilot study were shown to be completely subthreshold with no laser scars or any other complications

A second randomized controlled study was conducted on Ellex 2RT for DME was presented at ARVO 2010. The study was conducted in Adelaide, Australia comparing treatment of 22 eyes using 2RT with 18 eyes treated with conventional photocoagulation. This study demonstrated that 2RT was safe and at clinically as efficient as conventional photocoagulation.

This laser is currently undergoing clinical trials at CERA, Centre of Eye Research Australia. A 12 month report which includes 50 patients at 12 month follow up showed that the patients experienced improvements in visual acuity and reduction in drusen. Drusen decreased in 70% of treated eyes, demonstrating a partial reversal of the degenerative process which causes AMD. Using flicker and color thresholds, the trial showed that central visual function improved in 38% of treated eyes [31].

3. Scientific Hypothesis

In aging and AMD, the accumulation of lipid- and protein-rich deposits in BM results in an overall thickening and a structural re-organisation of BM.(Ramrattan et al., 1994a) A consequent decrease in hydraulic conductivity and impairment of transport through BM may play a central role in the pathogenesis of AMD. So improvement of the hydraulic conductivity across the BM should improve the transport to and from the choroid to the outer retina.

2RT is a nanosecond pulsed laser, which uses very low energy levels to produce limited effects that selectively target melanosomes within the RPE cells. This laser energy absorption by melanosomes within RPE cells causes microbubbles and cavitations to form, damaging a percentage of RPE cells within the laser spots without rupture of the cell membranes. The resultant effects are an upregulation of MMPs and cytokines and RPE cell migration. This should improve the hydraulic conductivity across BM to and from photoreceptors and delay the progression of AMD in terms of reduction of clinical markers(drusen, pigment abnormality), improvement in visual function (visual acuity, color and contrast sensitivity and rod and cone recovery dynamics).

Days 4 to 7



<-- RPE cell loss

Days 7 to 14



<--RPE cell migration rim of bruch's thinning.



→MMP 2 and 9 upregulation →cytokines release

Overall improved
hydraulic conductivity

4. Objectives

To assess the efficacy and safety of retina rejuvenation therapy (Ellex 2RT) in patients with large drusen ($\geq 125 \mu$) in at least one eye compared to standard care (no treatment).

Comparison of the outcomes of Ellex 2RT compared to observation (standard care) will be done on the following parameters at 12 and 24 months:

Efficacy analyses:

3. Primary outcome: Mean change in visual acuity at 12 months.
4. Secondary outcomes:
 - d. Mean change in visual acuity at 24 months.
 - e. Mean change in contrast sensitivity, microperimetry and flicker sensitivity at 12 and 24 months.
 - f. Changes in fundus morphology as measured by optical coherence tomography, colour fundus photographs at 12 and 24 months.

Safety analyses will be done by comparing the following between the two arms:

16. Proportion of patients developing CNV confirmed by fluorescein angiography at 12 and 24 months
17. Proportion of patients developing retinal atrophy as measured by fluorescein angiography, autofluorescence and OCT at 12 and 24 months
18. Proportion of patients who lost more than 15 ETDRS letters at 12 and 24 months.
19. Proportion of patients who lost more than 30 ETDRS letters at 12 and 24 months.
20. Any other complications observed at 12 and 24 months.

5. Study Purpose and Design

5.1 Study Rationale

We hypothesize that Ellex 2RT would improve retinal function and morphology of the retina in patients with age related maculopathy.

We hypothesize that 2RT treatment will produce significantly better outcomes with respect to visual function improvements than the current standard of care (no treatment).

5.2 Study Design

Plan of investigation and statistical power of the trial

This is a prospective randomized controlled trial that will compare the mean change in visual acuity at 12 months between the treatment group treated with Ellex 2RT and the observation group (standard care) in patients with age related maculopathy

Sample size (Statistical Power of the study of 80%)

A control sample of size 33, with a baseline ETDRS letters in the range 70-95, and 12 months ETDRS letters was used to provide estimates for the sample size calculation.

The mean score at baseline was 79.7, and the SD of the one year change from baseline EDTRS was 7.59. To be able to detect a difference of 5 EDTRS between arms, in the mean change from baseline to 12 months, based on t-test, at the 5% level of significance, and with an 80% power, would need 76 patients to be recruited. Allowing for 5% dropout the required sample size would be 80 patients, 40 in each arm using a 1:1 ratio. The data will be analysed using analysis of covariance which involves adjusting for baseline in order to increase the power and to provide narrower confidence intervals.

Patient Enrolment

We expect that we will recruit 90% of the patients from Medical Retina Clinics in King's College Hospital and Moorfields Eye Hospital. The rest of the patients will be obtained from referrals from local optometrists and other ophthalmologists.

The local optometrists will be made aware of this study and patients with age related maculopathy will be informed about the study and referred to the screening clinics in the research department of both institutions. Suitable patients will be informed of the study verbally and by means of a Patient Information

Sheet at the research clinics. Patients will be invited to attend a clinic dedicated to the study at both institutions after at least 24 hours. At this baseline visits written informed consent will be obtained from patients wishing to enter the study, prior to enrolment.

Withdrawal from Study

Patients have the right to withdraw from the study for any reason. The investigator also has the right to withdraw a patient at anytime due to failure to follow protocol, administrative or other reason.

Randomisation

Patients are randomised into 2 groups by means of an on-line computerised randomisation programme (randomization.com). The follow-up investigators will be masked of the randomization.

Patient Numbering

Each patient is uniquely identified by a unique study number. Once assigned to a patient, a number will not be reused.

6. Population

6.1 Inclusion Criteria

1. Patients of either sex aged 55 years or over
2. Diagnosis of age related maculopathy that meet the criteria of large drusen ($\geq 125 \mu$) in at least 1 eye.
3. Best corrected visual acuity in the study eye between 50 to 90 ETDRS letters at baseline visit.
4. Media clarity, pupillary dilation, and subject cooperation sufficient for adequate fundus photographs.
5. No previous macular laser therapy to study eye.
6. Written informed consent and willingness and ability to be followed up for 24 months.

6.2 Exclusion Criteria

1. Drusenoid PED, Choroidal neovascularisation and geographic atrophy in the study eye.
2. Macular ischaemia (FAZ $> 1000\mu\text{m}$ in diameter or moderate perifoveal capillary loss in fluorescein angiogram).

3. Macular oedema of any cause such as wet AMD, diabetic macular oedema, pseudophakic macular oedema or taut posterior hyaloid.
4. Co-existent ocular disease that in the investigator's discretion would lead to decrease visual acuity by 3 lines or more by end of 12 months.
5. No coexistent choroidal neovascularization or geographic atrophy in either eye.
6. History of thermal lasers or treatment with intravitreal antiVEGF agents or steroids for any retinal conditions in the study eye.
7. Participation in an investigational trial within 30 days of randomisation that involved treatment with any drug including those that has not received regulatory approval at the time of study entry.
8. Anticipated major ocular surgery (including cataract extraction) for the period of the trial.
9. Amblyopia in study eye.
10. Known allergy to fluorescein dye or to any component of the study drug
11. Pregnancy at baseline and the patient will be withdrawn from the study if she becomes pregnant during the course of the study.

7. Summary of study assessments

Time	Screening	#6 months post entry	#12 months post entry	#18 months post entry	#24 months post entry
Informed consent	x				
Ophthalmic history	x	x	x	x	x
Medical history	x	x	x	x	x
Visual acuity	x	x	x	x	x
Contrast sensitivity	x	x	x	x	x
Microperimetry	x	x	x	x	x
Flicker sensitivity	x	x	x	x	x
Ophthalmic examination	x	x	x	x	x

2 field photographs	x	x	x	x	x
Autofluorescence	x	x	x	x	x
Fluorescein angiography [§]	x				x
OCT	x	x	x	x	x
Randomisation	x				
Treatment	x				

§ at physician's discretion in all other visits- if choroidal neovascularisation is suspected

The following data will be recorded

DEMOGRAPHIC DATA

Date of Birth

Gender

Ethnicity

Smoking history (never/previous/current)

Family history of AMD: Members blind with AMD or having treatment for AMD

Past Ophthalmic history

Duration of visual loss (>6/12 or worse) if present

Right eye

Left eye

AMD HISTORY

International classification of AMD

right

left

Cataract history LOC classification

right

Left

8. Detailed assessment protocols.

8.1 Visual function tests

REFRACTION PROTOCOL

The subjective refraction is to be performed at 6m using a Snellen chart with the room lights on. Following refraction the best VAs are to be measured at 4m using ETDRS Chart 1 for the right eye and Chart 2 for the left eye. During the VA

measurements the room lights need to be switched off. Both eyes are refracted at the baseline visit and at 12 months and 24 months (final visit).

The VA in the non-study eye is measured as outlined above and the score recorded on the score sheet. If, at one of the follow-up visits, the VA in the non-study eye differs by two lines or more from the VA found at the initial visit, the eye needs to be refracted as well, and the VA measurement repeated.

1. INITIAL VA MEASUREMENT

At the baseline visit, measure initial VA, whilst the patient is wearing his/her own distance glasses or unaided (if patient doesn't have distance glasses), using ETDRS Chart RJChart3. At all follow-up visits use the previous study refraction, the fellow eye is lightly patched with a tissue.

ALWAYS measure VA in the study eye first, then the fellow eye.

- Instruct the patient that the chart contains letters only and no numbers. If the patient forgets this during the course of the examination, they should be reminded that the chart contains no numbers and asked for a letter instead of the number.
- Advise the patient that there are 5 letters on each line, and that they should attempt to read the line from left to right.
- The examiner must not point at any letters or read any letters out loud during the test. It is acceptable to briefly point at a line, should the patient have difficulty finding the next line.
- The patient should be instructed to read the letters slowly, about one letter per second.
- The patient should be encouraged to guess any letters that are difficult to read, and be instructed to make a definite decision. If the patient is unable to identify a certain letter they should tell the examiner that they are moving on to the next letter along the line.
- If the patient incorrectly identifies a letter and then proceeds to read the next letter, s/he cannot go back and correct the mistake later. It is permissible to allow correction as long as the patient has not started to read the next letter aloud.
- The patient should be asked (and encouraged) to move on to the next line, as long as they manage to correctly identify it.

2. RETINOSCOPY

- Retinoscopy should be performed using a light / duochrome chart at 6m.

3. SUBJECTIVE REFRACTION

- Subjective refraction should be carried out according to the methods routinely employed by the Visual Assessment Department at the respective departments using a standard Snellen chart at 6m

4. FINAL VA MEASUREMENT

Follow the protocol for measuring the VA's outlined in section 1, except use Chart 1 for the right eye and Chart 2 for the left, and follow the instructions for recording the final ETDRS-score and VA outlined below.

5. ETDRS-SCORE

- Each letter correctly identified is circled on the visual acuity form. Any letters read incorrectly are deleted, and letters, for which no guess has been made, are left unmarked. Each correct letter scores one point. The total for each line is recorded in the right-hand column (max.5), and the scores for each line added at the bottom.
- If the score is 20 or more, then 30 points are added automatically and the final VA score is recorded.
- If the total score is less than 20, then the acuity should be tested at 1m. It is then added to 4m score.

TESTING FOR "COUNT FINGERS", HAND MOVEMENTS, AND LIGHT PERCEPTION

If the patient's VA is so poor that he/she cannot correctly identify any letters on the chart when tested at one meter, then test for Count Fingers.

I. TESTING FOR COUNT FINGERS

The eye not being tested should be completely occluded with a patch. A light must be shone from behind the patient's head at the examiner's hand. The examiner holds the hand two feet in front of the patient's face and presents an arbitrary number of fingers in random order and repeated 5 times. Eccentric fixation, if present, should be encouraged.

If the patient correctly identifies 3 of the 5 presentations, then count fingers vision is noted, If not, then the patient must be tested for hand movements.

2. TESTING FOR HAND MOVEMENTS

The eye not being tested should be occluded with a patch. A light must be shone from behind the patient's head at the examiner's hand. The examiner's hand

should be moved two feet in front of the patient with all fingers spread out. The hand should be moved either horizontally or vertically at a constant speed of approx. one back and forth movement per second. The patient is asked to watch the examiner's hand and respond to the question "in which direction is my hand moving?" The examiner should not explain that it will be moving either from side to side or up and down. Correct answers at three out of five presentations suggest that hand movement vision is present. If not, then you must test for light perception.

3. TESTING FOR LIGHT PERCEPTION

Light perception should be tested with an indirect ophthalmoscope in a darkened room. The nd ophthalmoscope should be focused at 1 meter with the rheostat set at maximum voltage. From that distance the beam should be directed in and out of the eye at least four times, and the patient should be asked to respond when they see the light. If the examiner is convinced that the patient perceives light should be recorded as "Light Perception". If not, vision should be recorded as "No Light Perception".

8.2 Contrast sensitivity

After refraction, contrast sensitivity measurement will be done using the Pelli-Robson chart (Clement Clarke Inc., Columbus, OH) at a distance of 1 m and chart luminance of 80 to 120 cd/m². The right eye will be tested followed by the left eye on charts 1 and 2, respectively, with +0.75 D added to the patient's refraction. The patient will be asked to name each letter on the chart, starting with the high-contrast letters on the upper left-hand corner and reading horizontally across the entire line. As low-contrast letters can take some time to appear, the patient was given instructions to keep looking and not give up too soon. The optometrist will circle each letter read correctly and cross out each letter read incorrectly, with letters not attempted left unmarked. The test will be stopped when the patient failed to correctly identify two or more letters in a triplet. The letter-by-letter scoring will be used.

8.3 Microperimetry

Microperimetry will be performed using the Nidek MP 1 (Nidek Technologies, Padova, Italy) or equivalent device. This instrument allows the examiner to view the fundus on the computer monitor while it is imaged in real time by an infrared (IR) fundus camera (768 x 576 pixels resolution; 45° field of view). Fixation target and stimuli are projected on to the liquid crystal display (LCD) within the MP1 for

the subject to view. The examiner can also view the stimulus and fixation target as part of the IR image on the computer monitor.

The study eye will be tested and the contralateral eye will be patched during the test. Pupils will be dilated with one drop each of tropicamide 1% and phenylephrine 2.5% at least 15 minutes prior to microperimetry. Microperimetry will be performed by an experienced examiner. The examination will be conducted in a darkened room. The following parameters will be used: a fixation target consisting of red ring, 1° in diameter; white, monochromatic background at 4 apostilb (asb), stimulus size Goldman III, with 200 milliseconds projection time; and a customized radial grid of 30 stimuli covering the central 10° (centred on the fovea), 2° apart (outer stimuli). The starting stimulus light attenuation will be set at 10 dB. A 4-2-1 double-staircase strategy will be used with an automatic eye tracker that compensates for eye movements. Pretest training was performed, and a 5-minute mesopic visual adaptation will be allowed before starting the test. The mean retinal sensitivity will be evaluated within central 10°, covering approximately 3 mm of central retinal area on the OCT map. The “9 in 1 layout” printout page (or equivalent) produced by the Nidek MP1 software provides indices related to microperimetry performance, retinal sensitivity and fixation characteristics will be printed out and recorded. The duration of each microperimetry examination and the average eye motion speed (°/sec) will also be recorded as indicators of test performance. The change in fixation stability and retinal sensitivity.

8.4 Flicker sensitivity

The Medmont perimeter will be used to perform static and flicker visual field evaluation of the central 10°. The Macula pattern will be used. Targets will be 0.5° in diameter, with a maximum spot brightness of 320 cd/m² and will be shown on a 3.2 cd/m² background. Spot presentation will occur for 200 ms in static perimetry and for 800 ms in flicker perimetry. Thresholding will be achieved with a 6/3 dB staircase.

8.5 Autofluorescence

The degree of RPE atrophy caused by the laser will be assessed using this technique. Images of fundus autofluorescence will be recorded after pupillary dilation using a retinal angiograph (Heidelberg Engineering, Heidelberg, Germany) scanning laser ophthalmoscope with a 40° field-of-view mode. The

ametropic corrector will be employed to correct for refractive error (up to ± 12 diopters) and to focus on the structure of interest. At least 24 single autofluorescence images of 512×512 pixels will be acquired in series mode with a frequency of 12 images per second. The best 10 images will be selected for automatic alignment, and a mean image will be obtained. As a result, a single image will be obtained for each eye. The areas of low autofluorescence will be measured and compared at baseline and final visit.

8.6 2-Field Colour and Macular Stereo Fundus Photography

AIM:

To grade the macula with **30 degrees** magnification

METHOD:

2 field and macular stereo photographs must be obtained as follows:

2- field retinal photography

1. Centred on the disc with the temporal border on the macula
2. Centred on the macula with the temporal border over the centre of the disc.

SAMPLING TIME:

Macular stereo photos will be taken at baseline and at 12 and 24 months

8.7 Fundus Fluorescein Angiography (FFA)

FFA will be performed in all subjects at baseline to exclude CNV and therefore study suitability. FFA will be repeated in all subjects at 12 and 24 months.

FFA will be performed to assess presence of CNV at physician's discretion. FFAs done up to 2 weeks prior to the baseline visit may be used instead of baseline FFA.

Field 1 - Macula: Centre the macula at the intersection of the cross hairs in the ocular. It is important that good even illumination is used at all times and that the flash settings are kept at the correct levels to ensure this.

The timing for the procedure is as follows: -

1. Before the injection of the fluorescein dye,
2. Position camera on F1 of eye to be treated (index eye) prior to injection.
3. 5ml of fluorescein is injected rapidly (in less than 5secs if possible).

Early or Transit Phase:

1. The 1st photograph of F1 of the index eye is taken at the start of the injection and the 2nd at the end of the injection. The purpose of this is to document the time taken to inject the dye.
2. 15-30 sec (F1 index eye): - Take a rapid series of about 10-16 exposures at intervals of about 1 to 2 seconds.

Mid Phase:

1. 30 - 45 seconds: F1 of the index eye
2. 50 seconds - 1 min: F1 of the fellow eye
3. 2 min: F1 of the index and fellow eye
4. 2½-3 min: F1 of index eye

Late Phase:

1. 5 min: F1 of index eye and fellow eye

Digital files must include the following information about each patient:

1. Study ID number
2. Date of birth
3. Date of angiogram. The information can then be stored in the research department until masked analysis by graders.

8.8 Spectral Domain Optical Coherence Tomography

Optical Coherence Tomography (OCT) will be assessed on both eyes. These assessments will be performed by an OCT certified photographer. OCT imaging will be performed using the Spectralis and OTI OCT. Scanning protocols will include raster and line scans. The analysis of the OCT images will be performed by two independent retinal specialists for features of macular drusen and presence, disruption or absence of the high reflectance bands corresponding to the external limiting membrane and inner-segment / outer-segment photoreceptor junction, RPE-Bruch's membrane and choroid.

9. Treatment Regime

Treatment spot size:	400 micron spot
Total number of laser spots per eye:	A total of at least 25 laser spots
Energy range:	70 – 120mJ/cm ²
Energy setting:	Energy increased while applying test nasal mid-peripheral area until a faintly visible spot is observed.

Reduce the energy to 70% of this setting then apply the grid pattern

Contact lens:

Area Centralis 1:1 laser contact lens (or equivalent)

Treatment Protocol:

3. Treatment one: Ellex 2RT, 400µm diameter spot, 2 rings of concentric subthreshold laser spots applied, at 2000µm (5 ½ spots sizes out from the fovea) and 2800µm (7 ½ spot sizes out from the fovea). So a total of at least 25 spots will be applied.

OR

4. No treatment or observation (standard care)

10. Adverse Events

10.1 Adverse Events

Safety evaluations will be performed by recording clinical adverse events at each visit.

1. Foveal burn
2. Conversion to wet AMD
3. Break in Bruch Membrane, evidenced by blood or pigment released at time of treatment as reported by ophthalmologist.
4. RPE atrophy increase as measured by autofluorescence.

10.2 Procedures for Recording and Reporting Adverse Events

A “serious adverse incident” is one which:

- led to a death
- led to a serious deterioration in the health of the patient, user or others and includes:
- a life threatening illness or injury
- a permanent impairment to a body structure or function

- a condition requiring hospitalisation or increased length of existing hospitalisation
- a condition requiring otherwise unnecessary medical or surgical intervention and which might have led to death or serious deterioration in health had suitable action or intervention not taken place. This includes a malfunction of the device such that it has to be monitored more closely or temporarily or permanently taken out of service
- led to foetal distress, foetal death or a congenital abnormality or birth defect
- might have led to any of the above

.Reporting Responsibilities

All SAEs, will be reported immediately to the Chief Investigator. All serious adverse incidents, whether initially considered to be device related or not, will be reported to the UK Competent Authority - the MHRA Devices Group. These reports should initially be made as soon as possible once the Chief Investigator has been made aware of the incident. Copies of all Serious Incident forms will be sent by the Chief Investigator to the Sponsor and the REC.

Reporting timelines are as follows:

SUSARs which are fatal or life-threatening must be reported not later than 7 days after the sponsor is first aware of the reaction. Any additional relevant information must be reported within a further 8 days.

SUSARs that are not fatal or life-threatening must be reported within 15 days of the sponsor first becoming aware of the reaction.

The reporting of 2 SUSAR will lead to termination of the trial.

The Chief Investigator will provide an annual report of all SARs (expected and unexpected), and SAEs which will be distributed to the Sponsor, MHRA and the REC.

All other AEs are to be collected and reported from baseline to end of study (24 months).

11.Data Monitoring

11.1 Data collection

Data will be collected on clinical report forms and entered into the study database.

11.2 Data analysis of efficacy

The analysis will be conducted at 12 and 24 months.

11.3 Planned analysis

Baseline characteristics of patients in each treatment arm will be summarized. Analysis of covariance will be used to assess whether any observed difference in mean visual acuity at 12 and 24 months (after adjusting for baseline difference in visual acuity) is statistically significant. If any imbalance in other important prognostic factors is evident regression analysis will be conducted adjusting for those factors to assess the impact. Data will be analysed according to the group to which patients were originally assigned (i.e. intention to treat).

We will provide the 12 and 24 months analyses of:

Efficacy analyses:

1. Primary outcome: Mean change in visual acuity at 12 months.
2. Secondary outcomes:
 - a. Mean change in visual acuity at 24 months.
 - b. Mean change in contrast sensitivity, microperimetry and flicker sensitivity at 12 and 24 months.
 - c. Changes in fundus morphology as measured by optical coherence tomography, colour fundus photographs at 12 and 24 months.

Safety analyses will be done by comparing the following between the two arms:

1. Proportion of patients developing CNV confirmed by fluorescein angiography at 12 and 24 months
2. Proportion of patients developing retinal atrophy as measured by fluorescein angiography, autofluorescence and OCT at 12 and 24 months

3. Proportion of patients who lost more than 15 ETDRS letters at 12 and 24 months.
4. Proportion of patients who lost more than 30 ETDRS letters at 12 and 24 months.
5. Any other complications observed at 12 and 24 months.

12. Ethics and Regulatory Approvals

The trial will be submitted through IRAS for ethics approval and MHRA for approval of clinical investigation for non CE-marked medical device.

13. Milestones and targets for the work

Ethical Approval to be obtained by 1st Aug 2011.

Recruitment and randomisation of first patient by 15th Aug.

30 eyes to be recruited by December 2011.

Complete 80 eyes by end of March 2012

6-monthly follow up for 2 years.

Publication of results by June 2014.

14. Quality Assurance

The Generic model name for the 2RT system is: Product Name – Regeneris and the Product Code – LR1532.

The Quality assurance certificate is provided by the manufacturer, Ellex, along the investigators brochure.

15. Publication policy

All results pertaining to the trial will be released within 1 year post completion of trial.

16. Finance

JP Moulton Charitable Trust will be providing funding for staffing and running of the trial.

Ellex will be providing the laser Ellex 2RT for the trial.

The trial will be sponsored by King's College Hospital NHS Foundation trust.

17. Signature of Chief Investigator

Miss Sobha Sivaprasad
Consultant Ophthalmologist
King's College Hospital

III. Consent form, Patient information sheet



King's College Hospital NHS Foundation Trust

King's College Hospital
Denmark Hill
London SE5 9RS

www.kch.nhs.uk
Direct tel: 020 3299 1722
Direct fax: 020 3299 3738

CONSENT FORM

Efficacy and safety of retinal rejuvenation using Ellex 2RT laser in age-related maculopathy (RETILASE trial)

Name of Principal Researcher: Miss Sobha Sivaprasad

Patient Identification Number for this trial:

Please initial box

1 I confirm that I have read and understood the information sheet dated _____ for the above study and have had the opportunity to ask questions.

2. I understand that my participation is voluntary and that I am free to withdraw at any time, without giving any reason, without my medical care or legal rights being affected.

3. I understand that sections of any of my medical notes may be looked at by responsible individuals from King's College Hospital or from regulatory authorities where it is relevant to my taking part in research. I give permission for these individuals to have access to my records.

4. I agree to take part in the above study.

Name of Patient Date Signature

Name of Person taking consent Date Signature
(if different from researcher).

Name of researcher Date Signature

Name of witness Date Signature 3 copies: 1 for

King's College Hospital NHS Foundation Trust

King's College Hospital
Denmark Hill
London SE5 9RS

www.kch.nhs.uk
Direct tel: 020 3299 1722
Direct fax: 020 3299 3738

PATIENT INFORMATION SHEET

1. Study title: Efficacy and safety of retinal rejuvenation using Ellex 2RT laser in age-related maculopathy (RETILASE trial)

2. Invitation paragraph

You are being invited to take part in a research study. Before you decide it is important for you to understand why the research is being done and what it will involve. Please take time to read the following information carefully and discuss it with friends, relatives and your GP if you wish. Ask us if there is anything that is not clear or if you would like more information. Take time to decide whether or not you wish to take part.

Thank you for reading this.

3. What is the purpose of the study?

Age related macular degeneration is the leading cause of blindness amongst people above age of 55 years. 90% of AMD are dry, manifesting as yellowish deposits (drusen) in the retina. Most of these patients would have no loss in visual acuities, but frequently complain of changes in contrast as well as increased need of brighter lights for reading. Overtime, these patients may progress into wet AMD, with new vessel formation and bleeding in the macula. This is an average of 10% per annum.

Currently, wet AMD requires multiple treatments and are selectively beneficial. There is to date, no method that has proven to be of benefit in the prevention of

advanced AMD except high doses of vitamins in a select group. Prior work has shown that laser reduces the drusen in the retina and improves vision.

Ellex 2RT is a newly developed nanosecond, non thermal laser which has 500 times lower energy level than conventional laser. Hence, it is painless and does not penetrate and cause destruction to the neural layers(photoreceptor layer). Preliminary lab and clinical work has also shown that 2RT rejuvenates the retina, causing resorption of drusen and improvements in central visual acuity.

The purpose of this study is to prove that 2RT improves visual function and improves the features of the retina. Only one of your eyes will be subjected to 2RT.

You will have a 50% chance of being randomized into one of the 2RT treatment protocol.

The trial takes 24 months.

4. Has the study been approved by an Ethics Committee?

Yes the study has been given a favourable opinion by the Research Ethics Committee. It has also been approved by King's College Hospital Research Governance committee and the Medicines and Healthcare Products Regulatory Agency (MHRA).

5. Why have I been chosen?

You have been asked to be part of the study as you meet the inclusion criteria for the study, that is to say that you have early or intermediate AMD in at least one eye and the level of your vision meets the entry standard, you have no other eye disease and you are not pregnant. 69 other patients will be needed for the study. If you decide to take part in the study, this agreement will be irrespective of which of the 2 groups you are randomized to.

6. Do I have to take part?

It is up to you to decide whether or not to take part. If you do decide to take part you will be given this information sheet to keep and be asked to sign a consent form. If you decide to take part you are still free to withdraw at any time and without giving a reason. This will not affect the standard of care you receive. If you do not wish to take part in this study you will not be at a disadvantage and will continue to receive normal clinical management.

7. What will happen to me if I take part?

If you agree to take part, you will be asked, to undergo a series of baseline investigations to determine whether you meet the entry criteria. In addition to your normal investigations you will have. Some of the investigations will be done in City University.

1.a Detailed refraction (measurement for glasses), vision, contrast, colour and flicker tests.

2. Fundus fluorescein angiography (FFA), (a special dye will be injected through your arm veins and photographs taken by a computer)

3. Optical Coherence Tomography(OCT) and autofluorescence,(a painless and noninvasive procedure whereby you will have to follow a blue light on a screen and a computer will analyse the details of the back of your eye.

4. After receiving the laser treatment in the study eye, you will be followed up every 6 months for 2 years.

8. What do I have to do?

There are no lifestyle restrictions. You may eat and drink as normal and take your normal medication. You will be able to give blood. If you become pregnant no harm will occur to the unborn child as a result of the trial but you will be withdrawn from the study.

9. What is the drug or procedure that is being tested?

The therapy being tested is the retinal rejuvenation therapy, a new technique to deliver laser into the eye.

10. What are the alternatives for diagnosis or treatment?

The alternative to this novel therapy is observation (no treatment given)

11. What are the side effects of taking part?

Patients in both Groups will not be exposed to side effects over and above those of routine clinical care.

12. What are the possible disadvantages or risks of taking part?

If you have private medical insurance you should check with the company before agreeing to take part in the trial. You will need to do this to ensure that your participation will not affect your medical insurance.

13. What are the possible benefits of taking part?

We hope that the treatment will help you. However, this cannot be guaranteed. The information we get from this study is intended to help us design and perform further similar large studies in the future with the intention of prevention of advanced AMD

14. What if new information becomes available?

Sometimes during the course of a research project, new information becomes available about the treatment/drug that is being studied. If this happens, your research doctor will tell you about it and discuss with you whether you want to continue in the study. If you decide to withdraw your research doctor will make arrangements for your care to continue. If you decide to continue in the study you will be asked to sign an updated consent form.

Also, on receiving new information your research doctor might consider it to be in your best interests to withdraw you from the study. He/she will explain the reasons and arrange for your care to continue.

15. What happens when the research study stops?

After the trial has ended, your follow up will continue in the normal clinical settings with regular follow up in your clinic.

16. What if something goes wrong?

If you are harmed due to someone's negligence, then you may have grounds for a legal action but you may have to pay for it. Regardless of this, if you wish to complain about any aspect of the way you have been approached or treated during the course of this study, the normal National Health Service complaints mechanisms may be available to you.

17. Will my taking part in this study be kept confidential?

All information that is collected about you during the course of the research will be kept strictly confidential. Any information about you which leaves the hospital or surgery will have your name and address removed so that you cannot be recognised from it. With your consent, we would like to inform your GP and your diabetic consultant of your participation in the trial.

18. What will happen to the results of the research study?

At the end of the trial we expect to publish the results in ophthalmic journals. These results will be available shortly after the close of the trial in Jan 2014. You

will not be identified in any report or publication. You can obtain a copy of the published results by contacting your research doctor.

19. Who is organizing and funding the research?

The research is being funded by a charity, JP Moulton Charitable Trust. The money is used to fund the tests needed for the research.

20. Contact for Further Information

Your contact research doctor is

Miss. Sobha Sivaprasad (chief Investigator).

Address: King's College Hospital, Denmark Hill, London SE5 9RS

Telephone: 020 3299 1722

Fax: 020 3299 3738

Thank you for your time reading this form and for considering taking part in this study.

This Patient Information Sheet is for you to keep.

